Developing new metal-based chemistry for dentifrice formulations

Barret, Marie C.

Award date:
2001

Awarding institution:
University of Bath

Developing New Metal-based Chemistry for Dentifrice Formulations

Submitted by Marie C. Barret

for the degree of PhD

of the University of Bath

2001

Marie C. Barret

ProQuest LLC
789 East Eisenhower Parkway
P.O. Box 1346
Ann Arbor, MI 48106-1346

Abstract

This thesis has been divided into two main sections. Chapter I contains the Introduction to the work. The remaining chapters detail the synthesis, characterisation and biological testing of the compounds produced.

Chapter I provides an introduction to toothpaste and to the problems associated with the dental plaque. It also looks at the chemistry of three metals (copper, zinc and tin) and at the background to the research on cyclic α-hydroxyketones.

Chapter II contains a brief introduction on some commercially available α-hydroxyketones. The tin(IV), tin(II), zinc(II) and copper(II) complexes of these ligands have been prepared and characterised by standard spectroscopic techniques. Three of the tin(IV) complexes (hinokitiol)$_2$SnCl$_2$, (ethyl maltol)$_2$SnF$_2$ and (hinokitiol)$_2$SnF$_2$ were studied by single-crystal X-ray diffraction. The structures of Sn(maltol)$_2$, Sn(tropolone)$_2$, Zn(tropolone)$_2$, Zn(hinokitiol)$_2$, Cu(hinokitiol)$_2$.pyridine and a new structure of Cu(hinokitiol)$_2$ have also been obtained. Finally the results of the biological tests are presented.

Chapter III describes the synthesis and characterisation of a series of 1-alkyl-3-hydroxypyridin-4-ones and their M(II) complexes (M= Cu, Zn, Sn). The structures of two copper and two zinc compounds are reported, having been determined by X-ray crystallography. This chapter also details the results of the anti-bacterial assays of the ligands and of their copper and zinc complexes.

Chapter IV describes the synthesis and characterisation of a number of aminotropones and their copper(II) complexes. One ligand, 2-benzylaminotropone, was studied by single-crystal X-ray diffraction. The structures of two of the copper derivatives, Cu(2-methylaminotropone)$_2$ and Cu(2-ethylaminotropone)$_2$, are also given.

Acknowledgements

I would like to thank Kieran Molloy for his help, advice and continual encouragement during these three years.

I would also like to thank Mary Mahon for her help with the crystallographic analysis, Jon Steed at Kingston College for the crystal structures of $Sn(maltol)_2$ and $Sn(tropolone)_2$ and Alan Carver for all the elemental analyses.

My thanks also go to the people in the laboratory 1.35 for their advice and friendship (Aliki, Graeme, Leopardo, etc) and to Anna, Arach, Christelle, Fred, Koko and Selma for their support during the last year and for making my time at Bath so enjoyable.

A special thank to Ross "euuuh" Harrington for his patience and guidance through the solution of the crystal structures and to Tim "poulet" Thorpe for his help with the organic synthesis.

Merci aussi á ma mamounette et á mon papounet pour leurs encouragements durant cette thèse.

Finally I would like to thank Jon Creeth and Peter Hall, my supervisors at Unilever for their assistance and everyone else in the Unilever Dental labs for all their help during my placements.

Financial support for this project from Unilever Research Port sunlight Laboratories is gratefully acknowledged.

Abbreviations

b	broad
bipy	bipyridine
BHI	Brain Heart Infusion
^{n}Bu	^{n}butyl
Bz	benzyl
d	doublet
CEE	L-Cysteine Ethyl Ester
DMSO	dimethylsulfoxide
en	1,2-diaminoethane
Et	ethyl
ether	diethyl ether
EtOH	ethanol
HAP	hydroxyapatite
Hacrp	4-hydroxy-6-methyl-3-[-3-dimethylaminoacryloyl]-2H-pyran-2-one
Hdep	1,2-diethyl-3-hydroxypyridin-4-one
Hdmp	1,2-dimethyl-3-hydroxypyridin-4-one
HEtma	ethyl maltol
hfa	hexafluoroacetylacetonato
Hhino	hinokitiol
Hhmp	2-methyl-3-hydroxypyridin-4-one
Hkoj	kojic acid
Hma	maltol
Hmep	1-ethyl-2-methyl-3-hydroxypyridin-4-one
Htrop	tropolone
m	multiplet
Me	methyl
MeOH	methanol
NMR	nuclear magnetic resonance spectroscopy

No.	number
IR	infrared spectroscopy
I.S	isomer shift
OD	optical density
PBS	phosphate buffered saline
pmdt	N,N,N',N'',N''-pentamethyldiethylenetriamine
^{i}Prop	*iso*-propyl
^{n}Prop	^{n}propyl
py	pyridine
q	quartet
Q.S	quadrupole splitting
s	singlet
SDS	sodium dodecylsulphate
S.Warneri	*Staphlococcus.warneri*
t	triplet
TC	tropocoronate
THF	tetrahydrofuran
Ts	tosyl
ZCT	zinc citrate trihydrate

Chapter I

Chapter II

Chapter III

Chapter IV

Conclusion

Appendices

Chapter I

1.1 What is toothpaste?

Toothpastes appeared on the market around the turn of the XX century having evolved from toothsoaps and toothpowders. The function of toothpaste is twofold. It serves a cosmetic function to clean the teeth (by removal of stain, plaque and food debris) and freshen the mouth, and also a therapeutic function in delivering a range of therapeutic agents to control caries, plaque, gingivitis, etc.

Toothpastes are the ideal vehicles for the delivery of therapeutic agents since they are:

- Mass market family products
- Easy and pleasant to use
- Provide direct application of therapeutic agents to the tooth surface and oral tissues

The plaque causes most oral problems: plaque bacteria produce acid, especially in the presence of sugar, which can cause tooth decay. It follows that improved dental health can be achieved by the removal of plaque and the prevention of further plaque growth using suitable anti-bacterial agents. An anti-bacterial agent can act in several ways, by preventing the biofilm formation, disrupting the existing biofilm, inhibiting further biofilm growth or killing particular organisms in the biofilm. Therapeutic agents are only one of the several components of toothpaste. The Table 1.1 shows basic toothpaste formulation.[1]

Table 1.1: Basic toothpaste formulation.

Component	Level (wt/wt%)
Water	1.0-28.0
Humectant	27.0-70.0
Detergent	1.5-3.0
Flavour	1.0-1.5
Abrasive	4.0-55.0
Thickener	0.6-1.5
Structurant	0.0-5.0
Opacifier	0.0-1.0
Therapeutic agent(s)	qs
Sweetener	qs
Colour	qs
Stabilisers	qs

Exact formulations depend upon the type of abrasive chosen, which then affects the choice of therapeutic agents. Here is a brief description of the major components and their role in the toothpaste.

The role of **water** is to dissolve and disperse the therapeutic agents; the **humectant** is there to lower water-activity. There are two major humectants: sorbitol, a solid, which is used as a 70% aqueous solution called sorbitol syrup or neosorb70; and glycerol, which is a liquid.

Sorbitol $HOCH_2[CH(OH)]_4CH_2OH$

Glycerol $HOCH_2CH(OH)CH_2OH$

The most common **detergent** (or surfactant) is sodium dodecylsulphate (SDS), also called sodium laurylsulphate.

SDS $CH_3CH_2CH_2CH_2CH_2CH_2CH_2CH_2CH_2CH_2CH_2CH_2OSO_3^- Na^+$

The detergent serves a number of roles: it creates foam which is important as consumers do not like non-foaming toothpastes; it dissolves and disperses the water-insoluble flavours; it helps cleaning the teeth.

Flavour types are highly conservative, being dominated by mints either singly (peppermint or spearmint) or together as double mint. Peppermint is the most popular dental flavour since it has the ability to deliver the sensation of freshness to most of consumer palates. It contains about 50% of menthol.

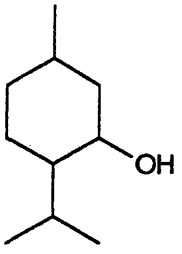

Menthol

The **abrasive** is used mainly to clean the teeth, but it also contributes the body of the toothpaste. The three major abrasives are silica (SiO_2), chalk ($CaCO_3$) and alumina $[Al(OH)_3]$. Unilever is mainly using silica and alumina. Chalk does not permit the use copper complexes because they decompose at the high pH.

1.2 Dental plaque

Before explaining the role of the therapeutic agents, it is of importance to first describe what plaque is and then what are its consequences.

Dental plaque is a complex mass of bacteria that forms on the exposed surface of teeth.[2] It is the single major factor responsible for two of the most common oral human diseases:

- Dental caries
- Periodontal disease

Dental plaque is a very complex phenomenon and there is still a lot to learn about it. It is known that plaque is made up of saliva, bacteria and food particles and that it can adhere very tenaciously to teeth, especially where their surface is irregular or discontinuous.

Dental calculus, known as tartar, is also involved in the build-up of plaque. Tartar is a hard deposit formed around the gum margin. The exact process by which calculus appeared is as yet to be defined in detail. It acts as an ideal substrate on which further plaque build-up occurs. This makes plaque even more difficult to remove, as gum margins are areas of the mouth which are hard to clean with a conventional toothbrush.

Methods of physical removal of the plaque, such as tooth brushing and flossing, are the most common ways to control it. However the most problematic plaque usually lies in the most inaccessible areas of the mouth, where it does a lot of damage.

Consequently, a better way to reduce the plaque involves the use of anti-bacterial agents in commercially available dental care products.

1.3 Periodontal disease and dental caries

There is not an exact definition of **periodontal disease** but its presence is often indicated by inflammatory gingivitis, which manifests itself as bleeding around the gingival margin during and after brushing. The disease appears to be caused by bacterial contamination of the gingival margin, so prevention can be achieved through early and effective removal of the plaque from this area.[3]

Most people suffer from mild periodontitis, although relatively harmless by itself, if left unchecked it may lead to full periodontitis. When periodontal disease becomes more serious, there is gradual withdrawal of the gum around the teeth, causing the teeth to loosen and eventually fall out. It is estimated that more teeth are lost in this way than through the actual decay of the teeth.[4] The proportion of elderly persons in the population is increasing in many countries and emphasis has been made on finding measures, which will encourage tooth retention.[5] Improving knowledge about the cause and effect of periodontal disease should help to find an effective prevention and cure for this condition. In particular, using better anti-bacterial agents in toothpastes would be an effective and reliable way of improving gum health.

Dental caries is also a disease primarily caused by plaque, which leads to the physical decay and eventually loss of the teeth. Dental caries occur when bacteria present in the plaque film generate lactic acid. They metabolise carbohydrates from food and in doing so produce lactic acid. Then, the acid produced penetrates the acquired pellicle and reacts with the mineral (hydroxyapatite) HAP in the enamel. The acid is said to de-mineralise the tooth enamel leading to calcium deficient apatites. When the de-mineralisation occurs, the surface of the enamel is weakened and gives way to the formation of cavities and eventually to the destruction of the tooth. The formation of a cavity can expose the nerves, causing a painful toothache.

In the past few decades, evidence suggests that dental caries have shown a marked reduction in the UK, some European countries and the US.[6-9] This is due to overall

better oral hygiene and also to the finding that dietary restriction of sugar is the most effective method of prevention against dental caries.[10] The change in the toothpaste market from non-fluoride formulations to fluoride in virtually all the pastes is also a major factor. The fluoridation of public water supplies has helped as well.

1.4 Therapeutic agents

They are several kinds of **therapeutic agents**: anti-caries agents, anti-bacterial agents, anti-tartar agents and anti-sensitive tooth agents.

Historically sodium fluoride (NaF) was the first **anti-caries agent** to be incorporated into toothpaste during the early 1940's, following the success of water-fluorination in reducing dental caries. The understanding of fluoride's role in tooth decay prevention started in 1901 when Dr. McKay moved to Colo (Colorado, US).[11] He found out that people there had brown stains on their teeth and that their teeth were very resistant to tooth decay. He discovered later that this was due to the town's drinking water, which was naturally rich in fluorides. Subsequent research determined that water fluoride levels below 1ppm prevent tooth decay without staining.

Fluoride reduces dental caries in two ways:

- It reduces the ability of bacteria in plaque to generate lactic acid
- It helps remineralise the tooth areas where acid attacks have already begun

It is the fluoride ion itself that is active, the chemical compound it is part of does not matter. However, when making fluoride toothpaste it is important to choose the right abrasives. The first formulations using NaF were not active since the fluoride reacted with the calcium present in the abrasive (particularly chalk) to form insoluble calcium fluoride.[1] Today, however, sodium fluoride has found use again in silica formulations and is the major anti-caries agent.

Anti-bacterial agents can be divided into two classes: metal ion anti-bacterial agents and organic anti-bacterial agents.

The **metal ion** anti-bacterial agents are generally limited to water-soluble salts of zinc, copper and tin.[1] Out of these three metals **zinc** has received the most exploitation. Clinical data, both *in vivo* and *in vitro*, have shown that regular exposure to toothpaste containing zinc inhibits plaque growth.[6] One of the first metal additives used in toothpaste was zinc citrate [$Zn_3(citrate)_2.3H_2O$, ZCT] in 1944[1] which showed great anti-bacterial activity and is still used today. Recently zinc has been shown to inhibit odour formation. Bad breath is a major concern to the general population and oral care products (toothpaste, mouth rinse, chewing-gum) have succeed in masking it when containing metal ions, especially zinc.[12]

Whilst **copper** figures strongly in the patent literature it has not found success in commercial formulations due to its tendency to give a metallic taste to toothpaste.

Tin(II) fluoride (SnF_2) has also been used in toothpaste since the early 1950's and was initially employed as an anti-caries agent. It was believed to be an inorganic source of fluorine, but it is the stannous ion itself, Sn^{2+}, which is now known to be very active rather than the fluorine. However, it suffered from various problems, one of them being its tendency to give a yellow/brown discoloration to the teeth. The major one is that Sn(II) is particularly susceptible to hydrolysis and oxidation, which causes precipitation in the presence of water. As only Sn(II) is believed to be active, it is necessary to prevent the oxidation to Sn(IV), which is possible by the addition of a specific stabilising agent. Tin(II) compounds are known to react with polyhydroxy compounds such as sorbitol[13] and since a large proportion of toothpaste is sorbitol, it is very likely that a chemical interaction occurs between them. This type of interaction seems to provide stability to the Sn^{2+}. A co-polymer of maleic anhydride and methoxyethylene of molecular weight greater than 30,000 $gmol^{-1}$ has been found to form chelates with stannous fluoride and so provide effective protection from oxidation in a similar manner to sorbitol.[14]

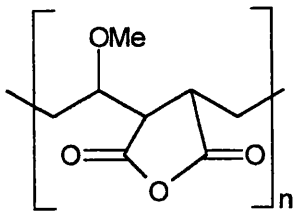

Methoxyethylene/maleic co-polymer

Another approach has involved the use of an organic anti-oxidant in the formulation. The compound, typically propyl gallate, has been found to be compatible with the other ingredients and to consequently reduce the tendency for tin(II) to oxidise with as low as only 1% incorporated into the toothpaste.[15]

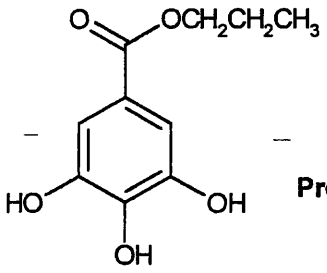

Propyl gallate

Today, SnF_2 has been replaced by stannous pyrophosphate [$Sn_2P_2O_7$].

The only **organic anti-bacterial** agent finding extensive use in toothpaste is triclosan.

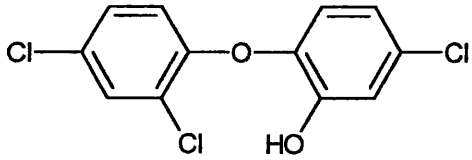

Triclosan

A study in 1995[16] showed there was no significant difference between the triclosan toothpaste and fluoride toothpaste. The triclosan toothpaste offers only moderate plaque inhibitory properties when compared to conventional toothpaste, but whilst its use as a single anti-plaque agent has given only modest reduction in plaque level, its use in combination with zinc citrate has improved plaque reduction.[17] A possible

explanation is that while the zinc ions are more effective on existing plaque, triclosan acts to prevent the re-growth.

However, one major problem with triclosan is the current tendency for reducing the use of chlorinated organic compounds. It is clear, regarding the current legislation, that a more environmentally friendly alternative to triclosan would be desirable.

Another disadvantage of triclosan is its poor solubility in distilled water (about 1ppm at 20°C). A way around this problem is to emulsify triclosan with a suitable surfactant such as SDS to form a micellar phase. However, upon dilution in the mouth the surfactant concentration falls below the critical micelle concentration and triclosan precipitates, loosing its efficacy.

An alternative method for improving the delivery of triclosan is to incorporate a lipophilic copolymer of methoxyethylene and maleic acid into the dentifrice. This has been found to enhance the oral retention of triclosan in the mouth.[18,19]

The most recent technique to increase the water solubility of triclosan is to react triclosan with phosphoryl chloride ($POCl_3$) to produce triclosan phosphate.[20]

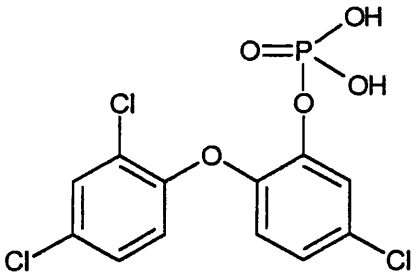

Triclosan phosphate

This compound is soluble in both water (>10%w/w at 20°C) and toothpaste and has been found to be more active than triclosan alone. A possible explanation is that triclosan phosphate, being water soluble, can bind to phosphatases in saliva, bacteria cell walls and plaque fluids through its phosphate functional group. Once bound to these specific sites the triclosan phosphate liberates free triclosan *via* the action of phosphatase enzymes on the functional group.

1.5 The chemistry of copper and zinc

Copper and zinc are **transition metals**. Their electronic configurations are as follows:

- For copper: $1s^2 2s^2 2p^6 3s^2 3p^6 3d^{10} 4s^1$
- For zinc: $1s^2 2s^2 2p^6 3s^2 3p^6 3d^{10} 4s^2$

Strictly speaking, the term transition element applies to an element with a partly filled *d* or *f* subshell, so excludes those with d^0, d^{10}, f^0 or f^{14}. However, it is convenient to include copper, silver and gold in this classification as these elements commonly form ions with partly filled *d* subshell. Despite the fact that they and their ions have d^{10} electron configuration, zinc, cadmium and mercury are also considered together with the transition elements.

The transition elements are all metals, which conduct heat and electricity well. The metals of Group 11 (copper, silver, gold) have the highest electrical and thermal conductivities known.

1.5.1 Copper

Copper was discovered early in human history. This is hardly surprising as it occurs native in several parts of the world. In Roman times, much of the copper used came from the island of Cyprus, hence the Latin name for copper at that time as *aes cyprium*. Over the year it became *cuprum* from which the modern symbol Cu is derived.[21] The formation of copper through charcoal reduction appears to have been known by 3500BC and the copper/tin alloy bronze is believed to have been discovered before 3000BC, leading to "the Bronze Age". Copper is the second metal after iron in its usefulness down the ages. Brass, a copper alloy formed with zinc, appeared much later than that of bronze, around 1400BC in Palestine.[22] Copper does not appear to be very toxic towards humans and a typical diet usually includes between 2 and 5 mg of copper per day.[21]

Copper belongs to the Group 11, with also silver and gold. Each of the three elements exhibits the oxidation states +I, +II and +III, with Ag being most commonly +I and Au +III. Cu(II) is the most stable oxidation state of copper in

aqueous solution. The electronic configuration of Cu^{2+} is $1s^2 2s^2 2p^6 3s^2 3p^6 d^9$ and the unpaired electron makes the copper complexes paramagnetic and coloured (e.g: copper acetate is blue, Cu(tropolone)$_2$ is dark green, etc).

The most common coordination numbers for Cu(II) complexes are four, five and six. In each structure a variation from idealised geometries occurs through bond length and bond angle distortion.

Four-coordinate Cu(II) compounds:

Four-coordinate Cu(II) complexes exhibit both square planar.[23-25] and tetrahedral geometries. In $Cs_2[CuBr_4]$ and $Cs_2[CuCl_4]$, the $[CuX_4]^{2-}$ ions have a slightly squashed tetrahedral shape.[26] An X-ray crystal structure analysis of the copper complex of 3-methylacetylacetone has been carried out.[23] The copper atom adopts a square planar geometry as shown Figure 1.5.1.

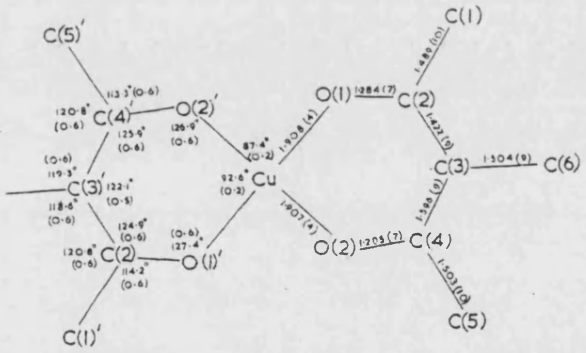

Figure 1.5.1: Structure of Cu(3-methylacetylacetone)$_2$ with bond lengths (Å).[23]

The Cu-O bonds [1.908(4), 1.907(4) Å] are equivalent and are consistent with earlier work.[27,28]

Five-coordinate Cu(II) compounds:[29,30]

Five-coordinate, square pyramidal geometry is less common for Cu(II) complexes. The crystal structure of Cu(2-[(2-oxy-phenyl)iminomethyl]phenolato).(1,10-phenanthroline) consists of monomeric molecules in which the copper atom has a distorted square pyramidal form (Figure 1.5.2).[31] The angles N(18)-Cu-N(42) (107°)

and N(31)-Cu-N(42) (77.2°) are wider and narrower respectively than in an ideal square pyramidal complex (90°). The Cu-O bonds are of similar length and are close to values observed for other five coordinate copper(II) compounds.[32]

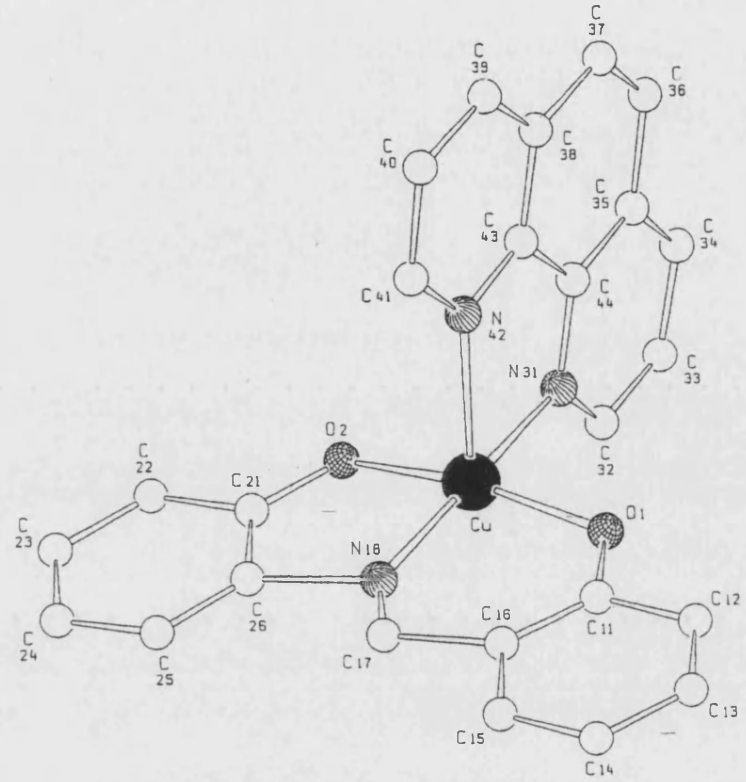

Figure 1.5.2: The molecular structure of Cu(2-[(2-oxy-phenyl)iminomethyl]phenolato).(1,10-phenanthroline).[31]

Five-coordinate copper can also adopt a trigonal bipyramidal geometry.[33,34] The structure of [Cu(en)(pmdt)]$(ClO_4)_2$ (en: 1,2-diaminoethane; pmdt: N,N,N',N'',N''-pentamethyldiethylenetriamine) was determined by X-ray crystallography.[35] The geometry around the copper ion is very close to regular trigonal bipyramidal (Figure 1.5.3).

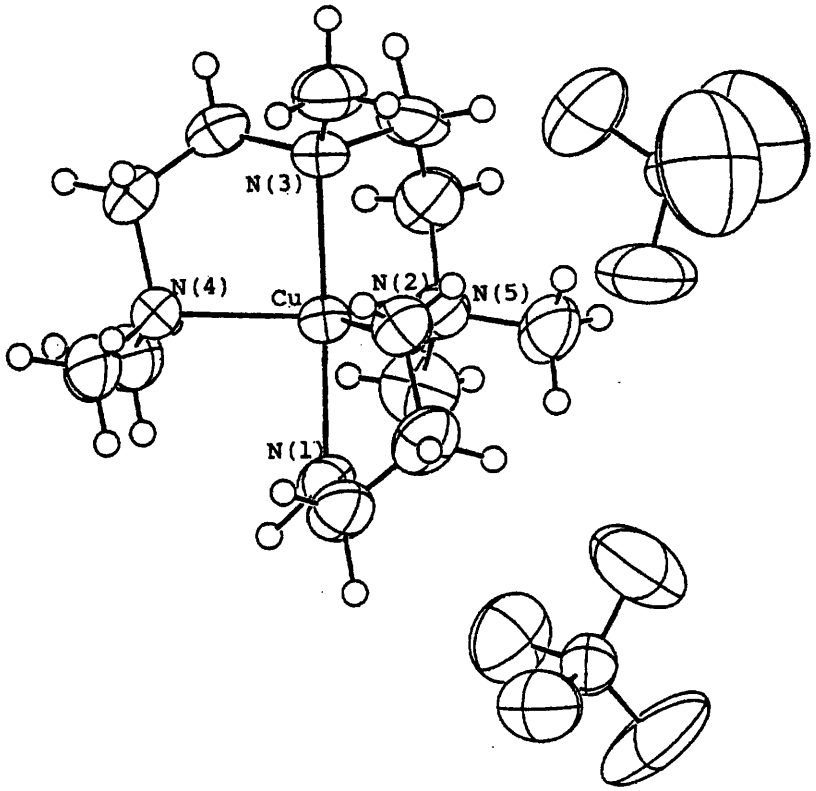

Figure 1.5.3: The structure of [Cu(en)(pmdt)](ClO$_4$)$_2$.[35]

Six-coordinate Cu(II) compounds:

Complexes of general formula CuL_6 tend to have a distorted octahedral geometry. Regular octahedral coordination is very rare due to the presence of the $3d^9$ configuration, which causes a distortion. This is known as the Jahn-Teller effect and can be explained with Crystal Field Theory (CFT). The distortion usually leads to an elongation of two bonds, giving four short and two long Cu-L distances (*i.e.*: 4+2 coordination). An example is given Figure 1.5.4 with $[Cu(NO_2)_6]^{4-}$.

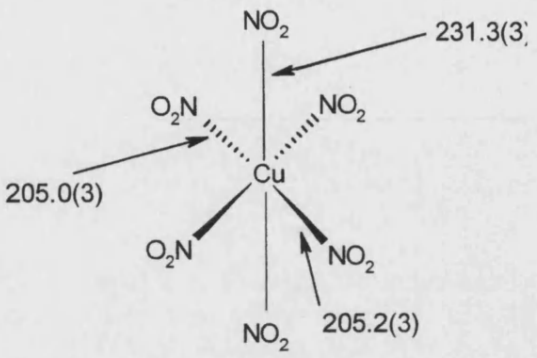

Figure 1.5.4: Structure of $[Cu(NO_2)_6]^{4-}$ with Cu-N bonds in pm.[22]

More rarely the distortion leads to two short bonds and four long ones (*i.e.*: 2+4 coordination). For example, the X-ray structure of K_2CuF_4, shows an array of fluoride ions in which each copper atom is surrounded by six fluoride ions, two *trans* at 195pm and four at 208pm.[36]

From other examples[37,38] it can be noted that bidentate ligands are bonded to the copper atom in the equatorial plane, with other monodentate ligands adopting axial positions. Figure 1.5.5 shows the crystal structure of Cu(N-acetyl-β-alaninato)$_2$.2H_2O[37] as an example of this.

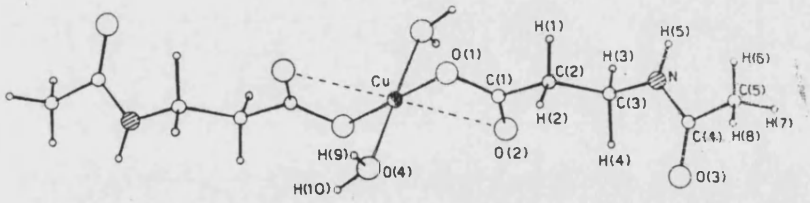

Figure 1.5.5: The structure of Cu(Ac-β-ala)$_2$.2H_2O.[37]

In this case the copper atom increases its coordination number to six with the oxygen atoms of two water molecules.

1.5.2 Zinc

Zinc is widely distributed over the earth's surface and is found concentrated into sulphide, carbonate, silicate and phosphate rocks. The use of alloys of zinc, especially those with copper (brass) and tin, antedate those of the pure metal by several thousand years.[21] Brass contains from 20–45% of zinc, together with copper and sometimes other metals. Zinc itself was probably first extracted in India and then on larger scale in China. Zinc has an important role in several enzymes. It is the second most important transition metal after Fe.[26] It is generally accepted that the toxicity of zinc is very low and a wide range of compounds are permitted for use in food or food containers.[21]

The elements of the Group 12, zinc, cadmium and mercury, all have two *s* electrons beyond a completed *d* shell. Removal of the *s* electrons results in divalent compounds and the oxidation state (+II) is characteristic of the group. Hg(I) compounds are also important, but oxidation states higher than (II) do not occur. This is because removal of more electrons would destroy the symmetry of a completed *d* shell. Also, these elements have d^{10} electronic configuration and so cannot produce *d-d* spectra and hence the majority of their compounds are white.

Coordination numbers 4, 5 and 6 are also most common in Zn^{2+} chemistry.

Four-coordinate Zn(II) compounds:

Four-coordinated Zn(II) occurs largely as tetrahedral complexes. Many complexes are known such as $[Zn(CN)_4]^{2-}$, $[Zn(pyridine)_2Cl_2]$,[26] or $[(\eta^3\text{-}Tp^{Ph})Zn(anthranilate)]$.[39] The molecular structure of $[(\eta^3\text{-}Tp^{Ph})Zn(anthranilate)]$ is shown in Figure 1.5.6. Anthranilate acts as oxygen ligand intermediate between monodentate and bidentate with Zn-O bond distances of 1.93 and 2.46 Å.

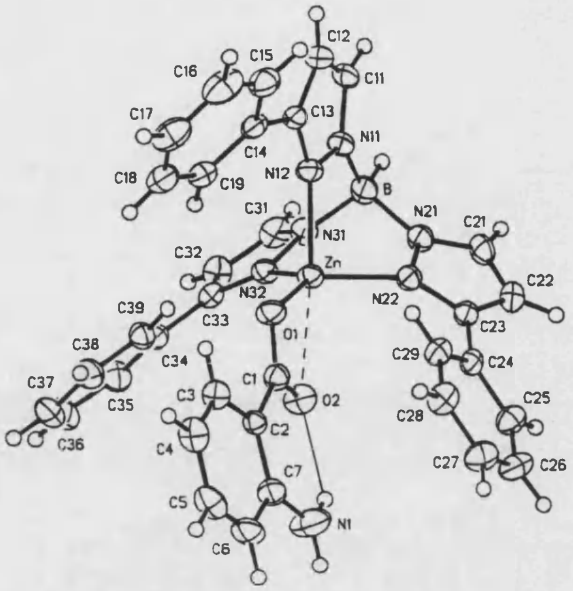

Figure 1.5.6: Molecular structure of [(η^3-Tp^{Ph})Zn(anthranilate)].[39]

Five-coordinate Zn(II) compounds:

Five-coordination is less common for Zn(II), but examples include Zn(terpyridyl)Cl_2 which has a trigonal bipyramidal structure.[26] There are examples of five-coordinate zinc complexes with less clearly defined geometry.[40,41] The molecular structure of $[Zn(mmpcd)]ClO_4$ (mmpcd: $(Me_2pzCH_2)_2NC_2H_3CH_3NHC_5H_6CSSCH_3$) shows a distorted trigonal bipyramidal geometry for the zinc(II) ion (Figure 1.5.7).[42]

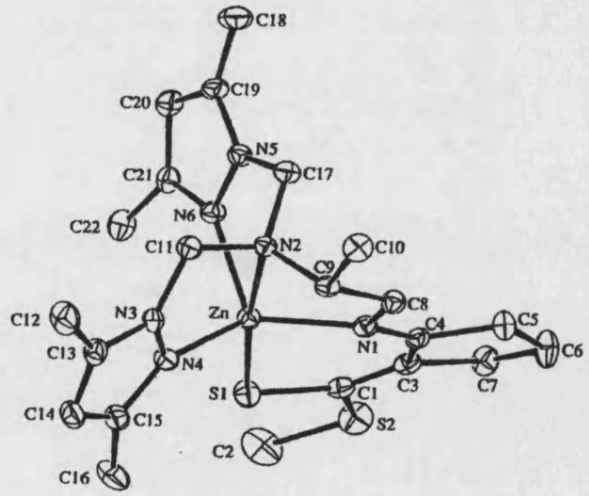

Figure 1.5.7: Structure of [Zn(mmpcd)]$^+$.[42]

The ligand is pentadentate, utilising all potential donors atoms in coordination. There are no Zn•••perchlorate interactions.

There are very few examples of square pyramidal coordination, one is in $[Zn_2L_2][ClO_4]_2$ (L= {2-bis[2-(pyridyl)ethyl]aminomethyl}phenolate.[43] Another one is seen in the structure of Zn(II) complex of macrocyclic tetraimine (Figure 1.5.8).

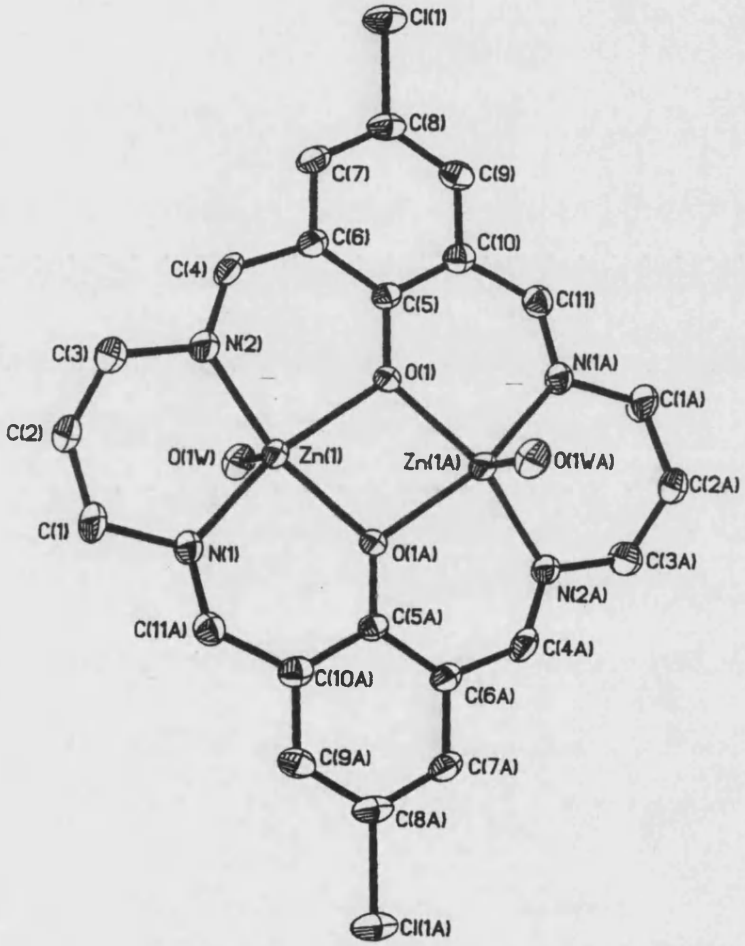

Figure 1.5.8: Structure of zinc complex.[44]

The structure consists of a complex cation countered by two independent perchlorate anions. The donor atoms of the macrocyclic ligand occupy the base plane, while two coordinating water molecules, situated inversely, occupy the apical position.

Six-coordinate Zn(II) compounds:

Zinc forms a number of six coordinate octahedral complexes.[45-47] The examples cited in this thesis are all composed of two bidentate ligands in the square plane and with two molecules of water in the axial positions. The structure of $Zn(hfa)_2(OH_2)_2$ (hfa: hexafluoroacetylacetonato) is given Figure 1.5.9. The Zn-O bond lengths are all similar, ranging from 2.0–2.2 Å.

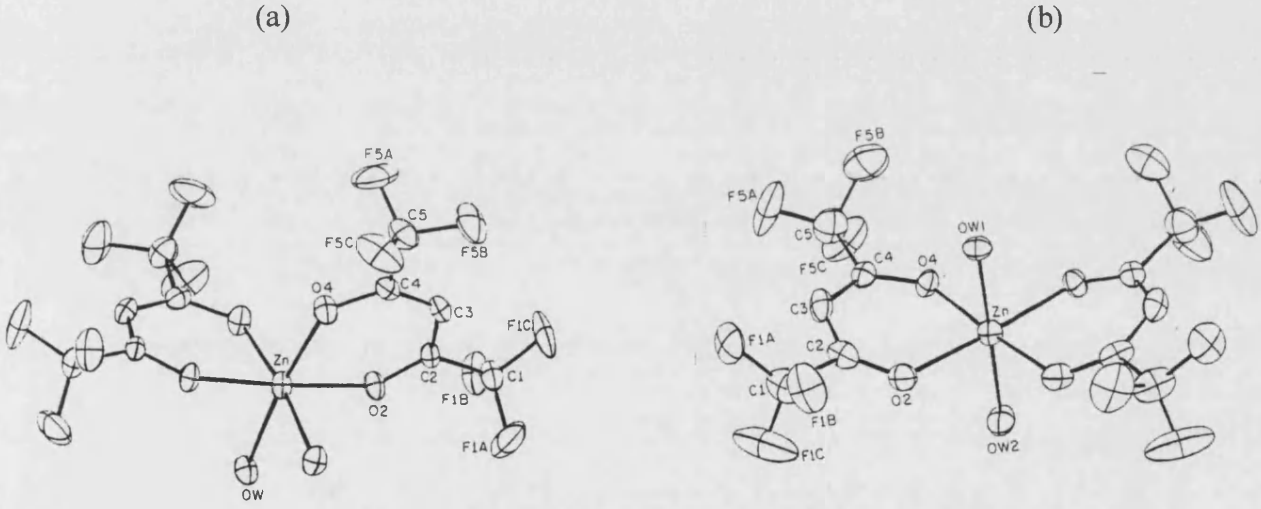

Figure 1.5.9: View of the complex $[Zn(hfa)_2(OH_2)_2]$, (a) cis-isomer, (b) trans-isomer.[47]

It is possible to see *cis* and *trans* isomerism in some of these complexes. Both compounds have been prepared separately, but the details for such behaviour are outside the scope of this thesis.

1.6 The chemistry of tin

Tin has been used with copper to form the alloy bronze since ca. 3000BC, even though isolation of the pure metal probably only dates from ca. 800BC. In the UK, tin has been mined in Cornwall from Roman times, but today the mines are closed because they have became uneconomic. The main uses of tin are electroplating steel to make tin plates and making alloys. Tin plate is extensively used for making cans for food and drinks.[26]

Tin is one of the Group 14 elements, together with carbon, silicon, germanium and lead. It has the electronic structure [Kr] $4d^{10}5s^25p^2$. The change from non-metal to metal with increasing atomic number is well illustrated in Group 14, where C and Si are non-metals, Ge has some metallic properties and Sn and Pb are metals. The increase in metallic character on descending the group also shows itself in the increased tendency to form M^{2+} and the increase stability of the +II oxidation state in general. Lead is the only element of the group where the lower oxidation state (+II) is favoured. In the case of the tin the +IV state is more stable than the +II state, but the energy difference between the two oxidation states is quite small (electrochemical potential for the reaction $Sn^{2+} - 2e^- \rightarrow Sn^{4+}$ 0.1364V).[48] Tin(II) compounds are susceptible to facile aerobic oxidation, which causes problems during their preparation.

With a ground state configuration of $5s^25p^2$ tin can form covalent tin(II) compounds with use of two unpaired *p*-electrons. If the $5s^2$ electrons do not take part in bond formation, the bond angle in such an SnX_2 molecule would be 90°. Normally however, the *s*-electrons are incorporated into an sp^2 hybridised bond situation and the resultant bond angle is about 120°.

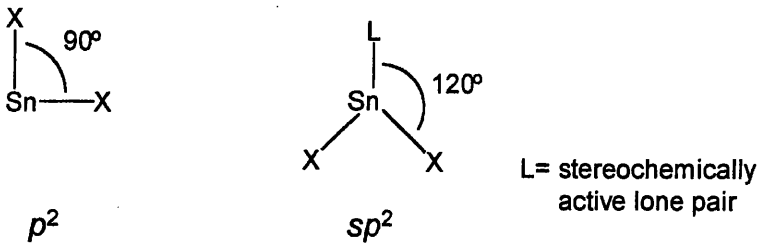

Bivalent tin complexes wherever possible adopt structures in which the metal achieves a coordination number greater than two, either by chelation, complexation or bridging. Examples of coordination geometries are given Figure 1.6.1. The basic unit is usually recognisable as a trigonal pyramid (**I**), but additional bond or contacts are often present, leading to distorted pseudo-trigonal bipyramidal (**II**), square-based pyramidal (**III**), octahedral (**IV**), distorted octahedral (**V**), or facially capped trigonal prismatic (**VI**). Through all these geometries the coordination number for the tin atom varies from 2 to 9, the most common geometries are **I, II** and **III**.

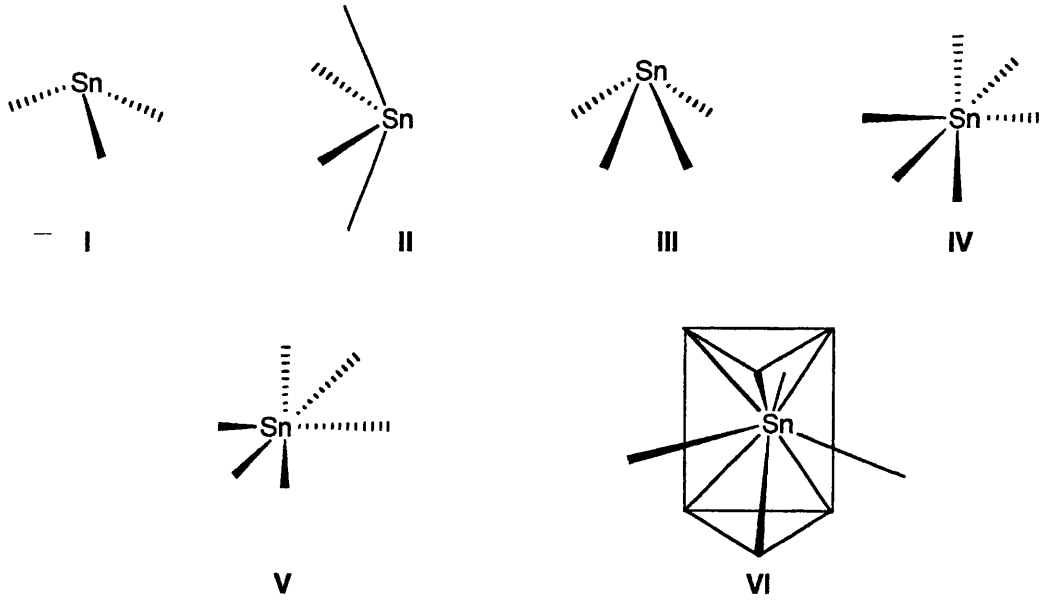

Figure 1.6.1: Different coordination geometries for Sn(II).

The Table 1.6.1 shows some possible coordination geometries for stannous compounds together with known examples.

In the majority of the Sn(II) complexes the lone pair is stereochemically active. This is indicated by a vacancy in the coordination sphere accompanied by the expected distortion of the regular geometries. It is usual to find distorted structures, which are sometimes difficult to distinguish from each other. For example it may be difficult to differentiate a four-coordinate square-based pyramidal (**III**) from a distorted pseudo-trigonal bipyramidal (**II**).

Table 1.6.1: Sn(II) geometries.

Coordination number	Coordination geometry	Example	Ref.
2	Angular	$Sn(OC^tBu_3)_2$	49
3	Trigonal planar	$(OC)_5Cr.Sn[CH(SiMe_3)_2]_2$	50
3	Pyramidal	$K_2Sn_2(CH_2C_2O_4)_3$	51
4	Square pyramidal	$Sn[N(SePPh_2)_2\text{-}Se,Se']_2$	52
4	Ψ-trigonal bipyramidal	$Sn(CEE)_2$ (CEE: L-Cysteine Ethyl Ester)	53
6	Octahedral	Cubic SnSe	54
9	Trifacially capped trigonal prismatic	$SnBr_2$	55

Angular coordination: It is claimed from spectroscopic evidence that $Sn(OC^tBu_3)_2$ has the same structure as the germanium complex.[49] $Ge(OC^tBu_3)_2$ in the solid sate is a two-coordinate compound, due to the steric bulk effect of the ligands (Figure 1.6.2). The Ge-O bond lengths are 1.896(6) and 1.832(11) Å. The structure has an exceptionally small [O-Ge-O] angle of 85.9(4)°, which is quite surprising as the ligand is bulky.

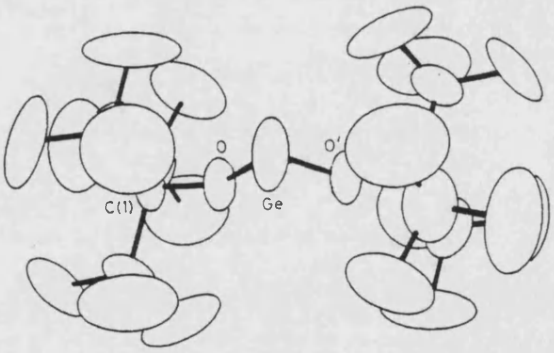

Figure 1.6.2: The structure of $Ge(OC^tBu_3)_2$.[49]

Trigonal planar coordination: The crystal structure of $(OC)_5Cr.Sn[CH(SiMe_3)_2]_2$ consists of a three-coordinate tin. The [C-Sn-C] angle is 98°, which is distorted from the ideal geometry (120°). The average bond length Sn-C is 2.185 Å.

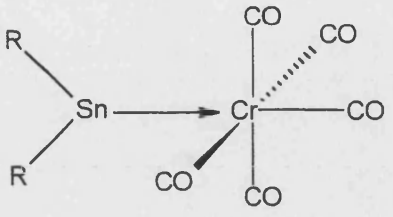

R= $CH(SiMe_3)_2$

Figure 1.6.3: The structure of $(OC)_5Cr.Sn[CH(SiMe_3)_2]_2$.[50]

Trigonal pyramidal coordination: The structure of potassium [hydrogen(bismaleato)]stannate(II) has been reported and found to adopt a polymeric anionic system $Sn_2[(CH_2C_2O_4)_3]_n^{2n-}$ (Figure 1.6.4).[51]

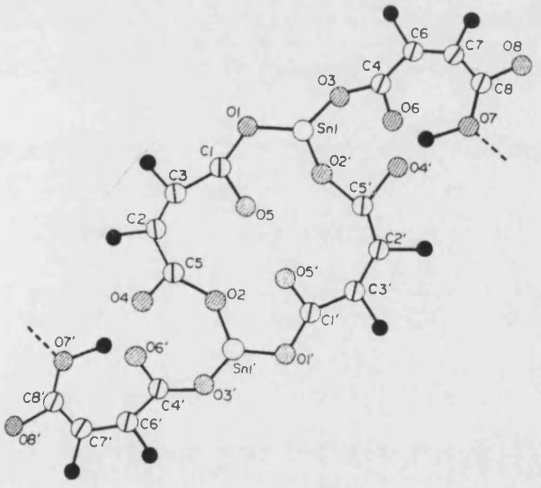

Figure 1.6.4: The 14-membered ring system in $Sn_2[(CH_2C_2O_4)_3]_n^{2n-}$.[51]

The tin atom adopts a pyramidal geometry. Each tin atom is bonded to two different types of maleate group; one is a bridging bidentate ligand and the other one a unidentate monoprotomaleato group. The Sn-O distances to the maleate and monoprotomaleate ligands are 2.199 and 2.212 Å respectively.

Square pyramidal coordination: The structure of the distorted tetragonal pyramidal complex of $Sn[N(SePPh_2)_2\text{-}Se,Se']_2$ is described by Cea-Olivares *et al.*[52] They also reported the first example of a true square planar tin(II) compound, an isomer of $Sn[N(SePPh_2)_2\text{-}Se,Se']_2$ (Figure 1.6.5).

The distorted pyramidal molecule presents two types of Sn-Se bonds, long ones of 2.943(2) Å and short ones of 2.803(2) Å, both being longer than the Sn-Se bond lengths in the square planar isomer.

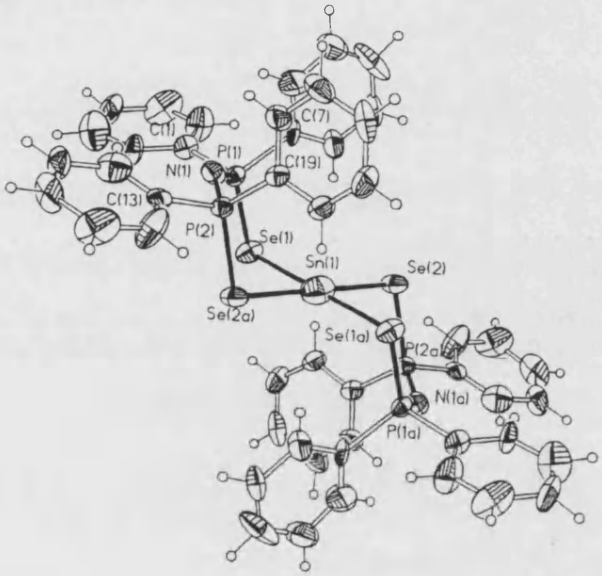

Square planar

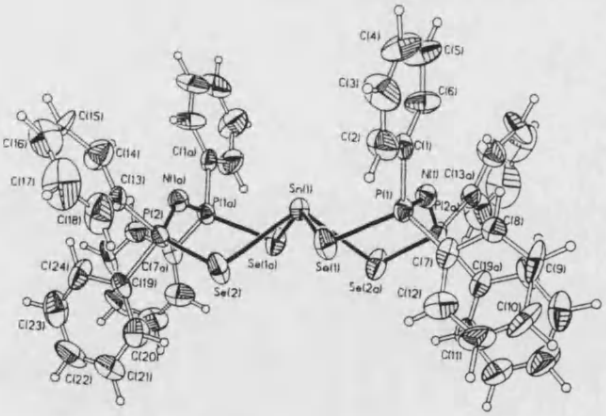

Distorted square pyramidal

Figure 1.6.5: The two structures adopted by $Sn[N(SePPh_2)_2\text{-}Se,Se']_2$.[52]

Pseudo-trigonal bipyramidal coordination: The crystal structure of $Sn(CEE)_2$ (CEE: L-Cysteine Ethyl Ester) has been obtained[53] and shown to have a Ψ-trigonal bipyramidal geometry (Figure 1.6.6). The average bond distance for Sn-S is 2.52 Å and is typical of stannous complexes, while the average Sn-N distance of 2.48 Å is slightly longer than those previously reported.

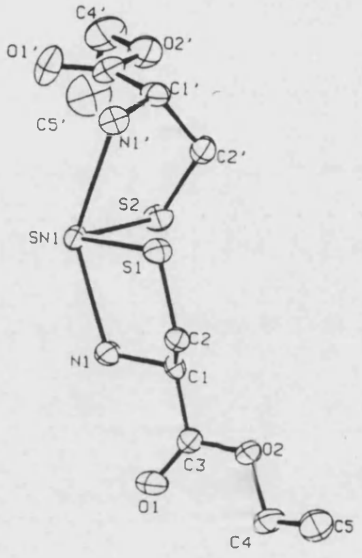

Figure 1.6.6: The structure of bis(ethylcysteinato) tin(II).[53]

Octahedral coordination: It has been noted that SnTe[56] and cubic SnSe[54] adopt both the NaCl lattice. These are covalent species in which both lobes of the three *p* orbitals of the tin(II) bond to six neighbours. In case of the cubic SnSe, the average bond distance is 3.00 Å.

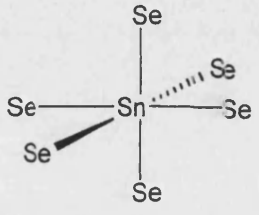

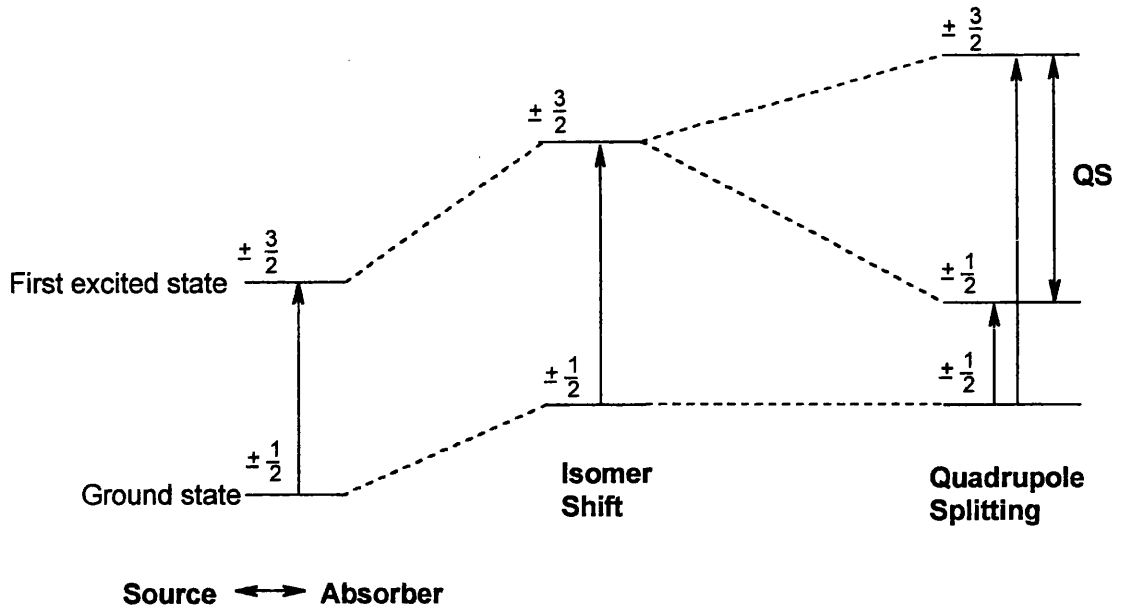

Figure 1.6.8: Nuclear energy levels, Isomer Shift and Quadrupole Splitting in ^{119m}Sn Mössbauer spectroscopy.[48]

Isomer Shift, I.S, (δ):

The I.S measures the total electron density on the Mössbauer atom. It is the electron density at the nucleus that is important. Since only *s*-electrons have finite probability of occurring at the nucleus, the I.S measures the difference in valence *s*-orbital populations of the tin atom relative to the standard material (usually SnO_2). In Sn(II) complexes, the electronic configuration is $5s^2$, so the *s*-electron density is greater than in the tin atom ($5s^25p^2$). In Sn(IV) compounds, the electronic configuration is $5s^0$. The two $5s$ have been used in bonding, reducing the *s*-electron density. The isomer shift varies as follows:

Tin(IV) δ = -0.5 to +2.1 mms^{-1}

Tin(II) δ = +2.5 to +5.0 mms^{-1}

Quadrupole Splitting, Q.S, (Δ):

Q.S arises from an unsymmetrical distribution of electric charge about the nucleus. So the magnitude of the Q.S represents the asymmetry of the electron cloud around the nucleus. Such asymmetry may occur directly through the presence of lone electron pairs (*i.e.*: non-bonding electrons) or indirectly through the bonding interactions. If the asymmetry of the tin nucleus is spherical, there will be a zero electric field gradient (EFG) and so a single line will be observed. However if there is an EFG at the nucleus, a doublet spectrum will be observed.

In general the magnitude of the QS is related to the differing electronegativities and coordination geometries of the surrounding ligands. In the case of most of tin(IV) compounds the Δ value can give a precise information about the coordination number, because definite ranges of QS exists for particular ligand configurations. However, this is different for the tin(II) complexes due to the presence of the active lone pair, which can produce irregular and unpredictable geometries. This causes the data to be difficult to interpret and less useful in assigning coordination geometries.

As mentioned previously, only tin(II) compounds are believe to be active in toothpaste, so in order to see how the stannous complexes behave in toothpaste formulations, Mössbauer spectroscopy has been applied to a range of products such as $Sn_2P_2O_7$ (Figure 1.6.8.).[57] The Mössbauer spectrum of $Sn_2P_2O_7$ (a) is typical of polymeric Sn(II) species, with broad linewidths due to the presence of multiple tin environments. The spectrum of $Sn_2P_2O_7$ once incorporated into toothpaste (b) shows clearly the presence of a tin(IV) impurity. This oxidation of the stannous ions is due to interactions with other components present in the paste and the oxygen in the air.

(a)

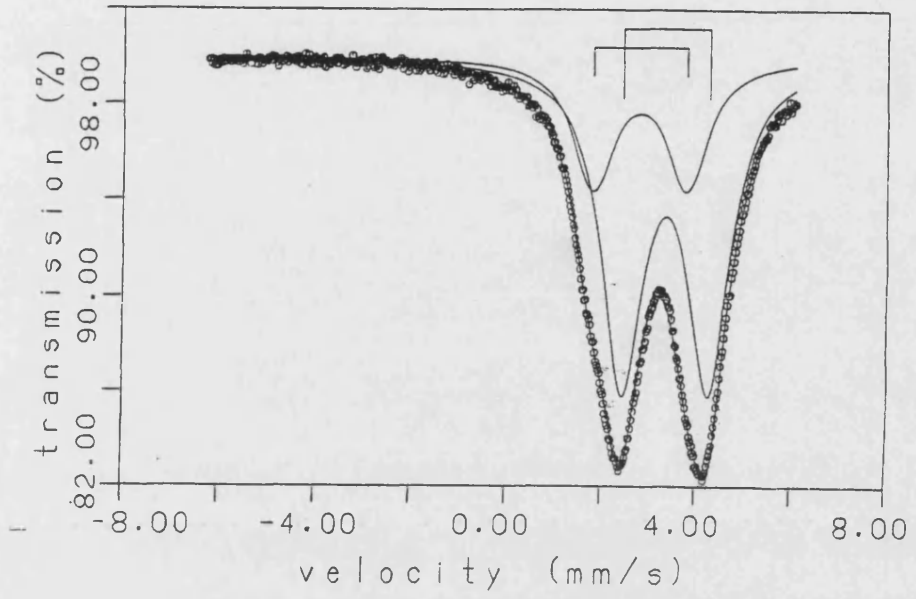

(b)

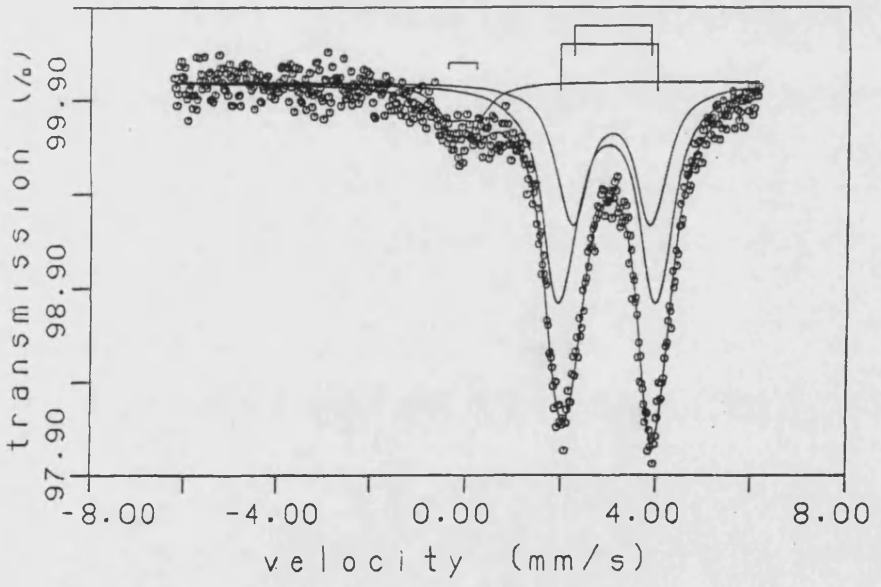

Figure1.6.8: The Mössbauer spectra of (a) solid $Sn_2P_2O_7$ and (b) $Sn_2P_2O_7$ as a dentifrice component.[57]

^{119}Sn Nuclear Magnetic Resonance (NMR)

Tin has three naturally occurring isotopes with spin ½ (all the others have spin zero) (Table 1.6.2). In practice only the two more abundant isotopes are of any consequence.

Table 1.6.2: Tin nuclei with spin ½.

Nucleus	^{115}Sn	^{117}Sn	^{119}Sn
Natural abundance (%)	0.35	7.61	8.58

Although both ^{117}Sn and ^{119}Sn can be used, usually the latter is chosen because of its superior abundance and receptivity. Spectra in which tin is involved in coupling to other nuclei are readily recognisable. This can be illustrated by the ^{1}H and ^{13}C spectra of $Sn(CH_3)_4$ (Figure 1.6.9).[58]

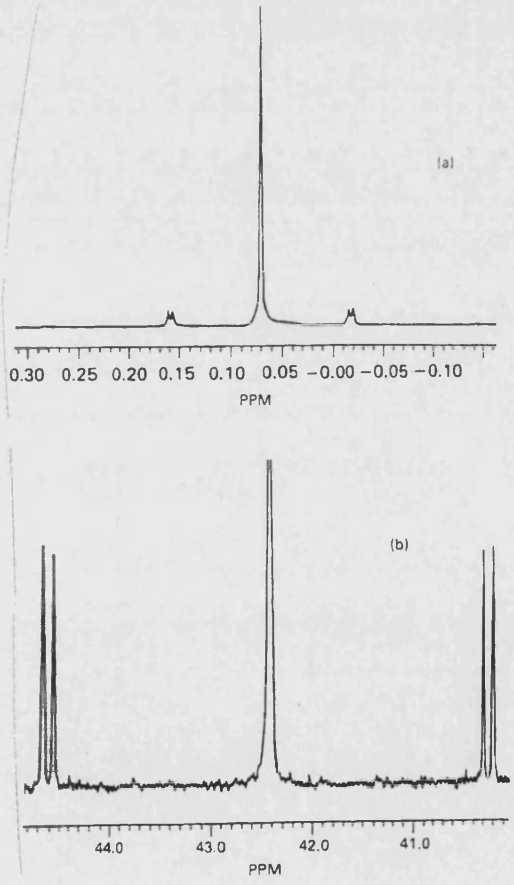

Figure 1.6.9: Satellites due to ^{117}Sn and ^{119}Sn in the spectra of $Sn(CH_3)_4$. (a) the ^{1}H spectrum; (b) the expanded ^{13}C spectrum. $^{2}J(^{117}Sn\text{-}^{1}H) = 52Hz$; $^{2}J(^{119}Sn\text{-}^{1}H) = 54Hz$; $^{1}J(^{117}Sn\text{-}^{13}C) = 317Hz$; $^{1}J(^{119}Sn\text{-}^{13}C) = 329Hz$

Tetramethyltin is the universally adopted standard for ^{119}Sn chemical shifts. Tin chemical shifts span a large range (>4000ppm) and the value is affected by a number of parameters (coordination number of the tin, electronegativity of the group attached to it, etc.). The number of tin(II) compounds which have been studied by ^{119}Sn NMR is relatively small, probably due to the relatively low solubilities of most stannous compounds. A selection of ^{119}Sn chemical shifts for Sn(II) compounds is given Table 1.6.3.

Table 1.6.3: selected ^{119}Sn NMR data for Sn(II) compounds.

Compound	δ (ppm)	Reference
$SnCl_2.NH(CH_3)_3$	-111.8	59
$SnCl_2.Py$	-294.0	59
$SnCl_2.DMF$	-324.1	60
$SnCl_2.DMSO$	-369.5	59
$SnBr_2.DMSO$	-319.5	60
$SnBr_2.DMF$	-202.1	60
$SnF_2.DMSO$	-629.0	60
$(Me_5C_5)_2Sn$	-2129	61
$(C_5H_5)_2Sn$	-2199	62

1.7 Copper, zinc and tin complexes of maltol and related ligands

Previous works at the University of Bath[63] and at Unilever Research centre have shown very interesting antibacterial activity for copper(II) and zinc(II) complexes of maltol (Hma), ethyl maltol (HEtma) and hinokitiol (Hhino). These ligands belong to a group of compounds called cyclic α-hydroxyketones. α-Hydroxyketone ligands have a ketone and a hydroxyl group adjacent to one another.

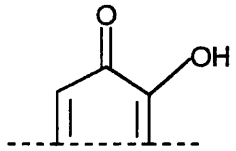

This type of ligand has recently shown biological and medicinal properties and their complexation with different metals have been studied.[64-66]

The Cu(II) and Zn(II) complexes were formed using copper or zinc acetate in a water and ethanol mix (Scheme 1.7.1).

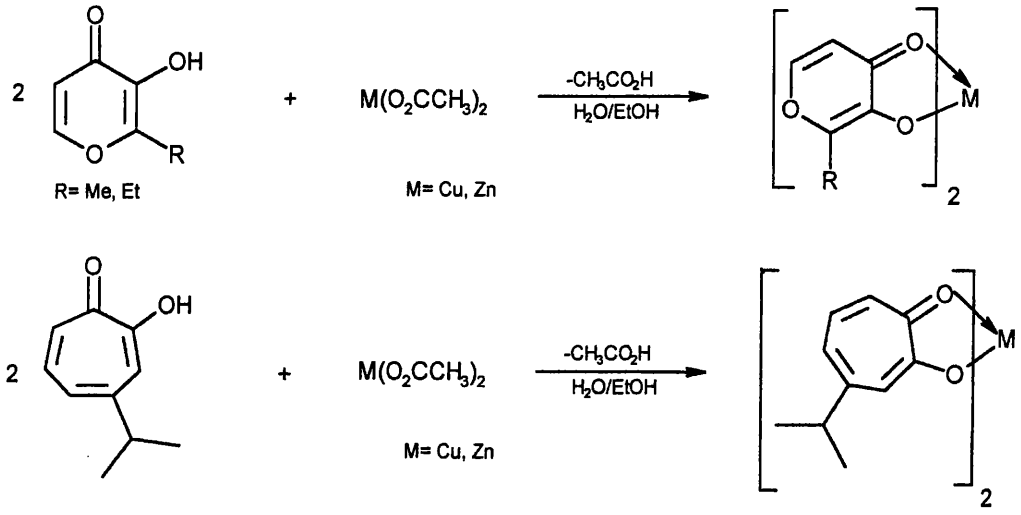

Scheme1.7.1: Synthesis of Cu(II) and Zn(II) complexes.

All the compounds were characterised by elemental analysis and infrared spectroscopy and the zinc species also by ^{1}H and ^{13}C NMR. The elemental analysis suggests that the zinc complexes are hydrated and this is supported by the infrared spectra (a broad peak present at ca. 3300cm^{-1}). The infrared results also are good

evidence for the formation of M(II) ma/Etma/hino complexes by the removal of the hydroxyl proton and chelation by the carbonyl oxygen. The ^{1}H NMR spectra for the zinc compounds agree with this theory, as there was no peak in the region where hydroxyl proton should appear. Further evidence can be seen in the crystal structure of Cu(hinokitiol)$_2$ (Figure 1.7.1).[63] The copper atom is four-coordinate and adopts a square planar geometry. The Cu-O bonds are equivalent, 1.900(2) Å for Cu-O(2) and 1.904(3) Å for Cu-O(1), and the [O(1)-Cu-O(2)] bond angle is 83.8(1)°.

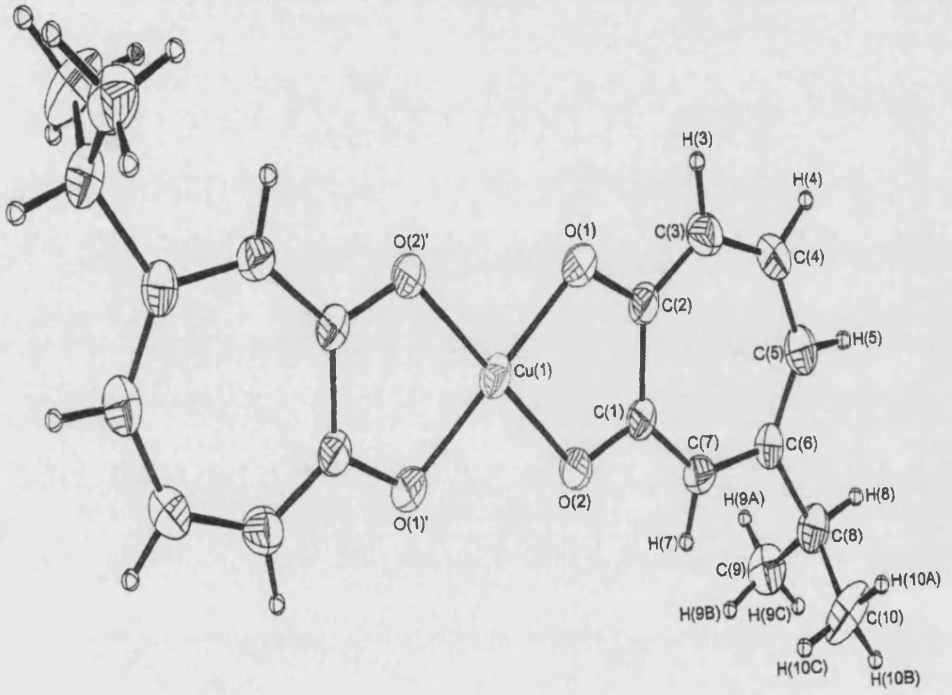

Figure 1.7.1: The structure of Cu(hinokitiol)$_2$.[63]

The Cu-O distances are in agreement with other Cu complexes, such as Cu(tropolone)$_2$.[24] The bis(tropolonato)Cu(II) complex was obtained from a mixture of tropolone (Htrop) and copper acetate and crystallised from dioxane and acetic acid. The Cu(II) atom is also square planar and as expected coordinated to the ligand *via* the oxygen atoms (Figure 1.7.2).

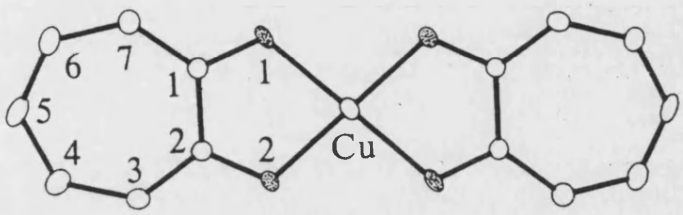

Figure 1.7.2: Bis(tropolonato)Cu(II). Oxygen atoms are shaded.[24]

Pyridinones belong to the cyclic α-hydroxyketones family and have also been extensively studied for medicinal purposes. They are six-membered ring species, like Hma and HEtma, in which the oxygen atom is being replace by an amine. Cu(1,2-dimethyl-3-hydroxypyridin-4-one)$_2$ [1,2-dimethyl-3-hydroxypyridin-4-one: Hdmp], and Cu(1,2-diethyl-3-hydroxypyridin-4-one)$_2$ [1,2-diethyl-3-hydroxypyridin-4-one: Hdep] are other examples where the copper is bonded to the oxygen atoms and adopts a square planar geometry (Figure 1.7.3).[25] The reaction of cupric chloride with the appropriate ligand gave the final product.

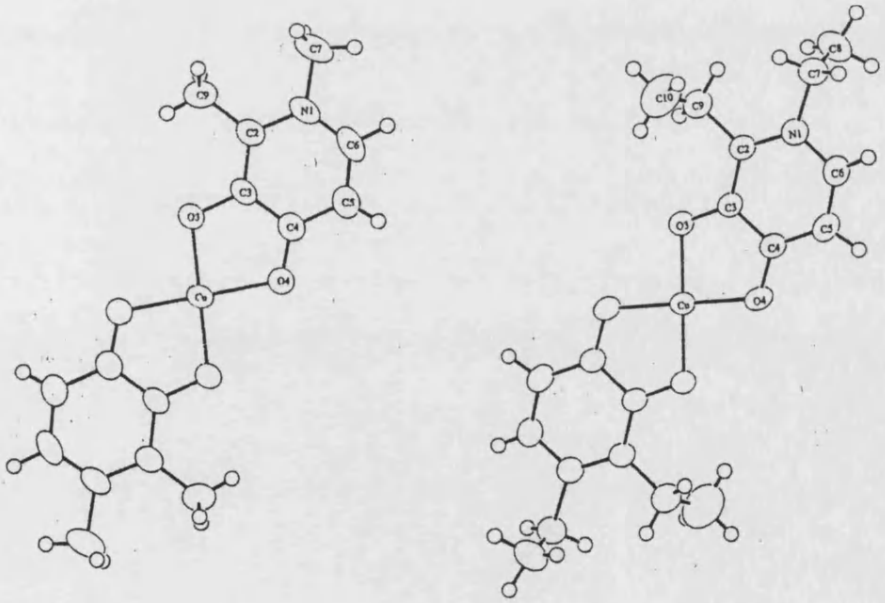

Figure 1.7.3: The crystal structures of Cu(dmp)$_2$ (left) and Cu(dep)$_2$ (right).[25]

Burgess *et al* synthesised and characterised $Zn(ma)_2$ and $Zn(dmp)_2$.[40] The bis(maltolato)Zn(II) complex was prepared from zinc sulfate heptahydrate in water and maltol in a 1:1 methanol: water mixture, whereas $Zn(dmp)_2$ was prepared by adding the ligand to Zn(II) chloride dissolved in methanol. The structure of $Zn(maltol)_2$ is shown inFigure 1.7.4. The structure is unusual for two reasons. First there are in the unit cell two molecules with different coordination numbers, five and six, for the zinc ion and second the five-coordinate zinc atom is in a distorted square pyramidal coordination environment (not a very common geometry for Zn, *c.f.* Section 1.5.2).

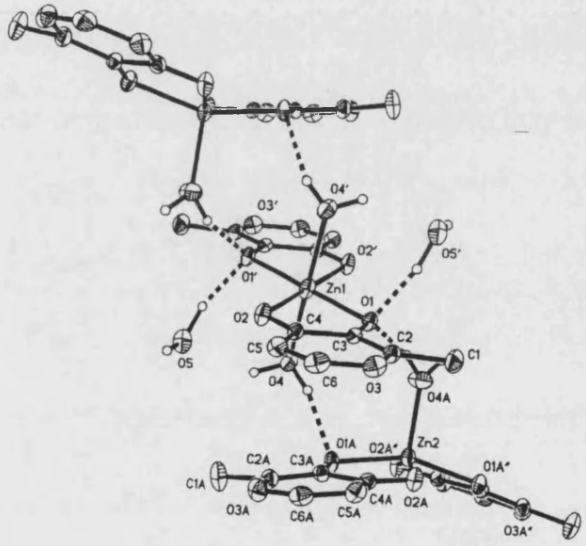

Figure 1.7.4: The crystal structure of $Zn(maltol)_2$.[40]

The overall structure can be described as layers of **ABA** sandwiches, with the layer **A** consisting of the five-coordinated zinc complex and the layer **B** of the six-coordinate complex. The zinc to oxygen (water) distance in the five-coordinated compound is 2.01 Å. In the octahedral complex, the two waters are *trans* to each other and the Zn-O bond length is 2.26 Å. The zinc to maltol-oxygen distances are in the range of 2.01–2.08 Å.

The structure of $Zn(dmp)_2$ is given Figure 1.7.5 and again the zinc has a coordination number of five and has a distorted square pyramidal geometry.

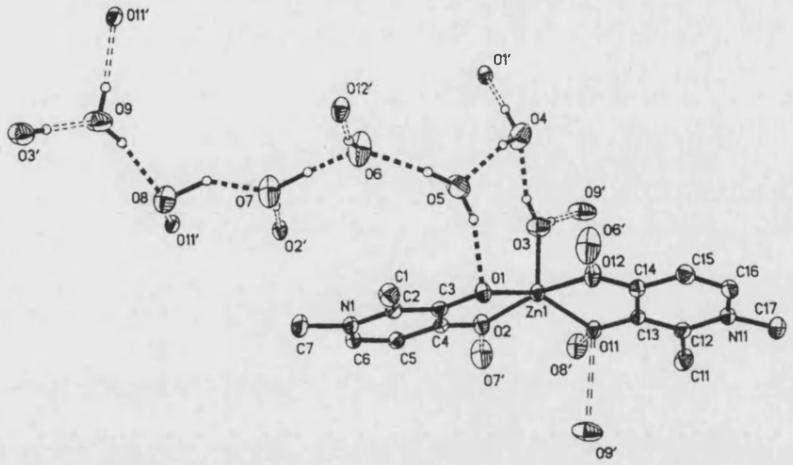

Figure 1.7.5: The molecular structure of $Zn(dmp)_2.7H_2O$. [40]

There are seven molecules of water in the unit cell and O7′, O8′ and O9′ can be seen to block the sixth coordination site at the zinc, but without interacting with the metal. The zinc to water-oxygen distance is 2.05 Å, longer than in the five-coordinated zinc(II)(maltol) complex. The zinc to hydroxypyridinonate-oxygen bond lengths are between 2.02 and 2.05 Å.

Tin(IV) complexes of cyclic α-hydroxyketones have been well-known for the past forty years, but nothing has yet been reported about any tin(II) compounds. Complexes of the type SnL_2X_2 (L= tropolone, X=Cl, Br, I) were first reported in 1964.[67] Later on similar complexes with kojic acid were reported by Tanaka *et al.*[68] More recently, six coordinate tin(IV) compounds of the type SnL_2X_2 have been prepared and characterised by elemental analysis, ^1H and ^{119}Sn NMR and mass and vibrational spectroscopy.[69] The reactions were carried out using tin tetrahalides (SnX_4 with X= Cl, Br and I) and different variety of ligands [L= Hma, kojic acid (Hkoj), Htrop, 2-methyl-3-hydroxypyridin-4-one (Hhmp), Hdmp, and Hdep].

Complexes of the type SnL_2X_2 can exist as geometrical isomers (Figure 1.7.6). All isomers are seen by NMR spectroscopy in cases where slow exchange was reached and where the chemical shift differences between the inequivalent sites are resolvable.

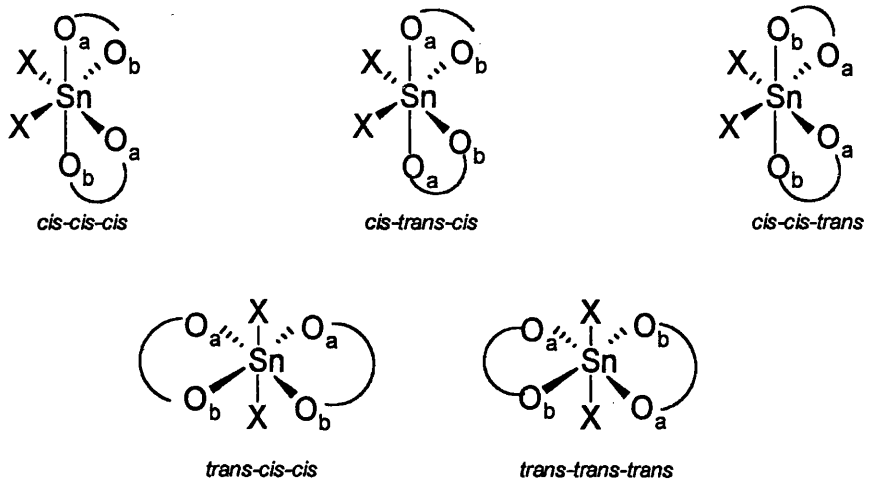

Figure 1.7.6: Geometrical isomers of SnL_2X_2.[69]

The chemical shifts for the ^{119}Sn NMR of the compounds are given Table 1.7.1.

Table 1.7.1: ^{119}Sn NMR chemical shifts for SnL_2X_2 complexes.

Complex	Chemical shift		
L	X= Cl	X= Br	X= I
Maltol	-469.7, -474.9	-647.5, -666.1	-1147.6, -1209.9
Kojic acid	-464.4, -469.9	-645.8, 666.4	-1139.6, -1194.9
Tropolone	-477.2	-672.6	_
Hhmp	-475.5, -477.6, -479.6	-643.8, -650.3, -657.1	_
Hdmp	-472.9, -474.7, -476.7	-644.1, -650.3, -656.9	_
Hdep	-473.3, -475.3, -477.4	-642.9, -649.1, -655.9	_

Woollins *et al* attributed the two set of resonances for L= Hma and Hkoj to the three possible *cis* isomers. The peaks intensity ratio was 2:1, which might be because the resonances of the two of these isomers are co-incident.

The X-ray structures of $Sn(ma)_2Cl_2.CHCl_3$ and $Sn(trop)_2Cl_2$ have been determined.[69] $Sn(ma)_2Cl_2.CHCl_3$ has the *cis-cis-trans* configuration, whereas $Sn(trop)_2Cl_2$ has the *cis-cis-cis* one (Figure 1.7.7). In both cases the coordination environment of the tin is approximately octahedral.

(a)

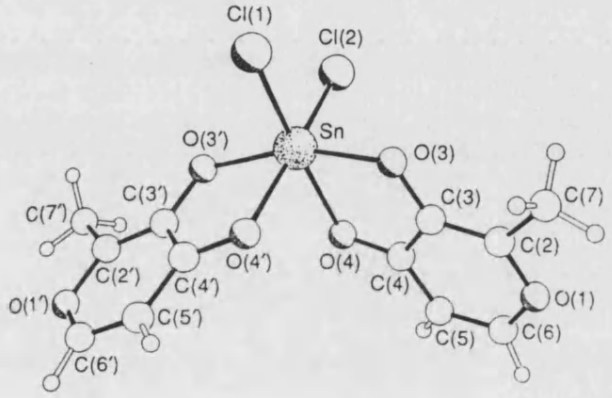

(b)

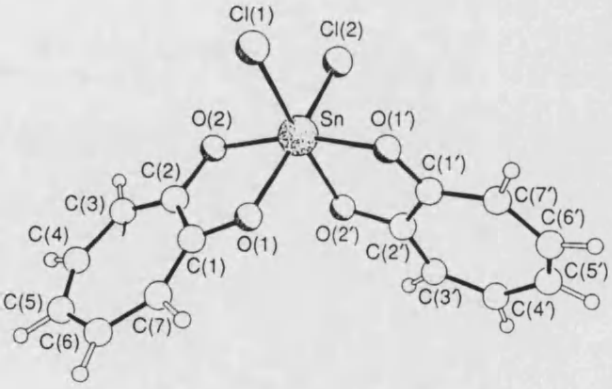

Figure 1.7.7: The structures of $Sn(maltol)_2Cl_2$ (a) and $Sn(tropolone)_2Cl_2$ (b).[69]

Recently Burgess *et al* have established the structures of $Sn(Etma)_2Cl_2$[70] and $Sn(Etma)_2I_2$.[71] In both structures the halides are *cis* to each other, but the SnL_2I_2 shows the *cis-cis-cis* isomer, while SnL_2Cl_2 shows the *cis-cis-trans* arrangement like $Sn(ma)_2Cl_2$.The Sn-O distances are similar for the three compounds and are given Table 1.7.2.

Sn(1-methyl-2-ethyl-3-hydroxypyridin-4-one)$Cl_3(H_2O)$, (1-methyl-2-ethyl-3-hydroxypyridin-4-one: Hmep) has also been characterised by Burgess *et al*[70] in an attempt to synthesise the SnL_2Cl_2 version of the compound. The tin atom is six-coordinated with a tin-water bond and is in a distorted octahedral environment. The tin to water-oxygen bond distance [2.132(3) Å] is comparable to analogous distances in other tin(IV) complexes containing coordinated water.[72,73]

SnL_3X complexes have also been reported.[74] These compounds were synthesised by Woollins *et al* using tin tetrahalides (SnX_4, X= Cl, Br and I) and three equivalent of the ligands (Hhmp and Hdmp) in the presence of a base. For the tropolone complex, there are two steps to its formation. First $Sn(trop)_2Cl_2$ is synthesised and then a further equivalent of tropolone is added and gives the desired compound. The complexes with Hkoj or Hma could not be prepared.

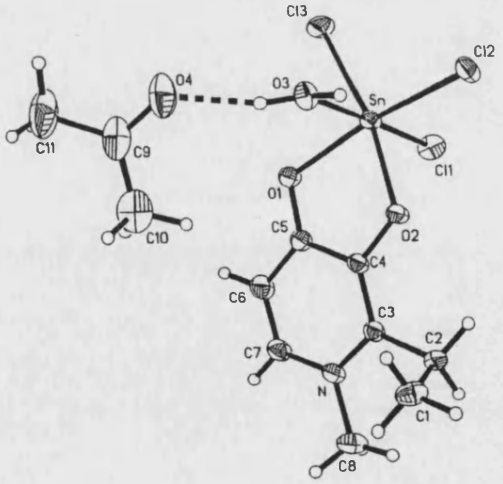

Figure 1.7.8: The structure of Sn(1-methyl-2-ethyl-3-hydroxypyridin-4-one)$Cl_3(H_2O)$[70]

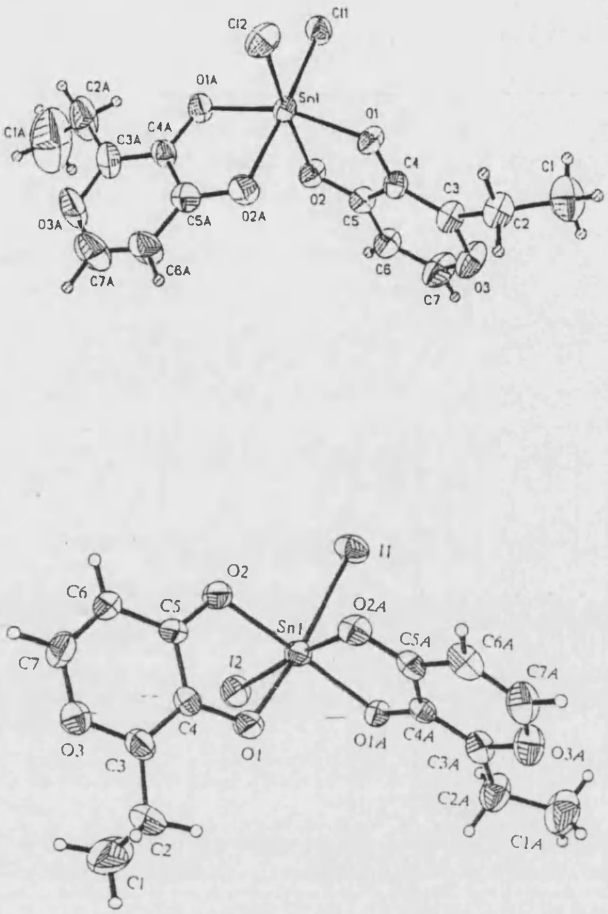

Figure 1.7.9: The structures of $Sn(Etma)_2Cl_2$[70] and $Sn(Etma)_2I_2$[71]

Tris(ma)monohydroxytin(IV) is another example of a tris complex,[63] and was formed in an attempt to synthesise Sn(II) maltolate. The coordination sphere around the tin atom is composed of seven oxygens (six from the maltol and one from the hydroxyl group) in an approximate pentagonal bipyramidal geometry (Figure 1.7.10). The Sn-O bonds, on average 2.14 Å, are similar to those observed in related compounds. For the tris(tropolonato)monohydroxytin(IV) the average Sn-O bond length is 2.12 Å.[75]

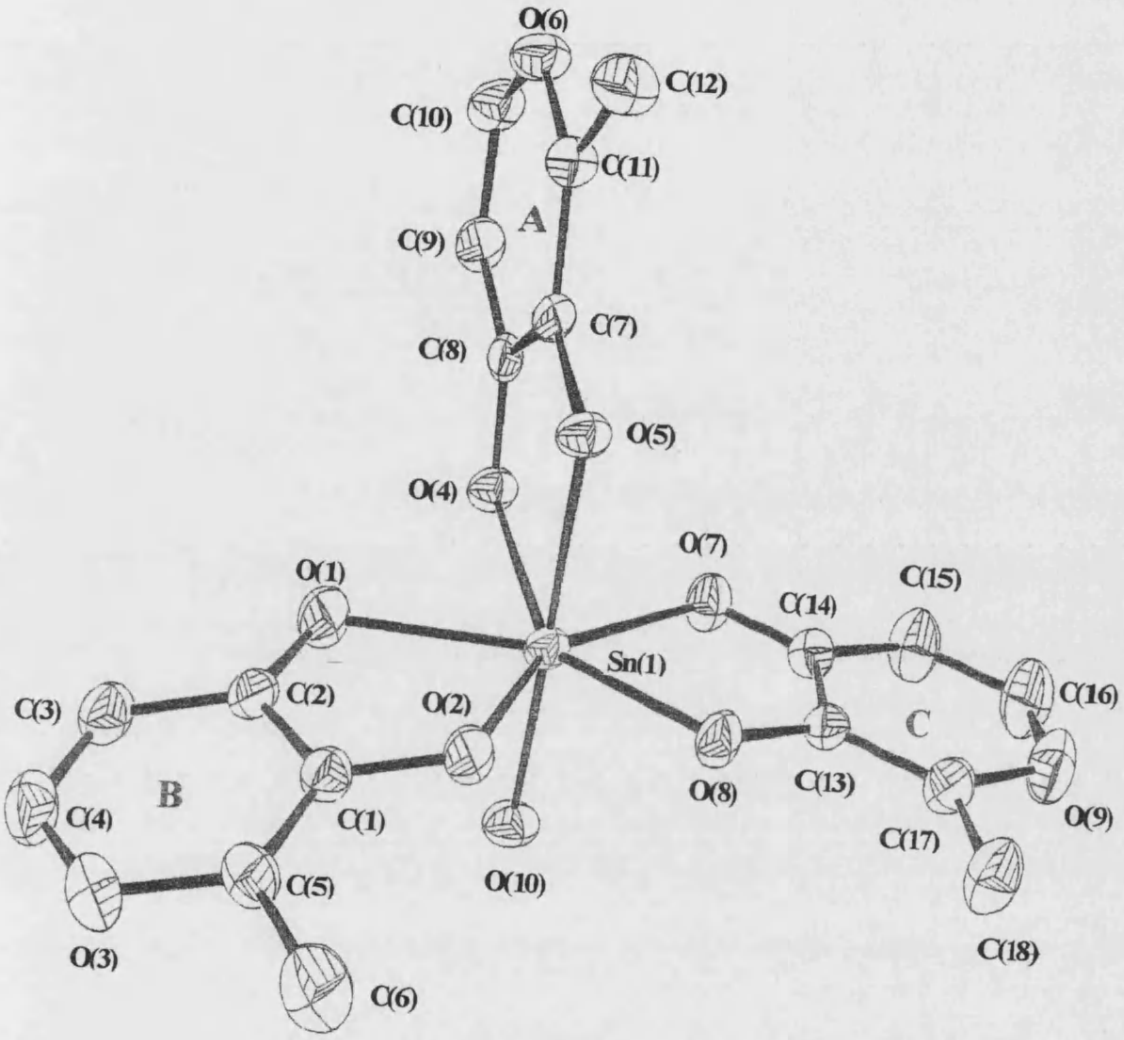

Figure1.7.10: The structure of tris(maltolato)monohydroxytin(IV).[63]

Table 1.7.2 gives the metal to α-hydroxyketone-oxygen bond distances in various complexes, while the Table 1.7.3 gives a range of [C–O] bond lengths.

Table 1.7.2: Coordination number of the metal and [M–O] bond lengths.

Compound	Metal CN	M-O distance Å	Reference
$Cu(hino)_2$	4	1.900(2); 1.904(3)	63
$Cu(trop)_2$	4	1.915(3)	24
$Cu(dmp)_2$	4	1.913; 1.908	25
$Cu(dep)_2$	4	1.913; 1.923	25
$Zn(ma)_2$	5 and 6	2.033(2); 2.075(2); 2.010(2); 2.076(2)	40
$Zn(dmp)_2$	5	2.021(2); 2.050(2); 2.034(2); 2.047(2)	40
$Sn(ma)_2Cl_2.CHCl_3$	6	2.041(7); 2.050(7); 2.135(7); 2.149(9)	69
$Sn(trop)_2Cl_2$	6	2.101(17); 2.059(15); 2.071(16); 2.065(15)	69
$Sn(Etma)_2Cl_2$	6	2.052(6); 2.043(6); 2.136(5); 2.115(7)	70
$Sn(Etma)_2I_2$	6	2.054(5); 2.067(4); 2.130(5); 2.127(5)	71
$Sn(ma)_3O$	7	2.280(3); 2.096(3); 2.219(3); 2.053(3); 2.268(3); 2.089(3)	70
$Sn(mep)Cl_3(H_2O)$	6	2.050(2); 2.089(2)	63

Table 1.7.3: [C–O] distances.

Compound	[C-O] bond / Å	[C=O] bond / Å	Reference
$Cu(hino)_2$	1.296(5)	1.293(5)	63
$Cu(trop)_2$	1.302(5)	1.286(5)	24
$Cu(dmp)_2$	1.344	1.300	25
$Cu(dep)_2$	1.383	1.309	25
$Zn(dmp)_2$	1.334; 1.335	1.292; 1.293	40
$Sn(ma)_2Cl_2.CHCl_3$	1.344(12); 1.355(12)	1.277(10); 1.284(13)	69
$Sn(trop)_2Cl_2$	1.348(25); 1.350(28)	1.303(29); 1.309(27)	69
$Sn(Etma)_2Cl_2$	1.315(9); 1.342(11)	1.285(10); 1.306(13)	70
$Sn(Etma)_2I_2$	1.351(8); 1.321(8)	1.274(8); 1.281(9)	71
$Sn(memp)Cl_3(H_2O)$	1.315(9);1.342(11)	1.285(10);1.306(13)	70
$Sn(ma)_3O^-$	1.321(5); 1.332(5); 1.318(5)	1.266(5); 1.268(5); 1.273(5)	63

1.8 Aim of the project

As described previously,[63,76] works on α-hydroxyketone metal-based complexes have shown very interesting anti-bacterial results. The studies have convincingly demonstrated the therapeutic potential of these systems.

Table 1.8.1: Antiplaque activity of some metal complexes.

Antiplaque activity

	Maltol	Ethyl maltol	Hinokitiol
zinc(II)	×	×	✓
copper(II)	✓	✓✓	✓✓

×= Activity no greater than standard toothpaste

✓= Activity greater than standard toothpaste

✓✓= Activity much greater than standard toothpaste

The efficacy of the compounds is evaluated against different bacteria and the results compare with the antiplaque activity of a standard paste. CuL_2 (L= hino, Etma, ma) and zinc(hino)$_2$ complexes are the first examples where a ligand enhances the antiplaque activity of these metal ions in toothpaste. Previous compounds (such as zinc citrate, copper sulphate) showed the same antiplaque activity as the ion Cu^{2+} or Zn^{2+} itself. Moreover, the ligand/metal ion complexes were shown to be compatible with standard toothpaste. So a new perspective of research was found.

The aim of this project is to prepare and characterise new metal-hydroxyketones complexes for testing in toothpaste. The metals used are Cu(II), Zn(II) and Sn(II), as only Sn(II) is believed to be active. The ligands must be orally safe and the complexes they form with the metals must be soluble in either water, alcohol or acetone. There is a range of chemicals which have cyclic α-hydroxyketone motif and which can be purchased directly from chemical companies. Examples are maltol, ethyl maltol, tropolone, kojic acid, purpurogallin, etc.

Concerning the tin complexes, the tin atom needs to be stable to oxidation and the complexes need also to be soluble. This could be a problem, as most of the tin(II)

species are air sensitive and if they are not, they are often sparingly soluble in any common organic solvents.

No explanation has yet been given concerning the mode of action of the cyclic α-hydroxyketones/metal complexes. This is a relatively new area and research is currently being carried out at Unilever Research. This is another part of the project, as two weeks a year have been spent at Unilever in order to understand better the testing procedures.

1.9 References

1) Riley P. I., "An introduction to toothpaste formulation technology," Unilever, **1991**.

2) *Dental Science and Dental Art*; S. M. Gordon ed. Philadelphia, **1938**.

3) Mandel I. D.; Gaffar A., *J. Clin. Periondotol.* **1986**, *13*, 249.

4) *Unilever Dental Research* **1994**.

5) Wagg, B. J., *Community Dent. Health* **1984**, *1*, 11.

6) Harrap G. J.; Saxton C. A.; Best J. S., *J. Periodont. Res.* **1983**, *18*, 634.

7) Peterson G. H.; Bratthall D., *Eur. J. Oral Sci.* **1996**, *104*, 436.

8) Chan J. T.; Koh S. H., *Caries Res.* **1996**, *30*, 88.

9) Kiritsy M. C.; Levy S. M.; Warren J. J.; Guha-Chowdhury N.; Heilman J. R.; Marshall T., *J. Am. Dent. Assoc.* **1996**, *127*, 895.

10) McDonald S. P.; Cowell, C. R.; Sheiman A., *Brit. Dent. J.* **1981**, *151*, 118.

11) McKoy M., *Chemical & Engineering News* **2001**, 42.

12) Meningaud J. P.; Bado F.; Favre E.; Bertrand J. C.; Guilbert F., *Revue de Stomatologie et de Chirurgie Maxillo-faciale* **1999**, *100*, 240.

13) Langer H. G., *US Patent* **1990**, 3 227 707.

14) Cuhonen C. H., *US Patent* **1990**.

15) Waterfield P. C., *Eur. Patent* **1992**, 0 514 966.

16) Binney A.; Addy M.; McKeown S.; Everatt L., *J. Clin. Periondont.* **1995**, *22*, 830.

17) Lane R. M., *Eur. Patent* **1985**, 0 161 899.

18) Nabi N.; Mukerjee C.; Schmid R.; Gaffar A., *Am. J. Dent.* **1989**, *2*, 197.

19) Nabi N., *US Patent* **1990**, 4 894 220.

20) Francis D. M., *Inernational Patent* **1993**.

21) Bailard J. C.,*Comprehensive Inor. Chem.*; Pergamon Press Ltd:, **1975**; Vol. 3.

22) Jones C. J., *d- and f- Block Chemistry*; The royal Society of Chemistry: Cambridge, **2001**.

23) Robertson I.; Truter,M. R., *J. Chem. Soc (A)* **1967**, 309.

24) Berg J.; Pilotti A.; Soderholm A.; Karlsson B., *Acta Cryst.* **1978**, *B34*, 3071.

25) El-Jammal A.; Howell P. L.; Turner M. A.; Li N.; Templeton D. M., *J. Med. Chem.* **1994**, *37*, 461.

26) Lee D. J., *Concise Inor. Chem.*; Chapman & Hall: London, 1996.

27) Carmichael J. W.; Steinrauf L. K.; Belford R. L., *J. Chem. Phys.* **1965**, *43*, 3959.

28) Hon P. K.; Pfluger C. E.; Belford R. L., *Inorg. Chem.* **1966**, *5*, 516.

29) Castellani C. B.; Rizzi M., *Polyhedron* **1990**, *9*, 2061.

30) Haouri M.; Hommel H.; Ouada H. B.; Legrand A. P.; Maaref H.; Gharbi A.; Jouini A., *J. Phys. : Condens. Matter* **1995**, *7*, 3023.

31) Labisbal E.; Garcia-Vasquez J. A.; Romero J.; Picos S.; Sousa A., *Polyhedron* **1995**, *14*, 663.

32) Carugo O.; Castellani C. B.; Rizzi M., *Polyhedron* **1990**, *9*, 2061.

33) Murakami T.; Kita S., *Inorg. Chim. Acta* **1998**, 247.

34) Dittler-Klingemann A. M.; Hahn F. E., *Inorg. Chem.* **1996**, *35*, 1996.

35) Murakami T.; Takei T.; Ishikawa Y., *Polyhedron* **1996**, *15*, 4391.

36) Winter M. J., *d-Block Chemistry*; Oxford University Press: Oxford, **1994**.

37) Battaglia L. P.; Corradi A. B.; Marcotrigliano G.; Menabue L.; Pellacani G. C., *Inorg. Chem* **1981**, *20*, 1075.

38) Grand A.; Rey P.; Subra R., *Inorg. Chem* **1983**, *22*.

39) Kremer-Aach A.; Klaui W.; Bell R.; Strerath A.; Wunderlich H.; Mootz D., *Inorg. Chem.* **1997**, *36*, 1552.

40) Ahmed S. I.; Burgess J.; Fawcett J.; Parsons S. A.; Russell D. R.; Laurie S. H., *Polyhedron* **2000**, *19*, 129.

41) Tanase T.; Yun J. W.; Lippard S. J., *Inorg. Chem.* **1995**, *34*, 4220.

42) Bhattacharyya S.; Kumar S. B.; Dutta S. K.; Tiekink E. R. T.; Chaudhury M., *Inorg. Chem.* **1996**, *35*, 1967.

43) Adams H.; Bailey N. A.; Fenton D. E.; He Q. Y., *J. Chem. Soc., Dalton Trans.* **1996**, 2857.

44) Huang W.; Gou S.; Hu D.; Xu Y.; Chantrapromma S.; Meng Q., *J. Mol. Chem. Struc.* **2001**, *561*, 121.

45) Braibanti A.; Pellinghelli M. A.; Tiripicchio A.; Camellini M. T., *Acta Cryst* **1971**, *B27*, 1240.

46) Singh K. D.; Jain S. C.; Sakore T. D.; Biswas A. B., *Acta Cryst* **1975**, *B31*, 990.

47) Adams R. P.; Allen H. C., *Inorg. Chim. Acta* **1986**, *119*, 67.

48) Harrison P. G., *Chemistry of tin*; P. J. Smith ed.; Blackie Academic & Professional: London, **1998**.

49) Fjeldberg T.; Hitchcock P. B.; Lappert M. F.; Smith S. J.; Thorne,A. J., *J. Chem. Soc. Chem. Comm.* **1985**, 939.

50) Goldberg D. E.; Harris D. H.; Lappert M. F.; Thomas K. M., *J. Chem. Soc., Chem. Commun.* **1976**.

51) Donalson J. D.; Grimes S. M.; Nicolaides A.; Smith P. J., *Polyhedron* **1985**, *4*, 391.

52) Cea-Olivares R.; Novosad, J.; Woollins J. D.; Slawin A. M. Z.; Garcia-Montalvo V.; Espinosa-Perez G.; Garcia-y-Garcia P. G., *J. Chem.Soc., Chem. Commun.* **1996**, 519.

53) Anderson J. E.; Sawtelle S. M.; Thompson J. S.; Nguyen S. A. K.; Calabrese J., *Inorg. Chem.* **1992**, *31*, 2778.

54) Rundle R. E.; Olson D. H., *Inorg. Chem.* **1964**, *3*, 596.

55) Anderson J., *Acta Chem. Scand.* **1975**, *A29*, 956.

56) Tremel W.; Hoffman R., *Inorg. Chem.* **1987**, *26*, 118.

57) Deacon P. R., *Preparation, characterisation and anti-bacterial activity of orally viable tin(II) salts.*; University of Bath, **1994**.

58) Parish R. V., *NMR, NQR, EPR, and Mossbauer spectroscopy in Inorganic Chemistry*; Ellis Horwood Limited: Chichester, **1990**.

59) Chun-Hsu C.; Geanangel R. A., *Inorg. Chem.* **1980**, *19*, 110.

60) Mimi-Yeh H.; Geanangel R. A., *Inorg. Chim. Acta* **1981**, *52*, 113.

61) Jutzi P.; Hielscher B., *Organometallics* **1986**, *5*, 1201.

62) Harris R. F.; Mann B. E., *NMR and The Periodic Table*, **1978**.

63) Wright P., *The synthesis and characterisation of novel Sn(II), Zn(II) and Cu(II) compounds for anti-bacterial evaluation*; University of Bath, **1999**.

64) Ahmet M. T.; Frampton C. S.; Silver J., *J. Chem. Dalton Trans.* **1988**, 1159.

65) Caravan P.; Gelmini L.; Glover N.; Herring F. G.; Li H.; McNeill J. H.; Rettig S. J.; Setyawati I. A.; Shuter E.; Sun Y.; Tracey A. S.; Yuen V. G.; Orvig C., *J. Am. Chem. Soc.* **1995**, *117*, 12759.

66) Abrahams I.; Choi N.; Henrick K.; Joyce H.; Matthews R. W.; McPartlin M., *Polyhedron* **1994**, *13*, 513.

67) Muetterties E. L.; Wright C. M., *J. Am. Chem. Soc.* **1964**, *86*, 5132.

68) Otera J.; Kawasaki Y.; Tanaka T., *Inorg. Chim. Acta* **1967**, *1*, 294.

69) Denekemp C. I. F.; Evans D. F.; Slawin A. M. Z.; Williams D. J.; Wong C. Y.; Woollins J. D., *J. Chem. Soc, Dalton Trans.* **1992**, 2375.

70) Alshehri S.; Burgess J.; Fawcett J.; Parsons S. A.; Russell,D. R., *Polyhedron* **2000**, *19*, 399.

71) Lu Z.; Burgess J.; Fawcett J.; Russell D. R., *Acta Cryst.* **1999**, *C55*, 2051.

72) Isaacs N. W.; Kennard C. H. L., *J. Chem. Soc, A* **1970**.

73) Barnes J. C.; Sampson, H. A.; Weakley T. J. R., *J. Chem. Soc, Dalton Trans.* **1980**, 949.

74) Denekemp, C. I. F.; Evans, D. F.; Woollins, J. D., *J. Chem. Soc., Dalton Trans.* **1993**, 1489.

75) Park J. J.; Collins D. M.; Hoard J. L., *J. Am Chem. Soc.* **1970**, *92*, 3636.

76) *Unilever Internal Report*, **1998**.

Chapter II

2.1 Introduction to cyclic α-hydroxyketone ligands

As mentioned in the Introduction, compounds that have a ketone and a hydroxyl group adjacent to one another have recently shown biological and medicinal activity.

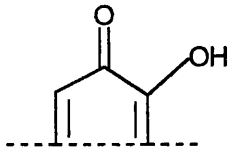

Maltol (3-hydroxy-2-methyl-4-pyrone) and ethyl maltol (3-hydroxy-2-ethyl-4-pyrone) are examples of cyclic α-hydroxyketones (Figure 2.1). They are both non-toxic food additives used in the baking industry.[1]

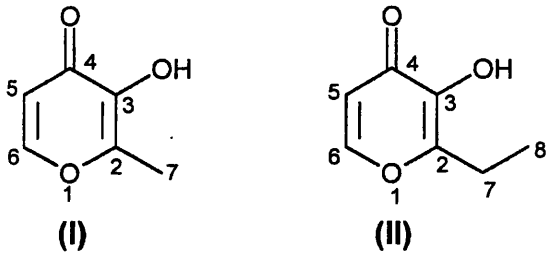

Figure 2.1: Maltol (I) and ethyl maltol (II), including atom numbering.

Maltol (Hma) and ethyl maltol (HEtma) differ in the group attached to C_2. It was of interest to see if this small change, from a methyl group to an ethyl group, affected the activity of the metal complexes in toothpaste.

Hma and HEtma are known to form chelates with various metals *via* the two oxygen atoms and in the 1980's studies were directed towards the use of their metal complexes for medicinal applications, both therapeutic and diagnostic. $Fe(ma)_3$ is used for the treatment of iron deficiency anaemia.[2] Hma has been shown to possess the ideal properties: forming a soluble iron(III) (stable to oxidation and reduction), neutral and non-toxic complex.

Hma is also an appropriate ligand for the study of aluminium delivery into the brain in Alzheimer's disease.[3] It forms a neutral six-coordinate complex which is stable at physiological pH and therefore can penetrate the cell membrane. The unique combinations of biologically significant properties has led to the wide use of $Al(ma)_3$ in the study of aluminium neurotoxicity.

Orvig *et al* have conducted more studies of the complexes formed by aluminium and gallium with maltol and prepared the compounds from aqueous solution.[4] It was found out that the complexes are water soluble at neutral pH and that they remained neutral, which help them to bring the metals into and out of mammalian cells. As part of a continuing study of neutral, water-soluble complexes of neurological interest, Orvig *et al* have synthesised $Ph_2B(ma)$,[5] and bis(maltolato)oxovanadium,[6] which is a potent insulin mimetic agent for the treatment of diabetes. They also studied the complex of maltol with technetium that has potential application in brain and heart imaging.[7]

$In(ma)_3$ and $In(Etma)_3$ have been synthesised and are used for the radio-labelling of leucocytes with ^{111}In.[8] Both ligands bind In to form neutral complexes which can penetrate cell membranes. Maltol and ethyl maltol have also found utilisation as contrast agents in Magnetic Resonance Imaging (MRI) where they form a complex with gadolinium.[9]

3-hydroxy-6-hydroxymethyl-4-pyrone, more commonly known as kojic acid (Hkoj), also fits into the category of cyclic α-hydroxyketone (Figure 2.2). It is used in cosmetics as a whitening agent because of its ability to inhibit tyrosinase, which is responsible for melanization in animals and browning in plants.[10]

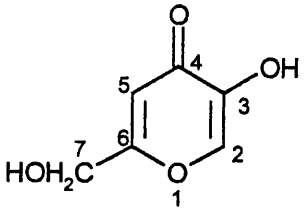

Figure 2.2: Kojic acid, including atom numbering.

This ligand is interesting in that it may help to stabilise more easily its tin(II) complex with the help of its extra hydroxyl group, in much the way that sorbitol has been used to stabilise other the Sn(II) species.[11] A study of the complexes formed by Al and Ga with kojic acid has been conducted.[4] Like maltol, kojic acid forms water-soluble complexes with the metals and has been shown to be a possible chelator for aluminium overload. The kojic acid complex of In has been prepared[12] and has similar properties to those of Al and Ga (water soluble, lipophilic, etc).

The first ligand incorporating the cyclic α-hydroxyketone function used at Unilever was 2-hydroxy-4-propylcyclohepta-2,4,6-trien-1-one, more commonly called hinokitiol (Hhino) (Figure 2.3). Hinokitiol was first isolated from the essential oil of the Formosan Hinoki tree by Nozoe in 1936.[13] It shows antimicrobial properties at relatively low dosages and has a wide antimicrobial spectrum against general bacteria. No resistant bacteria has yet been found. It is known that hinokitiol decomposes in light, particularly UV, but its salts or complexes are relatively stable.[14]

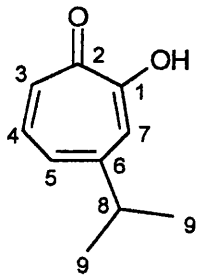

Figure 2.3: Hinokitiol, including atom numbering.

Despite the increasing amount of data to support its biological effects, the application of hinokitiol in medicine has been limited to Japan. It has been used mainly as a component in oral-care and hair-care products. Hinokitiol has therapeutic effects in preventing and controlling redness, swelling, bleeding and puss formation in gingiva and it also helps remove bad breath.[15-17] Hinokitiol has an effect on hair and patent applications have been filed relating to its use in hair-care products.[18-20]

There are many other applications for hinokitiol such as food preservative,[21] insecticide,[22] anti-fungal[23] or even fertiliser.[24] $In(hino)_3$ has also been shown to be capable of labelling blood cells.[25]

Tropolone (Htrop), formally 2-hydroxycyclohepta-2,4,6-trien-1-one, contains the α-hydroxyketone function (Figure 2.4). It is a very well known compound and has been studied extensively during the last thirty to forty years. The organic chemistry relating to tropolone compounds has given rise to a new branch of chemistry known as troponoid chemistry.

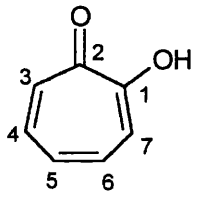

Figure 2.4: Tropolone, including atom numbering.

Tropolone is a non-benzenoid aromatic compound. It is a seven-membered ring as is hinokitiol, with one hydrogen attached to C_6. As for maltol and ethyl maltol, which have a methyl and ethyl group respectively at C_2, tropolone and hinokitiol differ in the group attached to C_6. It was of interest to compare the activity in toothpaste of the tropolone/metal complexes with the hinokitiol/metal complexes and see how the absence of the i-propyl group affects the antibacterial properties of metal complexes.

In nature, many compounds have been isolated containing the tropolone nucleus, thus the great interest in research laboratories for tropolone. Tropolone is able to form a wide range of coordination compounds with metals.[26-29] Chelate complex of ^{111}In with tropolone has been shown to be capable of labelling blood cells.[25] A bis-tropolonato derivative of Co(III), $[Co(trop)_2L]^+$ with L= N, N'-diethylethylenediamine, has been synthesised and suggested to be of potential use in the treatment of cancer.[30]

2.2 Results and Discussion: Tin compounds

2.2.1 Synthesis of the tin(IV) complexes SnL_2X_2

In previous studies, Unilever Research mixed directly in the paste the α-hydroxyketone (HL) and SnF_2 and claimed they obtained very efficient complexes, which were assumed to be SnL_2. In order to isolate and fully characterise the tin(II) species, some reactions of SnX_2 (X= Cl, F) with maltol, ethyl maltol and hinokitiol were attempted (Scheme 2.1).

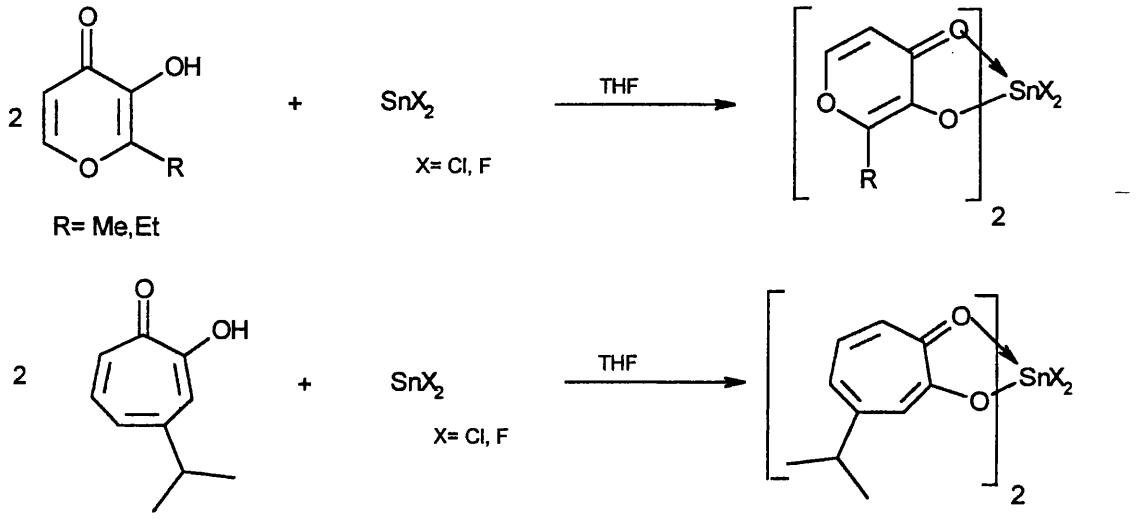

	maltol	ethyl maltol	hinokitiol
Cl	**(1)**	**(2)**	**(3)**
F	**(4)**	**(5)**	**(6)**

Scheme 2.1: Synthesis of SnL_2Cl_2 and SnL_2F_2.

It was, however, found that the products obtained are not the ones expected but are in fact SnL_2X_2. The Mössbauer data (Table 2.1) and elemental analysis clearly indicate that the compounds obtained were not tin(II), but tin (IV). An oxidative addition takes place by a mechanism that is unknown at the moment. The formation of $Sn(acac)_2F_2$ from SnF_2 and Hacac has been reported[31] and oxygen was claimed to be the oxidant.

All the six compounds were identified and crystals suitable for X-ray crystallography were obtained for the bis-(Etma)difluorotin **(5)**, the bis-(hino) dichlorotin **(3)** and the bis-(hino)difluorotin **(6)**.

Table 2.1: Mössbauer data for the SnL_2X_2 complexes.

Compound	I.S (mms^{-1})	Q.S (mms^{-1})
(1)	0.25	0.42
(2)	0.31	0.49
(3)	0.26	0.48
(4)	0.00	0.52
(5)	-0.01	0.56
(6)	-0.07	0.32

The compounds **(1)** and **(2)** are known and have already been prepared and characterised by Evans *et al*[32] and Burgess *et al*[33] respectively. In both cases the methods involved the use of $SnCl_4$ as starting material.

Each ^{119}Sn Mössbauer spectrum consists of a doublet with an Isomer Shift (I.S) varying between -0.07 and -0.31 mms^{-1}, which clearly indicates that the tin is in the +4 oxidation state and has a high coordination number. The Quadrupole Splitting (Q.S) values are close to zero (0.32–0.56), which indicate that the tin atom is in a symmetrical environment (absence of a lone pair). This is due to the small difference in electronegativity between the oxygen and halogen atoms.

^{119}Sn NMR provided information regarding the environment around the tin atom and, as explained in the Introduction, complexes of the type SnL_2X_2 can exist as five geometrical isomers.[32] The three fluorinated complexes showed strong coupling to the fluorine atoms, J = 2232–2293 Hz.

One triplet signal is seen, which means the compounds only exist as a single form which crystallography has shown to be the *cis-cis-trans* isomer.

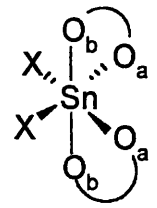

cis-cis-trans isomer

The three chlorinated compounds showed two singlets, which, according to Evans *et al*,[32] can be attributed to the three possible *cis* isomers.

Table 2.2: ^{119}Sn NMR data.

Compound	Chemical shift (ppm) & multiplicity	$^{1}J(^{119}Sn\text{-}^{19}F)$ (Hz)
(1)	-470; -475 [a]	–
(2)	-465; -471 [b]	–
(3)	-478 [c]	–
(4)	-594, t	2293
(5)	-595, t	2286
(6)	-603, t	2232

[a] literature values: -470; -475 ppm,[32] [b] literature values: -468; -473 ppm,[33] [c] (trop)$SnCl_2$: -478 ppm.[32]

All the chemical shifts are typical of tin(IV) species and the values are comparable with those obtained previously by Evans *et al*[32] and Burgess *et al*[33] (Table2.2). $Sn(hino)_2Cl_2$ exhibits one signal in the ^{119}Sn NMR spectrum (-478ppm) at an identical position to that of $Sn(tropolone)_2Cl_2$.[32]

^{1}H NMR spectra were recorded for the six compounds in deuterated solvents, either DMSO or chloroform. The peaks were relatively easy to assign to the protons of the complexes.

For **(1)** and **(4)** the three methyl protons (H_7) give a singlet at 2.57 and 2.45 ppm respectively. There are also two doublets at 7.22, 8.70 ppm and 7.80, 8.55 ppm respectively that are assigned to the protons in the C_5 and C_6 positions.

For **(2)** and **(5)** the ^{1}H NMR spectra consist of a triplet at 1.25 and 1.23 ppm, respectively, corresponding to CH_3 and a quartet at 2.98 and 2.95 ppm respectively corresponding to CH_2. There are also two doublets at 6.76, 8.80 ppm and 6.82, 8.12 ppm respectively that are assigned to the protons in the C_5 and C_6 positions.

For **(3)** and **(6)** the six methyl protons give a doublet at 1.23 ppm for both compounds and the proton (H_8) is found at 2.96 and 2.97 ppm as a septet. There are singlets at 7.35 and 7.41, respectively, which are assigned to the proton in the C_7 position. It has not been possible to assign with certainty the peaks corresponding to H_3, H_4 and H_5, as they are all based in a region between 7.76-7.77 ppm. For the six compounds, there was no peak in the spectrum due to the hydroxyl group, which supports the fact that the deprotonated hydroxyl group is involved in bonding to the metal ion.

The ^{13}C NMR spectra were recorded for the six compounds in deuterated solvents, either DMSO or chloroform. The spectra showed the right number of carbons and all the peaks were assigned (See Experimental).

The infrared spectra are relatively similar, as one would expect. There is no band relative to the ν(O–H) mode, which is a good evidence for the formation of the metal complexes by the removal of the hydroxyl proton. The ν(C=O) band at 1650 cm^{-1} in the starting materials is shifted to lower wavenumbers by around 30-70 cm^{-1} in the complexes, which indicates the chelation by the oxygen C=O→M. The bands at 1610 and 1550 cm^{-1} due to ν(C=O) and ν(C=C) are also shifted to a lower

wavenumbers. These finding are consistent with the ones in the literature, the C=O and C=C stretching frequencies all decrease by *ca.* 40 cm^{-1} (Table 2.3).

Table 2.3: Infrared absorptions (cm^{-1}) for SnL_2X_2 (L=α-hydroxyketone, X= halogen).

Compound	υ(C=O) & υ(C=C)	Reference
Maltol	1650, 1610, 1550	34
(1)	1610, 1560, 1503	This work
(2)	1605, 1549, 1505	This work
(3)	1581, 1512	This work
(4)	1619, 1503	This work
(5)	1609, 1548, 1511	This work
(6)	1582, 1511	This work
$Sn(ma)_2Cl_2$	1618, 1510, -	35
$Sn(ma)_2Ph_2$	1618, 1520, -	35
$Al(ma)_3$	1610, 1570, 1515, 1465	4
$Ga(ma)_3$	1610, 1570, 1505, 1460	4
$Fe(ma)_3$	1600, 1575, 1500	34

Recrystallisation at room temperature from either methanol **(5)** or chloroform/cyclohexane **(3, 6)** afforded crystals suitable for X-ray crystallography. The structures of **(3)**, **(5)** and **(6)** are very similar and are shown Figures 2.5–2.7.

(5) crystallises in the tetragonal space group $P4_12_12$, while **(3)** and **(6)** both crystallise in the monoclinic space group $P2_1/c$. As expected, the tin is bonding to the ligands via the oxygens. The C-O^- groups are *trans* to each other, the C=O groups are *cis* to each other and *trans* to the halogen (*cis-cis-trans* isomer).

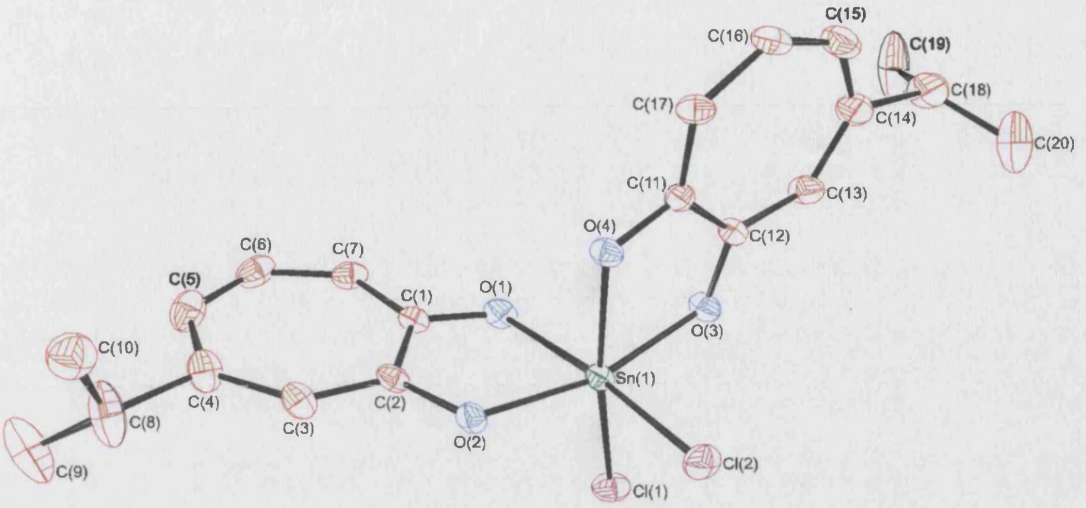

Figure 2.5: The structure of $Sn(hino)_2Cl_2$, ***(3)***.

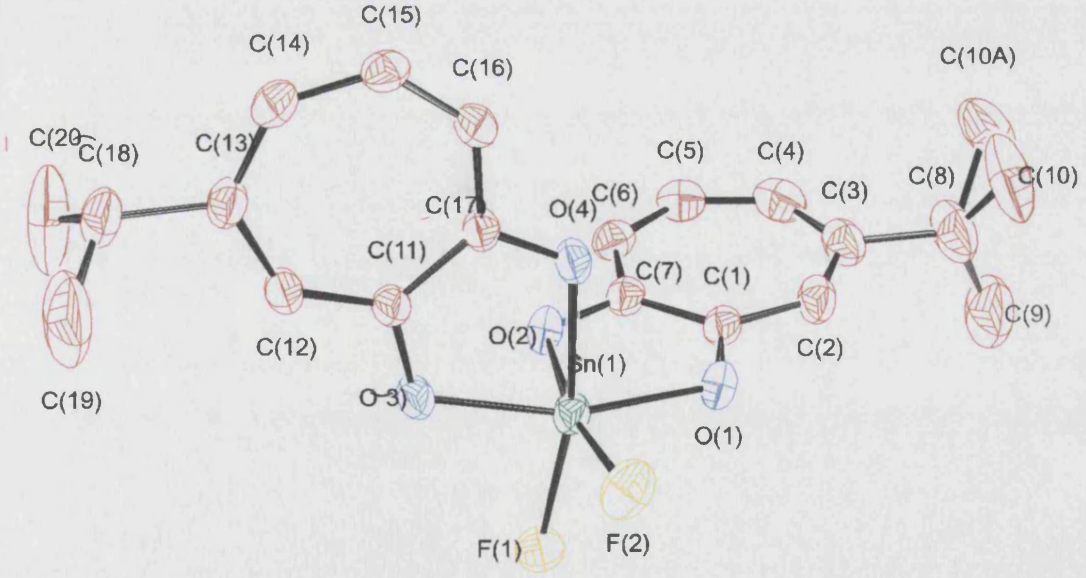

Figure 2.6: The structure $Sn(hino)_2F_2$, ***(6)***.

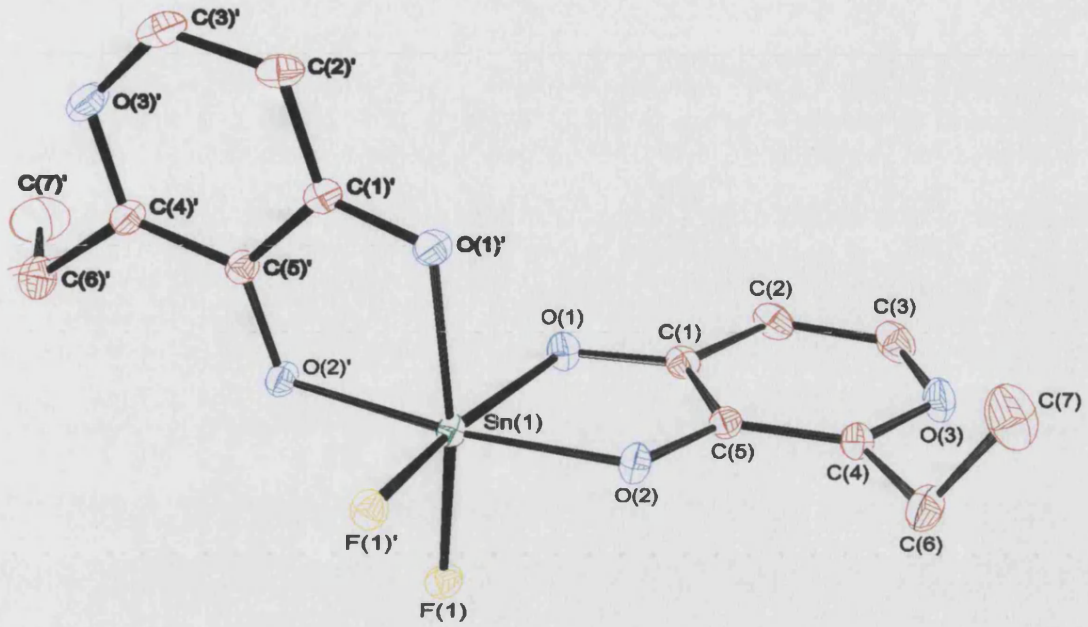

*Figure 2.7: The structure of of $Sn(Etma)_2F_2$, **(5)**.*

The [Sn-O] bond lengths in the Sn(IV) complexes are typical of other [Sn-O] bond lengths found in the literature[32,33] (Table 2.4).

Table 2.4: Sn-O bond lengths in selected Sn(IV) complexes

Compound	[Sn-O(-C)] bond / Å	[Sn←O(=C)] bond / Å	Reference
(1)	2.041(7); 2.050(7)	2.135(7); 2.149(9)	32
(2)	2.052(6); 2.043(6)	2.136(5); 2.115(7)	33
(5)	2.028(1)	2.110(1)	This work
(3)	2.050(4); 2.071(4)	2.061(4); 2.088(4)	This work
(6)	2.049(2); 2.053(2)	2.072(2); 2.082(2)	This work
$Sn(trop)_2Cl_2$	2.071(16); 2.065(15)	2.101(17); 2.059(15)	32

The [C=O] bond is significantly shorter than the one involving the hydroxyl oxygen. This is consistent with the previous observation that one of the [Sn-O] bonds was longer than the other. It can be concluded that only a partial delocalisation of [C-O] double bond character has occurred.

Table 2.5: C-O bond lengths in selected Sn(IV) complexes

Compound	[C-O] bond / Å	[C=O] bond / Å	Reference
(1)	1.344(12)	1.277(10)	32
(2)	1.315(9); 1.342(11)	1.285(10); 1.306(13)	33
(5)	1.330(6)	1.290(2)	This work
(3)	1.307(7); 1.307(6)	1.303(7); 1.302(6)	This work
(6)	1.310(4); 1.318(3)	1.306(4); 1.302(3)	This work
$Sn(trop)Cl_2$	1.350(28); 1.348(25)	1.309(27); 1.303(29)	32

The [C-O] and [C=O] are clearly distinguishable only for **(5)**. For **(3)** and **(6)** the [Sn-O(-C)] bonds and the [Sn←O(=C)] bond are more equivalent to each other than in the ethyl maltol derivatives, as are the [C-O] and [C=O] bond (Table 2.5). It means both the oxygen atoms of hinokitiol are involved in the π-electron delocalisation.

The [Sn–Cl] lengths in (**3**) [2.363(2); 2.369(2)Å] are typical of other complexes, for example $Sn(trop)_2Cl_2$ [2.359(8); 2.347(7)Å].[32] The [Sn–F] bonds in (**5**) [1.9471(9)Å] are *trans* to relatively long [Sn–O] bonds [2.110(1)Å] and are longer than those in (**6**) [1.926(2); 1.934(2)Å], which are *trans* to shorter [Sn–O] bonds [2.072(2); 2.082(2)Å]. These values are typical of Sn-F bonds where the halogen is not involved in bridging as in $Me_2[(PhMe_2Si)_3C]SnF$ [1.965Å] or $Ph_2[(Me_3Si)_3C]SnF$ [1.966Å].[36] The results are summarised Table 2.6.

Table 2.6: Sn-X (X= Cl, F) bond lengths in selected Sn(IV) complexes.

Compound	[Sn-X] bond / Å	Reference
(3)	2.363(2); 2.369(2)	This work
$Sn(trop)_2Cl_2$	2.359(8); 2.347(7)	32
(5)	1.9471(9)	This work
(6)	1.926(2); 1.934(2)	This work
$Me_2[(PhMe_2Si)_3C]SnF$	1.965	36
$Ph_2[(Me_3Si)_3C]SnF$	1.966	36

2.2.2 Synthesis of the tin(II) complexes SnL_2 via stannocene

A successful route to SnL_2 (L= ma, Etma, hino, trop) was found, using stannocene (7) as reagent. Stannocene $[(C_5H_5)_2Sn]$ was prepared from sodium cyclopentadienide $[C_5H_5Na]$ and tin dichloride $[SnCl_2]$. It was used because the tin atom can easily lose the C_5H_5 groups in reaction with protic ligands and replace them by the ligands. Much of tin(II) chemistry uses stannocene as a reagent.[37]

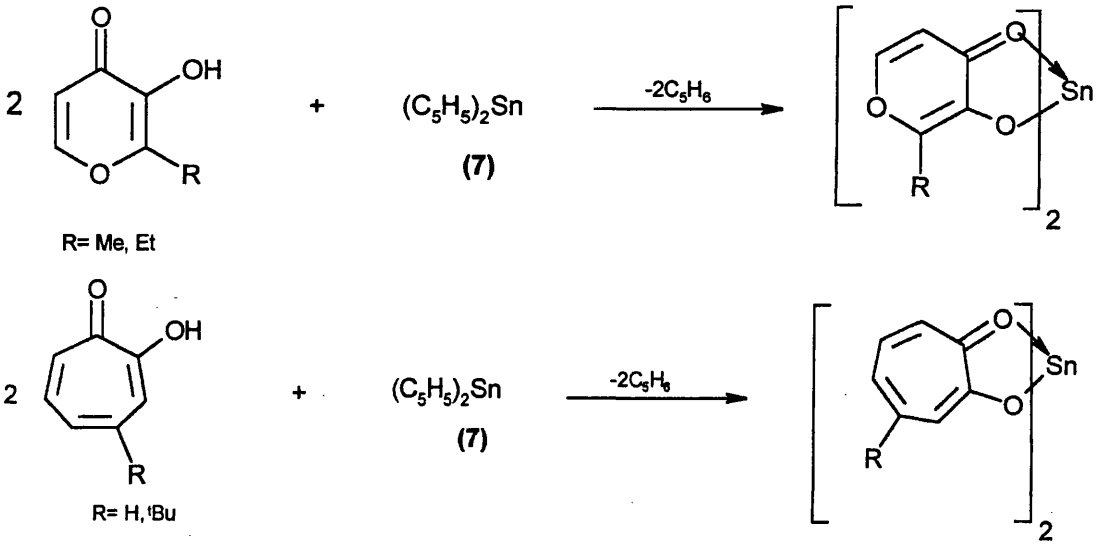

	maltol	ethyl maltol	hinokitiol	tropolone
tin(II)	**(8)**	**(9)**	**(10)**	**(11)**

Scheme 2.2: Synthesis of SnL_2.

The ^{119}Sn Mössbauer spectra of **(8)–(11)** each consists of a doublet. The data for these compounds clearly indicate they contain tin(II), but the spectra also show evidence of oxidised products. The I.S vary between 2.90 and 3.04 mms^{-1}, which indicates that the tin is in the +2 oxidation state. The Q.S values are close to 2 mms^{-1}, which indicates that the tin atom is in an asymmetrical environment. The environment of the tin atom is asymmetrical because of the presence of its lone-pair.

The four compounds have been synthesised and while the elemental analysis are close, the compounds are not pure enough for testing. It is very difficult to purify them due to their insolubility in all common organic solvents. No NMR spectrum has been recorded due to the lack of solubility of the compounds.

(10) has also been synthesised using $SnCl_2$ and water as solvent. Surprisingly this gave the Sn(II) complex rather than the $Sn(hino)_2Cl_2$ compound (*cf.*: Section 2.2.1).

2.2.3 Synthesis of the tin(II) complexes SnL_2 via tin alkoxides

An alternative to the use of stannocene are reactions involving tin(II) alkoxides. In this methodology tin(II) butoxide is be generated *in situ* from tin(II) methoxide, which has a good long-term stability when stored under N_2.

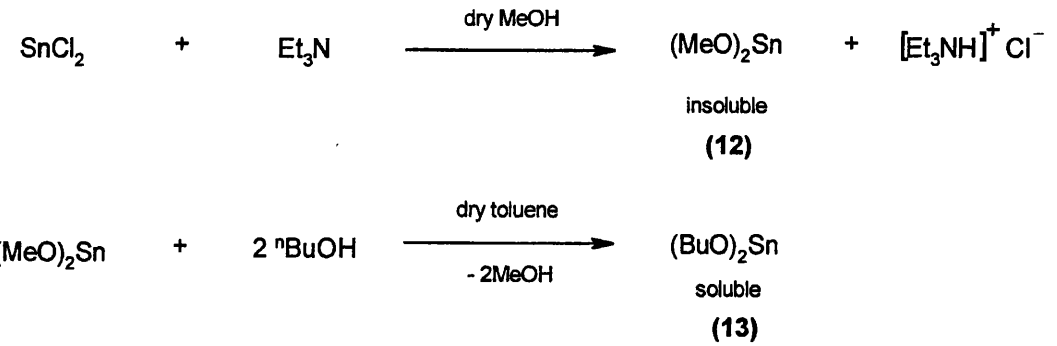

Tin alkoxides have apparently low solubility in organic solvents and are air and moisture sensitive. Their solubility increases as the length of the alkoxy chain increases.[38] Thus, while **(12)** is insoluble, the butoxide **(13)** is readily soluble in all common organic solvents and is more stable than stannocene.

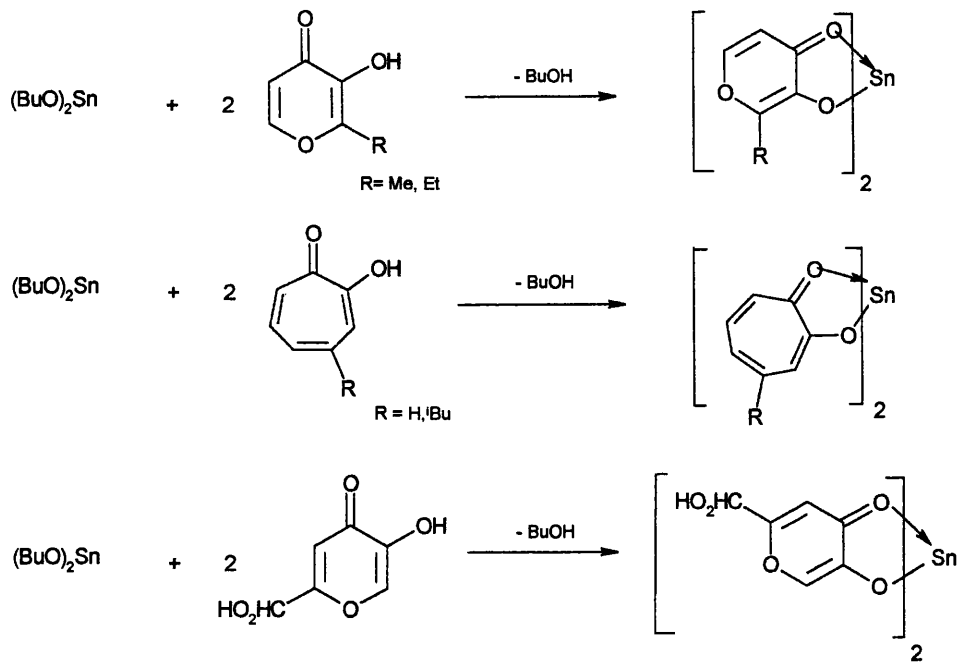

	ma	Etma	hino	trop	koj
tin(II)	**(8)**	**(9)**	**(10)**	**(11)**	**(14)**

Scheme 2.3: Synthesis of SnL_2.

The compounds **(8)–(11)** and **(14)** were successfully synthesised and their identity confirmed by the elemental analysis. Crystals suitable for X-ray crystallography were obtained for **(8)** and **(11)**. The results from the X-ray structural data are presented later in this Section.

Contrary to the previous compounds synthesised *via* stannocene, **(8)–(11)** are soluble in acetone (which is promising for the tests on the biofilm), whereas it proved impossible to dissolve **(14)** in any organic solvents. **(14)** precipitated immediately from the reaction solution and was very difficult to characterise and purify. This is possibly caused by the formation of intermolecular hydrogen bonds via the hydroxyl group on C_6 and/or intermolecular $CH_2(H)O{:}\rightarrow Sn$ coordination.

The infrared spectra of these compounds are similar to those of **(1)-(6)**. The ν(O-H) mode is absent for **(8)–(11)**. For **(14)**, ν(O-H) band at 3269 cm^{-1} is due to the

hydroxyl group on C_6. All the complexes show a ν(C=O) related band between 1564 and 1593 cm^{-1}, which is shifted to a lower wavenumber by around 57-86 cm^{-1} compared to the starting materials. ν(C=O) and ν(C=C) bands, between 1191 and 1521 cm^{-1}, are also shifted to lower wavenumbers.

The ^{1}H and ^{13}C NMR spectra were recorded in deuterated chloroform for **(8)–(11)**. The spectra of **(8)**, **(9)** and **(10)** are similar to the ones recorded for the SnL_2X_2 complexes (Section 2.1). The 3 methyl protons for **(8)** are found at 2.39 ppm as a singlet and for **(9)** are found at 1.08 ppm as a triplet. The CH_2 protons of **(9)** gave a quartet at 2.75 ppm. The protons in the five and six position appeared at 8.35 and 6.83 ppm and 7.76 and 6.57 ppm for **(8)** and **(9)**, respectively. The ^{1}H spectrum of **(11)** consisted of a multiplet between 7.14 and 7.64 ppm corresponding to the five protons. It was not possible to assign the peaks unambiguously.

The ^{13}C NMR spectra of **(8)** and **(9)** show six and seven carbon environments and all the peaks were assigned. For **(11)**, the spectrum consisted of four peaks corresponding to the four carbon environments, the compound being symmetrical.

The ^{119}Sn Mössbauer spectra confirmed that the tin atom is in the +2 oxidation state, as well as in an asymmetric environment. This non-symmetric environment is due to the lone pair of the tin atom. The data are identical to those of the products obtained using stannocene as reagent.

Table2.7: Mössbauer data for the SnL_2 complexes.

Compound	I.S (mms^{-1})	Q.S (mms^{-1})
(8)	2.96^{a}, 2.98^{b}	1.99^{a}, 2.03^{b}
(9)	3.01^{a}, 3.04^{b}	2.01^{a}, 2.02^{b}
(10)	2.93^{a}, 2.93^{b}	1.96^{a}, 1.96^{b}
(11)	2.91^{a}, 2.90^{b}	1.98^{a}, 1.99^{b}
(14)	3.11^{a}	1.95^{a}

[a] value obtained with alkoxides method, [b] value obtained with stannocene method

The complexes appeared to be relatively air and moisture stable in the solid state. The Mössbauer spectrum of **(8)**, which has been left in contact with air for two weeks, shows only a small amount of tin oxide (2%) (Figure 2.8). However, in solution, they are much less stable (100% SnO_2 after a week).

The long term stability of the tin complexes is unusual (related species such as Sn(β-diketonates)$_2$ are readily degraded in moist air to tin oxides) and of significant importance related to their use in toothpaste. Only tin(II) compounds are believe to be active and toothpaste formulations routinely require long shelfe lives during which the active complexes are in contact with an aqueous and aerobic cocktails of others additives.

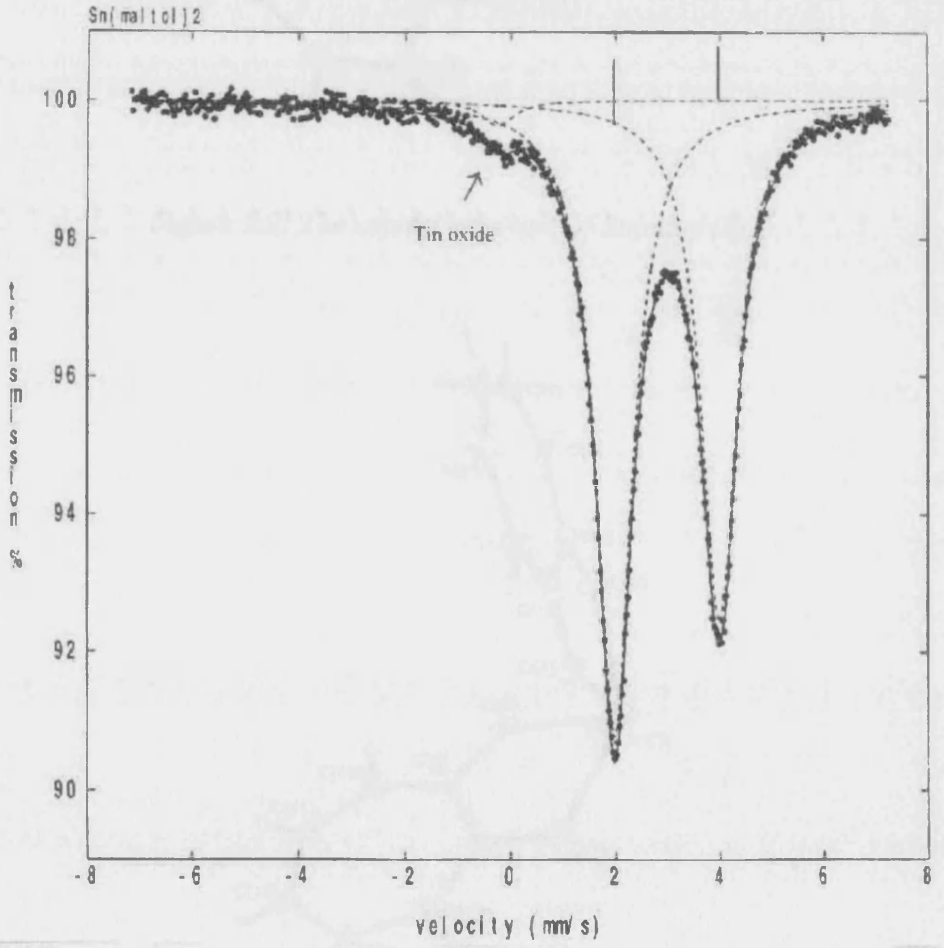

Figure 2.8: Mössbauer spectrum of Sn(ma)$_2$ after 2 weeks in contact with air.

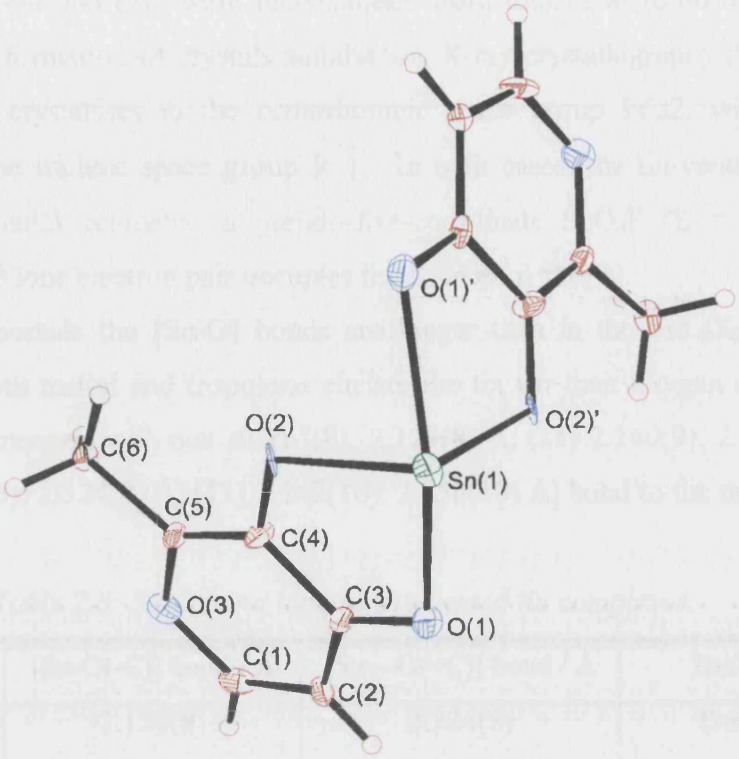

Figure 2.9: The crystal structure of $Sn(ma)_2$ ***(8)****.*

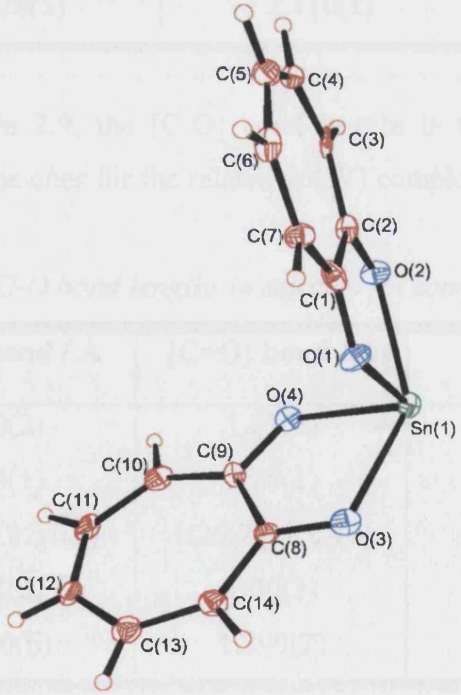

Figure 2.10: The crystal structure of $Sn(trop)_2$ ***(11)****.*

The products **(8)** and **(11)** were recrystallised from toluene at room temperature, resulting in the formation of crystals suitable for X-ray crystallography (Figures 2.9 and 2.10). **(8)** crystallises in the orthorhombic space group Fdd2, whereas **(11)** crystallises in the triclinic space group P $\bar{1}$. In both cases, the tin centre adopts a trigonal bipyramidal geometry, a pseudo-five-coordinate SnO_4E (E = lone pair), where the active lone electron pair occupies the equatorial site.

In both compounds the [Sn-O] bonds are longer than in the SnL_2X_2 analogues (Table 2.8). Both maltol and tropolone chelate the tin *via* their oxygen atoms in an anisobidentate manner, with one short [**(8)**: 2.129(8) Å; **(11)** 2.140(9); 2.140(10) Å] and one long [**(8)**: 2.324(8) Å; **(11)** 2.242(10); 2.258(10) Å] bond to the metal.

Table 2.8: Sn-O bond lengths in selected tin complexes.

Compound	[Sn-O(-C)] bond / Å	[Sn←O(=C)] bond / Å	Reference
(8)	2.129(8)	2.324(8)	This work
$Sn(ma)_2Cl_2$	2.041(7); 2.050(7)	2.135(7); 2.149(9)	32
(11)	2.140(9); 2.140(10)	2.242(10); 2.258(10)	This work
$Sn(trop)_2Cl_2$	2.071(16); 2.065(15)	2.101(17); 2.059(15)	32
$Sn(Etma)_2F_2$	2.028(1)	2.110(1)	This work

As can be seen in Table 2.9, the [C-O] bond lengths in the tin(II) compounds compare favourably with the ones for the related tin(IV) complexes.

Table 2.9: C-O bond lengths in selected tin complexes.

Compound	[C-O] bond / Å	[C=O] bond / Å	Reference
(8)	1.30(2)	1.27(2)	This work
$Sn(ma)_2Cl_2$	1.34(1)	1.28(1)	32
(11)	1.29(2); 1.31(2)	1.26(2); 1.27(2)	This work
$Sn(trop)_2Cl_2$	1.31(3)	1.30(3)	32
$Sn(Etma)_2F_2$	1.330(6)	1.290(2)	This work

2.2.4 Attempts to make SnL_3X and SnL_4 complexes

Due to the uncertainty concerning the activity of tin(IV) species in toothpaste, an attempt to attach three and four ligands to the tin atom has been made. Unfortunately it was unsuccessful and L_2SnCl_2 complexes **(1)** and **(2)** were obtained again.

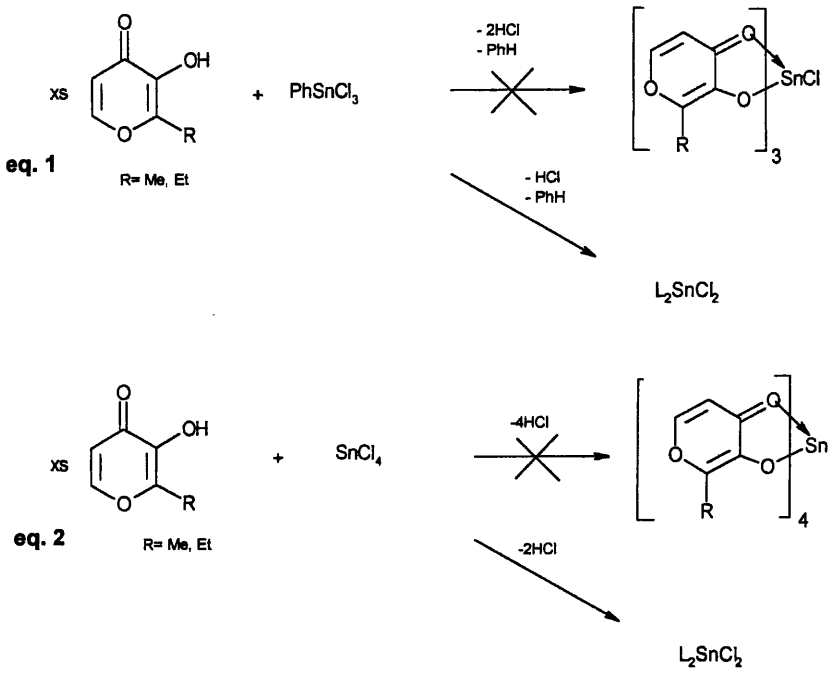

Scheme 2.4: Attempted synthesis of SnL_3Cl and SnL_4.

An attempt to prepare the SnL_3X compounds was made following a literature procedure[35] (eq. 1). S.Bhattacharya *et al*[35] have used maltol and $PhSnCl_3$ in a 2:1 ratio and have obtained $SnCl_2L_2$ compounds. It was assumed that using an excess of ligands, three or four ligands could be attached to the tin atom. So an excess of either maltol or ethyl maltol was added to a solution of $PhSnCl_3$, and held at reflux for three hours. But solids of compounds **(1)** and **(2)** were obtained by cooling to room temperature.

Another attempt to attach four ligands to the tin atom was made using $SnCl_4$ (eq. 2). A solution of maltol or ethyl maltol in excess in toluene was added to $SnCl_4$ under nitrogen. The reaction mixture was stirred for four hours and the solvent was removed *in vacuo*. This yielded again the compounds **(1)** and **(2)**.

2.3 Results and Discussion: Zinc(II) and Copper(II) compounds

2.3.1 Synthesis of the of the zinc(II) and copper(II) complexes

In order to compare the activity in toothpaste of the tin compounds, five known compounds with zinc or copper have been prepared,[39] whose activities have been discussed in the Introduction. These allowed results on the biological testing of new compounds to be compared with earlier data.

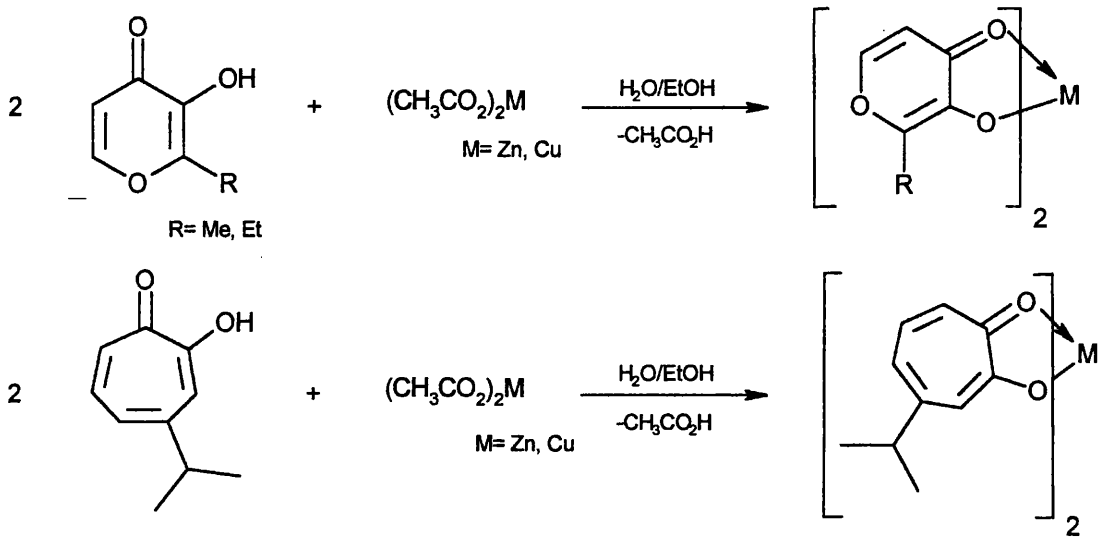

	ma	Etma	hino
Zn(II)	**(15)**	**(16)**	**(17)**
Cu(II)	**(18)**	**(19)**	**(20)**

Scheme 2.5: Synthesis of known ZnL_2 and CuL_2 complexes.

The Cu(II) complexes CuL_2 have the Cu atom adopting a four coordinate, square planar geometry. The Zn(II) complexes of maltol and ethyl maltol were found to be hydrated, whereas the Zn(II) complex of hinokitiol appeared to be anhydrous. Unilever has tested all these compounds and the hinokitiol derivatives seem to be particularly active.

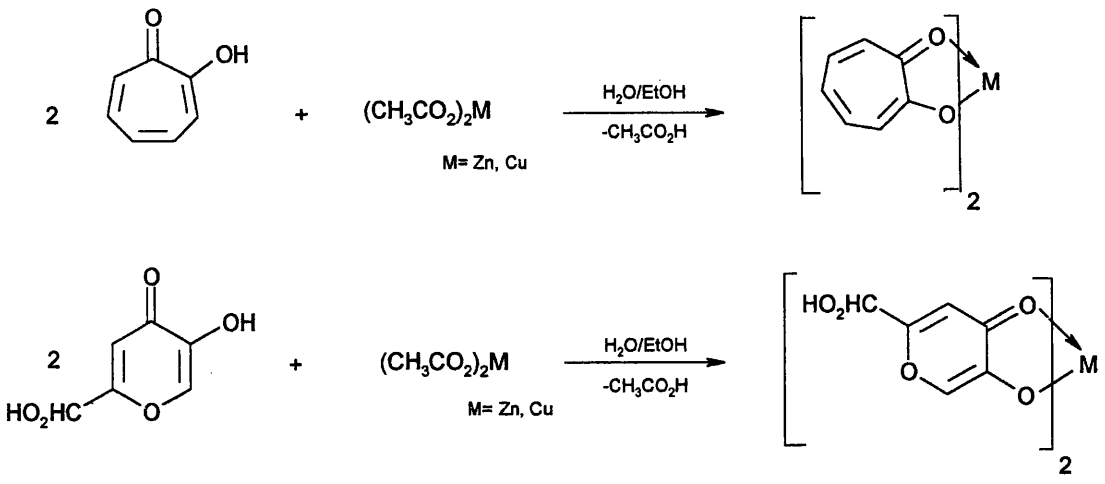

	trop	koj
Zn(II)	**(21)**	**(22)**
Cu(II)	**(23)**	**(24)**

Scheme 2.6: Synthesis of new ZnL_2 and CuL_2 complexes.

The elemental analysis confirmed the nature of **(21)–(24)**, and suggested that the two zinc complexes were both anhydrous. No NMR spectrum has been recorded for the copper(II) species because of the electronic configuration of Cu^{2+}. Cu^{2+} is d^9 and the odd electron makes the compound paramagnetic. Due to the lack of solubility in any organic solvents of **(21)** and **(22)** no spectrum has been obtained for the zinc compounds either.

The infrared spectra of the compounds are similar to those of the tin complexes. The ν(O-H) mode is absent for **(21)** and **(23)**. For **(22)** and **(24)** ν(O-H) band at 3050 and 3060 cm^{-1} is due to the hydroxyl group on C_6. For the zinc compounds **(21)** and **(22)** there is no broad peak around 3500 cm^{-1}, which supports the finding that these two complexes are not hydrated.

Crystals suitable for X-ray crystallography were obtained for **(17)** and **(21)** (Figures 2.11, 2.12). **(17)** crystallises in the monoclinic space group $P2_1/n$, whereas **(21)** crystallises in the monoclinic space group $P2_1/c$.

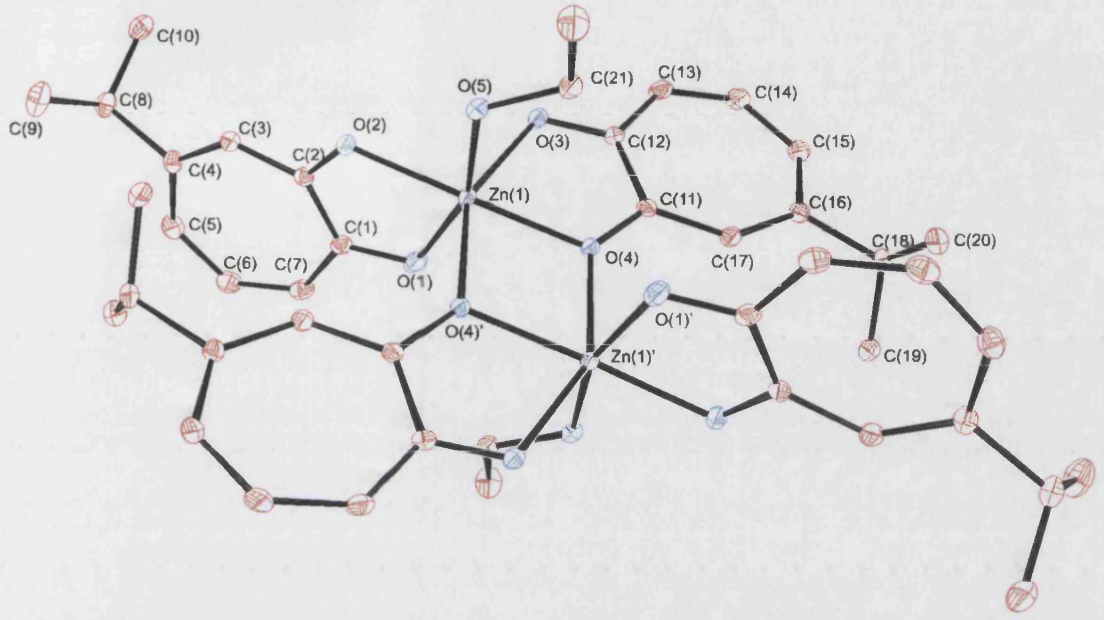

*Figure 2.11: The structure of $[Zn(hino)_2.EtOH]_2$, **(17)**.*

(17) forms a dimer in which a molecule of ethanol coordinates to each zinc atom, so that the coordination number of the zinc is six. Figure 2.13 shows that there are two types of hinokitiol ligand in the complex: one (ligand ***A***) co-ordinating to one zinc atom only and one (ligand ***B***) co-ordinating to the first zinc atom and also to the second *via* a bridging oxygen.

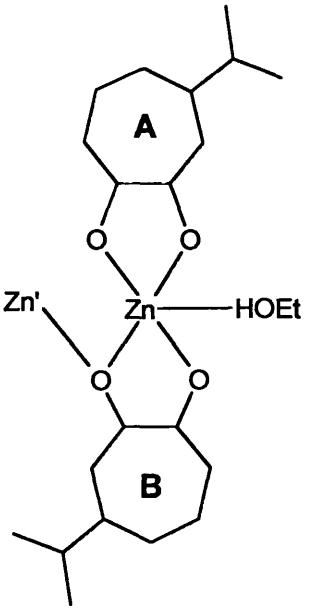

Figure 2.13: The two types of hinokitiol ligand in (17).

So one ligand is bridging while the other one is purely chelating, the remaining site in the zinc occupied by a molecule of ethanol. This structure is similar to the one of $Ni(trop)_2.H_2O$[40] except that in this case, ethanol is replaced by water.

(21) forms a polymer in the solid state. Each tropolone ligand chelates zinc and in addition bridges through only one of the available oxygen centres to an adjacent metal, so that the zinc atom is six-coordinate in distorted octahedral geometry. The structures of **(17)** and $Ni(trop)_2.H_2O$[40] can be seen as an ethanol/water-capped dimeric fragment of the polymer of **(21)**, the solvent molecules breaking the extended polymer of $Zn(trop)_2$.

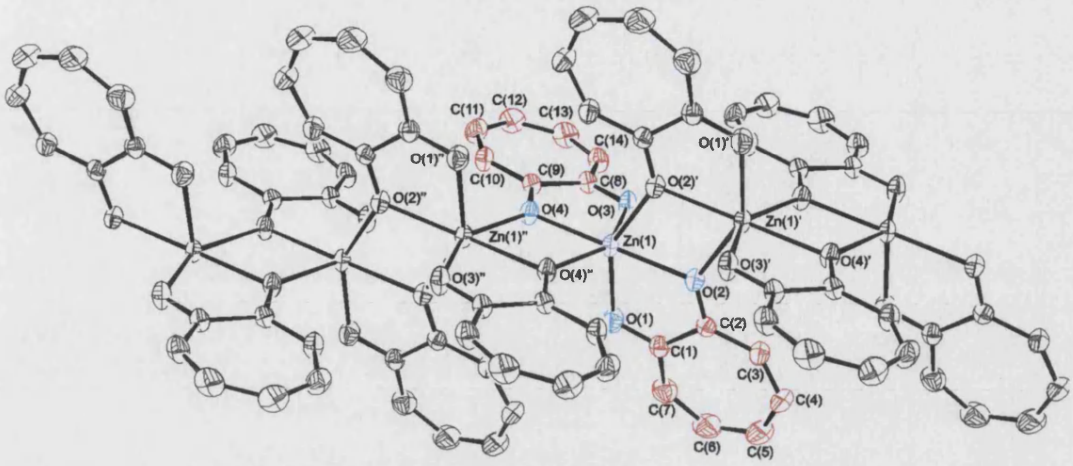

Figure 2.12: The crystal structure of Zn(trop)$_2$ ***(21)***.

For **(21)** a short [C=O] bond [1.261(3); 1.263(3) Å] and a long [C–O] bond [1.291(3); 1.299(3) Å] can be identified (Table 2.11). Contrary to other structures, in **(21)** this is the carbonyl oxygen, which binds to the zinc with the shortest bond [2.067(2); 2.051(2) Å], while the hydroxyl oxygen makes a weaker bond to the metal [2.149(2), 2.150(2) Å], presumably as a consequence of its bridging role (Table 2.10).

Table 2.10: C-O bond lengths in selected metal complexes.

Compound	[C-O] bond / Å	[C=O] bond / Å	Reference
(17)	1.287(2); 1.306(2)	1.277(2); 1.279(2)	This work
(21)	1.291(3); 1.299(3)	1.261(3); 1.263(3)	This work
Cu(hino)$_2$	1.296(5)	1.293(5)	39
Cu(trop)$_2$	1.302(5)	1.286(5)	41

For **(17)**, the correlation of [C–O]/[C=O] and [Zn–O] bond lengths follow the expected pattern, (specially in the purely chelating ligand), [Zn-O(-C)] bond [2.029(1), 2.075(1) Å] being shorter than the [Zn←O(=C)]bond [2.074(1); 2.107(1) Å] (Table 2.11).

The C(11)-O(4) bond [1.306(2) Å] is elongated as a result of the dual bonding role for O(4), but O(4) still forms a stronger bond to Zn [2.075(1) Å] than the carbonyl oxygen, O(3) [Zn-O(3): 2.107(1)Å].

Table 2.11: M-O bond length in selected metal complexes.

Compound	[M-O(-C)] bond / Å	[M←O(=C)] bond / Å	Reference
(17)	2.029(1), 2.075(1)	2.074(1); 2.107(1)	This work
(21)	2.149(2), 2.150(2)	2.067(2); 2.051(2)	This work
$Zn(ma).2H_2O$	2.033(2); 2.010(3)	2.075(2); 2.076(2)	9
$Cu(hino)_2$	1.900(2)	1.904(3)	39
$Cu(trop)_2$	1.915(3)	1.915(3)	41

Both structures differ from the ideal geometry; but the octahedral coordination about zinc in **(17)** is more regular than in **(21)**, due to the flexibility of the ethanol molecule in comparison to the second bridging tropolone in **(21)**. The bite angles differ from the ideal geometry because the ligands dictate them to be less than 90° [**(17)** O(1)-Zn-O(2): 78.63(5); O(3)-Zn-O(4): 76.35(4)°; **(21)** O(1)-Zn-O(2): 74.84(7); O(3)-Zn-O(4): 75.29(7)°]. In addition to the bite angles, the *trans* pair of atom angles also differ from the ideal value of 180° [**(17)** O(2)-Zn-O(4): 175.63(5)°; **(21)** O(1)-Zn-O(2′): 146.82(7) ; O(3)-Zn-O(4′): 147.81(7)°]. It can be seen in the *trans* angles O(4′)-Zn-O(5) [160.74(4)°] for **(17)** and O(3)-Zn-O(4′) [147.81(7)°] for **(21)** that the ethanol group allows more freedom than the rigid second bridging tropolone.

2.2.3 Structure and biological activity: the role of coordination number

It has been noticed that all the copper compounds (in which the copper is four-coordinate, in a square planar geometry) are active, whereas the zinc ones (in which the zinc is either five or six-coordinate) do not show any particular activity. So in order to assess the importance of metal coordination number on activity, it has been attempted to form Lewis base complexes of $Cu(hinokitiol)_2$, which is known to be active. **(20)** has been mixed with pyridine to form a complex of the form $Cu(hinokitiol)_2.L_n$ and hence change its properties. A 1:1 adduct with pyridine has been isolated **(25)**, which presumably contains five-coordinate copper. This is confirmed by the elemental analysis (found: C 63.7%; H 5.79%; N 2.85%, calculated: C 64.0%; H 5.76%; N 2.98%). Another 1:1 adduct with 2,2'-bipyridine has also been obtained **(26)**, which presumably contains six-coordinate copper. The elemental analysis indicates that there is only one bipyridine ligand attached to the copper atom (found: C 65.5%; H 5.48 %; N 5.83%, calculated: C 65.9%; H 5.49%; N 5.13%).

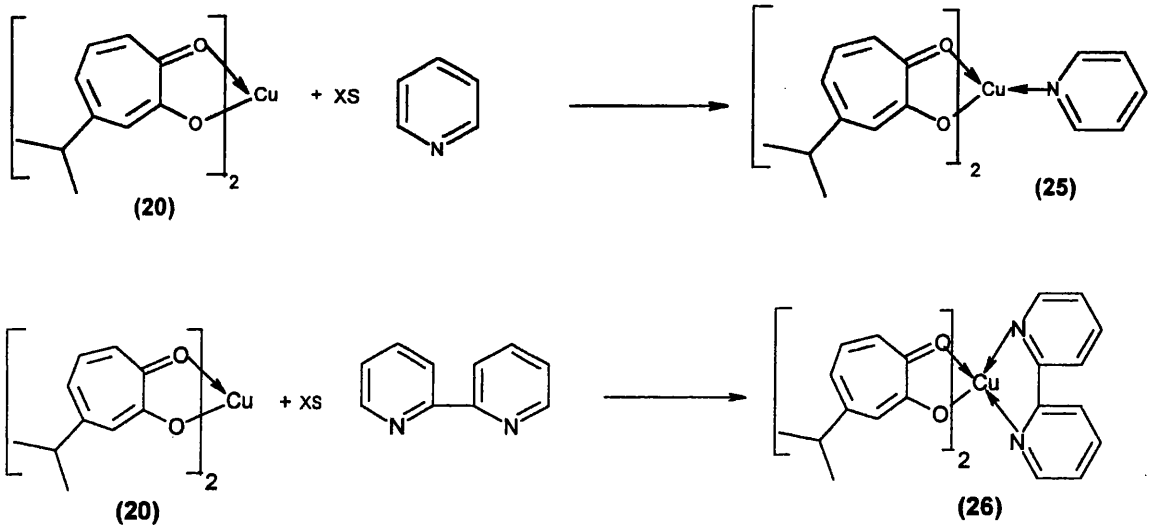

Scheme 2.7: Synthesis of Cu(hino) derivatives.

Recrystallisation of **(25)** from acetonitrile resulted in the formation of crystals suitable for X-ray crystallography. The crystal structure shows as expected a five-coordinate copper (Figure 2.14).

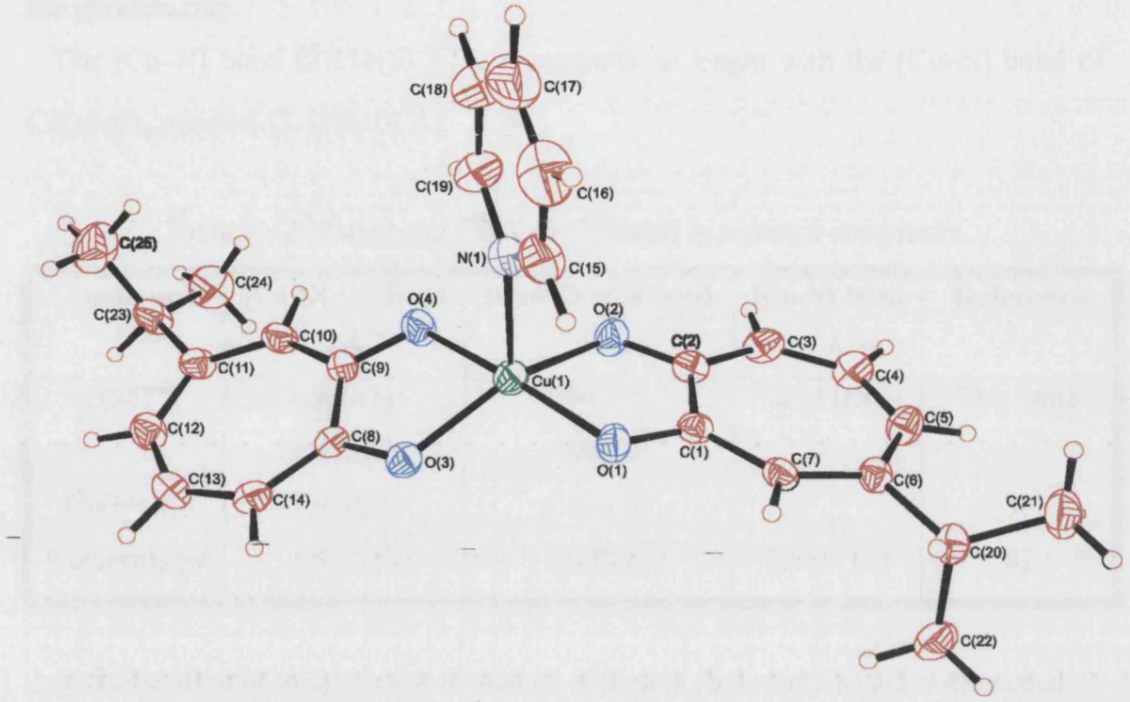

Figure 2.14: The crystal structure of Cu(hinokitiol)$_2$.pyridine ***(25)***.

(25) crystallises in the monoclinic space group $P2_1/n$, the copper adopts a square pyramidal geometry with the pyridine in the axial position. The structure is similar to the one obtained for Cu(acrp)$_2$.pyridine (Hacrp: 4-hydroxy-6-methyl-3-[-3-dimethylaminoacryloyl]-2H-pyran-2-one) (Figure 2.15).[42]

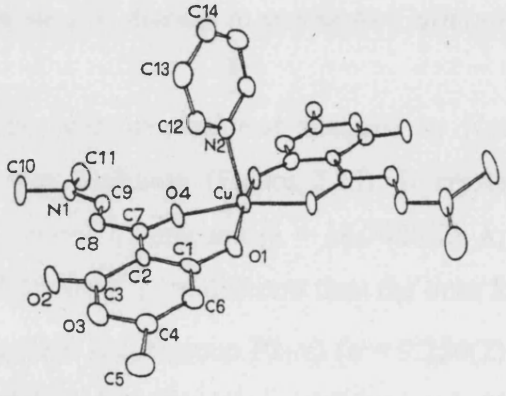

Figure 2.15: Structure of Cu(acrp)$_2$.pyridine.[42]

The [Cu–O] bond lengths [1.940(3); 1.933(3); 1.945(3); 1.965(3) Å] are longer than those observed in the Cu(hinokitiol)$_2$ complex [1.900(2); 1.904(3) Å].[39] This is the result of the interaction between the copper atom and the nitrogen atom N(1) of the pyridine ring.

The [Cu–N] bond [2.311(5) Å] is comparable in lenght with the [Cu–N] bond of Cu(acrp)$_2$.pyridine [2.310(10) Å].[42]

Table 2.12: Cu–O and Cu-N bond length in selected complexes.

Compound	[Cu-O(-C)] bond / Å	[Cu←O(=C)] bond / Å	[Cu-N] bond / Å	Reference
(25)	1.940(3); 1.933(3)	1.945(3); 1.965(3)	2.311(5)	This work
Cu(hino)$_2$	1.900(2)	1.904(3)	_	39
Cu(acrp)$_2$.py	1.911(5)	1.907(4)	2.310(10)	42

A similar attempt to synthesise an adduct with urea (Scheme 2.8) did not succeed.

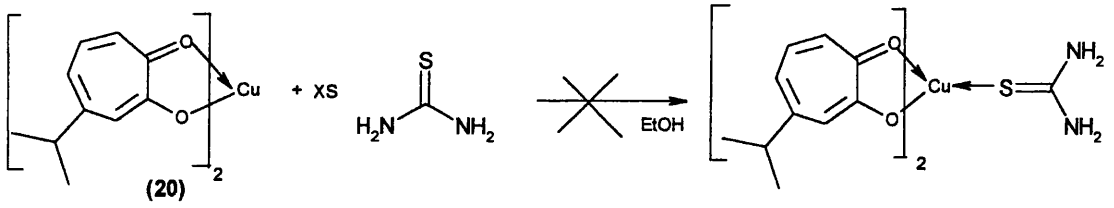

Scheme 2.8: Attempt to synthesise Cu(hino)$_2$.urea.

Some green crystals were obtained and analysed by X-ray crystallography. The structure showed it was Cu(hino)$_2$ (Figure 2.15). It crystallises in the monoclinic space group P2$_1$/n. The cell parameters [a = 16.7420(2) Å; b = 15.5370(2) Å; c = 18.3010(3) Å; β = 99.4000(6)°.] are different than the ones for the structure obtained by P. Wright[39] (monoclinic space group P2$_1$/c) [a = 9.254(2) Å; b = 9.997(2) Å; c = 11.124(3) Å; β = 113.86(2)°.].

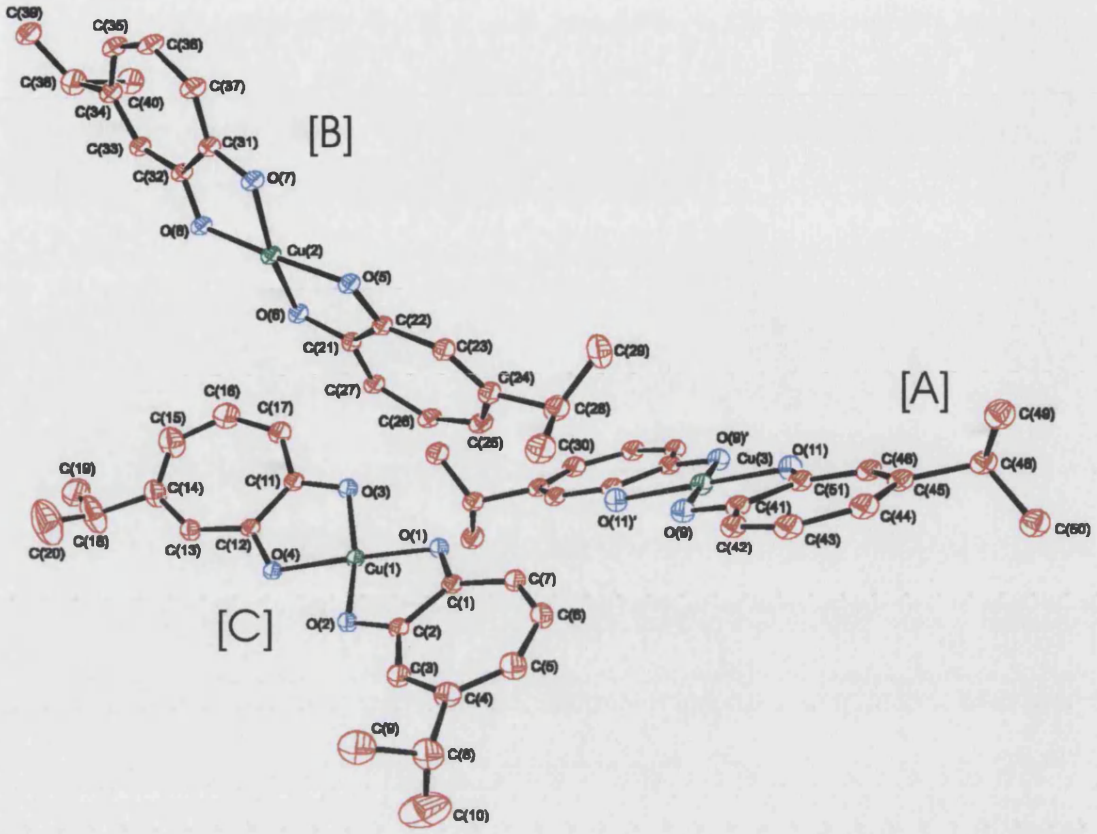

Figure 2.15: The structure of Cu(hino)$_2$ ***(20)***.

There are two and half molecules in the asymmetric unit, two molecules are in general positions, while the half molecule has the copper atom seated on an inversion centre, like for the earlier structure determination.[39] For each molecule the copper is nominally four-coordinate and in a square planar environment. The molecule generated by the inversion centre [molecule A containing Cu(3)] has the isopropyl groups adopting a *trans* configuration and it is also the case for one of the two other molecules [molecule B containing Cu(2)] and for P.Wright's structure determination.[39] However in the remaining molecule [molecule C containing Cu(1)] the isopropyl groups are *cis* to each other. This is unusual as for previous structures of α-hydroxyketones, the alkyl groups are *trans* to each other (*i.e.*: **(17)**, **(25)**, Cu(hino)$_2$,[39] Zn(ma)$_2$,[9] Sn(Etma)$_2$Cl$_2$[32]).

The two full molecules (B and C) are proximate to inversion centres and hence dimerize with nearby lattice neighbours (Figure 2.16). In the dimer of B the isopropyl groups sit on top of each other (head to head configuration), while in the dimer of C they are opposite (head to tail configuration).

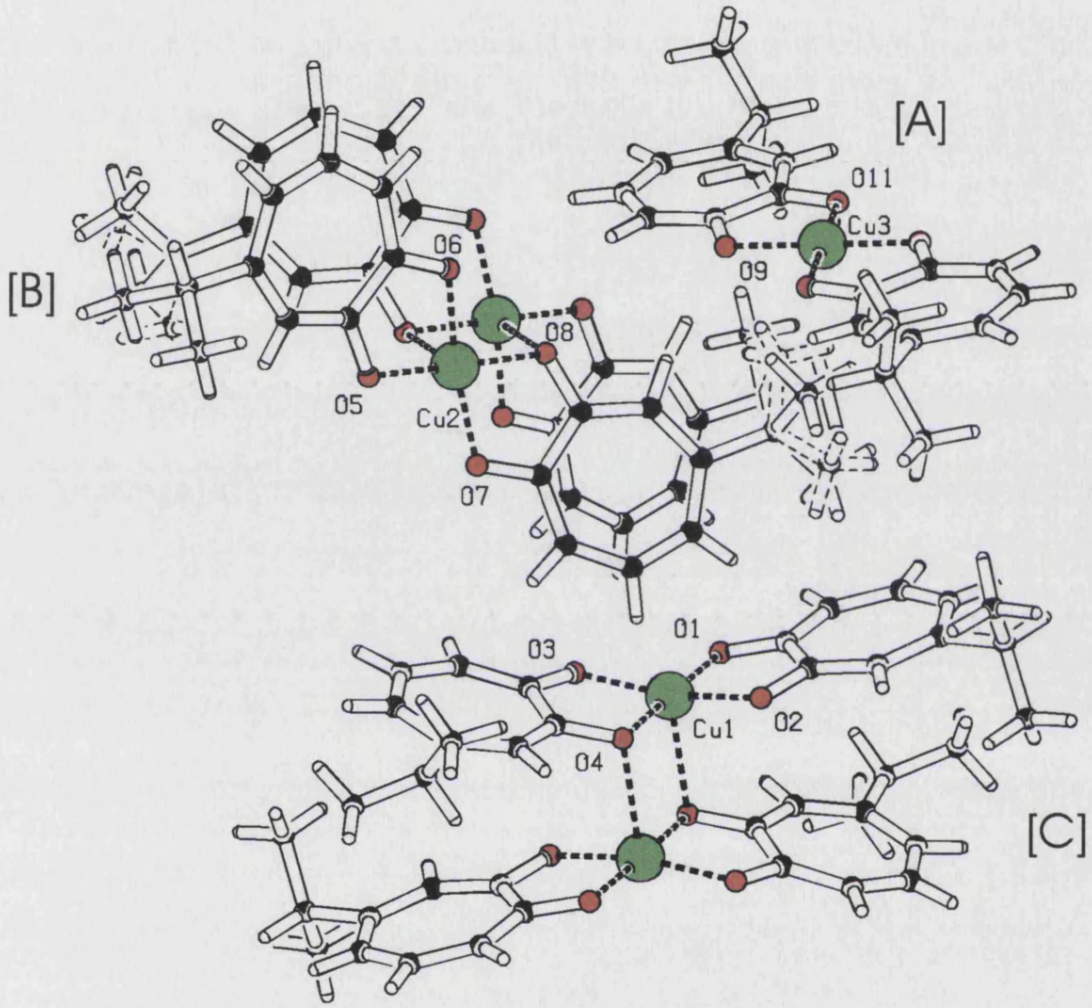

Figure 2.16: Dimers of Cu(hino)$_2$.

In undimerised molecule A, the [Cu–O] bond lengths [1.901(2); 1.909(2) Å] are similar than those observed in the earlier Cu(hino)$_2$ structure [1.900(2); 1.904(3) Å].[39] For B and C, the [Cu–O] bond lengths [1.919(2); 1.920(2); 1.932(2); 1.933(2) 1.915(2); 1.921(2); 1.922(2); 1.939(2) Å] are longer than those observed in the Cu(hinokitiol)$_2$ complex,[39] this being the result of the dimerization, similar to the effect of the pyridine coordination in **(25)**.

2.4 Biological Testing

All the tin(IV) compounds have been tested at Unilever. The copper(II) and the zinc(II) complexes of maltol, ethyl maltol and hinokitiol were sent in order to compare their activities, which are known, with the activity of the new tin(IV) compounds.

The complexes have been tested using the Plaque Growth Inhibition (PGI) assay (see Appendix). The species of orally derived bacteria used in the tests is *Staphlococcus Warneri* (*S.Warneri*). *S.Warneri* reflects clinical data more closely in metal ion system than any other bacteria. The PGI assay is a well-validated *in vitro* model of plaque inhibition effects, so the results can be related to *in vivo* clinical data.

The tests measure the antiplaque effect of the compounds, by the delay in biofilm regrowth, after treatment, to a certain pre-set optical density. The absorbance at 630 nm is used as a measure of cell density, because at this wavelength the bacterial cells absorb the radiation and not the molecules present in bacteria. The tests are stopped when it reaches an A_{630}=0.3.

Example of tests

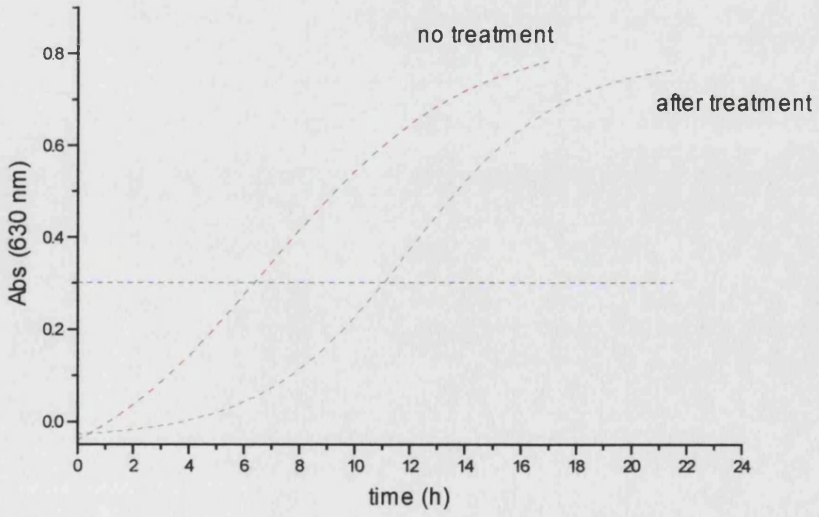

The delay indicates that cells in the biofilm have been killed or their growth inhibited by the compounds. The longer the regrowth time is, the more efficient is the complex.

The compounds must first be dissolved in either water, alcohol or acetone before adding to a model toothpaste solution. Then the solution is put on a biofilm for thirty seconds and washed three times with distilled water to mimic what is happening in the mouth during the brushing. After treatment the plates of biofilm are incubated at 37°c in a microtitre plate reader (Dynex Technologies DIAS) and growth monitored by measuring the absorbance at 630 nm every fifteen minutes for 16–23 hours.

It has been difficult to dissolve the tin(IV) complexes and at first an attempt to test them without previously dissolving them gave disappointing results. It was uncertain if this was because the compounds were not dissolved or because tin(IV) compounds are said not to be active. A second attempt was made and this time the complexes were dissolved in an ethanol/acetone mix. The results are shown in Table 2.13.

Table 2.13: Results of the PGI assay on the tin(IV) complexes [a].

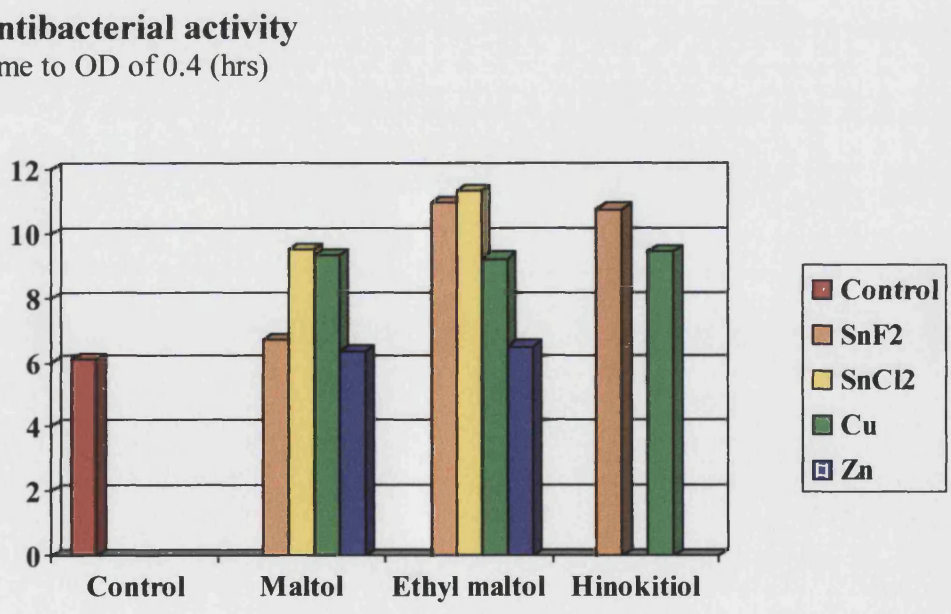

[a] *CuL_2, ZnL_2 also shown for comparison.*

The control toothpaste is a model toothpaste solution in which no metal or therapeutic agents of any sort have been incorporated. The zinc complexes show no particular activity and the copper ones are in the other hand relatively efficient. This confirms the previous tests.

All the tin compounds seem to be efficient. The complexes with ethyl maltol and Cl or F show a remarkably high activity. This is really important, as it is the first time evidence of the activity of tin(IV) compounds has been demonstrated. More tests need to be done. The problem of the tin complexes is that they are relatively acidic and this could affect the results, as the bacteria could be sensitive to such a low pH.

The pHs of the compounds as they were added to the biofilm were as follows: $Sn(ma)_2F_2$, $Sn(Etma)_2F_2$ and $Sn(hino)_2F_2$ were around pH 3.5, $Sn(ma)_2Cl_2$ and $Sn(Etma)_2Cl_2$ were around pH 3.1, $Cu(ma)_2$, $Cu(Etma)_2$ and $Cu(hino)_2$ were about pH 6.1–6.4, $Zn(ma)_2.2H_2O$ and $Zn(Etma)_2.2H_2O$ were the most neutral with pH's of between 7.4–7.9.

2.5 Experimental

Preparation of $(ma)_2SnCl_2$ (1)

A solution of maltol (0.78g; 6.22mmol) in dry THF (60mL) was added to a well stirred solution of tin(II) chloride (0.59g; 3.11mmol) in dry THF (20mL) under nitrogen. After stirring for two hours, the solution was refluxed and stirred for another two hours and then left in the freezer for twenty-four hours. A pale yellow solid appeared, which was recrystallised from methanol, yielding white crystals (0.48g; 35%).

Analysis: Found (calc. for $C_{12}H_{10}O_6SnCl_2$): C 32.7 (32.7)%; H 2.32 (2.27)%.

Mössbauer data (mms^{-1}): IS = 0.25, QS = 0.42

^{119}Sn NMR [δ(ppm), DMSO(d^6)]: -470, s; -475, s.

^1H NMR [δ(ppm), DMSO(d^6)]: 2.57 [3H, s, CH_3]; 7.22 [1H, d, H_6],
$J(^1H\text{-}^1H)$ = 4.94 Hz; 8.70 [1H, d, H_5],
$J(^1H\text{-}^1H)$ = 4.95 Hz.

^{13}C NMR [δ(ppm), DMSO(d^6)]: 15.4 [C_7];109.8 [C_5]; 145.7 [C_2]; 157.3 [C_3];
158.4 [C_6]; 172.1 [C_4].

IR data (NaCl plates, nujol, cm^{-1}): 1610, 1560 υ(C=O); 1503 υ(C=C);
1272, 1205 υ(C-O).

Preparation of $(Etma)_2SnCl_2$ (2)

The method described previously for **(1)** was utilised for ethyl maltol (0.82g; 5.79mmol) in dry THF (10mL) was added to tin dichloride (0.55g; 2.89mmol) in dry THF (20mL). Following this procedure, white crystals suitable for X-ray crystallography were obtained (0.68g; 50%).

Analysis: Found (calc. for $C_{14}H_{14}O_6SnCl_2$): C 36.0 (35.9)%; H 3.04 (2.99)%.

Mössbauer data (mms^{-1}): IS =0.31, QS = 0.49

^{119}Sn NMR [δ(ppm), DMSO(d^6)]: -465, s; -471, s.

^1H NMR [δ(ppm), DMSO(d^6)]: 1.25 [3H, t, CH_3]; 2.98 [2H, q, CH_2]; 6.76 [1H,s,H_6];
8.08 [1H, s, H_5].

^{13}C NMR [δ(ppm), DMSO(d^6)]: 10.4 [C_8]; 22.6 [C_7]; 109.9 [C_5];
146.1 [C_2]; 155.3 [C_6]; 160.9 [C_3]; 172.4 [C_4].

IR data (NaCl plates, nujol, cm^{-1}): 1605, 1549 υ(C=O); 1505 υ(C=C);
1274, 1194 υ(C-O).

Preparation of $(hino)_2SnCl_2$ (3)

The method described for **(1)** was repeated with hinokitiol (0.92g; 5.61mmol) in dry THF (50mL) added to tin dichloride (0.53g; 2.79mmol) in dry THF (20mL). A pale yellow solid was obtained. Recrystallisation from a solution of chloroform (20mL), in which cyclohexane (5mL) was slowly added, yielded the product as colourless crystals suitable for X-ray crystallography (0.21g; 15%).

Analysis: Found [calc. for $C_{20}H_{22}O_4SnCl_2$]: C 45.9 (46.5)%; H 4.27 (4.52)%.

Mössbauer data (mms^{-1}): IS =0.26, QS = 0.48

^{119}Sn NMR [δ(ppm), DMSO(d^6)]: -478, s.

^1H NMR [δ(ppm), DMSO(d^6)]: 1.23 [6H, d, CH_3]; 2.96 [1H, sept, H_8];
7.35 [1H, s, H_7]; 7.64-7.76 [3H, m, H_3, H_4, H_5].

^{13}C NMR [δ(ppm), DMSO(d^6)] : 23.6 [C_9]; 39.4 [C_8]; 127.1 [C_7],
$^3J(^{119}Sn\text{-}^{13}C)$ = 35.5 Hz; 128.2 [C_3],
$^3J(^{119}Sn\text{-}^{13}C)$ = 35.5 Hz; 131.9[C_5]; 140.6 [C_4];
164.7 [C_6]; 171.3 [C_2]; 171.7 [C_1].

IR data (NaCl plates, nujol, cm^{-1}): 1581 υ(C=O); 1512 υ(C=C);
1241, 1186 υ(C-O).

Preparation of $(ma)_2SnF_2$ (4)

A solution of maltol (0.88g; 7.00mmol) in absolute ethanol was added to a well-stirred solution of tin difluoride (0.55g; 3.50mmol) in dry THF (50mL) under nitrogen and gave a yellow solution. The solution was stirred for thirty minutes and then refluxed and stirred for two hours. The mixture was then left at room temperature for twenty-four hours and a pale orange precipitate appeared (1.00g; 70%).

Analysis: Found (calc. for $C_{12}H_{10}O_6SnF_2$): C 35.3 (35.4)%; H 2.52 (2.46)%.

Mössbauer data (mms^{-1}): IS = 0.00, QS = 0.52

^{119}Sn NMR [δ(ppm), $CDCl_3$]: -594, t, $^1J(^{119}Sn\text{-}^{19}F)$ = 2293 Hz.

^1H NMR [δ(ppm), $CDCl_3$]: 2.45 [3H, s, CH_3]; 7.8 [1H, d, H_6]; 8.55 [1H, d, H_5].

^{13}C NMR [δ(ppm), $CDCl_3$]: 15.5 [C_7]; 109.8 [C_5]; 145.7 [C_2]; 157.3 [C_3];
158.4 [C_6]; 172.1 [C_4].

IR data (NaCl plates, nujol, cm^{-1}): 1619 υ(C=O); 1503 υ(C=C); 1277, 1217 υ(C-O).

Preparation of $(Etma)_2SnF_2$ (5)

The synthetic method described above for **(4)** was repeated using ethylmaltol (0.80g; 6.38mmol) in absolute ethanol (30mL) and tin difluoride (0.50g; 3.19 mmol) in dry THF (50mL). A brown solid was obtained, which recrystallised from methanol (50mL) yielding yellow crystals suitable for X-ray crystallography (0.42g; 30%).

Analysis: Found (calc. for $C_{14}H_{14}O_6SnF_2$): C 37.8 (38.6)%; H 3.35 (3.22)%.

Mössbauer data (mms^{-1}): IS = -0.01, QS =0.56

^{119}Sn NMR [δ(ppm), $CDCl_3$]: -595, t, $^1J(^{119}Sn\text{-}^{19}F)$ = 2286 Hz.

^{19}F NMR [δ(ppm), $CDCl_3$]: -168, s.

^{1}H NMR [δ(ppm), $CDCl_3$]: 1.23 [3H, t, CH_3]; 2.95 [2H, q, CH_2]; 6.82 [1H, d, H_6];
8.12 [1H, d, H_5].

^{13}C NMR [δ(ppm), $CDCl_3$]: 10.8 [C_8]; 22.9 [C_7]; 110.4 [C_5]; 146.6 [C_2]; 155.9 [C_6];
161.8 [C_3]; 173.4 [C_4].

IR data (NaCl plates, nujol, cm^{-1}): 1609, 1548 υ(C=O); 1511 υ(C=C);
1274, 1197 υ(C-O).

Preparation of $(hino)_2SnF_2$ (6)

The method previously used to synthesise **(4)** was utilised with hinokitiol (1.05g; 6.38mmol) in absolute ethanol (40mL) and tin difluoride (0.5g; 3.19mmol) in dry THF (50mL). Recrystallisation from a solution of chloroform (20mL), in which cyclohexane (5mL) was slowly added, yielded the product as yellow crystals suitable for X-ray crystallography (0.32g; 21%).

Analysis: Found [calc. for $C_{20}H_{22}O_4SnF_2$]: C 49.6 (49.7)%; H 4.67 (4.56)%.

Mössbauer data (mms^{-1}): IS = -0.07, QS = 0.32

^{119}Sn NMR [δ(ppm), $CDCl_3$]: -603.2, t, $^1J(^{119}Sn\text{-}^{19}F)$ = 2232 Hz.

^{19}F NMR [δ(ppm), $CDCl_3$]: -167, s.

^{1}H NMR [δ(ppm), $CDCl_3$]: 1.23 [6H, d, CH_3]; 2.97 [1H, sept, H_8];
7.41 [1H, s, H_7]; 7.65-7.77[3H, m, H_3, H_4, H_5].

^{13}C NMR [δ(ppm), $CDCl_3$]: 23.4 [C_9]; 39.2 [C_8]; 127.3 [C_7],
$^{3}J(^{119}Sn\text{-}^{13}C)$ = 38.5 Hz; 128.3 [C_3],
$^{3}J(^{119}Sn\text{-}^{13}C)$ = 38.5 Hz; 132.4 [C_5]; 140.8 [C_4];
164.9 [C_6]; 171.4 [C_2], 171.8 [C_1],

IR data (NaCl plates, nujol, cm^{-1}): 1582 υ(C=O); 1511 υ(C=C); 1239, 1186 υ(C-O).

Preparation of stannocene, Cp_2Sn (7)

Sodium cyclopentadienide (47mL; 94mmol) was added to a solution of tin dichloride (9.48g; 50mmol) in dry THF (100mL) under nitrogen in a 2:1 ratio. The mixture was stirred and refluxed for one hour before removing the solvent *in vacuo.* Hexane (100mL) was then added to the solid obtained and stirred overnight. The solution was filtered through a canula and once the solvent removed *in vacuo*, yielded a yellow solid (3.97g; 32%).

Analysis: Found [calc. for $C_{10}H_{10}Sn$]: C 46.1 (48.3)%; H 4.02 (4.05)%.

Preparation of tin(II) methoxide and tin(II) butoxide (12) & (13)

Tin(II) alkoxides were prepared following a literature procedure.[38] Tin(II) methoxide was prepared using tin dichloride (12.16g; 64.10mmol), triethylamine (20mL) and dry methanol (200mL) under nitrogen. The white precipitate obtained was washed twice with methanol and then with diethylether to remove the amine salt. Then the tin(II) methoxide was added to a mixture of dry toluene (200mL) and dry butanol (9.5mL) where upon it is solubilised. The solvent was removed *in vacuo* and yielded a white solid (18.70g; 59%). The solution of **(13)** was used without isolation of the tin(II) butoxide.

Mössbauer data (mms^{-1}) for **(12)**: IS = 2.85, QS = 2.07

Preparation of $(ma)_2Sn$ (8)

Method 1 via tin alkoxides:

A solution of maltol (10.46g; 83.01mmol) in dry toluene (100mL) was added to a well-stirred solution of **(13)** (10.98g; 41.51mmol) in dry toluene (200mL) under nitrogen. The solution was stirred for two hours. The solution was left at room temperature and yielded pale yellow crystals suitable for X-ray crystallography (6.02g; 39%).

Analysis: Found [calc. for $C_{12}H_{10}O_6Sn$]: C 39.0 (39.0)%; H 2.75 (2.71)%.

Mössbauer data (mms^{-1}): IS =2.96, QS = 1.99

^1H NMR [δ(ppm), $CDCl_3$]: 2.39 [3H, s, CH_3]; 6.83 [1H, d, H_6],
$J(^1H\text{-}^1H) = 5.13$ Hz; 8.35 [1H, d, H_5],
$J(^1H\text{-}^1H) = 5.13$ Hz.

^{13}C NMR [δ(ppm), $CDCl_3$]: 15.5 [C_7]; 111.8 [C_5]; 148.2 [C_2]; 153.8 [C_3]; 155.6 [C_6]; 177.7 [C_4].

IR data (NaCl plates, nujol, cm^{-1}): 1570 υ(C=O); 1504 υ(C=C); 1265, 1199 υ(C-O).

Method 2 via stannocene:

A solution of maltol (0.96g; 7.59mmol) in dry ether (60mL) was added to a well-stirred solution of **(7)** (0.72g; 3.79mmol) in dry ether (100mL) under nitrogen in 2:1 ratio. The solution took a light yellow colour and was then stirred for two hours. The solvent was removed *in vacuo* and yielded a yellow solid (0.97g; 69%). Recrystallisation from common organic solvents was difficult due to the low solubility of the isolated material.

Analysis: Found [calc. for $C_{12}H_{10}O_6Sn$]: C 40.6 (39.0)%; H 3.32 (2.71)%.

Mössbauer data (mms^{-1}): IS = 2.98, QS = 2.03

Preparation of $(Etma)_2Sn$ (9)

Method 1 via tin alkoxides:

The method described previously for **(8)** was utilised with ethyl maltol (14.00g; 100.00mmol) in dry toluene (50mL) and **(13)** (13.23; 50.00mmol) in dry toluene (200mL). This yielded the compound as a pale yellow solid (13.06g; 66%).

Analysis: Found [calc. for $C_{14}H_{14}O_6Sn$]: C 42.4 (42.3)%; H 3.61 (3.53)%.

Mössbauer data (mms^{-1}): IS = 3.01, QS = 2.01

^1H NMR [δ(ppm), $CDCl_3$]: 1.08 [3H, t, CH_3]; 2.75 [2H, q, CH_2]; 6.57 [1H, d, H_6]; $J(^1H\text{-}^1H) = 5.27$ Hz; 7.76 [1H, d, H_5]; $J(^1H\text{-}^1H) = 4.98$s Hz.

^{13}C NMR [δ(ppm), $CDCl_3$]: 11.2 [C_8]; 22.4 [C_7]; 111.9 [C_5]; 153.0 [C_2]; 154.9 [C_6]; 158.8 [C_3]; 178.1 [C_4].

IR data (NaCl plates, nujol, cm^{-1}): 1564 υ(C=O); 1509 υ(C=C); 1261, 1191 υ(C-O).

Method 2 via stannocene:

The method described previously for **(8)** was utilised with ethyl maltol (1.03g; 7.38mmol) in dry ether (40mL) and **(7)** (0.70g; 3.69mmol) in dry ether (100mL). This yielded the compound as a yellow solid (0.43g; 29%).

Analysis: Found [calc. for $C_{14}H_{14}O_6Sn$]: C 42.4 (42.3)%; H 3.57 (3.53)%.

Mössbauer data (mms^{-1}): IS = 3.04, QS = 2.02

Preparation of $(hino)_2Sn$ (10)

Hinokitiol (0.50 g; 3.04 mmol) in ethanol (10 mL) was added to a well stirred solution of tin(II) chloride dihydrate (0.34g; 1.52 mmol) in water (20 mL) under nitrogen. The water was previously degassed for one hour. A precipitate appeared after 30 minutes and the solution was stirred for further hour. The solution was canula filtered and **8** dried under *in vacuo* (0.38 g, 56%).

Analysis: Found [calc. for $C_{20}H_{22}O_4Sn$]: C 54.2 (53.9)%; H 5.01 (4.95)%.

Mössbauer data (mms^{-1}): IS = 2.84, QS = 1.92

^1H NMR [δ(ppm), $CDCl_3$]: 1.21 [6H, d, CH_3]; 2.83 [1H, sept, H_8]; 6.94 [1H, s, H_7]; 7.26-7.43 [3H, m, H_3, H_4, H_5].

^{13}C NMR [δ(ppm), $CDCl_3$]: 23.7 [C_9]; 39.1 [C_8]; 125.2 [C_7]; 126.4 [C_3];
127.1 [C_5]; 138.0 [C_4]; 160.8 [C_6]; 177.0 [C_2];
177.5 [C_1].

IR data (NaCl plates, nujol, cm^{-1}): 1601 υ(C=O); 1524 υ(C=C); 1240, 1179 υ(C-O).

Method 2 via stannocene:

The methodology described for **(8)** was employed with hinokitiol (1.21g; 7.38mmol) in dry ether (40mL) and **(7)** (0.70g; 3.69mmol) in dry ether (100mL). A yellow product was obtained (0.69g; 42%).

Analysis: Found [calc. for $C_{20}H_{22}O_4Sn$]: C 55.0 (53.9)%; H 5.30 (4.95)%.

Mössbauer data (mms^{-1}): IS = 2.93, QS = 1.96

Preparation of $(trop)_2Sn$ (11)

Method 1 via tin alkoxides:

The method described previously for **(8)** was utilised with tropolone (1.00g; 8.15mmol) in dry toluene (20mL) and **(13)** (1.08g; 4.09mmol) in dry toluene (80mL). This yielded the compound as a pale yellow solid (0.55g; 37%).

Analysis: Found [calc. for $C_{14}H_{10}O_4Sn$]: C 46.6 (46.6)%; H 3.00 (2.77)%.

Mössbauer data (mms^{-1}): IS = 2.91, QS = 1.98

^{1}H NMR [δ(ppm), $CDCl_3$]: 7.14-7.64 (m, 5H, C_7H_5)

^{13}C NMR [δ(ppm), $CDCl_3$]: 124.3 [C_3]; 126.8 [C_4]; 139.7 [C_2]; 178.6 [C_1].

IR data (NaCl plates, nujol, cm^{-1}): 1593 υ(C=O); 1509 υ(C=C); 1254 υ(C-O).

Method 2 via stannocene:

The method described previously for **(8)** was utilised with tropolone (0.5g; 4.07mmol) in dry ether (20mL) and **(7)** (0.38g; 2.03mmol) in dry ether (100mL). This yielded the compound as a yellow solid (0.21g; 29%).

Analysis: Found [calc. for $C_{14}H_{10}O_4Sn$]: C 53.4 (46.6)%; H 3.44 (2.77)%.

Mössbauer data (mms^{-1}): IS = 2.90, QS = 1.99

Preparation of $(koj)_2Sn$ (14)

The methodology described for **(8)** was employed with kojic acid (0.82; 5.79mmol) in dry toluene (60mL) and **(13)** (0.76g; 2.88mmol) in dry toluene (80mL). A yellow product was obtained (0.52g; 45%). The solid was not soluble in any common organic solvents, so recrystallisation was impossible and no NMR study has beencarried out.

Analysis: Found [calc. for $C_{12}H_{10}O_6Sn$]: C 37.9 (41.7)%; H 2.85 (2.77)%.

Mössbauer data (mms^{-1}): IS = 3.11, QS = 1.95

IR data (NaCl plates, nujol, cm^{-1}): 3269 υ(O-H); 1572 υ(C=O); 1521 υ(C=C); 1261, 1147 υ(C-O).

Preparation of $(ma)_2Zn.2H_2O$ (15)

The method described by P. Wright[39] was repeated. A solution of maltol (1.27g; 10.00mmol) in a water/ethanol mix (25mL/25mL) was added to a well-stirred solution of zinc acetate (1.09g; 4.96mmol) in a water/ethanol mix (25mL/25mL). After stirring for two hours, the solution was refluxed and stirred for another two hours and then left at room temperature. A pale yellow crystalline product appeared (0.79g; 45%).

Analysis: Found [calc. for $C_{12}H_{14}O_8Zn$]: C 39.8 (40.9)%; H 4.19 (3.98)%.

^1H NMR [δ(ppm), $CDCl_3$]: 2.34 [3H, t, CH_3]; 6.54 [1H, d, H_6]; 8.12 [1H, d, H_5].

^{13}C NMR [δ(ppm), $CDCl_3$]: 14.8 [C_7]; 109.8 [C_5]; 149.8 [C_2]; 151.7 [C_3]; 153.6 [C_6]; 177.6 [C_4].

IR data (NaCl plates, nujol, cm^{-1}): 3500 broad υ(H-O-H), 1614, 1578 υ(C=O); 1517 υ(C=C); 1277, 1202 υ(C-O).

Preparation of $(Etma)_2Zn.2H_2O$ (16)

Following this procedure **(16)** was obtained using ethyl maltol (2.00g; 14.28mmol) in a water/ethanol mix (25mL/25mL) and zinc acetate (1.57g; 7.15mmol) in a water/ethanol mix (25mL/25mL). This yielded a beige solid (0.79g; 45%).

Analysis: Found (calc. for $C_{14}H_{18}O_8Zn$): C 44.5 (44.3)% H 4.83 (4.74)%.

^1H NMR [δ(ppm), $CDCl_3$]: 1.16 [3H, t, CH_3]; 2.79 [2H, q, CH_2]; 6.55 [1H, d, H_6]; 8.16 [1H, d, H_5].

^{13}C NMR [δ(ppm), $CDCl_3$]: 11.4 [C_8]; 21.4 [C_7]; 109.7 [C_5]; 151.0 [C_2]; 153.7 [C_6]; 154.1 [C_3]; 177.9 [C_4].

IR data (NaCl plates, nujol, cm^{-1}): 3480 broad υ(H-O-H), 1595, 1570 υ(C=O); 1508 υ(C=C); 1280, 1193 υ(C-O).

Preparation of $(hino)_2Zn$ (17)

Following the same procedure than for **(15)**, **(17)** was obtained using hinokitiol (0.20g; 1.22mmol) in a water/ethanol mix (25mL/25mL) and zinc acetate (0.12g; 6.11mmol) in a water/ethanol mix (25mL/25mL). This yielded yellow crystals (0.19g; 80%).

Analysis: Found [calc. for $C_{20}H_{22}O_4Cu$]: C 61.9 (61.6)%; H 5.72 (5.65)%.

^{1}H NMR [δ(ppm), DMSO(d^6)]: 1.23 [6H, d, CH_3]; 2.96 [1H, sept, H_8]; 7.35 [1H, s, H_7]; 7.64-7.76 [3H, m, H_3, H_4, H_5].

^{13}C NMR [δ(ppm), DMSO(d^6)]: 23.6 [C_9]; 39.4 [C_8]; 127.1 [C_7], $^3J(^{119}Sn\text{-}^{13}C)$ = 35.5 Hz; 128.2 [C_3], $^3J(^{119}Sn\text{-}^{13}C)$ = 35.5 Hz; 131.9[C_5]; 140.6 [C_4]; 164.7 [C_6]; 171.3 [C_2]; 171.7 [C_1].

IR data (NaCl plates, nujol, cm^{-1}): 1589 υ(C=O); 1506 υ(C=C); 1236 υ(C-O).

Preparation of $(trop)_2Zn$ (21)

The method described previously for **(15)** was utilised for tropolone (0.50g; 4.09mmol) in a water/ethanol mix (5mL/5mL) added to zinc acetate (0.45g; 2.05mmol) in a water/ethanol mix (25mL/25mL). Following this procedure, yellow crystals suitable for X-ray crystallography were obtained (0.56g; 89 %).

Analysis: Found [calc. for $C_{14}H_{10}O_4Zn$]: C 54.2 (54.8)%; H 3.33 (3.26)%.

IR data (NaCl plates, nujol, cm^{-1}): 1620, 1582 υ(C=O); 1523 υ(C=C); 1265, 1213 υ(C-O).

Preparation of (kojic acid)$_2$Zn (22)

The methodology described for **(15)** was employed with kojic acid (0.50; 3.52mmol) in a water/ethanol mix (5mL/5mL) and zinc acetate (0.39g; 1.76mmol) in a water/ethanol mix (25mL/25mL). A white product was obtained (0.50g; 82%). The solid was not soluble in any common organic solvents, so no NMR study has been possible.

Analysis: Found [calc. for $C_{12}H_{10}O_6Zn$]: C 41.2 (41.4)%; H 3.05 (2.88)%.

IR data (NaCl plates, nujol, cm^{-1}): 3500 broad υ(O-H), 1614, 1578 υ(C=O); 1517 υ(C=C); 1277, 1202 υ(C-O).

Preparation of (ma)$_2$Cu (18)

The methodology previously used by P. Wright was utilised.[39] A solution of maltol (0.50g; 3.97mmol) in a water/ethanol mix (25mL/25mL) was added to a well-stirred solution of copper acetate (0.39g; 1.95mmol) in a water/ethanol mix (50mL/50mL). After stirring for two hours, the solution was refluxed and stirred for another two hours and then left at room temperature. A pale green product appeared (0.57g; 91%).

Analysis: Found [calc. for $C_{12}H_{10}O_6Cu$]: C 45.7 (45.9)%; H 3.18 (3.19)%.

IR data (NaCl plates, nujol, cm^{-1}): 1612, 1573 υ(C=O); 1513 υ(C=C); 1279, 1213 υ(C-O).

Preparation of (Etma)$_2$Cu (19)

The method described previously for **(18)** was utilised for ethyl maltol (2.00g; 14.28mmol) in a water/ethanol mix (25mL/25mL) was added to copper acetate (1.43g; 7.16mmol) in a water/ethanol mix (100mL/100mL). A pale green solid was obtained (2.34g; 98%).

Analysis: Found [calc. for $C_{14}H_{14}O_6Cu$]: C 49.1 (49.2)%; H 4.07 (4.09)%.

IR data (NaCl plates, nujol, cm^{-1}): 1601,1562 υ(C=O); 1512 υ(C=C); 1279, 1188 υ(C-O).

Preparation of $(hino)_2Cu$ (20)

Following the same procedure as for **(18)**, **(20)** was obtained using hinokitiol (0.20g; 1.22mmol) in a water/ethanol mix (25mL/25mL) and copper acetate (0.12g; 6.11mmol) in a water/ethanol mix (25mL/25mL). This yielded dark green crystals (0.19g; 80%).

Analysis: Found [calc. for $C_{20}H_{22}O_4Cu$]: C 61.9 (61.6)%; H 5.72 (5.65)%.

IR data (NaCl plates, nujol, cm^{-1}) : 1589 υ(C=O); 1506 υ(C=C); 1236 υ(C-O).

Preparation of $(trop)_2Cu$ (23)

The method described for **(18)** was repeated with tropolone (0.50g; 4.09mmol) in a water/ethanol mix (5mL/5mL) added to copper acetate (0.41g; 2.05mmol) in a water/ethanol mix (30mL/30mL). A pale green solid was obtained (0.53; 85%).

Analysis: Found [calc. for $C_{14}H_{10}O_4Cu$]: C 55.3 (54.9)%; H 3.29 (3.27)%.

IR data (NaCl plates, nujol, cm^{-1}): 1601,1562 υ(C=O); 1512 υ(C=C); 1279, 1188 υ(C-O).

Preparation of $(koj)_2Cu$ (24)

The methodology described for **(18)** was employed with kojic acid (0.50; 3.52mmol) in a water/ethanol mix (5mL/5mL) and copper acetate (0.35g; 1.76mmol) in a water/ethanol mix (50mL/50mL). A pale green product was obtained (0.54g; 89%). The solid was not soluble in any common organic solvents, so recrystallisation to purify it was not possible.

Analysis: Found [calc. for $C_{12}H_{10}O_6Cu$]: C 37.9 (41.7)%; H 2.85 (2.89)%.

IR data (NaCl plates, nujol, cm^{-1}): 1601,1562 υ(C=O); 1512 υ(C=C); 1279, 1188 υ(C-O).

Preparation of $(hino)_2Cu$.(pyridine) complex (25)

Pyridine (5mL) was added to a solution of **(20)** (0.30g, 0.77mmol) in toluene (30mL). After stirring for twenty minutes, the solution was put in the freezer and a green solid appeared (0.06g; 17%). Some crystals suitable for X-ray crystallography were obtained.

Analysis: Found [calc. for $C_{25}H_{27}NO_4Cu$]: C 63.7 (64.0)%; H 5.79 (5.76)%;
N 2.85 (2.98)%.

IR data (NaCl plates, nujol, cm^{-1}): 1583, 1569 υ(C=O); 1496 υ(C=C);
1261,1231υ(C-O).

Preparation of (hino)$_2$Cu.(bipyridine) complex (26)

Bipyridine (1g, 6.25mmol) was dissolved in toluene (30 mL) and then added to a solution of **(20)** (0.40g, 1.03mmol) in toluene (50mL). The mixture was stirred for twenty minutes and then left at room temperature for few days, yielding a brown solid (0.44g, 78%).

Analysis: Found [calc. for $C_{30}H_{30}N_2O_4Cu$]: C 65.5 (65.9)%; H 5.48 (5.49)%;
N 5.83 (5.13)%.

IR data (NaCl plates, nujol, cm^{-1}): 1594, 1554 υ(C=O); 1511 υ(C=C);
1278,1199 υ(C-O).

2.5 References

1) Cavalieri L. F., *Chem. Rev.* **1947**, *41*, 525.
2) Ahmet M. T.; Frampton C. S.; Silver J., *J. Chem. Dalton Trans.* **1988**, 1159.
3) Finnegan M. M.; Rettig S. J.; Orvig C., *J. Am. Chem. Soc.* **1986**, *108*, 5033.
4) Finnegan M. M.; Lutz T. G.; Nelson W. O.; Smith A.; Orvig C., *Inorg. Chem.* **1987**, *26*, 2171.
5) Orvig C.; Rettig S. J.; Trotter J., *Can. J. Chem.* **1987**, *65*, 590.
6) Caravan P.; Gelmini L.; Glover N.; Herring F. G.; Li H.; McNeill J. H.; Rettig S. J.; Setyawati I. A.; Shuter E.; Sun Y.; Tracey A. S.; Yuen V. G.; Orvig C., *J. Am. Chem. Soc.* **1995**, *117*, 12759.
7) Luo H.; Rettig S. J.; Orvig C., *Inorg. Chem.* **1993**, *32*, 4491.
8) Ellis B. L.; Duhme A. K.; Hider R. C.; Bilayet-Hossein M.; Rizvi S.; Van-Der-Helm D., *J. Med. Chem.* **1996**, *39*, 3659.
9) Ahmed S.; Burgess J.; Hurman B.; Parsons S. A., *Polyhedron* **1994**, *13*, 23.
10) Cabanes J.; Chazarra S.; Garcia-Carmona F., *J. Pharm. Pharmacol.* **1994**, *46*, 982.
11) Langer H. G., *US Patent* **1990**, 3 227 707.
12) Matsuba C. A.; Nelson W. O.; Rettig S. J.; Orvig C., *Inorg. Chem.* **1988**, *27*, 3935.
13) Nozoe T., *Bull. Chem. Soc. Jpn.* **1936**, *11*, 295.
14) Takasago, *Takasago product literature.*
15) Nakasei, *Dental Outlook* **1958**, *15*, 1070.
16) Sato, *Dental Outlook* **1959**, *16*, 80.
17) Kudo, *Dental Outlook* **1970**, *36*, 743.
18) Yamashiki, *Patent JP* **1963**, 63-26498.
19) Isobe, *Patent JP* **1979**, 79-43054.
20) Taisho, P., *Patent JP* **1984**, 59-210010.
21) Takenaka, *Food Ind.* **1959**, 2, 51.
22) Takahashi, *Patent JP* **1975**, 75-40725.
23) Taisho, P., *Patent JP* **1974**, 74-85230.
24) Hikari-Kogyo, *Patent JP* **1969**, 69-20480.

25) Abrahams I.; Choi N.; Henrick K.; Joyce H.; Matthews R. W.; McPartlin M., *Polyhedron* **1994**, *13*, 513.

26) Avdeef A.; Costamagna J. A.; Fackler J. P., *Inorg. Chem.* **1974**, *13*, 1854.

27) Davis A. R.; Einstein F. W. B., *Inorg. Chem.* **1974**, *13*, 1880.

28) Griffin R. T.; Henrick K.; Matthews R. W.; McPartlin M., *J. Chem. Soc. Dalton Trans.* **1980**, 1550.

29) Lewinski J.; Zachara J.; Justyniak I., *Organometallics* **1997**, *16*, 4597.

30) Ware D. C.; Palmer H. R.; Brothers P. J.; Richard C. E. F.; Wilson W. R.; Denny W. A., *J. Inorg. Biochem.* **1997**, 215.

31) Stepanov A. G., *J. Organomet. Chem.* **1989**, *361*, 157.

32) Denekemp C. I. F.; Evans D. F.; Slawin A. M. Z.; Williams D. J.; Wong C. Y.; Woolins J. D., *J. Chem. Soc, Dalton Trans.* **1992**, 2375.

33) Alshehri S.; Burgess J.; Fawcett J.; Parsons S. A.; Russell D. R., *Polyhedron* **2000**, 19, 399.

34) Greaves S. J.; Griffith W. P., *Polyhedron* **1988**, *7*, 1973.

35) Bhattacharya S.; Seth N.; Gupta V. D.; Noth H.; Polborn K.; Tomann M.; Schwenk H., *Chem. Ber.* **1994**, *127*, 1895.

36) Al-Juaid S. S.; Dhaher S. M.; Earborn C.; Hitchcock P. B.; Smith J. D., *J. Organomet. Chem.* **1987**, *325*, 117.

37) *Chemistry of Tin*; P. J. Smith ed.; Blackie Academic & Professional: London, **1998**.

38) Gsell R.; Zeldin M., *J. Inorg. Nucl. Chem.* **1975**, *37*, 1133.

39) Wright P. *The synthesis and characterisation of novel Sn(II), Zn(II) and Cu(II) compounds for anti-bacterial evaluation*; University of Bath, **1999**.

40) Irving R. J.; Post M. L.; Povey D. C., *J. Chem. Soc., Dalton Trans.* **1973**, 697.

41) Berg J.; Pilotti A.; Soderholm A.; Karlsson B., *Acta Cryst.* **1978**, *B34*, 3071.

42) Carugo O.; Castellani C. B.; Rizzi M., *Polyhedron* **1990**, *9*, 2061.

Chapter III

3.1 Introduction to 1,2-dialkyl-3-hydroxypyridin-4-ones

Once all the ligands directly available from commercial sources had been combined with the metals, the focus was more on trying to synthesise new ligands. Different 1,2-dialkyl-3-hydroxypyridin-4-ones have been made (Figure 3.1) with the aim of varying the alkyl group (R') of the amine in order to assess its effect on the anti-bacterial activity of the metal derivatives.

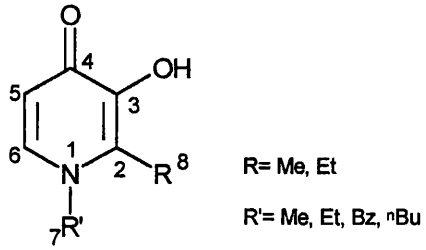

Figure 3.1: 1,2-dialkyl-3-hydroxypyridin-4-ones, including atom numbering.

Derivatives of hydroxypyridin-4-ones have been studied intensively due to their ability to form strong complexes with metals and their good oral bioavailability. 1-alkyl-3-hydroxypyridin-4-ones have shown medicinal potential as anti-tumour agents,[1,2] but their mechanism of action has yet to be established.

L-mimosine (a 3-hydroxypyridin-4-one amino acid derivative) was one of the first pyridinones to be studied. It has been used as a defleecing agent for sheep and has also shown depilatory properties.[3,4]

Hydroxypyridin-4-ones can be administrated orally and are water soluble, therefore they have been used as chelating agents in iron related diseases.[5] Iron is toxic when present in excess in the body and must be removed by chelation. Hdmp is known to form a complex with Fe^{3+} and is used in the treatment of Fe-overload diseases.[6] Hmep is another promising chelating agent for the treatment of iron overload in transfusion dependent thalassaemia patients.[7]

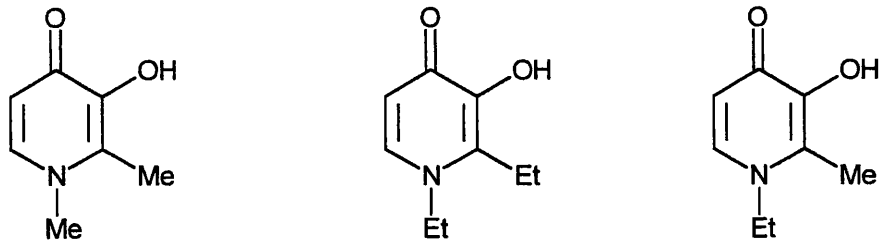

Figure 3.2: Structure of Hdmp, Hdep and Hmep.

Orvig *et al* have shown significant interest in maltol (*cf.*: Chapter II) and also hydroxypyridinones as binding groups for various metal ions.[8-10] Complexes with aluminium and gallium have shown to have the same properties as $Al(ma)_3$[9]: water solubility, hydrolytic stability and lipophilicity.[11] So Al and Ga complexes of this type of ligand could find considerable medical applications (Alzheimer's disease, tumour detection, etc).[12,13]

Orvig *et al* have prepared and characterised aluminium, gallium and indium complexes of various pyridinones in a one-pot-synthesis, by mixing together maltol, an amine and the appropriate metal(III) salt.[14,15] Neutral and anionic technetium complexes of the form $Tc(O)XL_2$ (where L= Hdmp and X= Cl) have also been synthesised by Orvig *et al* and shown to have potential use in brain and heart imaging.[16]

3.2 Results and Discussion: Copper(II) and Zinc(II) compounds

3.2.1 Synthesis of 1,2-alkyl-3-hydroxypyridin-4-ones

The method for the preparation of the 1,2-alkyl-3-hydroxypyridin-4-ones used either maltol or ethylmaltol as starting materials.[17] Although several methods for the preparations of these ligands have been reported[11,14,15,18] the one chosen was a direct one-step preparation (Scheme 3.1). The yields (14%-45%) are lower than those from the other methods, but maltol and ethylmaltol are both relatively cheap starting materials. Four different amines have been used: methylamine; ethylamine; benzylamine and ^{n}butylamine.

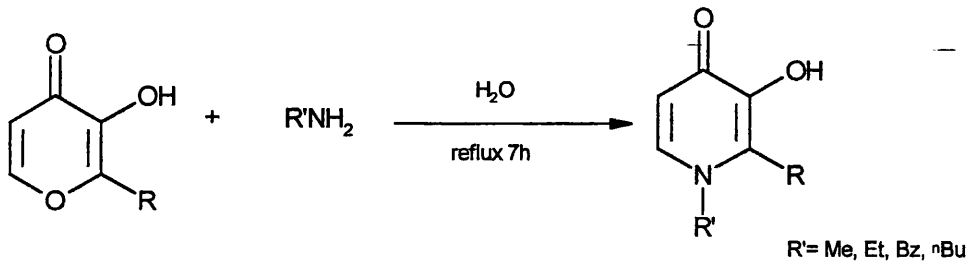

R'= Me, Et, Bz, ^{n}Bu

R= Me, Et

R'=	Me	Et	Bz	^{n}Bu
R= Me	**(27)**	**(28)**	**(29)**	**(30)**
R= Et	**(31)**	**(32)**	**(33)**	**(34)**

Scheme 3.1: Synthesis of 1,2-alkyl-3-hydroxypyridin-4-ones.

The ligands were recrystallised from hot water and were then used to prepare the Cu(II) and Zn(II) complexes (Scheme 3.2). **(27)**, **(28)** and **(30)–(33)** are known compounds, while **(29)** and **(34)** have been synthesised for the first time. The identity of the compounds was confirmed by elemental analysis, IR (Table 3.1) and ^{1}H and ^{13}C NMR.

Table 3.1: Infrared absorptions (cm^{-1}) for some ligands.

Compound	υ(C=O) & υ(C=C)	υ(C–N)	Reference
Maltol	1650, 1610, 1550	-	19
Hdmp	1630, 1560, 1520, 1495	1250	11
Hmep	1630, 1575, 1530, 1510	-	20
(27)	1629, 1567, 1529	1232	This work
(28)	1625, 1566, 1528	1227	This work
(29)	1627, 1576, 1526	1239	This work
(30)	1624, 1569, 1528	1234	This work
(31)	1624, 1570, 1521	1223	This work
(32)	1619, 1575, 1529	1236	This work
(33)	1620, 1548, 1529	1223	This work
(34)	1621, 1572, 1523	1238	This work

3.2.2 Synthesis of copper(II) and zinc(II) complexes

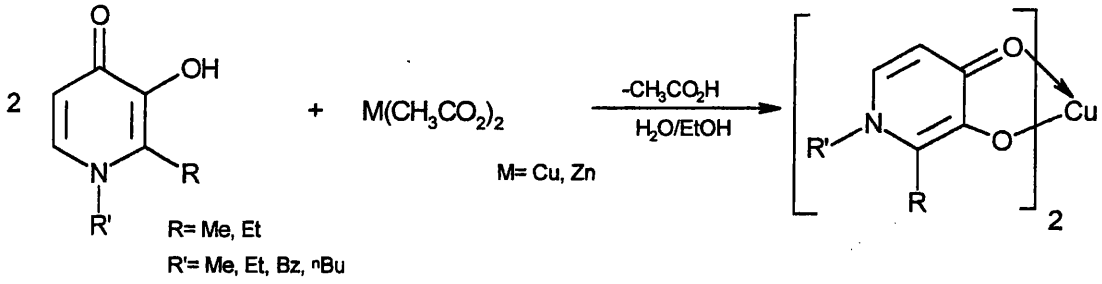

R= Me; R′=	Me	Et	Bz	^{n}Bu
Cu(II)	**(35)**	**(36)**	**(37)**	**(38)**
Zn(II)	**(39)**	**(40)**	**(41)**	**(42)**

R= Et; R′=	Me	Et	Bz	^{n}Bu
Cu(II)	**(43)**	**(44)**	**(45)**	**(46)**
Zn(II)	**(47)**	**(48)**	**(49)**	**(50)**

Scheme 3.2: Synthesis of CuL_2 and ZnL_2.

All the complexes **(35)-(50)** have been successfully synthesised and the crystal structures of **(41)**, **(45)**, **(46)** and **(47)** have been completed.

The elemental analysis confirms the nature of the complexes. The infrared spectra are consistent with those of related metal derivatives found in the literature and are summarized in Table 3.2.

Table 3.2: Infrared absorptions (cm^{-1}) for ML_2 (L=pyridinone, M=Cu, Zn).

Compound	υ(C=O) & υ(C=C)	Reference
(35)	1619, 1552, 1500, 1491	This work
(36)	1611, 1554, 1518, 1496	This work
(37)	1612, 1556, 1523, 1488	This work
(38)	1603, 1550, 1520, 1492	This work
(39)	1607, 1550, 1517, 1495	This work
(40)	1598, 1558, 1523, 1491	This work
(41)	1598, 1542, 1506, 1483	This work
(42)	1603, 1540, 1513, 1491	This work
(43)	1609, 1558, 1517, 1496	This work
(44)	1599, 1552, 1514, 1493	This work
(45)	1620, 1564, 1518, 1490	This work
(46)	1598, 1551, 1518, 1486	This work
(47)	1589, 1538, 1516, 1496	This work
(48)	1591, 1542, 1508, 1495	This work
(49)	1595, 1544, 1510, 1497	This work
(50)	1597, 1542, 1515, 1494	This work
$Tc(O)Cl(dmp)_2$	1615, 1555, 1505, 1495	16
$In(dmp)_3$	1605, 1550, 1505, 1490	21
$Al(dmp)_3$	1605, 1560, 1520, 1495	22
$Al(mep)_3$	1600, 1555, 1515, 1490	20
$Ga(dmp)_3$	1605, 1555, 1510, 1490	22

The ν(O–H) mode is absent for all the complexes and the ν(C=O) band in the starting materials is shifted to a lower wavenumber by around 30-70 cm^{-1} in the complexes. This is good evidence for the formation of the metal complexes by chelation *via* the two oxygen atoms.

The ^{1}H and ^{13}C NMR spectra were recorded for **(39)–(42)** and **(47)–(50)** in deuterated chloroform or water. The peaks were relatively easy to assign to the protons of the complexes (Table 3.2) and are similar to the ones for $Zn(ma)_2$ and $Zn(Etma)_2$.

Table 3.2: ^{1}H NMR data for ZnL_2 complexes.

Compound	Chemical Shift (ppm)			
	Me	Et	H_5	H_6
(39)	2.25	-	7.32	6.38
(40)	2.44	-	7.44	6.39
(41)	2.17	-	7.02	6.32
(42)	2.41	-	7.00	6.44
(47)	-	1.09, 2.83	7.35	6.20
(48)	-	1.40, 3.96	7.40	6.25
(49)	-	1.05, 2.64	7.03	6.31
(50)	-	1.21, 2.92	7.07	6.54
$Zn(ma)_2$ **(15)**	2.34	-	8.12	6.54
$Zn(Etma)_2$**(16)**	-	1.16, 2.19	8.16	6.55

Note: the chemical shifts for the N-R'groups have been omitted for clarity

The ^{13}C NMR spectra show the right number of carbons and all the peaks were assigned. The spectra are very similar to each other, apart for the data on the alkyl group attached to the nitrogen. These are now discussed in more detail. The methyl group attached to the nitrogen for **(39)** and **(47)** appeared at 16.4 and 19.2 ppm respectively. The spectra of **(40)** and **(48)** show two peaks for the N-Et group at 16.2 [CH_3] and 48.7 [CH_2] for both compounds. The spectra of **(41)** and **(49)** contain four peaks assigned to the benzyl group: 57.3 [CH_2] and 126.1, 127.7, 128.8 [CH

aromatic] for **(41)**; and 56.8 [CH_2] and 125.9, 127.6, 128.9 [CH aromatic] for **(49)**. The ^{13}C NMR spectra of **(42)** and **(50)** show four peaks belonging to the N-^{n}butyl group at 12.2 [CH_3], 19.5 [C_9H_2], 33.9 [C_8H_2], 54.4 [C_7H_2]; and 12.7 [CH_3], 19.6 [C_9H_2], 33.5 [C_8H_2], 54.3 [C_7H_2] respectively.

Recrystallisation from either hot methanol **(45)** or chloroform **(46)** gave crystals suitable for X-ray crystallography (Figures 3.1, 3.2). **(45)** and **(46)** both crystallise in the triclinic space group P-1. Other structures for $Cu(dmp)_2$ and $Cu(dep)_2$ have been obtained and cited,[23] but none of the crystallographic data has been published.

The asymmetric unit of **(45)** consists of half the copper complex molecule and one molecule of solvent (MeOH). The remainder is generated *via* the symmetry operation -x, -y, -z. The oxygen of the methanol molecule does not interact with the copper atom. However it is possible, based on the O2–O3 distance data, that there is a hydrogen bonding interaction between the alcoholic proton and O2, but this proton could not be located with certainty.

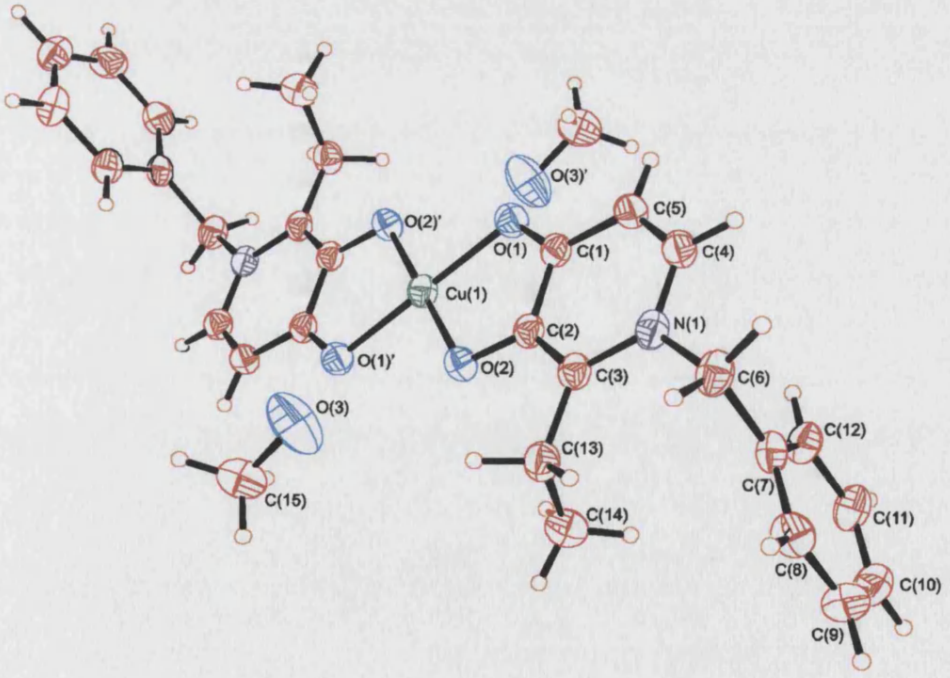

Figure 3.1: The structure of Cu(1-benzyl-2-ethyl-3-hydroxypyridin-4-one)$_2$.2MeOH ***(45)***.

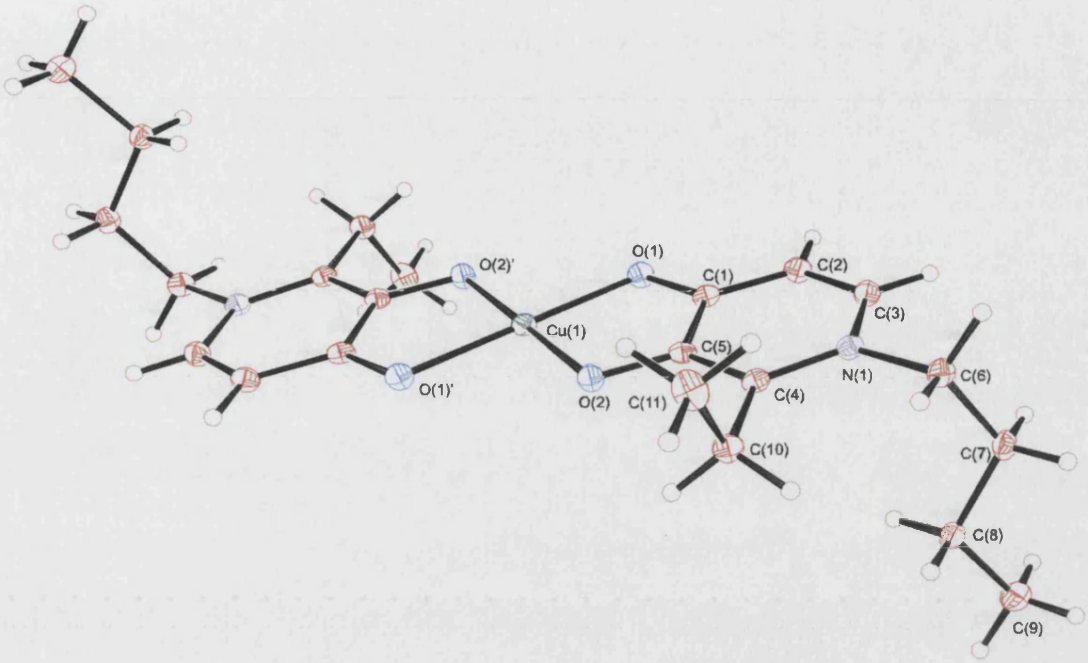

Figure 3.2: The structure of Cu(1-^{n}butyl-2-ethyl-3-hydroxypyridin-4-one)$_2$ ***(46)***.

Like for the previous structure, the asymmetric unit in **(46)** consists of half the copper complex molecule, the remainder being generated *via* the symmetry operation -x, -y, -z.

The Cu(II) complexes have the Cu atom adopting a four-coordinate, square planar geometry like other CuL_2 compounds, *e.g.*: Cu(dmp)$_2$,[23] Cu(dep)$_2$,[23] Cu(tropolone)$_2$,[24] or Cu(hinokitiol)$_2$.[25]

The [Cu-O] bond lengths in **(45)** are typical of other [Cu-O] bond lengths found in the literature (Table 3.2). However in the case of **(46)**, the [Cu←O(=C)] bond is much longer than in the other examples. Both ligands chelate the copper *via* their oxygen atoms in an anisobidentate manner, with one short [**(45)**: 1.904(2) Å; **(46)**: 1.916(1) Å] and one long [**(45)**: 1.916(2) Å; **(46)**: 2.057(1) Å] bond to the metal, this being more obvious for **(46)**.

Table 3.2: Cu-O bond length in selected metal complexes.

Compound	[Cu-O(-C)] bond / Å	[Cu←O(=C)] bond / Å	Reference
(45)	1.904(2)	1.916(2)	This work
(46)	1.916(1)	2.057(1)	This work
$Cu(dmp)_2$	1.913	1.928	23
$Cu(dep)_2$	1.913	1.923	23
$Cu(hino)_2$	1.900(2)	1.904(3)	25
$Cu(trop)_2$	1.915(3)	1.915(3)	24

As can be seen in Table 3.3, the [C-O] bond lengths in the Cu (II) compounds compare favourably with those of the other related complexes.

Table3.3: C-O bond lengths in selected copper complexes.

Compound	[C-O] bond / Å	[C=O] bond / Å	Reference
(45)	1.319(3)	1.292(3)	This work
(46)	1.328(2)	1.297(2)	This work
$Cu(dmp)_2$	1.344	1.300	23
$Cu(dep)_2$	1.383	1.309	23
$Cu(hino)_2$	1.296(5)	1.293(5)	25
$Cu(trop)_2$	1.302(5)	1.286(5)	24

The zinc products **(41)** and **(47)** were recrystallised from hot water, resulting in the formation of crystals suitable for X-ray crystallography. They both crystallise in the triclinic space group P-1.

The structure of **(41)** (Figure 3.3) is very similar to the one of $Pb(dmp)_2.7H_2O$[26] (Figure 3.4).

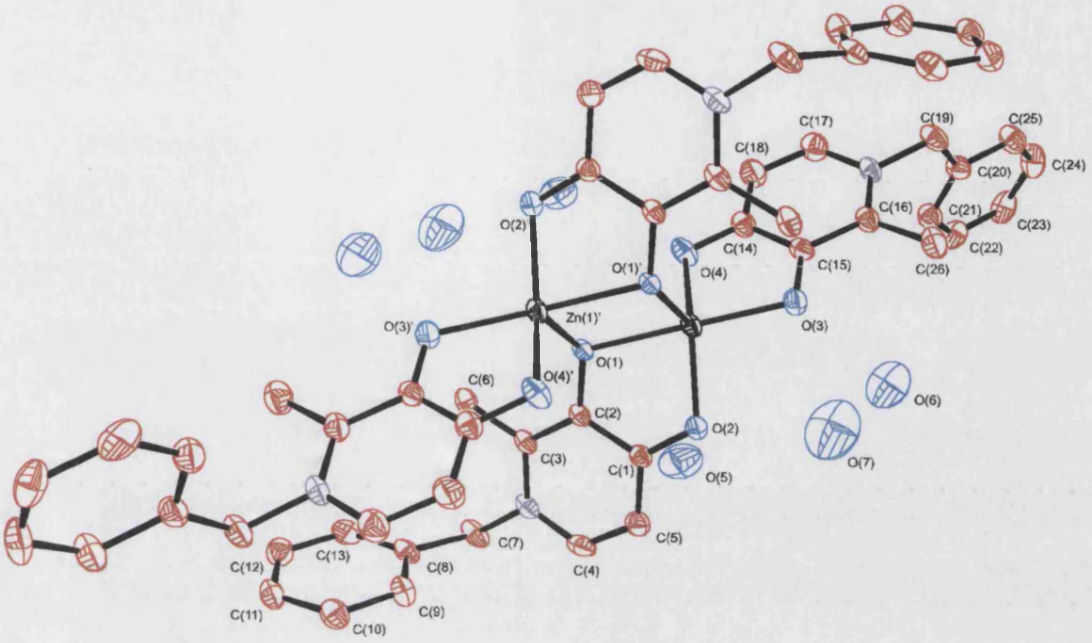

Figure 3.3: The structure of Zn(1-benzyl-2-methyl-3-hydroxypyridin-4-one)$_2$ ***(41)***.

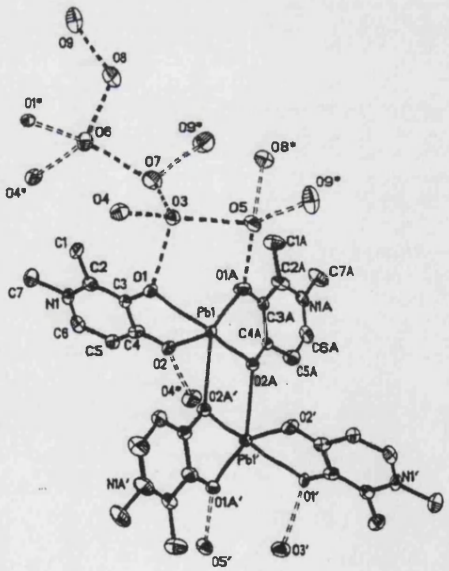

Figure 3.4: The structure of Pb(dmp)$_2$.[26]

In both compounds, the metal ion is five-coordinate and forms a dimer. Water molecules, which are hydrogen bonded to each other, form a polymer for **(41)** (Figure 3.5).

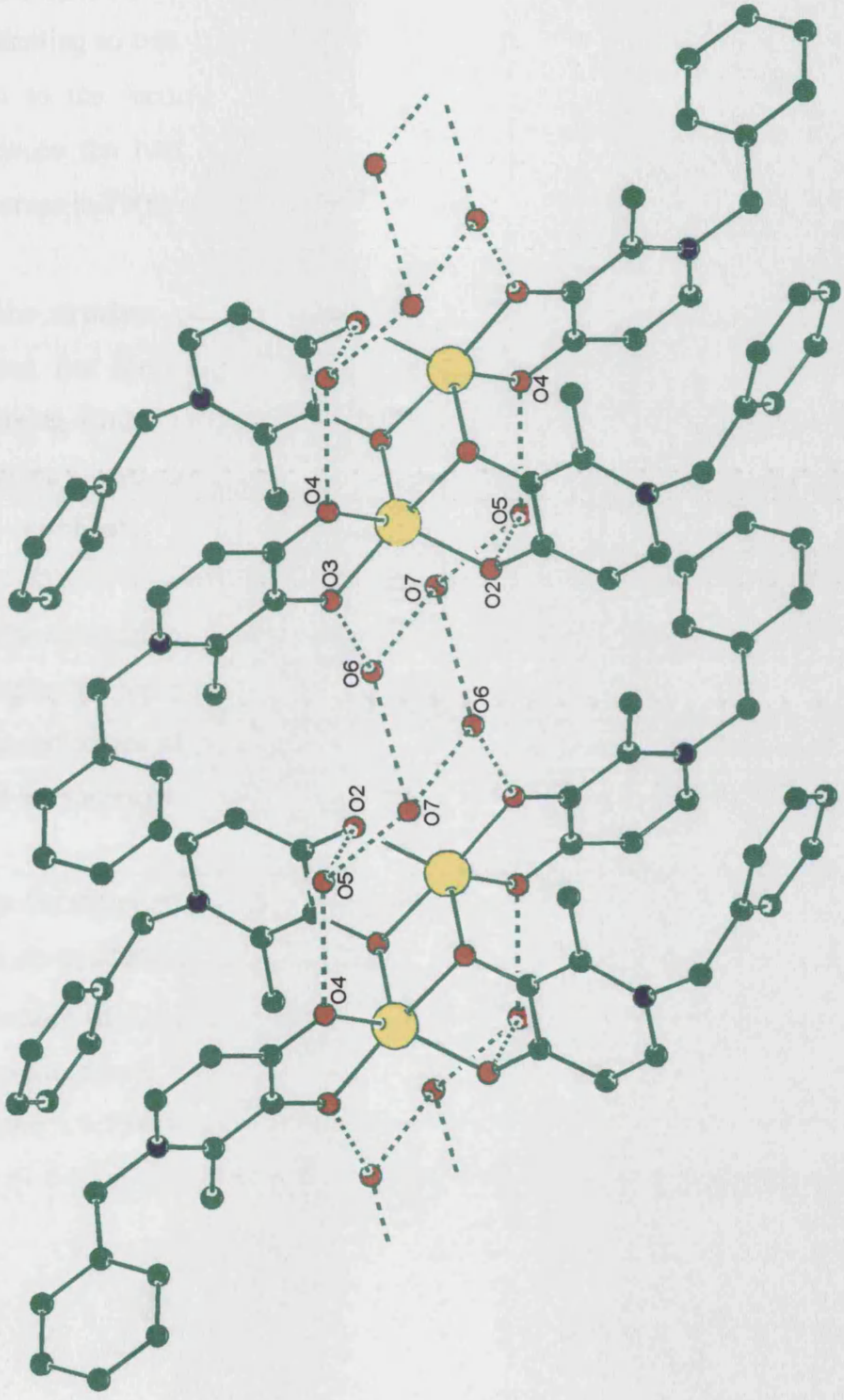

Figure 3.5: The extended structure of ***(41)***.

(Note: the hydrogens could not be reliably located and do not appear in the figure.)

The Zn(II) complex **(41)** has solvent (six molecules of water) incorporated to it (there are seven in the lead structure), but none of them is directly bonded to the zinc atom. There are two types of ligand in the complexes of **(41)** and $Pb(dmp)_2$: one co-ordinating to one metal atom only and one co-ordinating to the first metal atom and also to the second *via* a bridging oxygen. That is where the main difference lay between the two structures. In **(41)** the bridging oxygen is the hydroxyl oxygen, whereas in $Pb(dmp)_2$, it is the carbonyl oxygen which is involved in the bridging.

The structure of **(41)** is comparable to the structure of $Zn(hino)_2$ **(17)** complex which has been described Chapter II, Section 2.3.1. In **(17)** also, one ligand is bridging while the other one is purely chelating. But unlike **(41)**, in the structure of $Zn(hino)_2$, one molecule of ethanol is coordinated to the zinc atom, so that the zinc is six-coordinate.

The structure of **(41)** can also be compared with the structure of $Zn(trop)_2$ **(21)** (*cf.*: Chapter II, Section 2.3.1) and be seen as dimeric fragment of the polymer of **(21)**. The molecules of water in **(41)** are involved in a complex hydrogen bonding pattern and are therefore breaking the extended polymer it could have formed.

In the structure of **(47)**, a molecule of water is co-ordinated to the zinc atom, so that the co-ordination number of the zinc is five (Figure 3.6). This is similar to the structure of $Zn(dmp)_2$ obtained by Burgess *et al.*[26] In this complex also, the zinc is five-coordinate with one coordinated water molecule (*cf.*: Chapter I, Section 1.7, Figure 1.7.5).

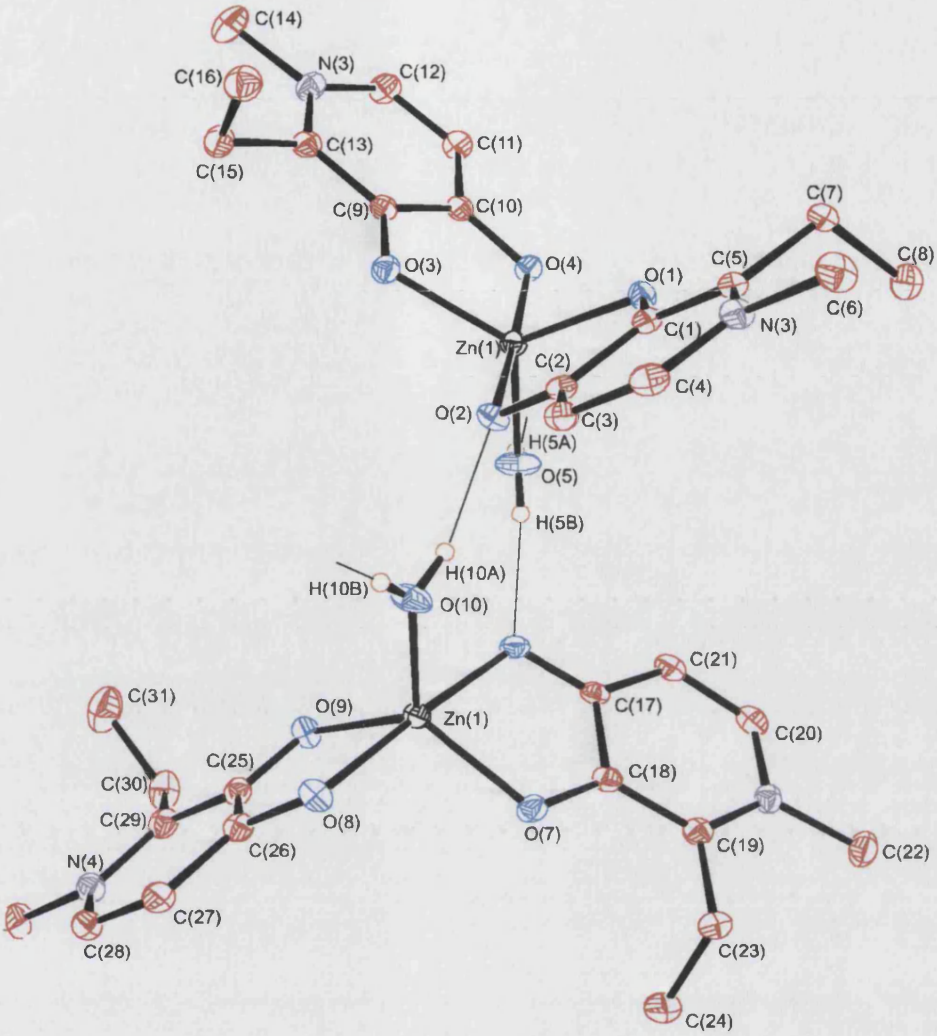

Figure 3.6: The structure of Zn(1-methyl-2-ethyl-3-hydroxypyridin-4-one)$_2$ ***(47)***.

For **(47)**, the hydrogens on the water molecules are involved in hydrogen bonding to the ligands. The result of this interaction is a one-dimensional molecular chain (Figure 3.7). Each water molecule is hydrogen bonded to two complexes *via* the carbonyl oxygen. In the structure of Zn(dmp)$_2$[26] the complex is heavily hydrated with seven waters per zinc ion. The difference to the structure of **(47)** is that in Zn(dmp)$_2$ the water molecule attached to the zinc interacts with another molecule of water and not an oxygen of the ligand. These water molecules hydrogen-bond each other and form extended chains, to block effectively the sixth coordination centre of the metal, without themselves interacting with the zinc. (This is similar to the way the six waters in **(41)** interact with each other.)

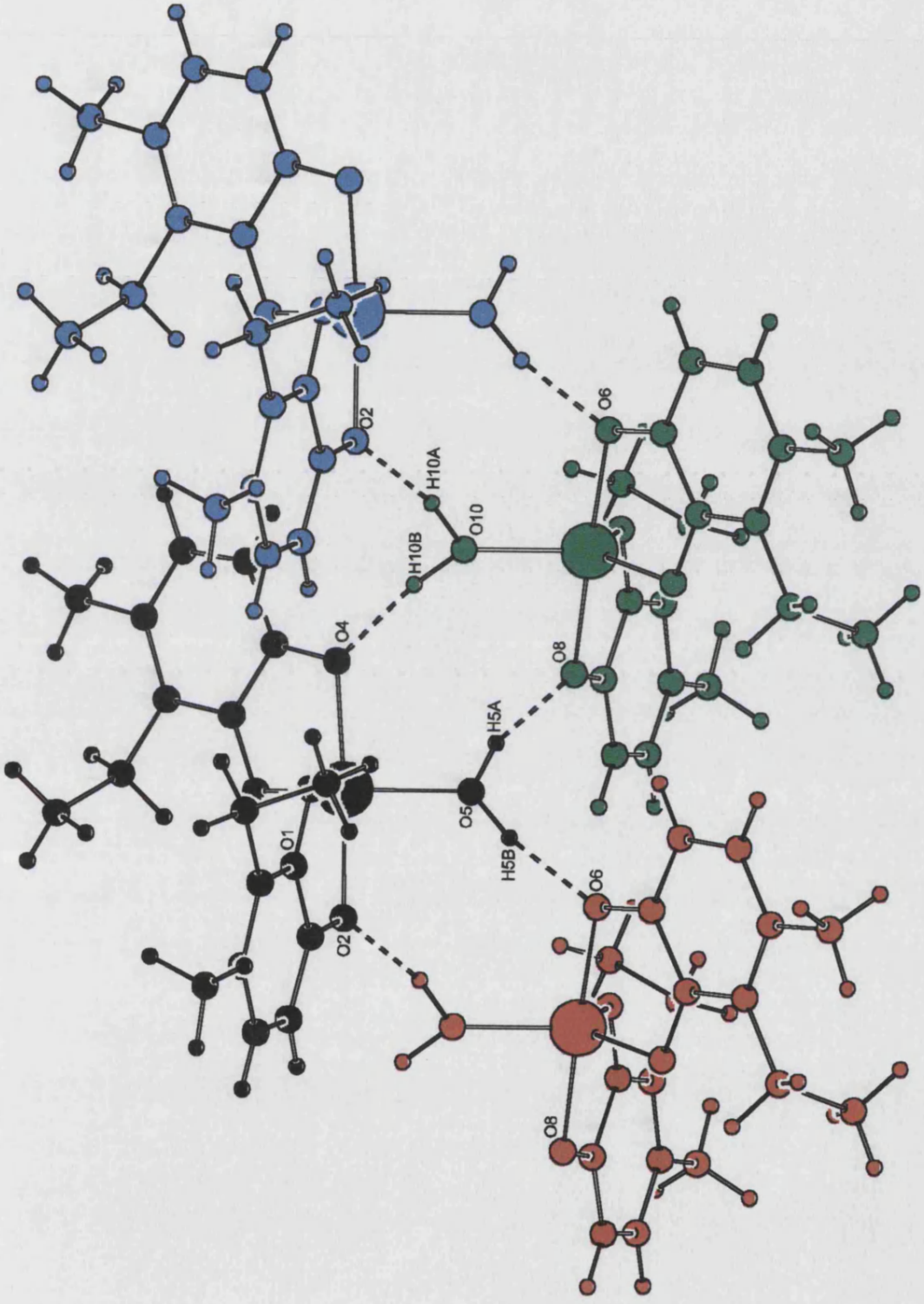

Figure 3.7: View of the polymeric chain structure of ***(47)***.

It can be noticed that the Zn(II) pyridinones complexes are extensively hydrogen bonded, with the hydrogen bonding involving water-water or water-(ligand-oxygen-donor) atom interactions. This is also true of other metal derivatives such as $Al(dmp)_3.12H_2O$[12] or $Pb(dmp)_2.7H_2O$.[26]

In both structures **(41)** and **(47)**, the zinc atom adopts a distorted trigonal bipyramidal geometry, whereas in the case of $Zn(dmp)_2$,[26] the zinc ion adopts a distorted square pyramidal geometry. The trigonal bipyramidal coordination about the zinc in **(47)** is slightly more regular than in **(41)** as a result of the flexible disposition of the water molecule in comparison to the second bridging 1-benzyl-2-methyl-3-hydroxypyridin-4-one. This difference is clearly manifest in the *trans*-angle [**(47)**: O(2)-Zn-O(4) 176.12(9)°; O(2)-Zn-O(4) 177.0(1)°; **(41)**: O(3)-Zn-O(1) 165.6(1)°].

The bite angles of the ligand **(29)** in **(41)** [O(1)-Zn-O(2) 80.0(1); O(3)-Zn-O(4) 82.2(1)°] are similar to those of the ligand **(31)** in **(47)** [O(1)-Zn(2)-O(2) 82.2(1); O(3)-Zn(2)-O(4) 82.5(1); O(6)-Zn(1)-O(7) 82.3(1); O(8)-Zn(1)-O(9) 82.2(1)°] and to those in $Zn(dmp)_2$ [O(1)-Zn-O(2) 81.68(8); O(11)-Zn-O(12) 81.59(9)°].[26]

In both compounds **(41)** and **(47)**, the ligands chelate the zinc atom *via* their oxygens with one short and one long bond to the metal (Table 3.4). As expected, for the chelating ligand in **(41)**, the hydroxyl oxygen binds the metal with the shortest bond [Zn(1)-O(3): 2.000(3) Å] and the carbonyl oxygen with the longest [Zn(1)-O(4): 2.048(3) Å]. However, for the bridging ligand, it is the carbonyl oxygen, which binds to the zinc with the shortest bond [Zn(1)-O(2): 2.008(3) Å], while the hydroxyl oxygen makes a weaker bond to the metal [Zn(1)-O(1): 2.136(3) Å], presumably as a consequence of its bridging role. This is different than in structure of $Zn(hino)_2$ **(17)**, in which the hydroxyl oxygen is more strongly bond to the metal, despite the fact that the [C-O] bond is elongated as a result of the dual bonding role. In case of the Pb(II) structure,[26] the metal-oxygen bonds in the bridging ligand are of similar length [Pb(1)-O(1A): 2.358(5); Pb(1)-O(2A): 2.370(5) Å]. Contrary to **(41)**, the [Pb←O(=C)] bond in the chelating ligand [Pb(1)-O(2): 2.300(5) Å] is shorter than

the [Pb-O(-C)] bond [Pb(1)-O(1): 2.544(5) Å]. This could be explained by the presence of a stereochemically active lone pair on the lead atom.[26]

For **(47)**, the carbonyl oxygen binds the metal with the longest bonds [Zn(2)-O(2): 2.046(2); Zn(2)-O(4): 2.055(2); Zn(1)-O(6): 2.063(2); Zn(1)-O(8): 2.067(3)Å], while the hydroxyl oxygen binds the zinc atom with the shortest bonds [Zn(2)-O(1): 2.018(2); Zn(2)-O(3): 2.003(2); Zn(1)-O(7): 2.000(3); Zn(1)-O(9): 1.990(2)Å]. The bond lengths are different than those of $Zn(dmp)_2$. The [Zn-O(-C)] bonds in **(47)** are shorter than the ones in $Zn(dmp)_2$, while the [Zn←O(=C)] bonds are longer than the ones in $Zn(dmp)_2$ (Table 3.4). This is the result of the interaction between the hydrogen on the water and the carbonyl oxygens in the structure of **(47)**.

Table 3.4: Zn-O bond length in selected metal complexes.

Compound	[Zn-O(-C)] bond / Å	[Zn←O(=C)] bond / Å	Reference
(41)	2.000(3); 2.136(3)	2.048(3); 2.008(3)	This work
(47)	1.990(2); 2.000(3)	2.063(2); 2.067(3)	This work
	2.003(2); 2.018(2)	2.046(2); 2.055(2)	
$Pb(dmp)_2$	2.544(5); 2.358(5)	2.300(5); 2.370(5)	26
$Zn(dmp)_2$	2.021(2); 2.050(2)	2.034(2); 2.047(2)	26
$Zn(hino)_2$ **(17)**	2.029(1), 2.075(1)	2.074(1); 2.107(1)	This work
$Zn(trop)_2$ **(21)**	2.149(2), 2.150(2)	2.067(2); 2.051(2)	This work
$Zn(ma)_2$	2.033(2); 2.010(2)	2.075(2); 2.076(2)	26

The zinc to water-oxygen distances in **(47)** are 2.015(3) Å for Zn(1)-O(10) and 2.009(3) Å for Zn(2)-O(5), shorter than in $Zn(dmp)_2.H_2O$ [2.043(3) Å],[26] but in the range of the five-coordinate $Zn(ma)_2.1.5H_2O$ [2.003(2) Å].[26]

Table3.5: C-O bond lengths in selected zinc complexes.

Compound	[C-O] bond / Å	[C=O] bond / Å	Reference
(41)	1.337(5); 1.338(6)	1.296(5); 1.288(6)	This work
(47)	1.312(4); 1.314(4)	1.305(4); 1.312(4)	This work
	1.315(4); 1.313(4)	1.299(4); 1.305(4)	
$Pb(dmp)_2$	1.313; 1.331	1.287; 1.291	26
$Zn(dmp)_2$	1.334; 1.335	1.292; 1.293	26
(17)	1.287(2); 1.306(2)	1.277(2); 1.279(2)	This work
(21)	1.291(3); 1.299(3)	1.261(3); 1.263(3)	This work

For **(41)**, the [C–O]/[C=O] bond lengths follow the expected pattern, with the [C=O] bonds being shorter than the [C–O] ones (Table 3.5). The [C=O] bonds in the chelating or bridging ligand are the same [C(1)-O(2): 1.296(5) Å; C(14)-O(4): 1.288(6) Å] and are similar to the ones found in the literature [$Zn(dmp)_2$: 1.292; 1.293 Å and $Pb(dmp)_2$: 1.287; 1.291 Å].[26] The same is true about the [C–O] bonds. They are not affected by the bridging, contrary to the ones in $Zn(hino)_2$. So it can be concluded that the bridging is weaker in **(41)** compared to **(17)**.

For **(47)**, both bonds appear to be of the same length, showing a greater bond delocalisation than in **(41)** or $Zn(dmp)_2$.

3.3 Results and Discussion: Tin compounds

3.2.2 Synthesis of the tin(II) complexes Sn(L)Cl

Because the 1-alkyl-3-hydroxypyridinones are only soluble in water, a successful route to SnL_2 other than using tin alkoxides as starting material has to be used. Another way (mentioned in Chapter II, Section 2.2.2) has been found using tin(II) chloride and water as solvent (Scheme 3.3).

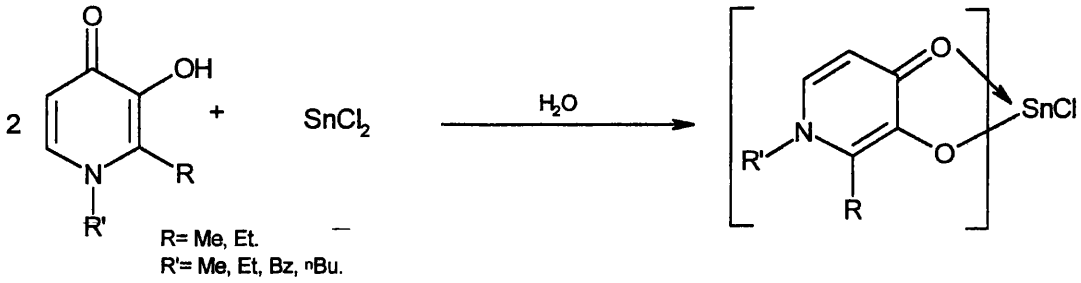

R= Me; R′=	Me	Et	Bz	^{n}Bu
Sn(II)	**(51)**	**(52)**	**(53)**	**(54)**
R= Et; R′=	Me	Et	Bz	^{n}Bu
Sn(II)	**(55)**	**(56)**	**(57)**	**(58)**

Scheme 3.3: Synthesis of Sn(L)Cl.

The elemental analysis (Table 3.6) clearly indicates that the compounds obtained were not SnL_2 as expected, but Sn(L)Cl. It appears that only one of the chlorines has been replaced by a ligand. A test made with silver nitrate, nitric acid and **(51)** mixed in water showed a white precipitate of silver chloride, which confirms the presence of chlorine in the compound. This reactivity has already been seen in the reaction of $SnCl_2$ with lactobionic acid.[25]

Table 3.6: Elemental analysis for the Sn(L)Cl complexes.

Compound	Carbon% found [calc.]	Hydrogen% found [calc.]	Nitrogen% found [calc.]
(51)	29.1; [28.8]	2.80; [2.74]	4.79; [4.79]
(52)	32.6; [31.4]	3.41; [3.26]	4.66; [4.57]
(53)	42.5; [42.4]	3.37; [3.26]	3.93; [3.80]
(54)	34.8; [35.9]	4.06; [4.18]	4.06; [4.18]
(55)	31.7; [31.4]	3.30; [3.26]	4.56; [4.57]
(56)	34.4; [33.7]	3.86; [3.74]	4.41; [4.37]
(57)	45.1; [44.0]	3.89; [3.66]	3.86; [3.66]
(58)	38.3; [37.9]	4.46; [4.59]	4.05; [4.02]

All the complexes **(51)–(58)** have been successfully synthesised and characterised. The infrared data are comparable to those for **(35)–(50)**. The ν(O–H) mode is absent for **(51)–(58)**. All the complexes show ν(C=O) bands between 1538 and 1600 cm^{-1}, which is shifted to lower wavenumbers by around 50 cm^{-1} than in the starting materials.

The Mössbauer data are typical of tin(II) complexes (Table 3.6). The Q.S values for some, but not all, complexes differ from the ones obtained for SnL_2 (Chapter II, Section 2.2.3), confirming the fact that only one of the halogens has been replaced by the ligand. The complexes seem to be relatively stable to oxidation, but their lack of solubility in common organic solvents makes them unsuitable to use in toothpaste formulation.

Table 3.7: Mössbauer data for the SnL_2X_2 complexes.

Compound	I.S (mms^{-1})	Q.S (mms^{-1})
(51)	3.04	1.97
(52)	3.16	1.85
(53)	3.16	1.91
(54)	3.18	1.84
(55)	3.10	1.85
(56)	3.19	2.01
(57)	3.08	2.02
(58)	3.11	1.84
$Sn(ma)_2$ **(8)**	2.98	2.03
$Sn(Etma)_2$ **(9)**	3.01	2.01

The ^1H and ^{13}C spectra of the tin compounds were recorded in deuterated DMSO due to the very low solubility of the complexes. The ^1H NMR data are given in Table 3.8 (Note: the chemical shifts for the N-R'groups have been omitted for clarity.)

Table 3.8: ^1H NMR data for Sn(L)Cl complexes.

Compound	Chemical Shift (ppm)			
	Me	Et	H_5	H_6
(51)	3.82	-	7.71	6.50
(52)	2.44	-	7.74	6.53
(53)	2.29	-	7.95	6.64
(54)	2.43	-	7.71	6.51
(55)	-	1.12, 2.87	7.68	6.50
(56)	-	1.33, 4.14	7.73	6.53
(57)	-	0.90, 2.68	7.86	6.58
(58)	-	1.13, 2.83	7.79	6.66
$Sn(ma)_2$ **(8)**	2.39	-	8.35	6.83
$Sn(Etma)_2$ **(9)**	-	1.08, 2.75	7.76	6.57

The ^{1}H spectra confirm the identity of the complexes. They are similar to the ones recorded for $Sn(ma)_2$ **(8)** and $Sn(Etma)_2$ **(9)** (Chapter II, Section 2.2.3) and to those obtained for the ZnL_2 complexes (Section 3.2.2).

The ^{13}C NMR spectra of the compounds show the right number of carbon environments and all the peaks were assigned. The spectra of **(51)–(58)** differ only by the alkyl group on the amine and their data are now discussed in more details.

The spectra of **(51)** and **(55)** show one peak for the N-Me group at 12.4 and 19.5 ppm. The ethyl group attached to the nitrogen for **(52)** and **(56)** appeared at 15.9 [CH_3] and 49.5 [CH_2] and at 12.7 [CH_3] and 49.1 [CH_2] respectively. The spectra of **(53)** and **(57)** show four peaks belonging to the benzyl group: 57.6 [CH_2] and 126.4, 128.1, 129.1 [CH aromatic] for **(53)**; and 57.1 [CH_2] and 126.3, 128.0, 129.0 [CH aromatic] for **(57)**. The ^{13}C NMR spectra of **(54)** and **(58)** contain four peaks assigned to the N-^{n}butyl group at 12.1 [CH_3], 19.1 [C_9H_2], 32.2 [C_8H_2], 54.2 [C_7H_2]; and 12.6 [CH_3], 19.4 [C_9H_2], 33.2 [C_8H_2], 53.9 [C_7H_2] respectively.

The data are comparable to those of the Zn(II) complexes described in the previous section 2.2.3.

3.4 Biological Testing

The tin compounds **(51)–(58)** appeared to be hardly soluble in any common organic solvents, which is a problem for biological testing. So none of them has been the subject of PGI assay. The PGI tests on zinc and copper derivatives were performed on *S.Warneri* and the same methodology was used as described for the tin complexes (Chapter II, Section 2.4). The results for the 1,2-dialkyl-3-hydroxypyridin-4-ones are shown in the Table 3.8. None of the ligands has been tested before, so it was of interest to see how their activity would be compare to their metal(II) complexes.

Table 3.8: Results of the PGI assay on the ligands [a].

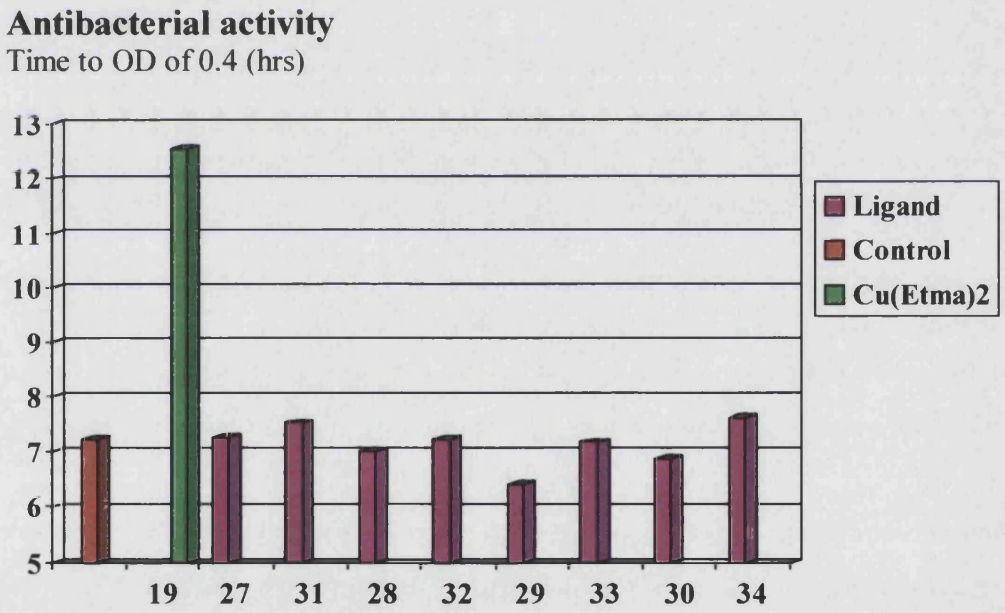

[a] *$Cu(Etma)_2$ **(19)** also shown for comparison.*

The ligands hardly show any anti-bacterial proprieties when compare to the control toothpaste (*i.e*: the control toothpaste is a model toothpaste solution in which no metal or therapeutic agents of any sort have been incorporated). The variation on the alkyl groups (R= Me, Et; R'= Me, Et, Bz, ^{n}Bu) does not seem to have any effect on their activity.

The compounds **(35)–(50)** were first dissolved in water and then added to a model toothpaste solution. The PGI assay results on the copper and zinc compounds are shown Table 3.9.

Table 3.9: Results of the PGI assay on the Cu(II) and Zn(II) complexes [a].

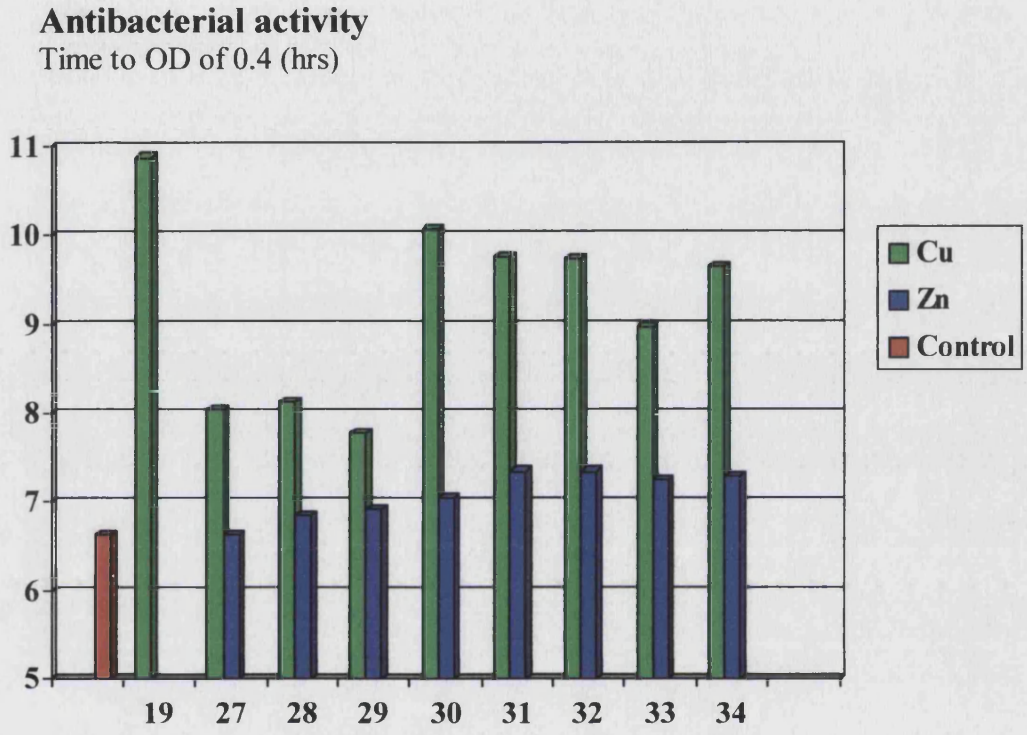

[a] *$Cu(Etma)_2$ **(19)** also shown for comparison.*

The copper complexes are more efficient than the zinc ones, as previously noticed for maltol and related metal derivatives (Chapter I, Section 1.8). The results are not very encouraging as none of the products showed a better activity than $Cu(Etma)_2$ complex. As for the ligands, the variation on the alkyl group does not seem to affect the anti-bacterial properties of the compounds. The metal complexes still show a greater anti-bacterial activity than the 1,2-alkyl-3-hydroxypyridin-4-ones on their own.

As noticed in Chapter II, the coordination number of the metals seems to affect the activity of the compounds. The Cu(II) complexes, which are four-coordinate [cf: structures of **(35)**,[23] **(44)**,[23] **(45)** and **(46)**], show a better activity than the Zn(II) compounds, which are five or six-coordinate [cf: structures of **(39)**,[26] **(41)** and **(47)**].

3.5 Experimental

All the 1-alkyl-2-methyl-3-hydroxypyrid-4-ones **(27)–(30)** and 1-alkyl-2-ethyl-3-hydroxy-pyrid-4-ones **(31)–(34)** were prepared following the same literature procedure.[17]

Preparation of 1-alkyl-2-methyl-3-hydroxypyrid-4-one (27)–(30)

1-methyl-2-methyl-3-hydroxypyrid-4-one **(27)** was prepared using maltol (5.00g; 0.04mol) and aqueous methylamine (40%) (10mL) in solution in water (100mL). The solution was refluxed and stirred for seven hours and then decolourising charcoal was added. The mixture was left for thirty minutes and was filtered. The solvent was evaporated in *vacuo* to give a dark brown solid and crystallisation from hot water gave fine white needles (2.47g; 45%)

Analysis for **(27)**: Found [calc. for $C_7H_9NO_2$]: C 60.1 (60.4)%; H 6.48 (6.47)%; N 10.00 (10.06)%.

^{1}H NMR [δ(ppm), $CDCl_3$]: 2.31 [3H, s, C-C*H*$_3$]; 3.68 [3H, s, N-C*H*$_3$]; 6.54 [1H, d, *H*$_5$]; J(^{1}H-^{1}H) = 7.16 Hz; 8.03 [1H, d, *H*$_4$]; J(^{1}H-^{1}H) = 7.16 Hz.

^{13}C NMR [δ(ppm), $CDCl_3$]: 11.8 [*C*$_7$H$_3$]; 16.1 [*C*$_6$H$_3$]; 111.3 [*C*$_5$H]; 133.8 [*C*$_1$]; 136.6 [*C*$_5$H]; 152.1 [*C*$_2$]; 169.1 [*C*$_3$].

IR data (NaCl plates, nujol, cm^{-1}): 3132 υ(O-H); 1629, 1567, 1529 υ(C=O) & υ(C=C); 1232 υ(C-N).

Following this procedure 1-ethyl-2-methyl-3-hydroxypyrid-4-one **(28)**, 1-benzyl-2-methyl-3-hydroxypyrid-4-one **(29)**, 1-^{n}butyl-2-methyl-3-hydroxypyrid-4-one **(30)** were obtained using maltol (5.00g; 0.04mol) and respectively aqueous ethylamine (70%) (10mL); benzylamine (10mL) and ^{n}butylamine (10mL). This yielded a brown crystalline product (1.59g; 26%) for **(28)**, a beige solid (1.17g; 14%) for **(29)** and pale yellow needles (1.31g; 18%) for **(30)**.

Analysis for **(28)**: Found [calc. for $C_8H_{11}NO_2$]: C 62.6 (62.7)%; H 7.22 (7.19)%;
N 9.01 (9.15)%.

^{1}H NMR [δ(ppm), $CDCl_3$]: 1.39 [3H, s, C-C*H*$_3$]; 2.40 [3H, t, N-CH$_2$-C*H*$_3$];
3.93 [2H, q, N-C*H*$_2$-CH$_3$]; 6.39 [1H, d, *H*$_5$];
J(^{1}H-^{1}H) = 7.15 Hz; 7.24 [1H, d, *H*$_4$]; J(^{1}H-^{1}H) = 7.14 Hz.

^{13}C NMR [δ(ppm), $CDCl_3$]: 11.6 [*C*$_8$H$_3$]; 16.2 [*C*$_7$H$_3$]; 48.7 [*C*$_6$H$_2$]; 111.4 [*C*$_4$H];
133.9 [*C*$_1$]; 136.0 [*C*$_5$H]; 158.4 [*C*$_2$]; 169.5 [*C*$_3$].

IR data (NaCl plates, nujol, cm^{-1}): 3152 υ(O-H); 1625, 1566, 1528 υ(C=O) & υ(C=C);
1227 υ(C-N).

Analysis for **(29)**: Found [calc. for $C_{13}H_{13}NO_2$]: C 72.7 (72.5)%; H 6.12 (6.05)%;
N 6.67 (6.51)%.

^{1}H NMR [δ(ppm), $CDCl_3$]: 2.12 [3H, s, C*H*$_3$]; 5.25 [2H, s, N-C*H*$_2$]; 6.20 [1H, d, *H*$_5$];
J(^{1}H-^{1}H) = 7.32 Hz; 7.06 [1H, d, *H*$_4$];
J(^{1}H-^{1}H) = 7.14 Hz; 7.29-7.76 [5H, m, C$_6$*H*$_5$].

^{13}C NMR [δ(ppm), $CDCl_3$]: 11.6 [*C*$_{13}$H$_3$]; 56.1 [*C*$_6$H$_2$]; 110.9 [*C*$_4$H];
126.1, 127.7, 129.0 [*C*H aromatic]; 137.1 [*C*$_1$];
138.7 [*C*$_5$H]; 145.8 [*C*$_2$]; 169.3 [*C*$_3$].

IR data (NaCl plates, nujol, cm^{-1}): 3174 υ(O-H); 1627, 1576, 1526 υ(C=O) & υ(C=C);
1239 υ(C-N).

Analysis for **(30)**: Found [calc. for $C_{10}H_{15}NO_2$]: C 65.9 (66.3)%; H 8.31 (8.29)%;
N 7.70 (7.73)%.

^{1}H NMR [δ(ppm), $CDCl_3$]: 0.96 [3H, t, C$_9$*H*$_3$]; 1.37 [2H, sextet, C$_8$*H*$_2$];
1.70 [2H, C$_7$*H*$_2$]; 2.39 [1H, s, C$_{10}$*H*$_3$]; 3.85 [2H, t, C$_6$*H*$_2$];
6.36 [1H, d, *H*$_5$]; J(^{1}H-^{1}H) = 7.03 Hz; 7.21 [1H, d, *H*$_4$];
J(^{1}H-^{1}H) = 7.41 Hz; 7.47 [1H, b s, O*H*].

^{13}C NMR [δ(ppm), $CDCl_3$]: 12.1 [*C*$_9$H$_3$]; 13.1 [*C*$_{10}$H$_3$]; 19.7 [*C*$_8$H$_2$]; 32.3 [*C*$_7$H$_2$];
53.8 [*C*$_6$H$_2$]; 111.7 [*C*$_5$H]; 133.2 [*C*$_1$]; 135.2 [*C*$_4$H];
156.6 [*C*$_2$]; 169.0 [*C*$_3$].

IR data (NaCl plates, nujol, cm^{-1}): 3152 υ(O-H); 1624, 1569, 1528 υ(C=O) & υ(C=C);
1234 υ(C-N).

Preparation of 1-alkyl-2-ethyl-3-hydroxypyrid-4-one (31)–(34)

The method described earlier for **(27)** was repeated for **(31)–(34)** using ethylmaltol (5.00g; 0.03mol) and the corresponding amine in excess in water (100mL). Aqueous methylamine (40%) (10mL) was used for **(31)** (2.03g; 33%), aqueous ethylamine (70%) (10mL) for **(32)** (1.82g; 27%), benzylamine (10mL) for **(33)** (1.44g; 16%) and ^{n}butylamine (10mL) for **(34)** (1.86g; 27%).

Analysis for **(31)**: Found [calc. for $C_8H_{11}NO_2$]: C 58.6 (62.7)%; H 7.28 (7.19)%; N 9.03 (9.15)%.

^{1}H NMR [δ(ppm), $CDCl_3$]: 1.20 [3H, t, CH_2-C*H*$_3$]; 2.80 [2H, q, C*H*$_2$-CH_3] 3.69 [3H, s, C*H*$_3$]; 6.32 [1H, d, *H*$_5$]; J(^{1}H-^{1}H) = 7.14 Hz; 7.19 [1H, d, *H*$_4$]; J(^{1}H-^{1}H) = 7.14 Hz; 7.63, [1H, b s, O*H*].

^{13}C NMR [δ(ppm), $CDCl_3$)]: 12.0 [*C*$_8$H$_3$]; 19.3 [*C*$_7$H$_2$]; 40.9 [*C*$_6$H$_3$]; 111.2 [*C*$_5$H]; 134.4 [*C*$_1$]; 137.3 [*C*$_5$H]; 145.7 [*C*$_2$]; 169.7 [*C*$_3$].

IR data (NaCl plates, nujol, cm^{-1}): 3158 υ(O-H); 1624, 1570 1511 υ(C=O) & υ(C=C); 1223 υ(C-N).

Analysis for **(32)**: Found [calc. for $C_9H_{13}NO_2$]: C 63.7 (64.7)%; H 7.80 (7.78)%; N 8.34 (8.38)%.

^{1}H NMR [δ(ppm), $CDCl_3$]: 1.23 [3H, t, N-CH_2-C*H*$_3$]; 1.41 [3H, t, C-CH_2-C*H*$_3$]; 2.82 [2H, q, C-C*H*$_2$-CH_3]; 3.96 [2H, q, N-C*H*$_2$-CH_3]; 6.40 [1H, d, *H*$_5$]; 7.25 [1H, d, *H*$_6$]; 7.47 [1H, s, O*H*].

^{13}C NMR [δ(ppm), $CDCl_3$]: 12.5 [*C*$_7$H$_3$]; 16.6 [*C*$_9$H$_3$]; 18.9 [*C*$_8$H$_2$]; 48.0 [*C*$_6$H$_2$]; 111.6 [*C*$_5$H]; 133.5 [*C*$_1$]; 135.8 [*C*$_4$H]; 145.7 [*C*$_2$]; 169.6 [*C*$_3$].

IR data (NaCl plates, nujol, cm^{-1}): 3144 υ(O-H); 1619, 1575, 1529 υ(C=O) & υ(C=C); 1236 υ(C-N).

Analysis for **(33)**: Found [calc. for $C_{14}H_{15}NO_2$]: C 69.6 (73.4)%; H 6.95 (6.55)%;
N 6.06 (6.11)%.

^{1}H NMR [δ(ppm), $CDCl_3$]: 1.14 [3H, d, C*H*$_3$]; 2.71 [2H, q, C*H*$_2$-CH$_3$];
4.78 [1H, b s, *OH*]; *5*.12 [2H, s, N-C*H*$_2$];
6.46 [1H, d, *H*$_5$]; 7.01 [1H, s, *H*$_4$];
7.35- 7.76 [5H, m, C$_6$*H*$_5$].

^{13}C NMR [δ(ppm), $CDCl_3$]: 11.7 [*C*$_{14}$H$_3$]; 18.5 [*C*$_{13}$H$_2$]; 55.5 [*C*$_6$H$_2$];
107.4 [*C*$_4$H]; 125.6, 127.6, 128.4 [*C*H aromatic];
133.5[*C*$_5$H]; 138.1 [*C*$_1$]; 157.3 [*C*$_2$]; 169.9 [*C*$_3$].

IR data (NaCl plates, nujol, cm^{-1}): 3174 υ(O-H); 1620, 1548, 1523,
1494 υ(C=O) & υ(C=C); 1223 υ(C-N).

Analysis for **(34)**: Found [calc. for $C_{11}H_{17}NO_2$]: C 67.4 (67.7)%; H 8.72 (8.72)%;
N 7.13 (7.18)%.

^{1}H NMR [δ(ppm), $CDCl_3$]: 0.87 [3H, t, C$_9$*H*$_3$]; 1.13 [3H, t, C$_{11}$*H*$_3$];
1.29 [2H, sextet, C$_8$*H*$_2$]; 1.64 [2H, C$_7$*H*$_2$];
2.69 [2H, q, C$_{10}$*H*$_2$]; 3.77 [2H, t, C$_6$*H*$_2$];
6.28 [1H, d, *H*$_5$]; J(^{1}H-^{1}H) = 7.42 Hz; 7.13 [1H, d, *H*$_4$];
J(^{1}H-^{1}H) = 7.47 Hz; 7.72 [1H, b s, O*H*].

^{13}C NMR [δ(ppm), $CDCl_3$]: 12.7 [*C*$_9$H$_3$]; 13.5 [*C*$_{11}$H$_3$]; 19.2 [*C*$_{10}$H$_2$];
19.6 [*C*$_8$H$_2$]; 33.5 [*C*$_7$H$_2$]; 53.1 [*C*$_6$H$_2$]; 111.2 [*C*$_5$H];
133.5 [*C*$_1$]; 136.2 [*C*$_4$H]; 145.6 [*C*$_2$]; 169.3 [*C*$_3$].

IR data (NaCl plates, nujol, cm^{-1}): 3162 υ(O-H); 1621, 1572, 1523 υ(C=O) & υ(C=C);
1238 υ(C-N).

Preparation of CuL_2 compounds

The method described by P. Wright[25] was repeated for **(35)–(38)**, **(43)–(46)**. A solution of the ligand in water/ethanol mix was added to a well-stirred solution of copper acetate in water/ethanol mix. After stirring for two hours, the solution was refluxed and stirred for another two hours and then left at room temperature.

Preparation of (1-methyl-2-methyl-3-hydroxypyrid-4-one)$_2$Cu (35)

A dark green solid was obtained using **(27)** (0.60g; 4.31mmol) and copper acetate (0.43g; 2.16mmol). Yield 64% (0.47g).

Analysis for **(35)**: Found [calc. for $C_{14}H_{16}N_2O_4Cu$]: C 49.6 (49.5)%; H 4.71 (4.71)%; N 8.26 (8.25)%.

IR data (NaCl plates, nujol, cm^{-1}): 1619, 1542, 1500, 1491 υ(C=O) & υ(C=C).

Preparation of (1-ethyl-2-methyl-3-hydroxypyrid-4-onate)$_2$Cu (36)

Following the procedure with **(28)** (0.70g; 4.57mmol) and copper acetate (0.45g; 2.29 mmol), **(36)** was obtained. Recrystallisation from hot methanol yielded green crystals (0.50g; 60 %).

Analysis for **(36)**: Found [calc. for $C_{16}H_{20}N_2O_4Cu$]: C 52.2 (52.2)%; H 5.53 (5.44)%; N 7.68 (7.61)%.

IR data (NaCl plates, nujol, cm^{-1}): 1611, 1554, 1518, 1496 υ(C=O) & υ(C=C).

Preparation of (1-benzyl-2-methyl-3-hydroxypyrid-4-onate)$_2$Cu (37)

The method described previously was utilised for **(29)** (0.55g; 2.56mmol) added to copper acetate (0.26g; 1.28mmol). Following this a green solid was obtained (0.55g; 86%).

Analysis for **(37)**: Found [calc. for $C_{26}H_{24}N_2O_4Cu$]: C 63.1 (63.5)%; H 4.84 (4.88)%; N 5.75 (5.69)%.

IR data (NaCl plates, nujol, cm^{-1}): 1612, 1556, 1523, 1488 υ(C=O) & υ(C=C).

Preparation of (1-^{n}butyl-2-methyl-3-hydroxypyrid-4-onate)$_2$Cu (38)

The methodology described earlier was employed with **(30)** (0.46g; 2.54mmol) and copper acetate (0.25g; 1.27mmol). A green solid was obtained (0.47g; 84%).

Analysis for **(38)**: Found [calc. for $C_{20}H_{28}N_2O_4Cu.H_2O$]: C 54.1 (54.4)%; H 6.83 (6.79)%; N 6.34 (6.43)%.

IR data (NaCl plates, nujol, cm^{-1}): 3559-3257 υ(H_2O); 1603, 1550, 1520, 1492 υ(C=O) & υ(C=C).

Preparation of (1-methyl-2-ethyl-3-hydroxypyrid-4-onate)$_2$Cu (43)

A dark green solid was obtained using **(31)** (0.41g; 2.78mmol) and copper acetate (0.27g; 1.39mmol). The yield of the reaction was 61% (0.31g).

Analysis for **(43)**: Found [calc. for $C_{16}H_{20}N_2O_4Cu$]: C 52.1 (52.2)%; H 5.50 (5.44)%; N 7.54 (7.61)%.

IR data (NaCl plates, nujol, cm^{-1}): 1609, 1558, 1517, 1496 υ(C=O) & υ(C=C).

Preparation of (1-ethyl-2-ethyl-3-hydroxypyrid-4-onate)$_2$Cu (44)

Following the procedure with **(32)** (0.47g; 2.81mmol) and copper acetate (0.28g; 1.40mmol), **(44)** was obtained (0.39g; 70%).

Analysis for **(44)**: Found [calc. for $C_{18}H_{24}N_2O_4Cu$]: C 54.8 (54.6)%; H 6.21 (6.06)%; N 7.17 (7.07)%.

IR data (NaCl plates, nujol, cm^{-1}): 1599, 1552, 1514, 1493 υ(C=O) & υ(C=C).

Preparation of (1-benzyl-2-ethyl-3-hydroxypyrid-4-onate)$_2$Cu (45)

The method described previously was utilised with **(33)** (0.50g; 2.18mmol) added to copper acetate (0.22g; 1.09mmol). Recrystallisation from hot methanol yielded green crystals (0.50g; 88%) suitable for X-ray-crystallography.

Analysis for **(45)**: Found [calc. for $C_{28}H_{28}N_2O_4Cu.2H_2O$]: C 60.3 (60.5)%; H 5.73 (5.76)%; N 5.09 (5.04)%.

IR data (NaCl plates, nujol, cm^{-1}): 3644-3253 υ(H_2O); 1620, 1564, 1518, 1490 υ(C=O) & υ(C=C).

Preparation of (1-^{n}butyl-2-ethyl-3-hydroxypyrid-4-onate)$_2$Cu (46)

The methodology described earlier was employed with **(34)** (0.60g; 3.08mmol) and copper acetate (0.31g; 1.54mmol). After recrystallisation from chloroform, a green solid was obtained (0.25g; 38%).

Analysis for **(46)**: Found [calc. for $C_{20}H_{30}N_2O_4Cu.2CHCl_3$]: C 58.0 (58.5)%; H 7.13 (7.09)%; N 6.22 (6.20)%.

IR data (NaCl plates, nujol, cm^{-1}): 1598, 1555, 1518, 1486 υ(C=O) & υ(C=C).

Preparation of ZnL_2 compounds

The methodology previously used by P. Wright was utilised.[25] A solution of the ligand in water/ethanol mix was added to a well stirred solution of zinc acetate in water/ethanol mix. After stirring for two hours, the solution was refluxed and stirred for another two hours and then left at room temperature.

Preparation of (1-methyl-2-methyl-3-hydroxypyrid-4-onate)$_2$Zn (39)

Following the procedure with **(27)** (0.46g; 2.59mmol) and zinc acetate (0.28g; 1.29mmol), **(39)** was obtained (0.32g, 53%). Recrystallisation from hot water gave colourless crystals.

Analysis for **(39)**: Found [calc. for $C_{14}H_{16}N_2O_4Zn.7H_2O$]: C 52.2 (52.2)%; H 5.53 (5.44)%; N 7.68 (7.61)%.

^{1}H NMR [δ(ppm), D_2O]: 2.25 [3H, s, C-C*H*$_3$]; 3.61 [3H, s, N-C*H*$_3$]; 6.38 [1H, d, *H*$_6$]; J(^{1}H-^{1}H) = 6.64 Hz; 7.32 [1H, s, *H*$_5$]; J(^{1}H-^{1}H) = 6.64 Hz.

^{13}C NMR [δ(ppm), D_2O]: 11.8 [*C*$_7$H$_3$]; 16.4 [*C*$_8$H$_3$]; 111.7 [*C*$_5$H]; 134.9 [*C*$_2$]; 135.6 [*C*$_6$H]; 157.3 [*C*$_3$]; 170.8 [*C*$_4$].

IR data (NaCl plates, nujol, cm^{-1}): 1607, 1550, 1527, 1495 υ(C=O) & υ(C=C).

Preparation of (1-ethyl-2-methyl-3-hydroxypyrid-4-onate)$_2$Zn (40)

The method described previously was utilised for **(28)** (0.48g; 3.13mmol) added to zinc acetate (0.34g; 1.56mmol). After recrystallisation in chloroform a white solid was obtained (0.45g; 78%).

Analysis for **(40)**: Found [calc. for $C_{16}H_{20}N_2O_4Zn.2CHCl_3$]: C 35.9 (35.5)%; H 3.68 (3.61)%; N 4.54 (4.60)%.

^{1}H NMR [δ(ppm), $CDCl_3$]: 1.36 [3H, t, N-CH$_2$-C*H*$_3$]; 2.44 [3H, s, C-C*H*$_3$]; 3.99 [2H, q, N-C*H*$_2$-CH$_3$]; 6.39 [1H, d, *H*$_6$]; J(^{1}H-^{1}H) = 6.81 Hz; 7.34 [1H, d, *H*$_5$]; J(^{1}H-^{1}H) = 6.83 Hz.

^{13}C NMR [δ(ppm), $CDCl_3$]: 11.6 [*C*$_8$H$_3$]; 16.2 [*C*$_9$H$_3$]; 48.7 [*C*$_7$H$_2$]; 111.4 [*C*$_5$H]; 133.9 [*C*$_2$]; 136.0 [*C*$_6$H]; 158.4 [*C*$_3$]; 169.5 [*C*$_4$].

IR data (NaCl plates, nujol, cm^{-1}): 1598, 1558, 1523, 1491 υ(C=O) & υ(C=C).

Preparation of (1-benzyl-2-methyl-3-hydroxypyrid-4-onate)$_2$Zn (41)

The methodology described earlier was employed with **(29)** (0.55g; 2.56mmol) and zinc acetate (0.28g; 1.28mmol). A yellow solid was obtained (0.53g; 84%). Recrystallisation from hot water gave crystals suitable for X-ray crystallography.

Analysis for **(41)**: Found [calc. for $C_{26}H_{24}N_2O_4Zn.3H_2O$]: C 58.9 (57.0)%;
H 5.46 (5.48)%; N 5.03 (5.11)%.

^{1}H NMR [δ(ppm), $CDCl_3$]: 2.17 [3H, s, C*H*$_3$]; *5*.29 [2H, s, N-C*H*$_2$];
6.32 [1H, d, *H*$_6$]; J(^{1}H-^{1}H) = 6.78 Hz; 7.02 [1H, d, *H*$_5$];
J(^{1}H-^{1}H) = 6.96 Hz; 7.28-7.61 [5H, m, C$_6$*H*$_5$].

^{13}C NMR [δ(ppm), $CDCl_3$]: 12.1 [*C*$_{14}$H$_3$]; 57.3 [*C*$_7$H$_2$]; 107.2 [*C*$_5$H];
126.1, 127.7, 128.8 [*C*H aromatic]; 132.9[*C*$_6$H];
137.2 [*C*$_2$]; 156.1 [*C*$_3$]; 171.2 [*C*$_4$].

IR data (NaCl plates, nujol, cm^{-1}): 1598, 1542, 1506, 1483 υ(C=O) & υ(C=C).

Preparation of (1-^{n}butyl-2-methyl-3-hydroxypyrid-4-onate)$_2$Zn (42)

A pale yellow solid was obtained using **(30)** (0.50g; 2.76mmol) and zinc acetate (0.30g; 1.38mmol). The yield of the reaction was 66% (0.39g).

Analysis for **(42)**: Found [calc. for $C_{20}H_{28}N_2O_4Zn.H_2O$]: C 52.0 (54.1)%;
H 6.57 (6.76)%; N 6.30 (6.31)%.

^{1}H NMR [δ(ppm), $CDCl_3$]: 0.92 [3H, t, C$_{10}$*H*$_3$]; 1.32 [2H, sextet, C$_9$*H*$_2$];
1.64 [2H, C$_8$*H*$_2$]; 2.41 [3H, s, C$_{11}$*H*$_3$]; 3.85 [2H, t, C$_7$*H*$_2$];
6.44 [1H, d, *H*$_6$]; J(^{1}H-^{1}H) = 6.96 Hz; 7.00 [1H, d, *H*$_5$];
J(^{1}H-^{1}H) = 6.96 Hz.

^{13}C NMR [δ(ppm), $CDCl_3$]: 12.2 [*C*$_{10}$H$_3$]; 13.5 [*C*$_{11}$H$_3$]; 19.5 [*C*$_9$H$_2$]; 33.9 [*C*$_8$H$_2$];
54.4 [*C*$_7$H$_2$]; 109.7 [*C*$_5$H]; 130.5 [*C*$_2$]; 133.0 [*C*$_6$H];
152.1 [*C*$_3$]; 170.2 [*C*$_4$].

IR data (NaCl plates, nujol, cm^{-1}): 1603, 1540, 1513, 1491 υ(C=O) & υ(C=C).

Preparation of (1-methyl-2-ethyl-3-hydroxypyrid-4-onate)$_2$Zn (47)

Following the procedure with **(31)** (0.43g; 2.81mmol) and zinc acetate (0.31g; 1.40mmol), **(47)** was obtained (0.40g; 77%). The complex was recrystallised from hot water.

Analysis for **(47)**: Found [calc. for $C_{16}H_{20}N_2O_4Zn$]: C 49.5 (52.0)%; H 5.75 (5.41)%; N 7.21 (7.58)%.

^{1}H NMR [δ(ppm), $CDCl_3$]: 1.09 [3H, t, C-CH_2-CH_3]; 2.83 [2H, q, C-CH_2-CH_3] 3.74 [3H, s, N-CH_3]; 6.20 [1H, d, H_6]; J(^{1}H-^{1}H) = 6.78 Hz; 7.35 [1H, d, H_5]; J(^{1}H-^{1}H) = 6.78 Hz.

^{13}C NMR [δ(ppm), $CDCl_3$]: 12.6 [C_9H_3]; 19.2 [C_7H_3]; 41.6 [C_8H_2]; 106.8 [C_5H]; 132.3 [C_6H]; 134.5 [C_2]; 155.5 [C_3]; 171.0 [C_4].

IR data (NaCl plates, nujol, cm^{-1}): 1589, 1538, 1516, 1496 υ(C=O) & υ(C=C).

Preparation of (1-ethyl-2-ethyl-3-hydroxypyrid-4-onate)$_2$Zn (48)

A white solid was obtained using **(32)** (0.52g; 3.11mmol) and zinc acetate (0.34g; 1.55mmol). The yield of the reaction was 68% (0.42g).

Analysis for **(48)**: Found [calc. for $C_{18}H_{24}N_2O_4Zn$]: C 54.1 (54.4)%; H 6.10 (6.04)%; N 7.13 (7.04)%.

^{1}H NMR [δ(ppm), $CDCl_3$]: 1.23 [3H, t, N-CH_2-CH_3]; 1.40 [3H, t, C-CH_2-CH_3]; 2.80 [2H, q, N-CH_2-CH_3]; 3.96 [2H, q, C-CH_2-CH_3]; 6.40 [1H, d, H_6]; J(^{1}H-^{1}H) = 7.12 Hz; 7.25 [1H, d, H_5]; J(^{1}H-^{1}H) = 7.15 Hz.

^{13}C NMR [δ(ppm), $CDCl_3$]: 12.5 [C_8H_3]; 16.6 [$C_{10}H_3$]; 19.0 [C_7H_2]; 48.0 [C_9H_2]; 111.6 [C_5H]; 133.5 [C_2]; 135.8 [C_6H]; 145.7 [C_3]; 169.6 [C_4].

IR data (NaCl plates, nujol, cm^{-1}): 1591, 1542, 1508, 1495 υ(C=O) & υ(C=C).

Preparation of (1-benzyl-2-ethyl-3-hydroxypyrid-4-onate)$_2$Zn (49)

The method described previously was utilised with **(33)** (0.50g; 2.18mmol) added to zinc acetate (0.24g; 1.09mmol). Recrystallisation from hot methanol yielded colourless crystals (0.51g; 88%).

Analysis for **(49)**: Found [calc. for $C_{28}H_{28}N_2O_4Zn$]: C 64.7 (64.4)%; H 5.95 (5.37)%; N 5.30 (5.37)%.

^{1}H NMR [δ(ppm), $CDCl_3$]: 1.05 [3H, t, C*H*$_3$]; 2.64 [2H, q, C*H*$_2$-CH$_3$]; 5.30 [2H, s, N-C*H*$_2$]; 6.31 [1H, d, *H*$_6$]; J(^{1}H-^{1}H) = 6.77 Hz; 7.03 [1H, s, *H*$_5$]; J(^{1}H-^{1}H) = 6.96 Hz; 7.27- 7.56 [5H, m, C$_6$*H*$_5$].

^{13}C NMR [δ(ppm), $CDCl_3$]: 12.8 [*C*$_{15}$H$_3$]; 18.6 [*C*$_{14}$H$_2$]; 56.8 [*C*$_7$H$_2$]; 107.2 [*C*$_5$H]; 125.9, 127.6, 128.9[CH aromatic]; 132.9[*C*$_6$H]; 137.7 [*C*$_2$]; 156.0 [*C*$_3$]; 171.6 [*C*$_4$].

IR data (NaCl plates, nujol, cm^{-1}): 1595, 1544, 1510, 1497 υ(C=O) &υ(C=C).

Preparation of (1-^{n}butyl-2-ethyl-3-hydroxypyrid-4-onate)$_2$Zn (50)

The methodology described earlier was employed with **(34)** (0.60g; 3.08mmol) and copper acetate (0.34g; 1.54mmol). A pale yellow solid was obtained (0.51g; 77%).

Analysis for **(50)**: Found [calc. for $C_{22}H_{32}N_2O_4Zn$]: C 56.3 (56.1)%; H 6.94 (7.02)%; N 5.95 (6.55)%.

^{1}H NMR [δ(ppm), $CDCl_3$]: 0.94 [3H, t, C$_{10}$*H*$_3$]; 1.21 [3H, t, C$_{12}$*H*$_3$]; 1.36 [2H, sextet, C$_9$*H*$_2$]; 1.71 [2H, C$_8$*H*$_2$]; 2.92 [2H, q, C$_{11}$*H*$_2$]; 3.90 [2H, t, C$_7$*H*$_2$]; 6.54 [1H, d, *H*$_6$]; J(^{1}H-^{1}H) = 6.78 Hz; 7.07 [1H, d, *H*$_5$]; J(^{1}H-^{1}H) = 6.78 Hz.

^{13}C NMR [δ(ppm), $CDCl_3$]: 12.7 [*C*$_{10}$H$_3$]; 13.5 [*C*$_{12}$H$_3$]; 19.5 [*C*$_{11}$H$_2$]; 19.6 [*C*$_9$H$_2$]; 33.5 [*C*$_8$H$_2$]; 54.3 [*C*$_7$H$_2$]; 108.9 [*C*$_5$H]; 131.1 [*C*$_2$]; 136.3 [*C*$_6$H]; 155.2 [*C*$_3$]; 171.1 [*C*$_4$].

IR data (NaCl plates, nujol, cm^{-1}): 1597, 1542, 1515, 1494 υ(C=O) & υ(C=C).

Preparation of Sn(L)Cl compounds

The same method was repeated for the eight compounds **(51)–(58)**. The ligand (2 equivalents) was added to a well stirred solution of tin(II) chloride dihydrate in water (20mL) under nitrogen. The water was previously degassed for one hour. A precipitate appeared after 30 minutes and the solution was stirred for another hour. The solution was filtered through a canula and the compound dried under *vacuo*.

Preparation of (1-methyl-2-methyl-3-hydroxypyrid-4-onate)SnCl (51)

Following the procedure with **(27)** (0.50; 3.60mmol) and $SnCl_2.2H_2O$ (0.40g; 1.80mmol), **(51)** was obtained (0.37g; 70%).

Analysis for **(51)**: Found [calc. for $C_7H_8NO_2SnCl$]: C 29.1 (28.8)%; H 2.80 (2.74)%; N 4.79 (4.79)%.

Mössbauer data (mms^{-1}): IS = 3.04, QS = 1.97.

^1H NMR [δ(ppm), DMSO(d^6)]: 2.41 [3H, s, N-CH_3]; 3.82 [3H, s, C-CH_3]; 6.50 [1H, d, H_6]; J(^1H-^1H) = 6.64 Hz; 7.71 [1H, s, H_5]; J(^1H-^1H) = 6.64 Hz.

^{13}C NMR [δ(ppm), DMSO(d^6)]: 12.4 [C_7H_3]; 42.5 [C_8H_3]; 108.9 [C_5H]; 134.5 [C_2]; 136.3 [C_6H]; 153.9 [C_3]; 168.9 [C_4].

IR data (NaCl plates, nujol, cm^{-1}): 1600, 1546, 1520 υ(C=O) & υ(C=C).

Preparation of (1-ethyl-2-methyl-3-hydroxypyrid-4-onate)SnCl (52)

The method described previously was utilised for **(28)** (0.50g; 3.26mmol) added to $SnCl_2.2H_2O$ (0.39g; 1.63mmol). This gave **(52)** as a white solid (0.33g; 66%).

Analysis for **(52)**: Found [calc. for $C_8H_{10}NO_2SnCl$]: C 32.6 (31.4)%; H 3.41 (3.26)%; N 4.66 (4.57)%.

Mössbauer data (mms^{-1}): IS = 3.16, QS = 1.85.

^1H NMR [δ(ppm), DMSO(d^6)]: 1.30 [3H, t, N-CH_2-CH_3]; 2.44 [3H, s, C-CH_3]; 4.16 [2H, q, N-CH_2-CH_3]; 6.53 [1H, d, H_6]; J(^1H-^1H) = 6.64 Hz; 7.74 [1H, d, H_5]; J(^1H-^1H) = 6.64 Hz.

^{13}C NMR [δ(ppm), DMSO(d^6)]: 11.9 [C_9H_3]; 15.9 [C_8H_3]; 49.5 [C_7H_2]; 109.6 [C_5H]; 133.7 [C_6H]; 135.4 [C_2]; 162.0 [C_3]; 168.6 [C_4].

IR data (NaCl plates, nujol, cm^{-1}): 1598, 1548, 1509 υ(C=O) & υ(C=C).

Preparation of (1-benzyl-2-methyl-3-hydroxypyrid-4-onate)SnCl (53)

The methodology described earlier was employed with **(29)** (0.50g; 2.32mmol) and $SnCl_2.2H_2O$ (0.26g; 1.16mmol). A beige solid was obtained (0.36g; 84%).

Analysis for **(53)**: Found [calc. for $C_{13}H_{12}NO_2SnCl$]: C 42.5 (42.4)%;
H 3.37 (3.26)%; N 3.93 (3.80)%.

Mössbauer data (mms^{-1}): IS = 3.16, QS = 1.91.

^1H NMR [δ(ppm), DMSO (d^6)]: 2.29 [3H, s, CH_3]; 5.46 [2H, s, N-CH_2];
6.64 [1H, d, H_6]; J(^1H-^1H) = 6.78 Hz;
7.16-7.38 [5H, m, C_6H_5]; 7.95 [1H, d, H_5];
J(^1H-^1H) = 6.77 Hz.

^{13}C NMR [δ(ppm), DMSO (d^6)]: 12.5 [$C_{14}H_3$]; 57.6 [C_7H_2]; 109.7 [C_5H];
126.4, 128.1, 129.1 [CH aromatic]; 134.2 [C_2];
135.8 [C_6H]; 157.1 [C_3]; 169.2 [C_4].

IR data (NaCl plates, nujol, cm^{-1}): 1599, 1542, 1491 υ(C=O) & υ(C=C).

Preparation of (1-^{n}butyl-2-methyl-3-hydroxypyrid-4-onate)SnCl (54)

A white solid (0.31g; 67%) was obtained using **(30)** (0.50g; 2.76mmol) and $SnCl_2.2H_2O$ (0.31g; 1.38mmol).

Analysis for **(54)**: Found [calc. for $C_{10}H_{14}NO_2SnCl$]: C 34.8 (35.9)%;
H 4.06 (4.18)%; N 4.06 (4.18)%.

Mössbauer data (mms^{-1}): IS = 3.18, QS = 1.84.

^1H NMR [δ(ppm), DMSO (d^6)]: 0.89 [3H, t, $C_{10}H_3$]; 1.30 [2H, sextet, C_9H_2];
1.66 [2H, C_8H_2]; 2.43 [3H, s, $C_{11}H_3$];
4.12 [2H, t, C_7H_2]; 6.51 [1H, d, H_6];
J(^1H-^1H) = 6.64 Hz; 7.71 [1H, d, H_5];
J(^1H-^1H) = 7.03 Hz.

^{13}C NMR [δ(ppm), DMSO (d^6)]: 12.1 [$C_{10}H_3$]; 13.6 [$C_{11}H_3$]; 19.1 [C_9H_2];
32.2 [C_8H_2]; 54.2 [C_7H_2]; 109.3 [C_5H]; 133.5 [C_2];
134.2 [C_6H]; 154.2 [C_3]; 168.9 [C_4].

IR data (NaCl plates, nujol, cm^{-1}): 1598, 1547, 1495 υ(C=O) & υ(C=C).

Preparation of (1-methyl-2-ethyl-3-hydroxypyrid-4-onate)SnCl (55)

Following the procedure with **(31)** (0.50g; 3.26mmol) and $SnCl_2.2H_2O$ (0.39g; 1.63mmol), **(55)** was obtained (0.34g; 68%).

Analysis for **(55)**: Found [calc. for $C_8H_{10}NO_2SnCl$]: C 31.7 (31.4)%; H 3.30 (3.26)%; N 4.56 (4.57)%.

Mössbauer data (mms^{-1}): IS = 3.10, QS = 1.85

^1H NMR [δ(ppm), DMSO (d^6)]: 1.12 [3H, t, CH_2-CH_3]; 2.87 [2H, q, CH_2-CH_3] 3.87 [3H, s, N-CH_3]; 6.50 [1H, d, H_6]; J(^1H-^1H) = 6.64 Hz; 7.68 [1H, d, H_5]; J(^1H-^1H) = 6.64 Hz.

^{13}C NMR [δ(ppm), DMSO (d^6)]: 11.8 [C_9H_3]; 19.5 [C_7H_3]; 40.1 [C_8H_2]; 109.2 [C_5H]; 134.7 [C_1]; 139.3 [C_6H]; 153.7 [C_3]; 169.5 [C_4].

IR data (NaCl plates, nujol, cm^{-1}): 1589, 1538, 1496 υ(C=O) & υ(C=C).

Preparation of (1-ethyl-2-ethyl-3-hydroxypyrid-4-onate)SnCl (56)

A white solid was obtained using **(32)** (0.50g; 2.99mmol) and $SnCl_2.2H_2O$ (0.34g; 1.49mmol). The yield of the reaction was 73% (0.35g).

Analysis for **(56)**: Found [calc. for $C_9H_{12}NO_2SnCl$]: C 34.4 (33.7)%; H 3.86 (3.74)%; N 4.41 (4.37)%.

Mössbauer data (mms^{-1}): IS = 3.19, QS = 2.01

^1H NMR [δ(ppm), DMSO (d^6)]: 1.13 [3H, t, N-CH_2-CH_3]; 1.33 [3H, t, C-CH_2-CH_3]; 2.84 [2H, q, N-CH_2-CH_3]; 4.14 [2H, q, C-CH_2-CH_3]; 6.53 [1H, d, H_6]; J(^1H-^1H) = 6.77 Hz; 7.73 [1H, d, H_5]; J(^1H-^1H) = 6.96 Hz

^{13}C NMR [δ(ppm), DMSO (d^6)]: 12.7 [C_8H_3]; 16.9 [$C_{10}H_3$]; 19.7 [C_7H_2]; 49.1 [C_9H_2]; 110.0 [C_5H]; 133.8 [C_6H]; 138.7 [C_2]; 154.1 [C_3]; 169.7 [C_4].

IR data (NaCl plates, nujol, cm^{-1}): 1596, 1541, 1507 υ(C=O) & υ(C=C).

Preparation of (1-benzyl-2ethyl-3-hydroxypyrid-4-onate)SnCl (57)

The method described previously was utilised with **(33)** (0.50g; 2.18mmol) added to $SnCl_2.2H_2O$ (0.25g; 1.09mmol). **(57)** was obtained as a white solid (0.27g; 64%).

Analysis for **(57)**: Found [calc. for $C_{14}H_{14}NO_2SnCl$]: C 45.1 (44.0)%;
H 3.89 (3.66)%; N 3.86 (3.66)%.

Mössbauer data (mms^{-1}): IS = 3.08, QS = 2.02.

^1H NMR [δ(ppm), DMSO (d^6)]: 0.90 [3H, t, CH_3]; 2.68 [2H, q, CH_2-CH_3];
5.44 [2H, s, N-CH_2]; 6.58 [1H, d, H_6];
J(^1H-^1H) = 6.59 Hz; 7.06- 7.37 [5H, m, C_6H_5];
7.86 [1H, s, H_5]; J(^1H-^1H) = 6.59 Hz.

^{13}C NMR [δ(ppm), DMSO (d^6)]: 12.2 [$C_{15}H_3$]; 19.8 [$C_{14}H_2$]; 57.1 [C_7H_2];
109.8 [C_5H]; 126.3, 128.0, 129.0 [CH aromatic];
135.9[C_6H]; 136.8 [C_2]; 157.3 [C_3]; 169.2 [C_4].

IR data (NaCl plates, nujol, cm^{-1}): 1599, 1540, 1506 υ(C=O) & υ(C=C).

Preparation of (1-^{n}butyl-2ethyl-3-hydroxypyrid-4-onate)SnCl (58)

The methodology described earlier was employed with **(34)** (0.50g; 2.56mmol) and $SnCl_2.2H_2O$ (0.29g; 1.28mmol). A white solid was obtained in 51% yield (0.23g).

Analysis for **(58)**: Found [calc. for $C_{11}H_{16}NO_2SnCl$]: C 38.3 (37.9)%;
H 4.46 (4.59)%; N 4.05 (4.02)%.

Mössbauer data (mms^{-1}): IS = 3.11, QS = 1.84.

^1H NMR [δ(ppm), DMSO (d^6)]: 0.87 [3H, t, C_9H_3]; 1.13 [3H, t, $C_{11}H_3$];
1.29 [2H, sextet, C_8H_2]; 1.67 [2H, C_7H_2];
2.83 [2H, q, $C_{10}H_2$]; 4.12 [2H, t, C_6H_2];
6.66 [1H, d, H_6]; 7.79 [1H, d, H_5].

^{13}C NMR [δ(ppm), DMSO (d^6)]: 12.6 [$C_{10}H_3$]; 13.6 [$C_{12}H_3$]; 19.1 [$C_{11}H_2$];
19.4 [C_9H_2]; 33.2 [C_8H_2]; 53.9 [C_7H_2]; 110.0 [C_5H];
135.4 [C_2]; 139.7 [C_6H]; 148.3 [C_3]; 168.1 [C_4].

IR data (NaCl plates, nujol, cm^{-1}): 1597, 1540, 1493 υ(C=O) & υ(C=C).

3.6 References

1) Hwang D. R.; Proctor G. R.; Driscoll J. S., *J. Pharm. Sci.* **1980**, *69*, 1074.

2) Li M.; Gu L.; Huang Z.; Xiao S.; Ma L., *Tetrahedron* **1999**, *55*, 2237.

3) Harris R. L. N., *Aust. J. Chem.* **1976**, *29*, 1329.

4) Harris R. L. N.; Stunzi H.; Perrin D. D.; Teitei T., *Aust. J. Chem.* **1980**, *33*, 2207.

5) Ghosh S.; Adsmond D. A.; Huotari J.; Grant D. J. W., *J. Pharm. Sci.* **1993**, *82*, 901.

6) Faller B.; Nick H., *J. Am. Chem. Soc* **1994**, *116*, 3860.

7) Xiao G.; Van-der-Helm D.; Hider R. C.; Dobbin P. S., *J. Chem. Soc., Dalton Trans.* **1992**.

8) Finnegan M. M.; Rettig S. J.; Orvig C., *J. Am. Chem. Soc.* **1986**, *108*, 5033.

9) Finnegan M. M.; Lutz T. G.; Nelson W. O.; Smith A.; Orvig C., *Inorg. Chem.* **1987**, *26*, 2171.

10) Orvig C.; Rettig S. J.; Trotter J., *Can. J. Chem.* **1987**, *65*, 590.

11) Nelson W. O.; Karpishin T. B.; Rettig S. J.; Orvig C., *Can. J. Chem.* **1988**, *66*, 123.

12) Nelson W. O.; Rettig S. J.; Orvig C., *J. Am. Chem. Soc.* **1987**, *109*, 4121.

13) Xiao G.; Van-der-Helm D.; Hider R. C.; Dobbin P. S.; Hall A. D.; Taylor P. D.; Sarpong P.; Porter J. B., *J. Med. Chem.* **1993**, *36*, 2448.

14) Zhang Z.; Hui T. L.; Orvig C., *Can. J. Chem.* **1989**, *67*, 1708.

15) Simpson L.; Rettig S. J.; Trotter J.; Orvig C., *Can. J. Chem.* **1991**, *69*, 893.

16) Luo H.; Rettig S. J.; Orvig C., *Inorg. Chem.* **1993**, *32*, 4491.

17) Kontoghiorghes G. J.; Sheppard L., *Inorg. Chim. Acta* **1987**, *137*, L11.

18) Harris R. L., *Aust. J. Chem.* **1976**, *29*, 1329.

19) Greaves S. J.; Griffith W. P., *Polyhedron* **1988**, *7*, 1973.

20) Nelson W. O.; Rettig S. J.; Orvig C., *Inorg. Chem.* **1989**, *28*, 3153.

21) Matsuba C. A.; Nelson W. O.; Rettig S. J.; Orvig C., *Inorg. Chem.* **1988**, *27*, 3935.

22) Nelson W. O.; Karpishin T. B.; Rettig S. J.; Orvig C., *Inorg. Chem* **1988**, *27*, 1045.

23) El-Jammal A.; Howell P. L.; Turner M. A.; Li N.; Templeton D. M., *J. Med. Chem.* **1994**, *37*, 461.

24) Berg J.; Pilotti A.; Soderholm A.; Karlsson B., *Acta Cryst.* **1978**, *B34*, 3071.

25) Wright P. *The synthesis and characterisation of novel Sn(II), Zn(II) and Cu(II) compounds for anti-bacterial evaluation*; University of Bath, **1999**.

26) Ahmed S. I.; Burgess J.; Fawcett J.; Parsons S. A.; Russell D. R.; Laurie S. H., *Polyhedron* **2000**, *19*, 129.

Chapter IV

4.1 Introduction to 2-alkylamino-4-alkyltropones

A new kind of ligand involving different donor atoms (N, O) has been synthesised, using tropolone or hinokitiol as a starting material (Figure 4.1).

It is particularly interesting to put an amino group instead of the hydroxyl group, in order to evaluate the effect of an alkyl group at this position on the activity of the compounds.

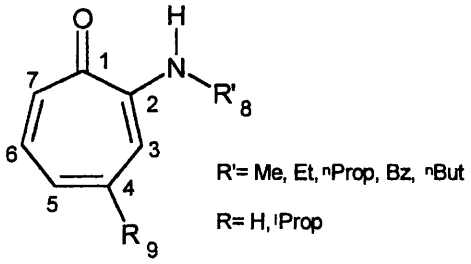

Figure 4.1: Alkylaminotropones, including atom numbering.

The 2-alkylaminotropone derivatives constitute a class of substances which could be of potential pharmaceutical interest,[1] but they have hardly been the objects of studies. No metal complexes with this type of ligand are known. In the literature, the aminotropones are mentioned only as a step to the synthesis of N-alkyl-2-(alkylamino)troponimines (Figure 4.2).[2-5]

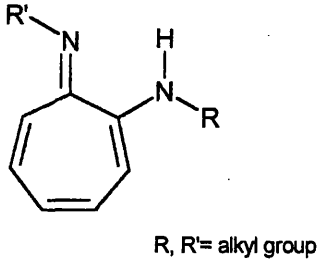

Figure 4.2: N-alkyl-2-(alkylamino)troponimines.

They can be easily prepared by a three-step procedure starting with tropolone Scheme 4.1). In the first step, tropolone is tosylated[6] or methoxylated.[7] The second step involves the direct nucleophilic displacement of the tosyl/methoxyl group, using

excess of primary amine. In the last step, the alkylaminotropone is ethylated with $Et_3O.BF_4$ and then treated with an excess of primary amine to obtain the N-alkyl-2-(alkylamino)troponimine.

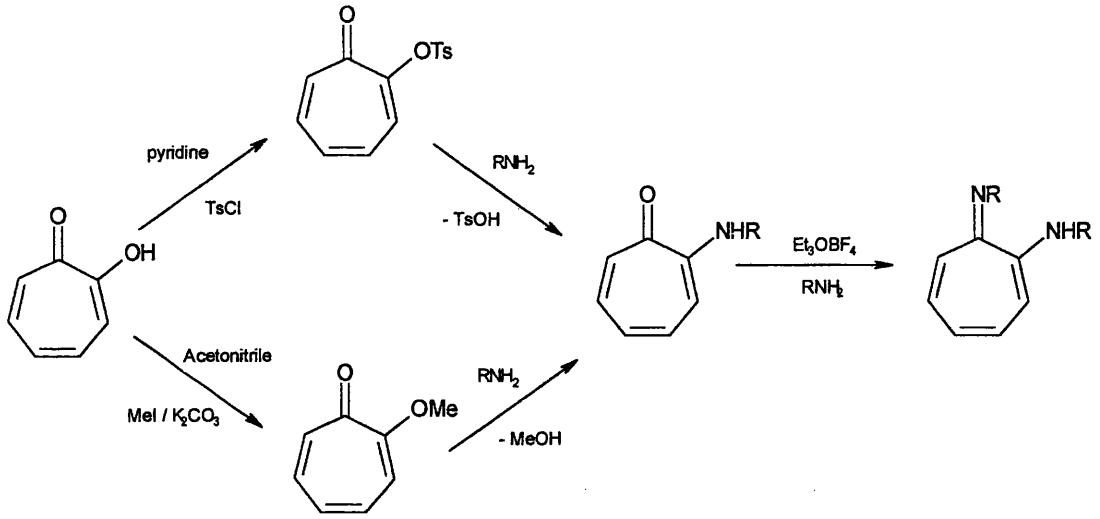

Scheme 4.1: Three-step procedure to N-alkyl-2-(alkylamino)troponimines.

In contrast to 2-alkylaminotropones, N-alkyl-2-(alkylamino)troponimines have attracted the attention of a number of research groups.

Dias *et al*[2,3] have been interested in the synthesis of metal adducts derived from aminotroponiminates, in order to stabilise the low-valent and low-coordinate main group species (Ga, Sn, In) (Figure 4.3).

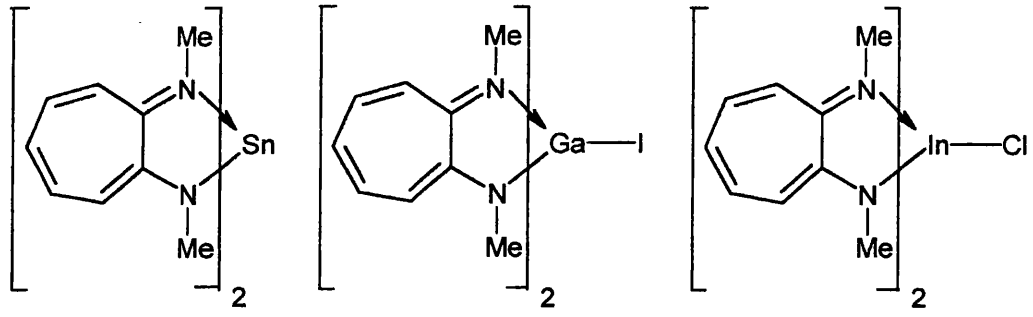

Figure 4.3: N-methyl-2-(methylamino)troponiminate complexes of Sn(II), Ga(III) and In(III).[3]

It has been shown that bis(aminotroponiminate)yttrium amides are active as catalysts for hydroamination/cyclisation catalysis.[8] Roesky *et al*[4,5] have also prepared bridged aminotroponiminate complexes of lanthanum, which could be potential catalysts for the polymerisation of terminal olefins (Figure 4.4). These bridged aminotroponiminate complexes are referred to as semi-tropocoronates, which are obtained in much higher yield starting from tropolone, than from the previous methods.[9,10]

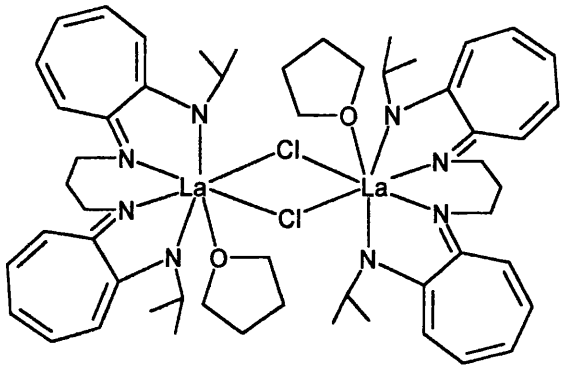

Figure 4.4: Bridged aminotroponiminate complex of lanthanum.[4]

Tropocoronate ligands are macrocycles in which two aminotroponiminate rings are connected together through polymethylene linker chains of length *n* and *m* (Figure 4.5).[11]

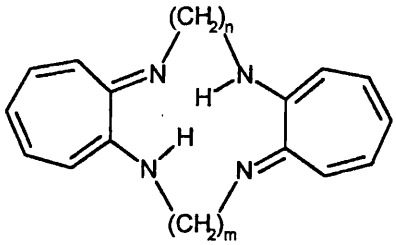

Figure 4.5: Tropocoronate.

Double deprotonation of the ligands provides a macrocycle capable of binding transition metals (such as zinc and cadmium)[11] to form neutral complexes. The four-coordinate geometries can be varied depending on *n* and *m*. The greater the sum (*n* + *m*), the more a complex twist from square planar towards tetrahedral geometry.

4.2 Results and Discussion: Copper(II) compounds

4.2.1 Synthesis of 2-alkylamino-4-alkyltropones

The tosylate compounds **(59)** and **(60)** were synthesised following a literature procedure.[6] Their identity was confirmed by elemental analysis.

Two methods[3,12] have been chosen for the preparation of the alkylaminotropones, depending on the amine used. If the amine is commercially available as a solution in water (*i.e.*: $MeNH_2$ 40%, and $EtNH_2$ 70%), the reaction was carried out in dichloromethane.[3] This method makes the purification of the product easier (straightforward separation of the dichloromethane layer from the mixture). If the amine does not come as a solution ($^nPropNH_2$, $BzNH_2$ and $^nBuNH_2$), the reaction was performed in DMSO.[12]

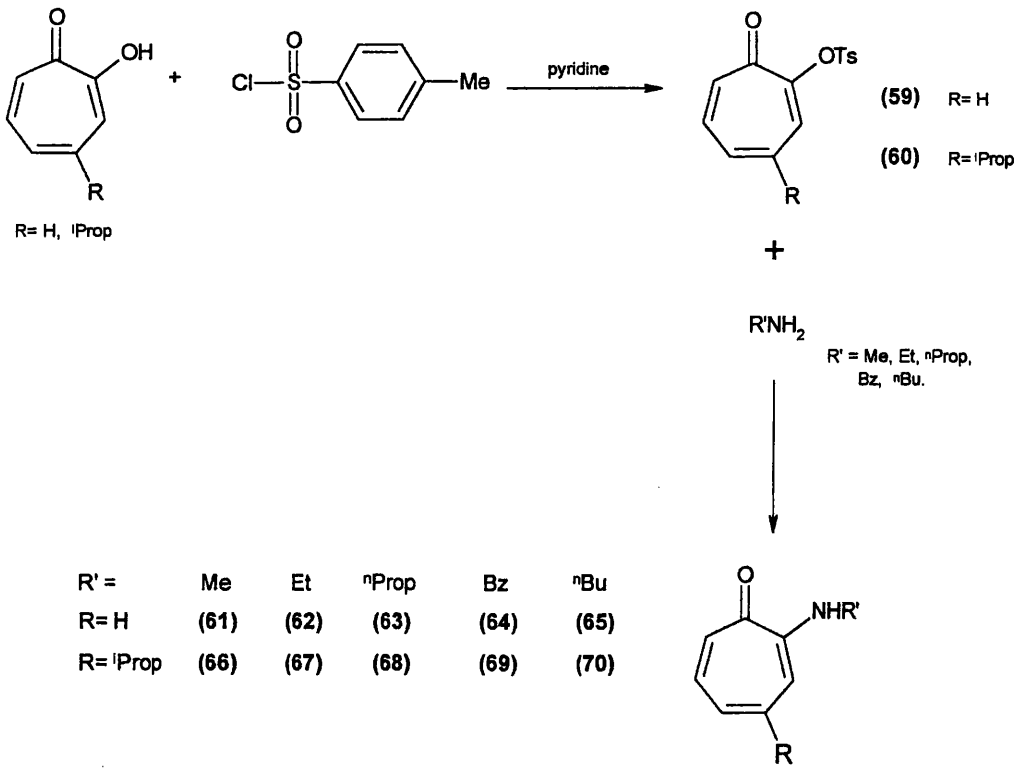

R' =	Me	Et	^{n}Prop	Bz	^{n}Bu
R= H	(61)	(62)	(63)	(64)	(65)
R= ^{i}Prop	(66)	(67)	(68)	(69)	(70)

Scheme 4.2: Synthesis of 2-alkylamino-4-alkyltropones.

It has been reported[13] that the reaction of hinokitiol with tosylchloride in the presence of pyridine gives a mixture of two compounds **I** and **II** in the ratio of 9:1 (Scheme 4.3).

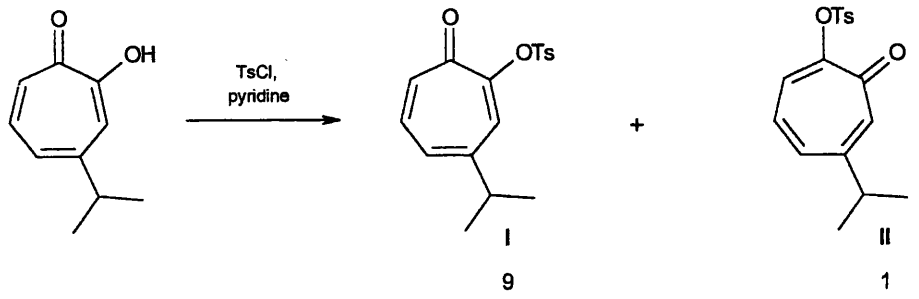

*Scheme 4.3: The mixture of **I** and **II**.*[13]

The compound **(60)** was used as a mixture, and no attempt was made to separate the two isomers.

The ligands **(61)-(65)** were characterised by elemental analysis, IR spectroscopy and ^{1}H and ^{13}C NMR. The NMR spectra were recorded in deuterated chloroform and confirm the identity of the products **(61)-(65)**. The spectra are very similar to each other except for the alkylamino group (Table 4.1).

Table 4.1: ^{1}H and ^{13}C NMR data for the alkylamino group.

Compound	^{1}H NMR data (ppm)	^{13}C NMR data (ppm)
(61)	2.95 [CH_3]	28.5 [CH_3]
(62)	1.31 [CH_3]; 3.28 [CH_2]	13.4 [CH_3]; 37.2 [CH_2]
(63)	0.94 [CH_3]; 1.64 [CH_2]; 3.18 [CH_2]	12.1 [CH_3]; 22.2 [CH_2]; 44.9 [CH_2]
(64)	4.44 [CH_2] *	*
(65)	0.94 [CH_3]; 1.40 [CH_2]; 1.63 [CH_2]; 3.22 [CH_2]	13.5 [CH_3]; 20.0 [CH_2]; 30.2[CH_2]; 42.3 [CH_2]

**Unable to distinguish with certainty the peaks between aromatic proton from the benzyl group and the tropone ring.*

The compounds **(66)-(70)** were characterised using microanalysis, IR spectroscopy and NMR. Due to the difficulty of assigning the peaks to **I** and **II** and to their overlapping, no NMR data are given. The signal due to the ^{i}propyl protons has been observed for every ligand, as well as the signals due to the alkylamino group. But their overlapping made it impossible to assign them with certainty.

The infra-red spectra for **(61)-(70)** are very similar as one would expect. The IR stretch observed at about 3300 cm^{-1} is characteristic of N–H mode and confirmed the replacement of the tosyl group by the amine (Table 4.2).

Table 4.2: Infrared absorptions (cm^{-1}) for some ligands.

Compound	υ(N–H)	υ(C=O) & υ(C=C)	Reference
(61)	3293	1629, 1590, 1510	This work
(62)	3301	1630, 1594, 1515	This work
(63)	3291	1637, 1595, 1512	This work
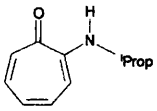	3290	-	2
(64)	3304	1632, 1591, 1512	This work
(65)	3307	1636, 1593, 1516	This work
(66)	3286	1633, 1595, 1514	This work
(67)	3308	1635, 1591, 1511	This work
(68)	3303	1632, 1592, 1511	This work
(69)	3314	1646, 1592, 1508	This work
(70)	3301	1635, 1593, 1511	This work

Crystals suitable for X-ray crystallography were obtained for **(64)** and the results from the X-ray structural study are now presented. Recrystallisation at room temperature from chloroform/cyclohexane afforded crystals of **(64)** suitable for X-ray crystallography. **(64)** crystallises in the monoclinic space group $P2_1/c$.

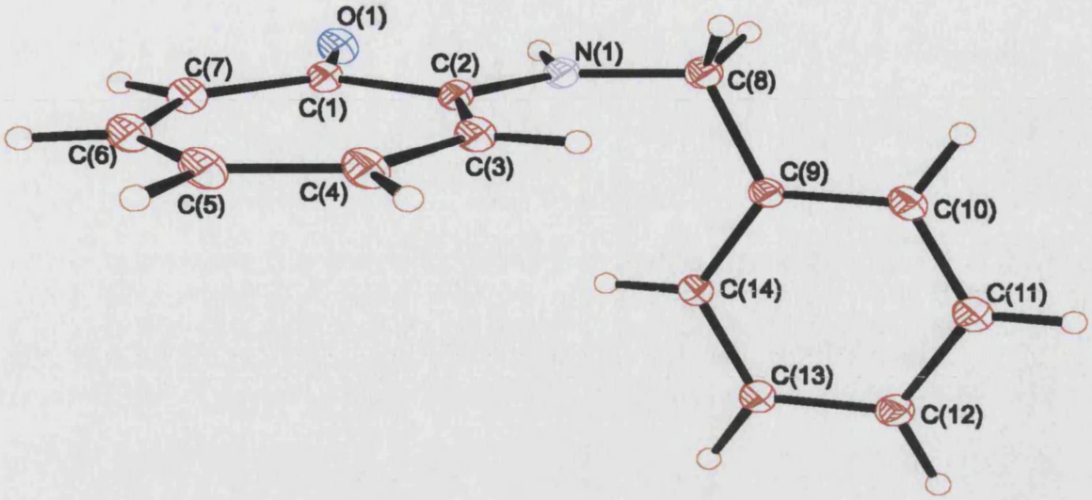

Figure 4.6: The structure of 2-benzylaminotropone ***(64)***.

The structure of tropolone and some tropolone derivatives have been studied.[14,15] It has been shown that tropolone,[14] as well as 3-chlorotropolone[16] and hinokitiol,[15] forms a bifurcated hydrogen bond with the carbonyl oxygen, one branch being intramolecular and other intermolecular. In this structure also, the intermolecular hydrogen bonds result in a dimer (Figure 4.7)

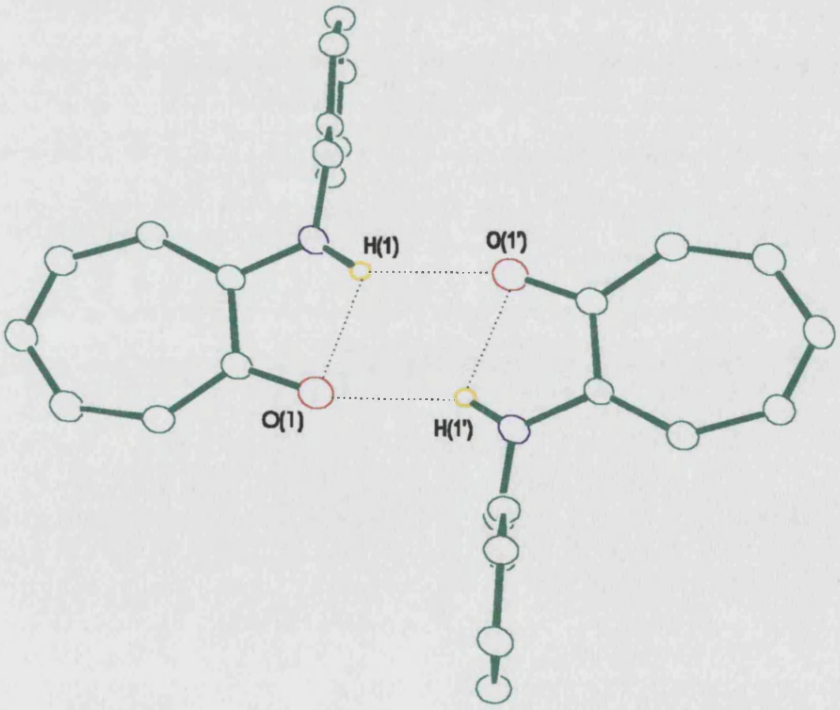

Figure 4.7: The dimer of 2-benzylaminotropone ***(64)***.

The distances O(1)···H(1) and O(1)···H(1') are 2.11 and 2.18 Å respectively. The value for the intermolecular bond O···H is similar to the one in 3-chlorotropolone (2.17 Å),[16] but larger than the corresponding value for tropolone (1.98 Å),[14] and hinokitiol (1.98 Å).[15] The hydrogen bonds in **(64)** are quite long and it can be concluded that the interaction is relatively weak.

The [C=O] bond length for **(64)** is given Table 4.3 with other [C=O] bond lengths found in the literature for related compounds. As can be seen, the [C=O] bond length of **(64)** compare favourably with the ones for the related tropolone compounds.

Table 4.3: C=O bond lengths in selected ligands.

Compound	[C=O] bond / Å	Reference
(64)	1.257(2)	This work
Tropolone	1.261(3)	14
3-Chlorotropolone	1.248(3)	16
Hinokitiol	1.247(4)	15

The torsion angle C(2)-N(1)-C(8)-C(9) between the seven-membered ring and the benzyl group is 76.1°.

4.2.2 Synthesis of copper(II) complexes

The ligands **(61)-(70)** were then used to prepare the Cu(II) complexes according to a method[17] used in earlier studies (Scheme 4.4).

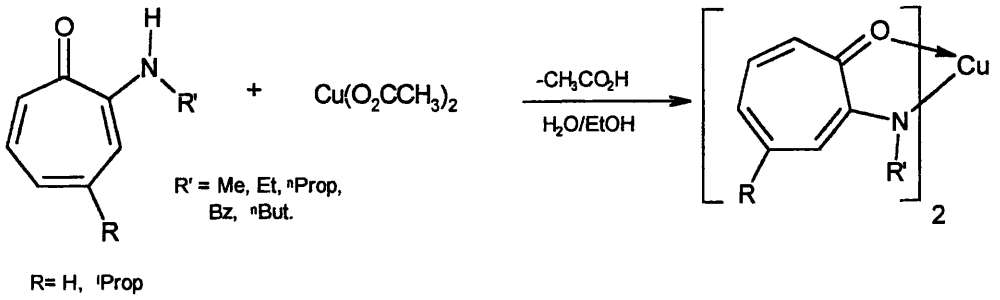

R′=	Me	Et	^{n}Prop	Bz	^{n}Bu
R= H	**(71)**	**(72)**	**(73)**	**(74)**	**(75)**
R= ^{i}Prop	**(76)**	**(77)**	**(78)**	**(79)**	**(80)**

Scheme 4.4: Synthesis of CuL_2

All the ten compounds were synthesised and crystals suitable for X-ray crystallography were obtained for **(71)** and **(72)**.

The elemental analysis confirms the identity of the compounds **(71)–(80)**, but they clearly indicate that the hinokitiol derivatives **(76)–(80)** are not pure [still a lot more pure than the ligands **(66)–(70)**]. Attempted recrystallisations from all common solvents, for the purpose of purification, proved unsuccessful.

The infrared spectra of the compounds are similar to those of the ligands, except that the ν(N-H) mode is absent. The ν(C=O) band that appears at 1630 cm^{-1} in the starting materials is shifted to a lower wavenumber by around 30-70 cm^{-1} in the complexes. This is good evidence for the formation of the metal complexes by chelation *via* the oxygen and the nitrogen atoms.

(71) crystallises in the monoclinic space group $P2_1/n$ and **(72)** crystallises in the monoclinic space group $P2_1/c$. The two complexes CuL_2 have the Cu atom adopting a four-coordinate, square planar geometry (Figures 4.8 and 4.9), like $Cu(trop)_2$,[18] $Cu(hino)_2$,[17] and most of the copper complexes in this thesis.

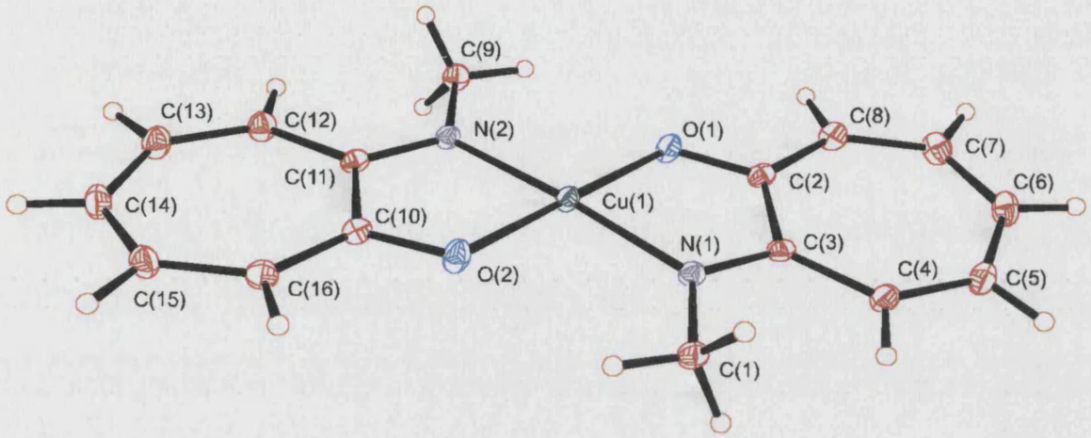

*Figure 4.8: The structure of Cu(2-methylaminotroponate)$_2$ **(71)**.*

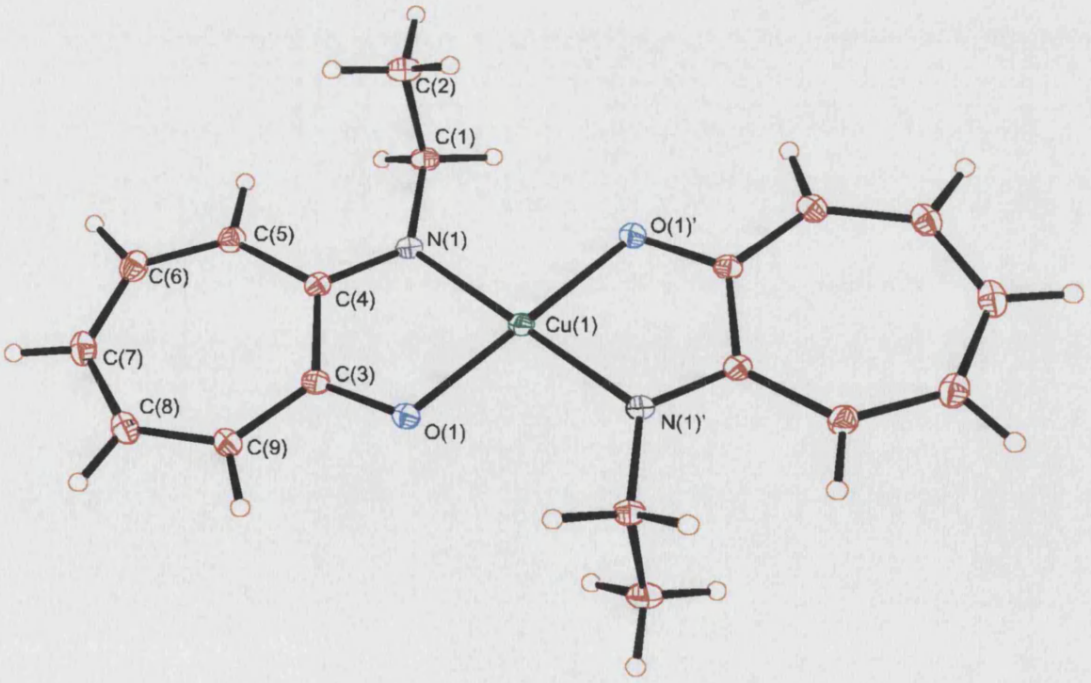

*Figure 4.9: The structure of Cu(2-ethylaminotroponate)$_2$ **(72)**.*

As expected the copper is bonding to the ligands via the oxygen and the nitrogen. Both compounds have the alkylamino groups adopting a *trans* configuration, which is the least sterically crowded arrangement. The *trans* isomer is the most favoured one in previous structures of α-hydroxyketones (*cf.*: Discussion about the structure of $Cu(hino)_2$, Chapter II, Section 2.2.3).

The [Cu←O(=C)] bonds in **(71)** and **(72)** are longer than those in the structures of $Cu(trop)_2$,[18] and $Cu(hino)_2$[17] (Table 4.3). It is due to the presence of the amino group. The [Cu-N] bond are similar to other [Cu-N] bond lengths found in the literature for Cu(II) tropocoronate complexes.

Table 4.3: Cu-X (X= N, O) bond length in selected complexes.

Compound	[Cu-N] bond / Å	[Cu-O(-C)] bond / Å	[Cu←O(=C)] bond / Å	Reference
(71)	1.928(1), 1.931(1)	-	1.934(1), 1.941(1)	This work
(72)	1.937(1)	-	1.931(1)	This work
$Cu(trop)_2$	-	1.915(3)	1.915(3)	18
$Cu(hino)_2$	-	1.900(2)	1.904(3)	17
Cu(TC-3,3)		-	-	19
Cu(TC-4,4)		-	-	19

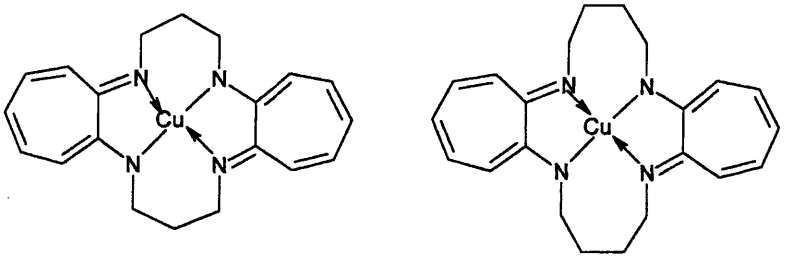

Cu(TC-3,3) Cu(TC-4,4)

Figure 4.10: The structures of Cu(TC-3,3) and Cu(TC-4,4).

The [C=O] bonds in **(71)** and **(72)** are of similar lengths than those in $Cu(trop)_2$,[18] and $Cu(hino)_2$[17] (Table 4.4). The [C-N] bonds also agree with those of Cu(TC-3,3) and Cu(TC-4,4).[19]

Table 4.4: C-X (X= N, O) bond lengths in selected complexes.

Compound	[C-N] bond / Å	[C-O] bond / Å	[C=O] bond / Å	Reference
(64)	1.346(2)	-	1.257(2)	This work
(71)	1.318(2), 1.320(2)	-	1.296(2), 1.309(2)	This work
(72)	1.325(2)	-	1.294(2)	This work
$Cu(trop)_2$	-	1.302(5)	1.286(5)	18
$Cu(hino)_2$	-	1.296(5)	1.293(5)	17
Cu(TC-3,3)		-	-	19
Cu(TC-4,4)		-	-	19

As expected, the [C=O] bond lengths, in both compounds **(71)** and **(72)**, are longer than those in the free ligand **(64)**. But surprisingly the [C-N] bond is shorter in the complexes than in the ligand.

The bite angles differ from the ideal geometry because the ligands dictate them to be less than 90°. The bite angles of the ligand **(61)** in **(71)** [O(1)-Cu-N(1): 82.04(5); O(2)-Zn-N(2): 82.26(5)] are similar to those of the ligand **(62)** in **(72)** [O(1)-Cu-N(1): 82.34(4)] and to those of Cu(TC-3,3) [O(1)-Cu-N(1): 82.34(4)] and Cu(TC-4,4) [O(1)-Cu-N(1): 82.34(4)].[19]

4.2.3 Structure and biological activity: the role of coordination number

In order to assess the importance of metal coordination number on activity and to complete the work done on the $Cu(hino)_2$ adducts (Chapter II, section 2.2.3), it has been attempted to synthesise a new chelating ligand using a diamine, which would

form a copper complex of higher than four coordination. The ligand was synthesised starting from 2-methoxytropone[7] (Scheme 4.5).

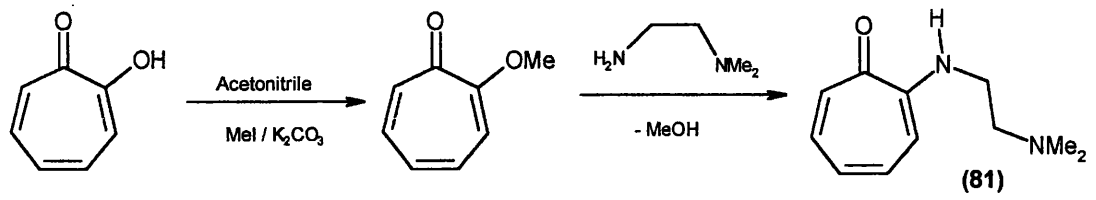

Scheme 4.5: synthesis of (81).

The elemental analysis indicates the nature of **(81)**, as do the ^{1}H and ^{13}C NMR. The compound is not completely pure, but the TLC shows only one spot. Some minor peaks in the NMR spectra have been attributed to solvents and despite all the effort no purification was possible.

Both NMR spectra were recorded in deuterated chloroform. The proton NMR is very similar to the one obtained by Nozoe *et al*[20] for 2-(2-aminoethylamino)tropone (Table 4.5).

Table 4.1: ^{1}H NMR data for (81) and related ligand.

Compound	^{1}H NMR data (ppm)
(81)	2.09 [NMe_2]; 2.51 [CH_2]; 3.26 [CH_2]; 6.41-7.08 [C_7H_5]; 7.42 [NH]
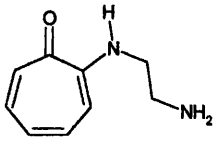	1.90 [NH_2]; 3.07 [CH_2]; 3.41 [CH_2]; 6.64-7.20 [C_7H_5]; 7.48 [NH]

The ^{13}C spectrum showed the right number of carbons and all the peaks were assigned (See Experimental).

Attempts to prepare the copper complex were made following the procedure used with the other alkylaminotropones (eq. 1)[17] or using Cu(II) chloride (eq. 2), but they did not work.

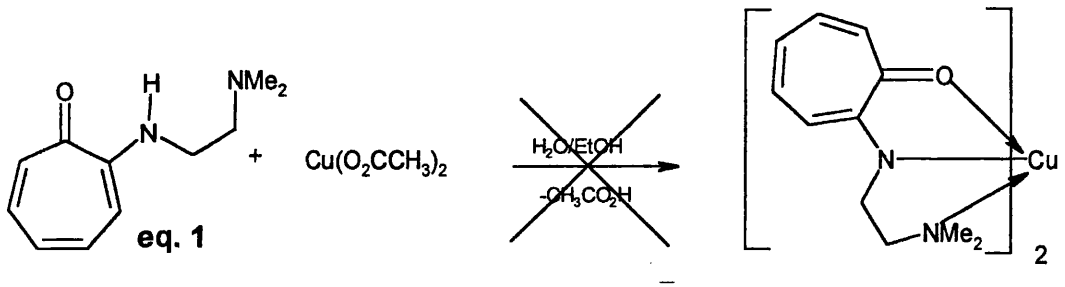

eq. 1

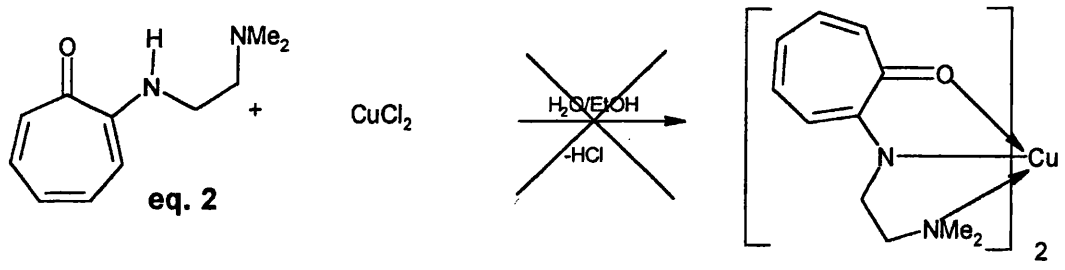

eq. 2

A mixture of a solid and an oil was obtained and any attempts to purify and separate them proved unsuccessful. An explanation could be that the acid produced HX (either acetic acid, eq.1 or hydrochloric acid, eq.2) is reacting with the NMe_2 group, preventing the formation of the wanted Cu(II) complex.

4.2.4 Attempts to synthesise the zinc(II) and tin (II) complexes

An attempt to prepare the Zn(II) derivatives of 2-alkylamino-4-alkyltropones was made following the same procedure as for the copper ones[17] (eq. 3), but this was unsuccessful.

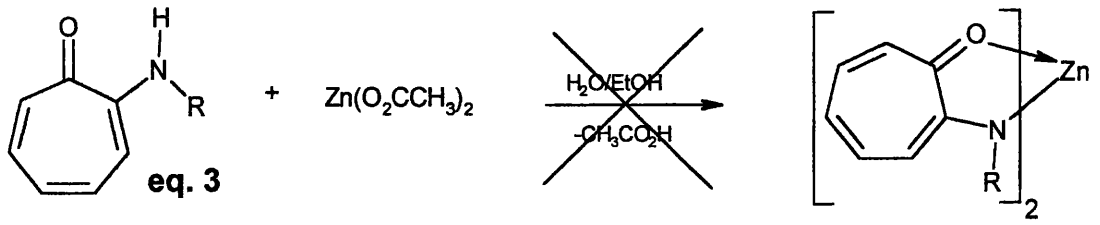

eq. 3

Scheme 4.6: Attempted synthesis of ZnL_2 via copper acetate.

Other attempts to synthesise the ZnL_2 compounds were made, using zinc dichloride (eq. 4) or diethyl zinc (eq. 5). A ligand was added to a solution of either $ZnCl_2$ in water/ethanol mixed or $Zn(Et)_2$ in hexane. The reactions were held at reflux for two hours and then the solvent removed *in vacuo*. But it was not possible to characterise or purify the mix obtained. The mixture was composed of a sticky oil and a solid that could not be separated.

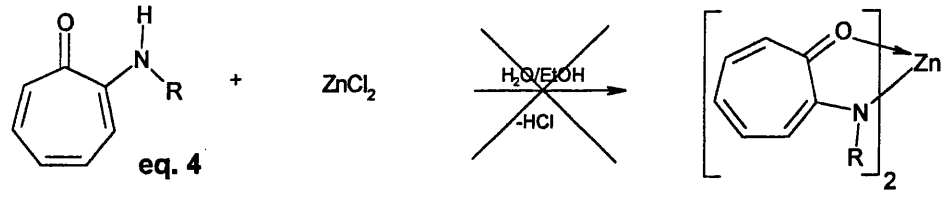

eq. 4

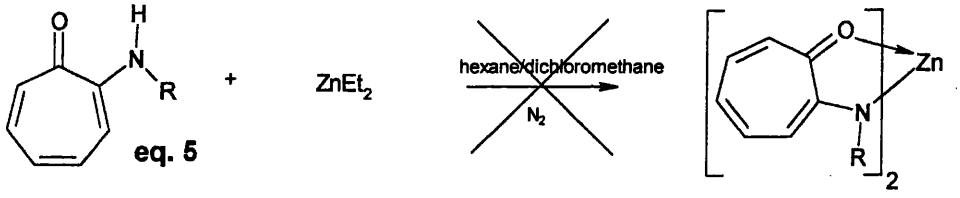

eq. 5

Scheme 4.6: Attempted synthesis of ZnL_2.

The tin(II) complexes were tried to be synthesised using the alkoxides route[21] (Chapter II, Section 2.2.3), but unfortunately this did not work.

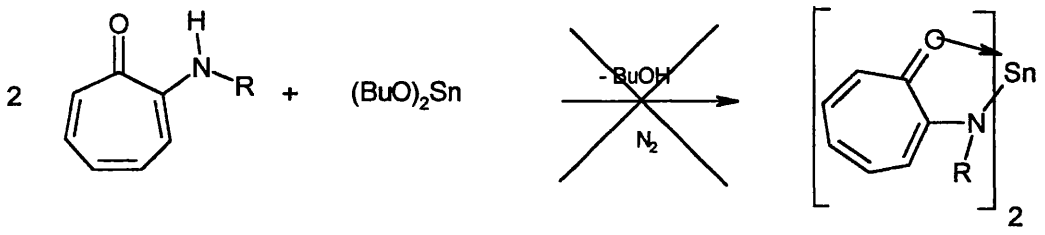

Scheme 4.7: Attempted synthesis of SnL_2.

The same problem occurs as for the zinc compounds. Any attempts to purify the mixture obtained have been unsuccessful.

4.3 Biological Testing

The results for the aminotropone compounds **(61)–(65)** and **(71)–(75)** are shown below. The hinokitiol derivatives **(66)–(70)** and **(76)–(80)** lack purity and have not been the object of anti-bacterial of PGI assay.

The tests were performed on *S.Warneri* and the same methodology was used as described for the tin complexes of maltol and related compounds in Chapter II, Section 2.4. As for the 1,2-dialkyl-3-hydroxypyridin-4-ones (Chapter III, Section 3.4) the ligands have been tested in order to compare their activities to those of the copper complexes (Table 4.4).

Table 4.4: Results of the PGI assay on the ligands [a].

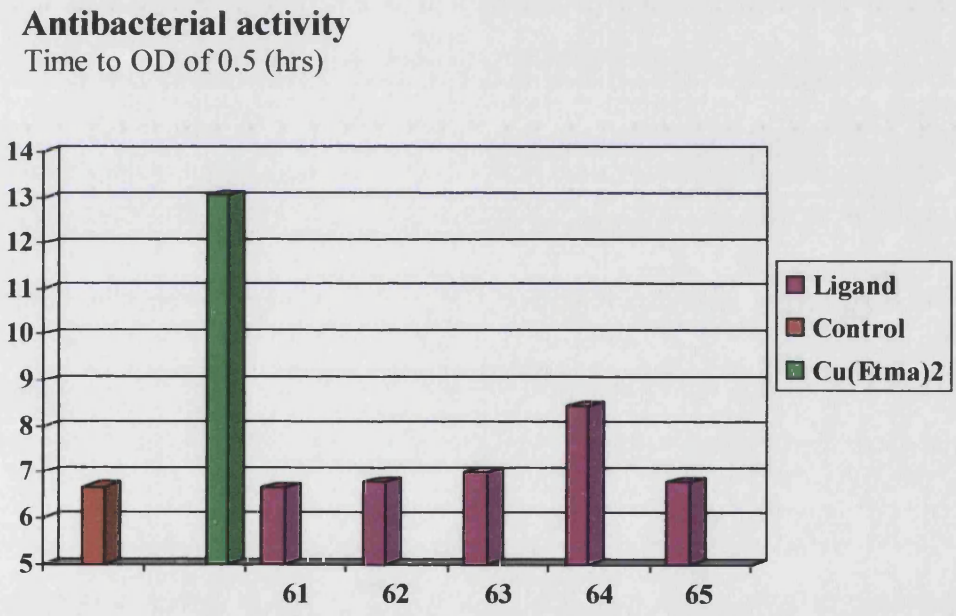

[a] *$Cu(Etma)_2$ also shown for comparison.*

The ligands hardly show any anti-bacterial proprieties when compared to the control toothpaste. The replacement of the alcohol function by an amine and the variation on the alkyl groups (R'= Me, Et, ^{n}Prop, Bz, ^{n}Bu) do not seem to influence their activity.

Only the PGI assay results on the copper compounds are shown Table 4.5, as it has not been possible to synthesise the zinc or tin derivatives.

Table 4.5: Results of the PGI assay on the copper complexes [a].

Antibacterial activity

Time to OD of 0.5 (hrs)

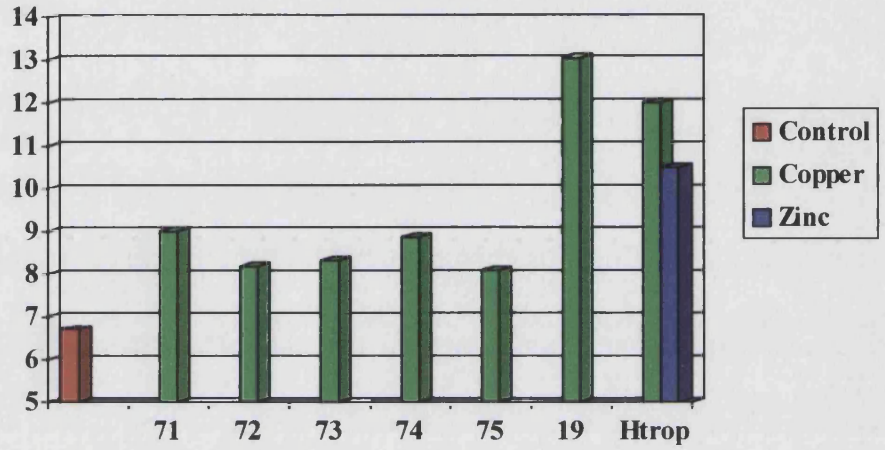

[a] *Cu(Etma)$_2$ **(19)**, Cu(trop)$_2$ and Zn(trop)$_2$ also shown for comparison.*

As for the Cu(1,2-alkyl-3-hydroxypyridin-4-one)$_2$ compounds (Chapter III, Section 3.4), none of the products showed a better activity than Cu(Etma)$_2$ complex. The fact that these compounds involved different donor atoms (N, O) seems to decrease their activity, when compare to the results for Cu(trop)$_2$ and Zn(trop)$_2$.

4.5 Experimental

Preparation of 2-*p*-toluenesulfonyltropolone (59)

Following the previously reported procedure[22] tropolone (5.00g; 40.98mmol) and *p*-toluenesulfonyl chloride (7.81g; 40.98mmol) were mixed together in dry pyridine (20mL). After thirty minutes, the mixture was filtered and the product obtained was then washed with cold water and dry under *vacuo*, yielding **(59)** as a white solid (11.18g; 98%).

Analysis for **(59)**: Found [calc. for $C_{14}H_{12}O_4S$]: C 61.0 (60.9)%; H 4.35 (4.34)%

Melting point: 156-158°C (156.5-157.5°C).[3]

Preparation of 2-*p*-toluenesulfonylhinokitiol (60)

The method described above[22] was applied to hinokitiol (5.00g; 30.48mmol). Hinokitiol and *p*-toluenesulfonyl chloride (5.81g; 30.48mmol) were mixed in dry pyridine (20mL) and the mixture was then washed with cold water and dried under *vacuo*, to obtain a pale yellow solid (9.31g; 96%).

Analysis for **(60)**: Found [calc. for $C_{17}H_{18}O_4S$]: C 64.6 (64.2)%; H 6.09 (5.66)%

The 2-alkylamino-tropones and 2-alkylamino-hinokitiols were prepared following literature procedures.[3,12] The method described by Rasika Dias *et al*[3] was repeated for **(61)**, **(62)** and **(66)**, **(67)**. The one from Pietra *et al*[12] was repeated for **(63)**–**(65)** and **(68)**–**(70)**.

Preparation of 2-methylaminotropone (61)

2-methylamino-tropone **(61)** was prepared using **(59)** (2.00g; 7.24mmol) in solution in dichloromethane (30mL) and aqueous methylamine (40%) (10mL). The mixture was stirred overnight at room temperature. Then the two layers were separated and the organic one was washed with water, dried with magnesium sulfate and concentrated under *vacuo* to obtain a yellow solid (0.76g; 78%).

Analysis for **(61)**: Found [calc. for C_8H_9NO]: C 61.0 (60.9)%; H 4.35 (4.34)%;
N 4.05 (4.02)%.

^{1}H NMR [δ(ppm), $CDCl_3$]: 2.95 [3H, s, N-CH_3]; 6.50-7.19 [5H, m, C_7H_5].

^{13}C NMR [δ(ppm), $CDCl_3$]: 28.5 [CH_3]; 107.3, 121.0, 127.3, 135.3, 136.3 [CH]; 155.5 [C_2]; 175.6 [C_3].

IR data (NaCl plates, nujol, cm^{-1}): 3293 υ(N-H); 1629, 1590 υ(C=O); 1510 υ(C=C).

Preparation of 2-ethylaminotropone (62)

The methodology described above was employed with aqueous ethylamine (70%) (10mL) and **(59)** (2.00g; 7.24mmol) in solution in dichloromethane (30mL). An orange oil **(62)** was obtained (0.77g, 71%).

Analysis for **(62)**: Found [calc. for $C_9H_{11}NO$]: C 71.9 (72.5)%; H 7.41 (7.38)%; N 9.32 (9.39)%.

^{1}H NMR [δ(ppm), $CDCl_3$]: 1.31 [3H, t, N-CH_2CH_3]; 3.28 [2H, q, N-CH_2CH_3]; 6.49-7.21 [5H, m, C_7H_5].

^{13}C NMR [δ(ppm), $CDCl_3$]: 13.4 [CH_3]; 37.2 [CH_2]; 108.4, 121.7, 128.0, 136.1, 136.9 [CH]; 155.2 [C_2]; 176.2 [C_3].

IR data (NaCl plates, nujol, cm^{-1}): 3301 υ(N-H); 1630, 1594 υ(C=O); 1515 υ(C=C).

Preparation of 2-^{n}propylaminotropone (63)

To a solution of **(59)** (2.00g, 7.24mmol) in dried DMSO (100mL) was added ^{n}propylamine (10mL) and the solution was stirred overnight. The mixture was poured into water and extracted with ether, then the ether layer was dried with magnesium sulfate and the solvent removed *in vacuo*. A brown oil **(63)** was obtained (0.81g, 68%).

Analysis for **(63)**: Found [calc. for $C_{10}H_{13}NO$]: C 72.7 (73.6)%; H 7.98 (7.97)%; N 8.65 (8.58)%.

^{1}H NMR [δ(ppm), $CDCl_3$]: 0.94 [3H, t, N-$CH_2CH_2CH_3$]; 1.64 [2H, m, N-$CH_2CH_2CH_3$]; 3.18 [2H, m, N-$CH_2CH_2CH_3$]; 6.49-7.21 [5H, m, C_7H_5].

^{13}C NMR [δ(ppm), $CDCl_3$]: 12.1 [$CH_2CH_2CH_3$]; 22.2 [$CH_2CH_2CH_3$]; 44.9 [$CH_2CH_2CH_3$]; 108.8, 122.1, 128.4, 136.5, 137.3 [CH]; 155.7 [C_2]; 176.5 [C_3].

IR data (NaCl plates, nujol, cm^{-1}): 3291 υ(N-H); 1637, 1595 υ(C=O); 1512 υ(C=C).

Preparation of 2-benzylaminotropone (64)

Following the same method than for **(63)**, a yellow solid was obtained using benzylamine (10mL) and **(59)** (2.00g; 7.24mmol). The yield of the reaction was 88% (1.34g). Recrystallysation from chloroform/cyclohexane gave yellow crystals suitable for X-ray analysis.

Analysis for **(64)**: Found [calc. for $C_{14}H_{13}NO$]: C 79.5 (79.6)%; H 6.26 (6.16)%; N 6.66 (6.63)%.

^{1}H NMR [δ(ppm), $CDCl_3$]: 4.44 [2H, s, CH_2]; 6.43-7.52 [10H, m, C_6H_5 and C_7H_5].

^{13}C NMR [δ(ppm), $CDCl_3$]: 46.5 [CH_2]; 108.4, 122.2, 127.5, 128.0, 130.1, 131.4, 136.1, 136.9 [*C*H]; 156.0 [C_2]; 175.8 [C_3].

IR data (NaCl plates, nujol, cm^{-1}): 3304 υ(N-H); 1632, 1592 υ(C=O); 1512 υ(C=C).

Preparation of 2-^{n}butylaminotropone (65)

Following the procedure with ^{n}butylamine (10mL) and **(59)** (2.00g; 7.24mmol), **(65)** was obtained (0.89g; 69%) as a brown-orange oil.

Analysis for **(65)**: Found [calc. for $C_{11}H_{15}NO$]: C 72.6 (74.6)%; H 8.57 (8.47)%; N 7.85 (7.90)%.

^{1}H NMR [δ(ppm), $CDCl_3$]: 0.94 [3H, t, N-$CH_2CH_2CH_2CH_3$];
1.40 [2H, m, N-$CH_2CH_2CH_2CH_3$];
1.63 [2H, m, N-$CH_2CH_2CH_2CH_3$];
3.22 [2H, t, N-$CH_2CH_2CH_2CH_3$];
6.49-7.21 [5H, m, C_7H_5].

^{13}C NMR [δ(ppm), $CDCl_3$]: 13.5 [$CH_2CH_2CH_2CH_3$]; 20.0 [$CH_2CH_2CH_2CH_3$];
30.2 [$CH_2CH_2CH_2CH_3$]; 42.3 [$CH_2CH_2CH_2CH_3$];
108.4, 121.7, 127.9, 136.1, 136.9 [*C*H]; 155.4 [C_2];
176.2 [C_3].

IR data (NaCl plates, nujol, cm^{-1}): 3307 υ(N-H); 1636, 1593 υ(C=O); 1516 υ(C=C).

Preparation of 2-methylamino-4-^{i}propyltropone (66), 2-ethylamino-4-^{i}propyltropone (67)

The method described earlier[3] for **(61)** and **(62)** was repeated for **(66)** and **(67)** using **(60)** (2.00g; 6.28mmol) and the corresponding amine in excess in solution in dichloromethane (30mL). Aqueous methylamine (40%) (10mL) was used for **(66)** (0.57g; 51%), aqueous ethylamine (70%) (10mL) for **(67)** (0.92g; 76%).

Analysis for **(66)**: Found [calc. for $C_{11}H_{15}NO$]: C 72.4 (74.6)%; H 8.25 (8.47)%; N 7.56 (7.90)%.

IR data (NaCl plates, nujol, cm^{-1}): 3286 υ(N-H); 1633, 1595 υ(C=O); 1514 υ(C=C).

Analysis for **(67)**: Found [calc. for $C_{12}H_{17}NO$]: C 73.1 (75.4)%; H 9.24 (8.89)%; N 6.37 (7.32)%.

IR data (NaCl plates, nujol, cm^{-1}): 3308 υ(N-H); 1635, 1591 υ(C=O); 1511 υ(C=C).

Preparation of 2-^{n}propylamino-4-^{i}propyltropone (68), 2-benzylamino-4-^{i}propyltropone (69), 2-^{n}butylamino-4-^{i}propyltropone (70)

Following the procedure for **(63)–(65)**, the three compounds **(68)–(70)** were obtained using **(60)** (2.00g; 6.28mmol) and ^{n}propylamine (10mL); benzylamine (10mL) and ^{n}butylamine (10mL) respectively. The yields of the reactions were as followed: **(68)** (0.51g; 39%), **(69)** (0.60g; 38%) and **(70)** (0.57g; 41%).

Analysis for **(68)**: Found [calc. for $C_{13}H_{19}NO$]: C 74.0 (76.1)%; H 9.49 (9.26)%; N 6.23 (6.82)%.

IR data (NaCl plates, nujol, cm^{-1}): 3303 υ(N-H); 1632, 1592 υ(C=O); 1511 υ(C=C).

Analysis for **(69)**: Found [calc. for $C_{17}H_{19}NO$]: C 70.6 (80.6)%; H 6.88 (7.50)%; N 6.79 (5.53)%.

IR data (NaCl plates, nujol, cm^{-1}): 3114 υ(N-H); 1646, 1592 υ(C=O); 1508 υ(C=C).

Analysis for **(70)**: Found [calc. for $C_{14}H_{21}NO$]: C 72.8 (76.7)%; H 9.10 (9.58)%; N 5.70 (6.39)%.

IR data (NaCl plates, nujol, cm^{-1}): 3301 υ(N-H); 1635, 1592 υ(C=O); 1511 υ(C=C).

Preparation of CuL_2 compounds

The method described by P. Wright[17] was repeated for **(71)–(80)**. A solution of the ligand in water/ethanol mix (1:1) was added to a well-stirred solution of copper acetate in water/ethanol mix (1:1). After stirring for two hours, the solution was refluxed and stirred for another two hours and then left at room temperature.

Preparation of Cu(2-methylaminotroponate)$_2$ (71)

A dark green solid was obtained using **(61)** (0.81g; 5.99mmol) and copper acetate (0.60g; 2.99mmol). The yield of the reaction was 99% (0.98g). Recrystallisation from ethanol gave crystal suitable for x-ray crystallography.

Analysis for **(71)**: Found [calc. for $C_{16}H_{16}N_2O_2Cu$]: C 57.9 (57.9)%; H 4.86 (4.82)%; N 8.40 (8.44)%.

IR data (NaCl plates, nujol, cm^{-1}): 1596, 1569 υ(C=O); 1518 υ(C=C).

Preparation of Cu(2-ethylaminotroponate)$_2$ (72)

Following the procedure with **(62)** (0.40g; 2.68mmol) and copper acetate (0.27g; 1.34 mmol), **(72)** was obtained. Recrystallisation from chloroform yielded green crystals (0.46g; 95 %) suitable for x-ray analysis.

Analysis for **(72)**: Found [calc. for $C_{18}H_{20}N_2O_2Cu$]: C 60.1 (60.0)%; H 5.66 (5.56)%; N 7.74 (7.78)%.

IR data (NaCl plates, nujol, cm^{-1}): 1595, 1540 υ(C=O); 1513 υ(C=C).

Preparation of Cu(2-^{n}propylaminotroponate)$_2$ (73)

The method described previously was utilised for **(63)** (0.55g; 2.56mmol) added to copper acetate (0.26g; 1.28mmol). Following this a green solid was obtained (0.55g; 86%).

Analysis for **(73)**: Found [calc. for $C_{20}H_{24}N_2O_2Cu$]: C 63.1 (63.5)%; H 4.84 (4.88)%; N 5.75 (5.69)%.

IR data (NaCl plates, nujol, cm^{-1}): 1597, 1570 υ(C=O); 1516 υ(C=C).

Preparation of Cu(2-benzylaminotroponate)$_2$ (74)

The methodology described earlier was employed with **(64)** (0.29g; 1.37mmol) and copper acetate (0.14g; 0.68mmol). A green solid was obtained (0.32g; 95%).

Analysis for **(74)**: Found [calc. for $C_{28}H_{24}N_2O_2Cu$]: C 68.9 (69.5)%; H 5.11 (4.96)%
N 5.77 (5.79)%.

IR data (NaCl plates, nujol, cm^{-1}): 1593, 1570 υ(C=O); 1513 υ(C=C).

Preparation of Cu(2-^{n}butylaminotroponate)$_2$ (75)

A green solid was obtained using **(65)** (0.46g; 2.59mmol) and copper acetate (0.26g; 1.29mmol). The yield of the reaction was 86% (0.46g).

Analysis for **(75)**: Found [calc. for $C_{22}H_{28}N_2O_2Cu$]: C 63.2 (63.5)%; H 6.79 (6.73)%;
N 6.80 (6.73)%.

IR data (NaCl plates, nujol, cm^{-1}): 1597, 1569 υ(C=O); 1515 υ(C=C).

Preparation of Cu(2-methylamino-4-^{i}propyltroponate)$_2$ (76)

The method described previously was utilised for **(66)** (0.50g; 2.82mmol) added to copper acetate (0.28g; 1.41mmol). Following this a green solid was obtained (0.21g; 42%).

Analysis for **(76)**: Found [calc. for $C_{22}H_{28}N_2O_2Cu$]: C 63.6 (63.5)%; H 6.73 (6.73)%;
N 6.45 (6.73)%.

IR data (NaCl plates, nujol, cm^{-1}): 1606, 1557 υ(C=O); 1512 υ(C=C).

Preparation of Cu(2-ethylamino-4-^{i}propyltroponate)$_2$ (77)

The methodology described earlier was employed with **(67)** (0.50g; 2.60mmol) and copper acetate (0.26g; 1.30mmol). A green solid was obtained (0.32g; 55%).

Analysis for **(77)**: Found [calc. for $C_{24}H_{32}N_2O_2Cu$]: C 67.9 (64.5)%; H 7.21 (8.27)%
N 4.80 (6.31)%.

IR data (NaCl plates, nujol, cm^{-1}): 1603, 1590 υ(C=O); 1510 υ(C=C).

Preparation of Cu(2-^{n}propylamino-4-^{i}propyltroponate)$_2$ (78)

A green solid was obtained using **(68)** (0.50g; 2.44mmol) and copper acetate (0.24g; 1.22mmol). The yield of the reaction was 62% (0.36g).

Analysis for **(78)**: Found [calc. for $C_{26}H_{36}N_2O_2Cu$]: C 66.9 (66.2)%; H 8.06 (7.63)%; N 5.74 (5.93)%.

IR data (NaCl plates, nujol, cm^{-1}): 1591, 1578 υ(C=O); 1512 υ(C=C).

Preparation of Cu(2-benzylamino-4-^{i}propyltroponate)$_2$ (79)

A dark green solid was obtained using **(69)** (0.50g; 1.97mmol) and copper acetate (0.20g; 0.98mmol). The yield of the reaction was 22% (0.12g).

Analysis for **(79)**: Found [calc. for $C_{34}H_{36}N_2O_2Cu$]: C 70.3 (71.9)%; H 6.12 (6.34)%; N 4.23 (4.93)%.

IR data (NaCl plates, nujol, cm^{-1}): 1617, 1589 υ(C=O); 1510 υ(C=C).

Preparation of Cu(2-^{n}butylamino-4-^{i}propyltroponate)$_2$ (80)

Following the procedure with **(70)** (0.50g; 2.28mmol) and copper acetate (0.23g; 1.14 mmol), **(80)** was obtained as a green solid (0.18g; 32%).

Analysis for **(80)**: Found [calc. for $C_{28}H_{40}N_2O_2Cu$]: C 65.6 (67.3)%; H 7.61 (8.00)%; N 5.72 (5.60)%.

IR data (NaCl plates, nujol, cm^{-1}): 1591, 1579 υ(C=O); 1511 υ(C=C).

Preparation of 2-methoxytropone

Following the previously reported procedure,[7] tropolone (1.00g; 8.19mmol), iodomethane (2.50g; 17.61mmol) and anhydrous potassium carbonate (2.00g; 14.47mmol) were refluxed together in dry acetonitrile (100mL). After three hours, the mixture was filtered and the product obtained was then washed with acetonitrile and dry under *vacuo*, yielding 2-methoxytropone, as a pale yellow oil (0.86g; 77%).

Analysis: ^{1}H NMR [δ(ppm), $CDCl_3$]: 3.76 [3H, s, O-CH_3]; 6.43-7.52 [5H, m, C_7H_5].

Preparation of 2-ethylaminotropone (81)

To a solution of **2-methoxytropone** (0.50g, 3.67mmol) in ethanol (20mL) was added N,N-dimethylethylenediamine (1mL) and the solution was refluxed for one hour. The solvent was removed *in vacuo* and the mixture obtained was poured into water and extracted with chloroform. Then the chloroform layer was dried with magnesium sulfate and the solvent removed *in vacuo*, yielding a dark yellow oil **(81)** (0.31g; 44%).

References

1) Bagli J. F.; St-Jacques M., *Can. J. Chem.* **1978**, *56*, 578.

2) Rasika-Dias H. V.; Jin W.; Ratcliff R. E., *Inorg. Chem.* **1995**, *34*, 6100.

3) Rasika-Dias H. V.; Jin W., *Inorg. Chem.* **1996**, *35*, 6546.

4) Roesky P. W., *Inorg. Chem.* **1998**, *37*, 4507.

5) Roesky P. W.; Burgstein M. R., *Inorg. Chem.* **1999**, *38*, 5629.

6) Von E Doering W.; Hiskey C. F., *J. Am. Chem. Soc.* **1952**, *74*, 5688.

7) Lal K.; Leckey N. T.; Watts W. E., *J. Organomet. Chem.* **1983**, *254*, 193.

8) Roesky P. W.; Burgstein M. R.; Berberich M. R., *Organometallics* **1998**, *17*, 1452.

9) Imajo S.; Nakanishi K.; Roberts M.; Lippard S. J.; Nozoe T., *J. Am. Chem. Soc.* **1983**, *105*, 2071.

10) Davis A. W.; Roberts M.; Zask A.; Nakanishi K.; Nozoe T.; Lippard S. J., *J. Am. Chem. Soc* **1985**, *107*, 3864.

11) Doerrer L. H.; Lippard S. J., *Inorg. Chem.* **1997**, *36*, 2554.

12) Biggi G.; Del Cima F.; Pietra F., *J. Am. Chem. Soc.* **1973**, 7101.

13) Yanagisawa T.; Kosakai K.; Tomiyama T.; Yasunami M.; Takase K., *Chem. Pharm. Bull.* **1990**, *38*, 3355.

14) Shimanouchi H.; Sasada Y., *Acta Cryst.* **1973**, *29*, 81.

15) Berg J. E.; Karlasson B.; Pilotti A. M.; Wiehager A. C., *Acta Cryst.* **1976**, *B32*, 3121.

16) Tsuji T.; Sekiya H.; Nishimura Y.; Mori, A.; Takeshita H., *Acta Cryst.* **1991**, *C47*, 2428.

17) Wright, P. *The synthesis and characterisation of novel Sn(II), Zn(II) and Cu(II) compounds for anti-bacterial evaluation*; University of Bath, **1999**.

18) Berg J.; Pilotti A.; Soderholm A.; Karlsson B., *Acta Cryst.* **1978**, *B34*, 3071.

19) Davis A. W.; Zask A.; Nakanishi K.; Lippard S. J., *Inorg. Chem* **1985**, *24*, 3737.

20) Nozoe T.; Ishikawa S.; Shindo K., *Heterocycles* **1989**, *28*, 733.

21) Gsell R.; Zeldin M., *J. Inorg. Nucl. Chem.* **1975**, *37*, 1133.

22) Reddington M. V., *J. Chem. Soc., Perkin Trans. I* **1998**, 143.

Conclusion

5.1 Conclusions and future work

i) Maltol and related compounds

The reactions SnX_2 + HL → SnL_2 (X= Cl, F; L= Hma, HEtma, Hhino) have been carried out in THF and have shown the products obtained are not the ones expected (SnL_2), but are in fact SnL_2X_2. The reaction seems to depend on the solvent, because when it is carried in water the oxidation does not occur and SnL_2 compounds are obtained. The products were characterised and the crystal structures of $Sn(hino)_2Cl_2$ **(3)**, $Sn(Etma)_2F_2$ **(5)** and $Sn(hino)_2F_2$ **(6)** were solved. The compounds have been tested against *S. Warneri* bacteria and appeared to be highly active. However, further tests need to be done to ensure this is not due to the low pH of the compounds in solution.

Tin(II) complexes of various cyclic α-hydroxyketones (L= Hma, HEtma, Hhino, Htrop and Hkoj) were obtained. A route involving stannocene as reagent and ether as solvent has first been used, but the product obtained lacked solubility and hence were poorly characterised. A successful route was discovered using tin alkoxides and the crystal structures of $Sn(ma)_2$ **(8)** and $Sn(trop)_2$ **(11)** have been obtained. The products were found to be notably air-stable despite adopting monomeric pseudo-trigonal bipyramidal structures (SnO_4E; E = stereochemically active lone electron pair) in which the ligands only chelate a single metal centre.

The synthesis of Zn(II) and Cu(II) compounds (L= Hma, Hetma, Hhino, Htrop and Hkoj) was achieved. All the complexes have been characterised and the structures of $Zn(hino)_2$ **(17)** and $Zn(trop)_2$ **(21)** were obtained. **(21)** is a polymer in the solid state, while **(17)** can be considered as an ethanol-capped dimeric fragment of the polymer of **(21)**, the solvent molecules breaking the extended polymer of $Zn(trop)_2$.

Derivatives of $Cu(hino)_2$ have been synthesised in order to understand the importance of metal coordination number on activity. A 1:1 adduct with pyridine **(25)** and another with 2,2'-bipyridine **(26)** have been isolated. The crystal structure

of **(25)** has been solved and has shown, as expected a five-coordinate copper. An unsuccessful reaction with urea gave crystals of $Cu(hino)_2$ **(20)**, which adopted a structure different t0 the previous obtained by P. Wright.

ii) 1,2-dialkyl-3-hydroxypyridin-4-ones

1,2-dialkyl-3-hydroxypyridin-4-ones have been synthesised using maltol or ethyl maltol as starting material and four different amines (methylamine; ethylamine; benzylamine and ^{n}butylamine). It was of interest to vary the alkyl group on the amine, in order to measure the steric effect on the anti-bacterial activity of the compounds.

The copper and zinc complexes have been obtained and characterised. Four compounds have been studied by X-ray crystallography: Zn(1-benzyl-2-methyl-3-hydroxypyridin-4-onate)$_2$ **(41)**, Cu(1-benzyl-2-ethyl-3-hydroxypyridin-4-onate)$_2$ **(45)**, Cu(1-^{n}butyl-2-ethyl-3-hydroxypyridin-4-onate)$_2$ **(46)** and Zn(1-methyl-2-ethyl-3-hydroxypyridin-4-onate)$_2$ **(47)**. None of the compounds was more active than their analogue $Cu(Etma)_2$ and no correlation was found between the variation on the amine and the anti-bacterial activity.

In the reactions with $SnCl_2$ and the ligands in water, only one of the halogens has been replaced by the ligand, giving compounds of the form Sn(L)Cl. The solubility of these compounds was on the whole very poor, so they have not been the objects of biological tests.

iii) Alkylaminotropones

A new kind of ligand, containing two different donor atoms (N, O) has been prepared starting from tropolone or hinokitiol, combined with five amines (methylamine; ethylamine; ^{n}propylamine; benzylamine and ^{n}butylamine). They have all been characterised and the structure of 2-benzylaminotropone **(64)** has been obtained.

The copper complexes have been synthesised and characterised. The crystal structures of Cu(2-methylaminotroponate)$_2$ **(71)** and Cu(2-ethylaminotroponate)$_2$ **(72)** were solved. Despite several attempts, it has not been possible to make the zinc and tin adducts. A diamino ligand has been synthesised in order to form an adduct with copper of higher coordination number than four, but it was not possible to obtain the copper complex.

A PGI assay was conducted on the ligands **(61)-(65)** and the Cu(II) complexes **(71)–(75)**. Their performance in the test was disappointing as they showed a lower activity than Cu(trop)$_2$. As for the pyridinones, variation of the alkyl group of the amine did not seem to have any effect; neither did the introduction of the nitrogen donor. It was impossible to purify the hinokitiol derivatives; therefore they have not been tested.

In all the crystal structures obtained for the copper complexes (except Cu(hino)$_2$ and Cu(hino)$_2$.py), the copper atom is four-coordinate adopting a square planar geometry. It has been noticed that all the copper compounds are active, when testing against *S.Warneri.* On the other hand, the crystal structures of the zinc compounds show the zinc in a coordination number greater than four (either five or six) often with solvent coordinated to the molecule, and these compounds always are less active than the copper derivatives. So clearly the coordination number of the metal appeared to play a role in the activity of the compounds. No explanation has yet been given concerning the mode of action of the cyclic α-hydroxyketones/metal complexes. This is a relatively new area and research is currently being done at Unilever Research, in order to understand better the testing and procedures. A possible mechanism is that the cyclic α-hydroxyketone helps solubilise the metal, so that the complex can take the metal into the cell where internal structures are damaged.

In conclusion it can be said that:

- Metal complexes are always better than ligands alone (comparison for pyridinones and tropolone derivatives) (Figure 5.1).

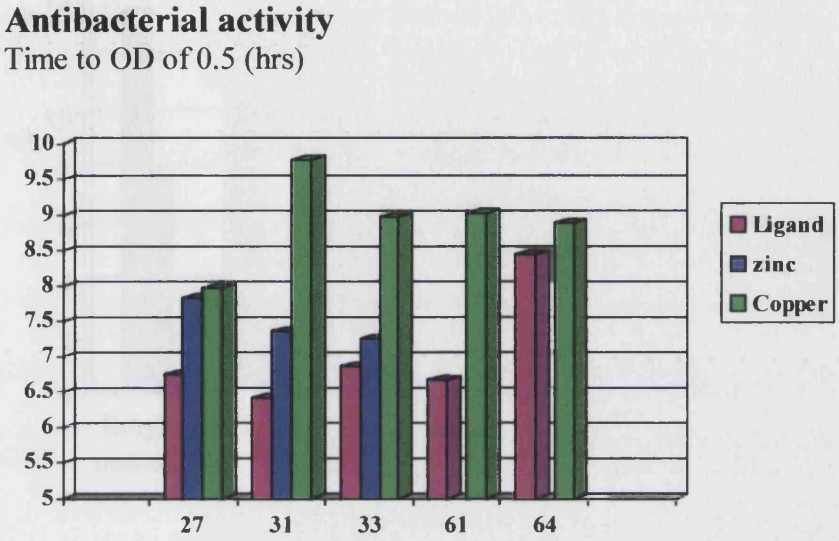

Figure 5.1: Antibacterial activity of some metal complexes versus related ligands.

- None of the new compounds has shown a greater activity than $Cu(Etma)_2$ (Figure 5.2).

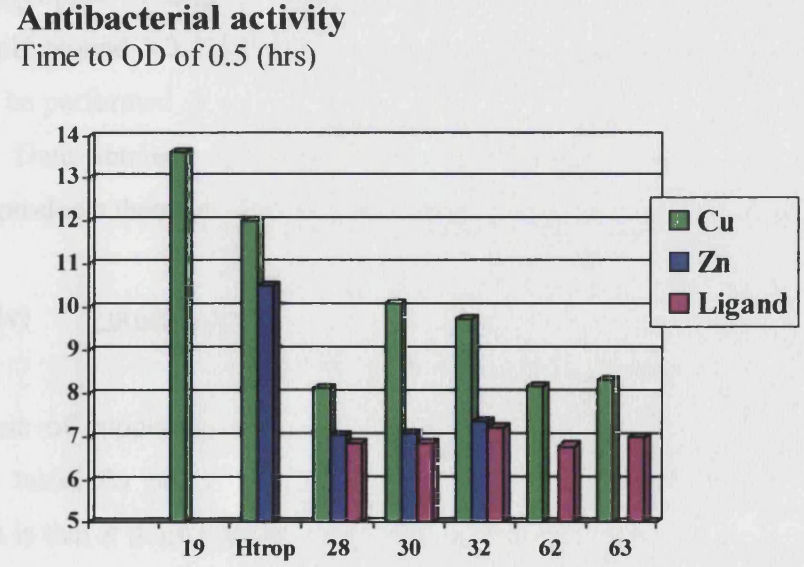

Figure 5.2: Antibacterial activity of some compounds versus $Cu(Etma)_2$ ***(19)****.*

- Ethyl maltol is the best among all the ligand tested (Figure 5.3).

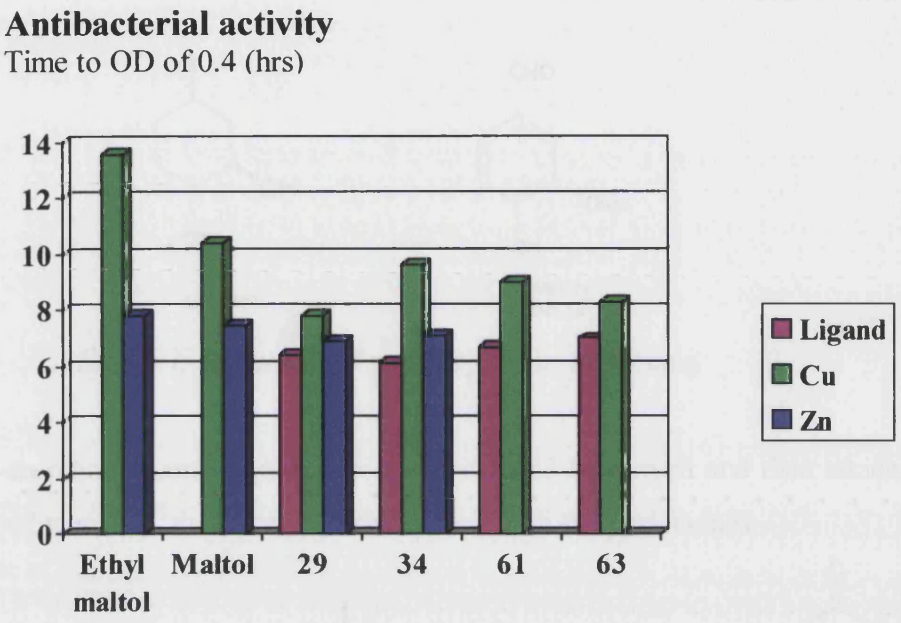

Figure 5.3: Antibacterial activity of ethyl maltol versus other ligands.

- Copper is the best of the three metals.

The SnL_2Cl_2 compounds, when tested against *S.Warneri*, seem to be more active than the copper or zinc related complexes, but the problem is that they are very acidic (pH around 3-3.5) and this could be responsible for their greater activity. Tests need to be performed at a higher pH (6.5-7.0) to demonstrate their true anti-bacterial activity. Data obtained for Zn(II) and Cu(II) show always a better activity for the copper products than for the zinc one (*cf* discussion above on CN number).

iv) Future work

The use of copper in toothpaste is not common, the main reason being its bad metallic taste. As previously stated, ethyl maltol is effective and cheap, the only problem is that it does not mask the taste of the copper. So the solution would be to combine the effectiveness of the α-hydroxyketones with a compound able to deliver

a nice flavour and hide any unwanted taste. Below are shown the structures of potential flavour molecules.

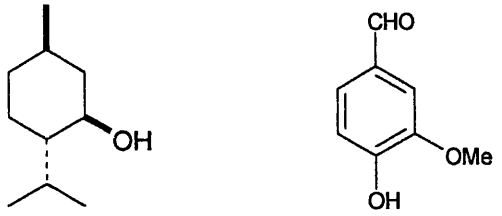

MENTHOL

VANILLIN
(VANILLA)

Figure I: Structures of various flavour molecules.

An amino-menthol or amino-vanillin compound could be formed and then attached to maltol or ethyl maltol, the same way it was done with the pyridinones.

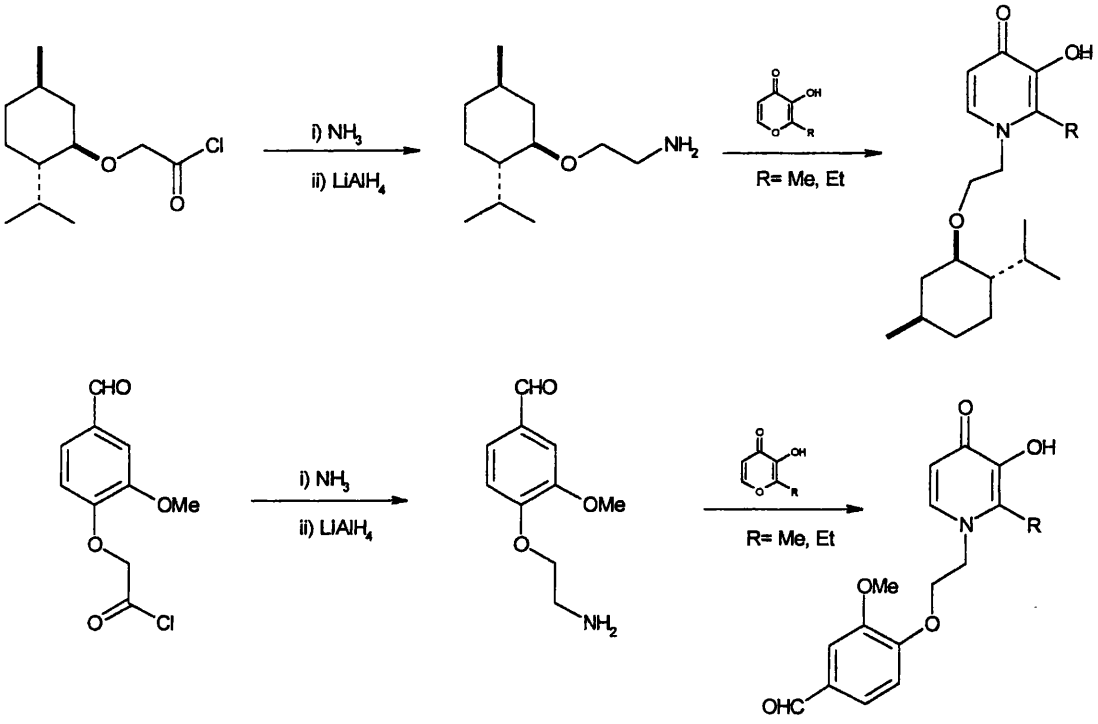

Such ligands, when combined with Cu(II), could deliver into the mouth a product with strong anti-bacterial properties (due to the presence of the α-hydroxyketone group), as well as a long lasting sensation of freshness (due to the presence of the flavour).

Appendix

Appendix A: Structures of the compounds (1)–(80)

The following pages are intended as an index of numbered compounds contained within Chapter II to IV.

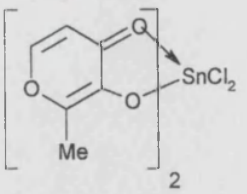

(1)

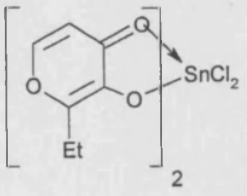

(2)

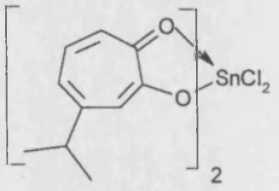

(3)

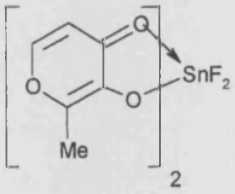

(4)

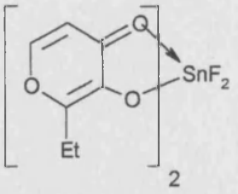

(5)

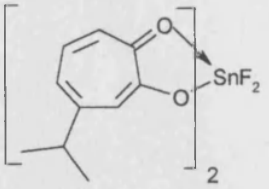

(6)

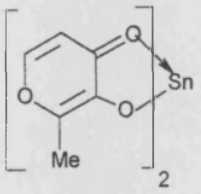

(8)

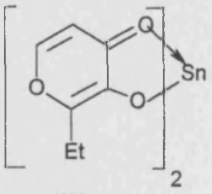

(9)

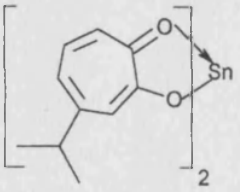

(10)

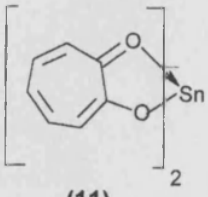

(11)

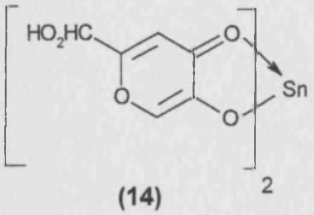

(14)

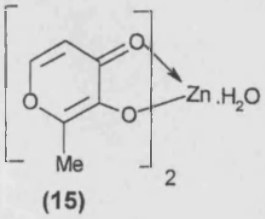

(15)

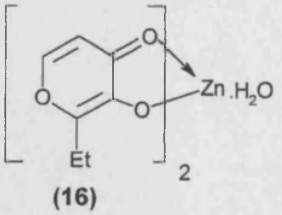

(16)

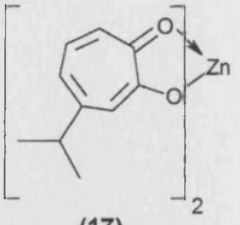

(17)

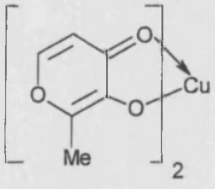

(18)

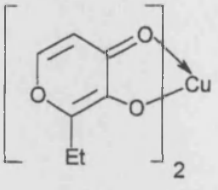

(19)

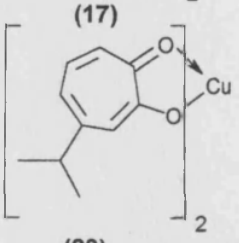

(20)

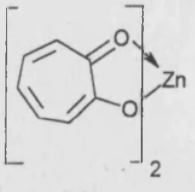

(21)

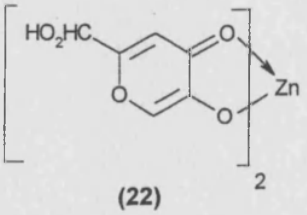

(22)

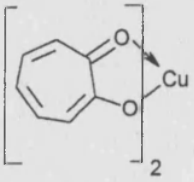

(23)

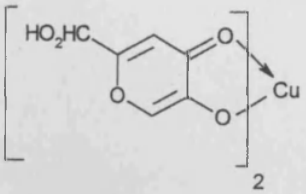

(24)

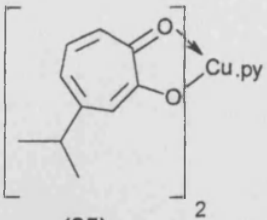

(25)

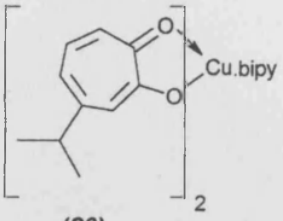

(26)

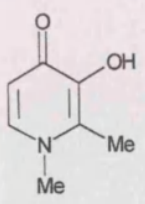

(27)

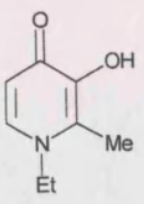

(28)

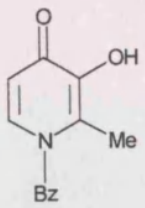

(29)

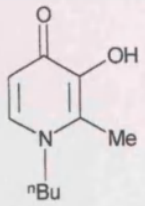

(30)

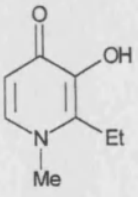

(31)

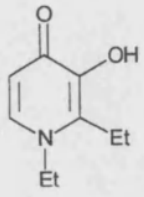

(32)

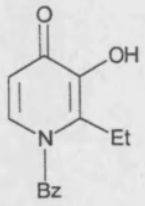

(33)

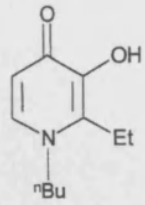

(34)

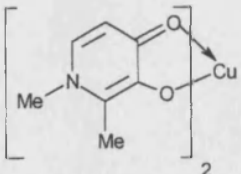

(35)

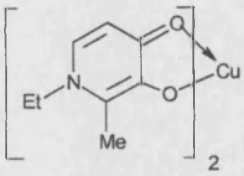

(36)

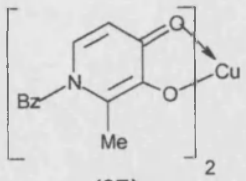

(37)

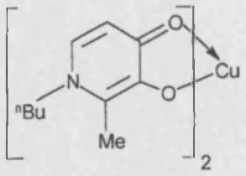

(38)

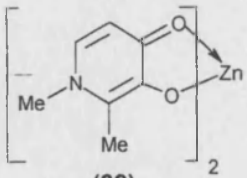

(39)

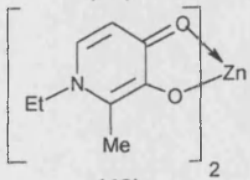

(40)

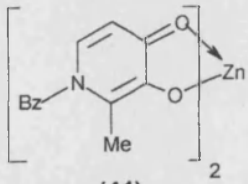

(41)

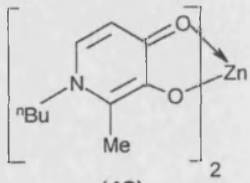

(42)

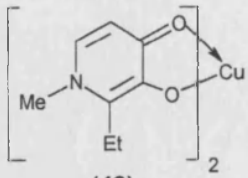

(43)

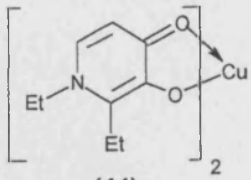

(44)

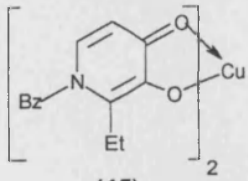

(45)

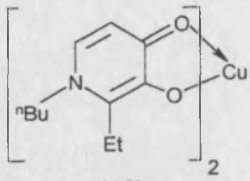

(46)

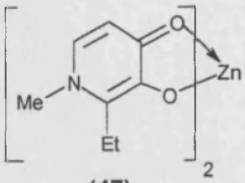

(47)

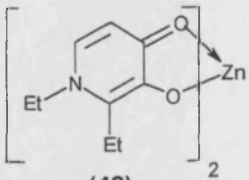

(48)

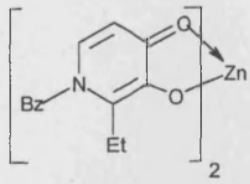

(49)

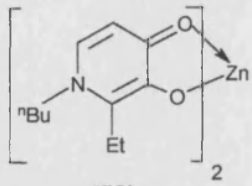

(50)

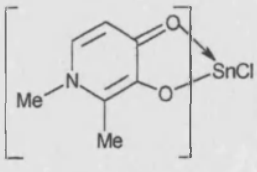

(51)

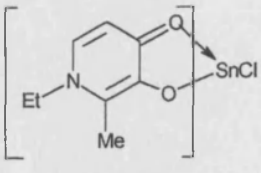

(52)

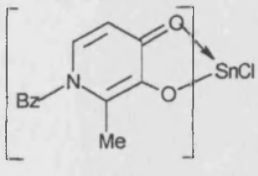

(53)

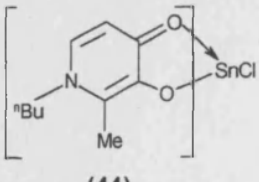

(44)

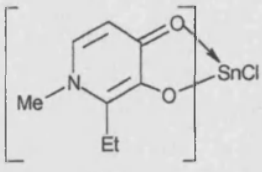

(55)

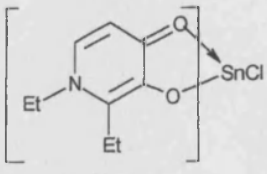

(56)

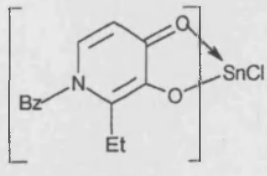

(57)

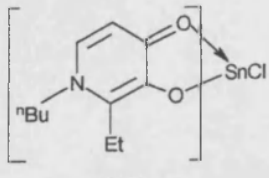

(58)

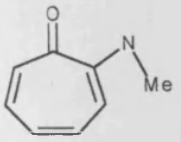

(61)

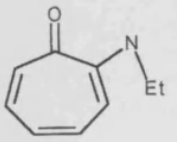

(62)

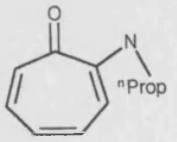

(63)

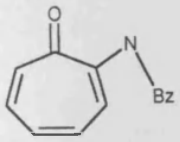

(64)

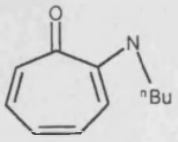

(65)

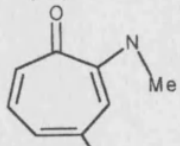

(66)

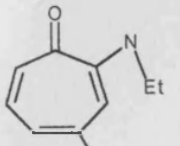

(67)

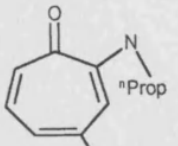

(68)

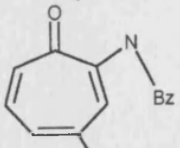

(69)

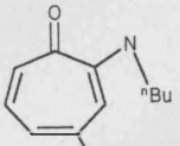

(70)

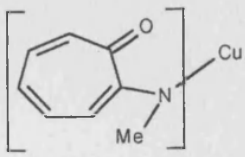

(71)

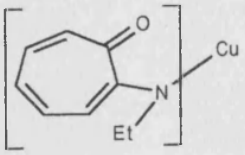

(72)

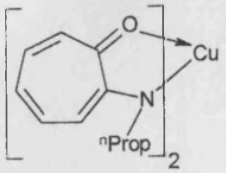

(73)

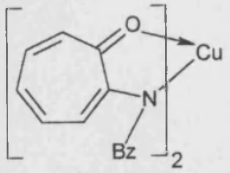

(74)

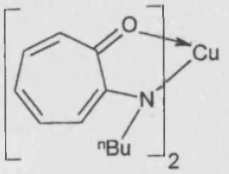

(75)

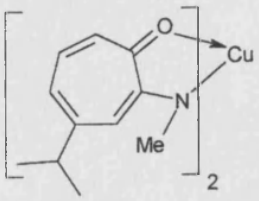

(76)

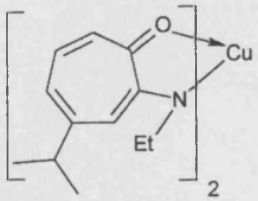

(77)

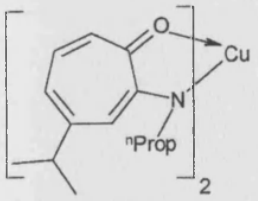

(78)

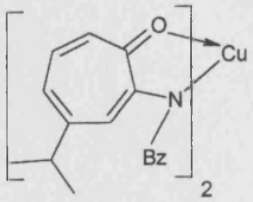

(79)

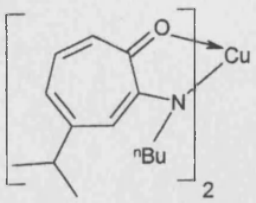

(80)

Appendix B: Experimental procedures

General Methods

Starting materials were commercially obtained and used without further purification. Maltol, ethyl maltol, kojic acid and all the amines (methyl, ethyl, ^{n}propyl, benzyl, ^{n}butyl) were purchased from Aldrich, while tropolone was bought from Avocado. Unilever provided hinokitiol.

Infrared spectra were recorded as nujol mulls between NaCl plates using a Nicolet 510P FT-IR spectrophotometer.

Elemental analyses were performed using a Carlo-Erba Strumentazione E.A. model 1106 microanalyser operating at 500°C.

^{1}H and ^{13}C NMR spectra were recorded on a Jeol JNM-GX270 FT spectrometer, while **^{119}Sn and ^{19}F NMR spectra** were recorded on a Jeol JNM-EX400 FT machine.

X-ray Crystallography

Crystal data are given in appendix **D–S**. Data for **(8)** and **(11)** were collected on an Enraf-Nonius CAD-4 diffractometer, while data for the rest of the compounds **(3)**, **(5)**, **(6)**, **(17)**, **(20)**, **(21)**, **(25)**, **(41)**, **(45)–(47)**, **(65)**, **(71)** and **(72)** were collected on a Nonius Kappa CCD machine. For all compounds, data were corrected for both extinction and absorption effects; hydrogens were added at calculated positions. Refinement was full matrix least-squares based on F^2. Structure determination and refinement was achieved using the SHELX suite of programmes;[1,2] drawings were produced using ORTEX.[3]

1) Sheldrick, G. M.: University of Göttingen, Göttingen, 1986.
2) Sheldrick, G. M.: University of Göttingen, Göttingen, 1997.
3) McArdle, P. *J. Appl. Cryst.* **1995**, *28*, 65.

Appendix C: Experimental procedures for the PGI assays

i) Preparation of *S.Warneri*-coated microtitre plates

The bacteria used for the tests were *Staphlococcus.warneri.* A subculture of *S.Warneri* was added to a Brain Heart Infusion (BHI) and incubated overnight at 37°C. The BHI with S.Warneri was then transferred to 10mL sterile centrifuge tubes and then spun for 5 minutes at 6000rpm. The supernatant was safely discarded and 5mL of sterile phosphate buffered saline (PBS) added to each tube. The bacteria were resuspended using a whirlmixer and the tubes recentrifuged. This procedure was repeated three times to thoroughly wash the bacteria. The bacteria were then suspended in PBS in 150mL sterilins to produce an optical density (OD) of O.2 relative to a PBS blank.

The 96-well plates on which the biofilms were coated were Corning, code 25860-96. Firstly. The wells from row A, No. 7-12 were covered with a strip of plate sealer, these wells form the "no-biofilm" control wells. Aliquots of 190μL of *S.Warneri* in PBS (OD 0.2) were then added to the remaining wells of the plate. Row A, No. 1-6 become "no-treatment" wells, leaving the remaining columns (B-H) for treatment with samples. The lids were then replaced on the plates which were then centrifuged to cause sedimentation of the bacteria.

The *S.Warneri*/PBS was shaken from the wells into a beaker containing Virkon. The plate was then patted firmly down a few times onto a piece of absorbent paper, before adding 200μL of sterile 20% glycerol in distilled water to all the biofilm wells. The plates were then used the same day they were made.

ii) Preparation of test samples and subsequent treatment of biofilms

A known weight of each compound to be tested was dissolved in a solvent (water, acetone, ethanol or the flavour). Experimental samples were added to the biofilm wells for 30 seconds. To facilitate this, all samples were first prepared and then added to separate clean 96-well plate in a slight excess (210μL). The first compound to be tested was added to the biofilm and left for 30 seconds. After 30 seconds the sample was removed by shaking the plate firmly over a beaker of Virkon, patting down on absorbent paper and filling the well with sterile distilled water. Typically 3 washes were needed.

The second test compound was then added to the biofilm plate and left for 30 seconds, tipped out and washed as before. This procedure was repeated for the remaining test solutions.

After the whole plate has been treated, it was washed once more and patted down. 200μL of BHI broth and 80μL of sterile oil were added to each of the wells. The plate was then placed in a plate reader, such as the Dynatech Dias. This enables the optical densities of the wells to be read over a period of up to 23 hours, whilst being incubated at 37°C. The OD (at 630nm) of the wells is then read every 15 minutes. The Dynatech has a kinetic programm which determines the mean times for the wells to reach a certain OD (in this case 0.3).

Appendix D: Crystal data and structure refinement for $Sn(hino)_2Cl_2$ (3)

Table 1. Crystal data and structure refinement for **(3)**.

Identification code	$Sn(hinokitiol)_2Cl_2$
Empirical formula	$C_{20}H_{22}Cl_2O_4Sn$
Formula weight	601.90
Temperature	170(2) K
Wavelength	0.71069 Å
Crystal system	Monoclinic
Space group	$P2_1/c$
Unit cell dimensions	a = 9.221(3)Å $\alpha = 90°$
	b = 25.904(9)Å $\beta = 91.80(3)°$
	c = 11.211(3)Å $\gamma = 90°$
Volume	2677(2) $Å^3$
Z	4
Density (calculated)	1.494 Mg/m^3
Absorption coefficient	1.184 mm^{-1}
F(000)	1204
Crystal size	0.25 x 0.25 x 0.2 mm
Theta range for data collection	2.21 to 25.02 °.
Index ranges	0<=h<=10; 0<=k<=30; -13<=l<=13
Reflections collected	5102
Independent reflections	4697 [R(int) = 0.0149]
Refinement method	Full-matrix least-squares on F^2
Data / restraints / parameters	4697 / 0 / 303
Goodness-of-fit on F^2	1.124
Final R indices [I>2σ(I)]	R1 = 0.0480 wR2 = 0.1205
R indices (all data)	R1 = 0.0672 wR2 = 0.1284
Largest diff. peak and hole	1.425 and -0.634 $eÅ^{-3}$
Weighting scheme	calc $w=1/[\sigma^2(Fo^2)+(0.0651P)^2+3.3611P]$ where $P=(Fo^2+2Fc^2)/3$

Table 2. Bond lengths [Å] and angles [°] for **(3)**.

Sn(1)-O(2)	2.050(4)
Sn(1)-O(3)	2.061(4)
Sn(1)-O(1)	2.071(4)
Sn(1)-O(4)	2.088(4)
Sn(1)-Cl(2)	2.363(2)
Sn(1)-Cl(1)	2.369(2)
O(1)-C(1)	1.303(7)
O(2)-C(2)	1.307(7)
O(3)-C(12)	1.307(6)
O(4)-C(11)	1.302(6)
C(1)-C(7)	1.390(8)
C(1)-C(2)	1.465(8)
C(2)-C(3)	1.384(8)
C(3)-C(4)	1.387(9)
C(4)-C(5)	1.379(9)
C(4)-C(8)	1.536(9)
C(5)-C(6)	1.401(10)
C(6)-C(7)	1.375(9)
C(8)-C(10)	1.41(2)
C(8)-C(9)	1.459(11)
C(11)-C(17)	1.391(8)
C(11)-C(12)	1.453(8)
C(12)-C(13)	1.384(8)
C(13)-C(14)	1.393(9)
C(14)-C(15)	1.383(10)
C(14)-C(18)	1.534(9)
C(15)-C(16)	1.368(9)
C(16)-C(17)	1.396(8)
C(18)-C(19)	1.26(2)
C(18)-C(20A)	1.44(2)
C(18)-C(20)	1.50(2)
C(18)-C(19A)	1.63(2)
C(21)-C(22)	1.28(2)
C(21)-C(31)	1.66(2)
C(21)-C(26)	1.86(2)
C(22)-C(31)	1.51(2)
C(22)-C(28)	1.64(2)
C(22)-C(27)	1.79(2)
C(24)-C(29)	1.40(3)
C(24)-C(25)	1.52(3)
C(24)-C(30)	1.64(3)
C(24)-C(31)	1.76(4)
C(24)-C(26)	1.78(3)
C(24)-C(27)	1.90(3)
C(25)-C(30)	0.83(2)
C(25)-C(29)	1.38(2)
C(25)-C(31)	1.53(3)
C(25)-C(26)	1.79(2)

C(26)-C(30)	1.11(2)
C(26)-C(31)	1.57(3)
C(27)-C(28)	1.19(2)
C(27)-C(29)	1.39(2)
C(27)-C(31)	1.80(3)
C(28)-C(31)	1.63(3)
C(28)-C(29)	1.94(2)
C(29)-C(31)	1.76(3)
C(30)-C(31)	1.58(3)
O(2)-Sn(1)-O(3)	164.9(2)
O(2)-Sn(1)-O(1)	78.21(14)
O(3)-Sn(1)-O(1)	92.6(2)
O(2)-Sn(1)-O(4)	90.3(2)
O(3)-Sn(1)-O(4)	76.98(14)
O(1)-Sn(1)-O(4)	86.0(2)
O(2)-Sn(1)-Cl(2)	90.48(11)
O(3)-Sn(1)-Cl(2)	97.63(12)
O(1)-Sn(1)-Cl(2)	168.01(11)
O(4)-Sn(1)-Cl(2)	90.12(11)
O(2)-Sn(1)-Cl(1)	101.01(12)
O(3)-Sn(1)-Cl(1)	91.08(11)
O(1)-Sn(1)-Cl(1)	91.32(12)
O(4)-Sn(1)-Cl(1)	167.62(11)
Cl(2)-Sn(1)-Cl(1)	94.79(6)
C(1)-O(1)-Sn(1)	114.2(3)
C(2)-O(2)-Sn(1)	115.8(3)
C(12)-O(3)-Sn(1)	115.7(3)
C(11)-O(4)-Sn(1)	115.4(3)
O(1)-C(1)-C(7)	118.2(5)
O(1)-C(1)-C(2)	116.6(5)
C(7)-C(1)-C(2)	125.2(5)
O(2)-C(2)-C(3)	117.5(5)
O(2)-C(2)-C(1)	114.9(5)
C(3)-C(2)-C(1)	127.5(5)
C(2)-C(3)-C(4)	131.8(6)
C(5)-C(4)-C(3)	127.4(6)
C(5)-C(4)-C(8)	117.2(6)
C(3)-C(4)-C(8)	115.4(6)
C(4)-C(5)-C(6)	126.9(6)
C(7)-C(6)-C(5)	131.8(6)
C(6)-C(7)-C(1)	129.4(6)
C(10)-C(8)-C(9)	118.9(11)
C(10)-C(8)-C(4)	112.5(11)
C(9)-C(8)-C(4)	114.6(7)
O(4)-C(11)-C(17)	118.3(5)
O(4)-C(11)-C(12)	115.3(5)
C(17)-C(11)-C(12)	126.4(5)
O(3)-C(12)-C(13)	117.2(5)
O(3)-C(12)-C(11)	116.0(5)
C(13)-C(12)-C(11)	126.8(5)

C(12)-C(13)-C(14)	132.2(6)
C(15)-C(14)-C(13)	126.1(6)
C(15)-C(14)-C(18)	117.7(6)
C(13)-C(14)-C(18)	116.2(6)
C(16)-C(15)-C(14)	129.1(6)
C(15)-C(16)-C(17)	130.6(6)
C(11)-C(17)-C(16)	128.6(6)
C(19)-C(18)-C(20A)	129.4(12)
C(19)-C(18)-C(20)	129.3(14)
C(20A)-C(18)-C(20)	37.4(9)
C(19)-C(18)-C(14)	114.4(11)
C(20A)-C(18)-C(14)	113.9(10)
C(20)-C(18)-C(14)	110.1(9)
C(19)-C(18)-C(19A)	36(2)
C(20A)-C(18)-C(19A)	110.2(11)
C(20)-C(18)-C(19A)	135.8(12)
C(14)-C(18)-C(19A)	111.9(9)

Appendix E: Crystal data and structure refinement for $Sn(Etma)_2F_2$ (5)

Table 3. Crystal data and structure refinement for **(5)**.

Identification code	$Sn(ethyl\ maltol)_2F_2$
Empirical formula	$C_{14}H_{14}F_2O_6Sn$
Formula weight	434.94
Temperature	170(2)°K
Wavelength	0.71069 Å
Crystal system	Tetragonal
Space group	$P4_12_12$
Unit cell dimensions	a = 8.704(1)Å $\alpha = 90°$
	b = 8.703(1)Å $\beta = 90°$
	c = 21.153(3)Å $\gamma = 90°$
Volume	1602.4 $Å^3$
Z	4
Density (calculated)	1.803 Mg/m^3
Absorption coefficient	1.642 mm^{-1}
F(000)	856
Crystal size	0.2 x 0.2 x 0.2 mm
Theta range for data collection	2.53 to 26.96 °.
Index ranges	0<=h<=11; 0<=k<=11; -26<=l<=26
Reflections collected	4080
Independent reflections	1746 [R(int) = 0.0120]
Refinement method	Full-matrix least-squares on F^2
Data / restraints / parameters	1741 / 0 / 107
Goodness-of-fit on F^2	1.106
Final R indices [$I>2\sigma(I)$]	R1 = 0.0120 wR2 = 0.0292
R indices (all data)	R1 = 0.0128 wR2 = 0.0311
Absolute structure parameter	0.00(2)
Largest diff. peak and hole	0.265 and -0.205 $eÅ^{-3}$
Weighting scheme	calc $w=1/[\sigma^2(Fo^2)+(0.0136P)^2+0.3472P]$ where $P=(Fo^2+2Fc^2)/3$
Extinction coefficient	0.00049(14)
Extinction expression	$Fc^*=kFc[1+0.001xFc^2\lambda^3/\sin(2\theta)]^{-1/4}$

Table 4. Bond lengths [Å] and angles [°] for **(5)**.

Sn(1)-F(1)#1	1.9470(9)
Sn(1)-F(1)	1.9471(9)
Sn(1)-O(2)	2.0282(11)
Sn(1)-O(2)#1	2.0283(11)
Sn(1)-O(1)	2.1102(11)
Sn(1)-O(1)#1	2.1104(11)
O(1)-C(1)	1.290(2)
O(2)-C(5)	1.330(2)
O(3)-C(3)	1.346(2)
O(3)-C(4)	1.350(2)
C(1)-C(2)	1.411(2)
C(1)-C(5)	1.430(2)
C(2)-C(3)	1.346(3)
C(4)-C(5)	1.366(2)
C(4)-C(6)	1.493(3)
C(6)-C(7)	1.522(3)
F(1)#1-Sn(1)-F(1)	93.41(6)
F(1)#1-Sn(1)-O(2)	89.25(4)
F(1)-Sn(1)-O(2)	95.67(4)
F(1)#1-Sn(1)-O(2)#1	95.68(4)
F(1)-Sn(1)-O(2)#1	89.25(4)
O(2)-Sn(1)-O(2)#1	172.83(7)
F(1)#1-Sn(1)-O(1)	169.56(4)
F(1)-Sn(1)-O(1)	90.35(4)
O(2)-Sn(1)-O(1)	80.68(4)
O(2)#1-Sn(1)-O(1)	94.11(5)
F(1)#1-Sn(1)-O(1)#1	90.35(4)
F(1)-Sn(1)-O(1)#1	169.56(4)
O(2)-Sn(1)-O(1)#1	94.12(5)
O(2)#1-Sn(1)-O(1)#1	80.67(4)
O(1)-Sn(1)-O(1)#1	87.65(7)
C(1)-O(1)-Sn(1)	110.56(9)
C(5)-O(2)-Sn(1)	111.71(9)
C(3)-O(3)-C(4)	120.79(14)
O(1)-C(1)-C(2)	123.53(14)
O(1)-C(1)-C(5)	118.49(14)
C(2)-C(1)-C(5)	118.0(2)
C(3)-C(2)-C(1)	118.9(2)
C(2)-C(3)-O(3)	122.5(2)
O(3)-C(4)-C(5)	120.6(2)
O(3)-C(4)-C(6)	113.49(14)
C(5)-C(4)-C(6)	125.9(2)
O(2)-C(5)-C(4)	122.3(2)
O(2)-C(5)-C(1)	118.48(14)
C(4)-C(5)-C(1)	119.2(2)
C(4)-C(6)-C(7)	113.2(2)

Appendix F: Crystal data and structure refinement for $Sn(hino)_2F_2$ (6)

Table 5. Crystal data and structure refinement for **(6)**.

Identification code	$Sn(hinokitiol)_2F_2$
Empirical formula	$C_{20}H_{22}F_2O_4Sn \bullet C_6H_{12}$
Formula weight	567.22
Temperature	293(2)°K
Wavelength	0.71069 Å
Crystal system	Monoclinic
Space group	$P2_1/c$
Unit cell dimensions	a = 8.7890(10)Å α = 90°
	b = 10.3920(10)Å β = 96.760(10)°
	c = 27.267(3)Å γ = 90°
Volume	2473.1(5) $Å^3$
Z	4
Density (calculated)	1.523 Mg/m^3
Absorption coefficient	1.078 mm^{-1}
F(000)	1160
Crystal size	0.2 x 0.2 x 0.2 mm
Theta range for data collection	2.10 to 24.97 °.
Index ranges	0<=h<=10; 0<=k<=12; -32<=l<=32
Reflections collected	4886
Independent reflections	4345 [R(int) = 0.0113]
Refinement method	Full-matrix least-squares on F^2
Data / restraints / parameters	4341 / 6 / 313
Goodness-of-fit on F^2	1.038
Final R indices [I>2σ(I)]	R1 = 0.0277 wR2 = 0.0745
R indices (all data)	R1 = 0.0367 wR2 = 0.0848
Largest diff. peak and hole	0.573 and -0.428 $eÅ^{-3}$
Weighting scheme	calc $w=1/[\sigma^2(Fo^2)+(0.0485P)^2+0.8359P]$ where $P=(Fo^2+2Fc^2)/3$
Extinction coefficient	0.0003(2)
Extinction expression	$Fc^*=kFc[1+0.001xFc^2\lambda^3/\sin(2\theta)]^{-1/4}$

Table 6. Bond lengths [Å] and angles [°] for **(6)**.

Sn(1)-F(2)	1.926(2)
Sn(1)-F(1)	1.934(2)
Sn(1)-O(1)	2.049(2)
Sn(1)-O(3)	2.053(2)
Sn(1)-O(2)	2.072(2)
Sn(1)-O(4)	2.082(2)
O(1)-C(1)	1.310(4)
O(2)-C(7)	1.306(4)
O(3)-C(11)	1.318(3)
O(4)-C(17)	1.302(3)
C(1)-C(2)	1.392(4)
C(1)-C(7)	1.452(4)
C(2)-C(3)	1.388(5)
C(3)-C(4)	1.398(6)
C(3)-C(8)	1.530(5)
C(4)-C(5)	1.365(6)
C(5)-C(6)	1.378(5)
C(6)-C(7)	1.385(5)
C(8)-C(10)	1.375(11)
C(8)-C(10A)	1.435(13)
C(8)-C(9)	1.452(7)
C(11)-C(12)	1.375(4)
C(11)-C(17)	1.447(4)
C(12)-C(13)	1.406(4)
C(13)-C(14)	1.379(5)
C(13)-C(18)	1.525(4)
C(14)-C(15)	1.379(5)
C(15)-C(16)	1.379(4)
C(16)-C(17)	1.396(4)
C(18)-C(20)	1.474(7)
C(18)-C(19)	1.485(7)
C(1A)-C(6A)	1.274(12)
C(1A)-C(2A)	1.389(10)
C(2A)-C(3A)	1.360(13)
C(2A)-C(4A)	2.02(2)
C(3A)-C(4A)	1.276(13)
C(4A)-C(5A)	1.344(13)
C(5A)-C(6A)	1.231(13)
F(2)-Sn(1)-F(1)	92.61(10)
F(2)-Sn(1)-O(1)	90.79(9)
F(1)-Sn(1)-O(1)	101.20(9)
F(2)-Sn(1)-O(3)	98.51(10)
F(1)-Sn(1)-O(3)	90.88(8)
O(1)-Sn(1)-O(3)	164.43(9)
F(2)-Sn(1)-O(2)	168.69(9)
F(1)-Sn(1)-O(2)	90.99(9)
O(1)-Sn(1)-O(2)	78.00(8)
O(3)-Sn(1)-O(2)	92.14(9)

F(2)-Sn(1)-O(4)	90.10(9)
F(1)-Sn(1)-O(4)	168.25(8)
O(1)-Sn(1)-O(4)	90.19(8)
O(3)-Sn(1)-O(4)	77.41(8)
O(2)-Sn(1)-O(4)	88.53(9)
C(1)-O(1)-Sn(1)	115.3(2)
C(7)-O(2)-Sn(1)	114.5(2)
C(11)-O(3)-Sn(1)	115.9(2)
C(17)-O(4)-Sn(1)	115.2(2)
O(1)-C(1)-C(2)	117.4(3)
O(1)-C(1)-C(7)	115.7(3)
C(2)-C(1)-C(7)	126.9(3)
C(3)-C(2)-C(1)	132.0(3)
C(2)-C(3)-C(4)	125.9(3)
C(2)-C(3)-C(8)	115.8(4)
C(4)-C(3)-C(8)	118.2(4)
C(5)-C(4)-C(3)	129.0(4)
C(4)-C(5)-C(6)	130.1(4)
C(5)-C(6)-C(7)	130.3(3)
O(2)-C(7)-C(6)	118.3(3)
O(2)-C(7)-C(1)	116.1(3)
C(6)-C(7)-C(1)	125.6(3)
C(10)-C(8)-C(10A)	57.6(9)
C(10)-C(8)-C(9)	125.4(8)
C(10A)-C(8)-C(9)	119.7(8)
C(10)-C(8)-C(3)	116.5(6)
C(10A)-C(8)-C(3)	115.0(7)
C(9)-C(8)-C(3)	112.0(4)
O(3)-C(11)-C(12)	117.2(3)
O(3)-C(11)-C(17)	115.4(2)
C(12)-C(11)-C(17)	127.4(3)
C(11)-C(12)-C(13)	132.3(3)
C(14)-C(13)-C(12)	125.6(3)
C(14)-C(13)-C(18)	117.8(3)
C(12)-C(13)-C(18)	116.5(3)
C(13)-C(14)-C(15)	129.0(3)
C(14)-C(15)-C(16)	130.5(3)
C(15)-C(16)-C(17)	129.7(3)
O(4)-C(17)-C(16)	118.4(2)
O(4)-C(17)-C(11)	116.1(2)
C(16)-C(17)-C(11)	125.5(3)
C(20)-C(18)-C(19)	112.8(5)
C(20)-C(18)-C(13)	112.8(4)
C(19)-C(18)-C(13)	112.5(4)
C(6A)-C(1A)-C(2A)	109.3(12)
C(3A)-C(2A)-C(1A)	111.2(11)
C(3A)-C(2A)-C(4A)	38.5(6)
C(1A)-C(2A)-C(4A)	90.4(9)
C(4A)-C(3A)-C(2A)	99.9(12)
C(3A)-C(4A)-C(5A)	112.5(14)

C(3A)-C(4A)-C(2A)	41.6(8)
C(5A)-C(4A)-C(2A)	95.4(10)
C(6A)-C(5A)-C(4A)	110(2)
C(5A)-C(6A)-C(1A)	119(2)

Appendix G: Crystal data and structure refinement for $Sn(ma)_2$ (8)

Table 7. Crystal data and structure refinement for **(8)**.

Identification code	$Sn(maltol)_2$
Empirical formula	$C_{12}H_{10}O_6Sn$
Formula weight	368.89
Temperature	100(2)°K
Wavelength	0.71070 Å
Crystal system	Orthorhombic
Space group	Fdd2
Unit cell dimensions	a = 18.908(8)Å $\alpha = 90°$
	b = 26.355(8)Å $\beta = 90°$
	c = 4.971(2)Å $\gamma = 90°$
Volume	2477(2) $Å^3$
Z	8
Density (calculated)	1.978 Mg/m^3
Absorption coefficient	2.083 mm^{-1}
F(000)	1440
Crystal size	0.40 x 0.08 x 0.08 mm
Theta range for data collection	2.65 to 24.99 °.
Index ranges	-23<=h<=24; -35<=k<=27; -6<=l<=6
Reflections collected	594
Independent reflections	440 [R(int) = 0.0525]
Refinement method	Full-matrix least-squares on F^2
Data / restraints / parameters	439 / 1 / 89
Goodness-of-fit on F^2	1.071
Final R indices [$I>2\sigma(I)$]	R1 = 0.0434 wR2 = 0.1059
R indices (all data)	R1 = 0.0530 wR2 = 0.1529
Absolute structure parameter	0.07(13)
Largest diff. peak and hole	0.620 and -0.483 $eÅ^{-3}$
Weighting scheme	calc $w=1/[\sigma^2(Fo^2)+(0.0748P)^2+4.7143P]$ where $P=(Fo^2+2Fc^2)/3$
Extinction coefficient	0.0026(5)
Extinction expression	$Fc^*=kFc[1+0.001xFc^2\lambda^3/\sin(2\theta)]^{-1/4}$

Table 8. Bond lengths [Å] and angles [°] for **(8)**.

Sn(1)-O(2)#1	2.129(8)
Sn(1)-O(2)	2.129(8)
Sn(1)-O(1)	2.324(8)
Sn(1)-O(1)#1	2.324(8)
C(1)-C(2)	1.327(14)
C(1)-O(3)	1.338(14)
C(2)-C(3)	1.424(14)
O(2)-C(4)	1.30(2)
O(3)-C(5)	1.38(2)
O(1)-C(3)	1.27(2)
C(4)-C(5)	1.37(2)
C(4)-C(3)	1.458(13)
C(5)-C(6)	1.511(13)
O(2)#1-Sn(1)-O(2)	94.5(4)
O(2)#1-Sn(1)-O(1)	81.4(3)
O(2)-Sn(1)-O(1)	74.8(3)
O(2)#1-Sn(1)-O(1)#1	74.8(3)
O(2)-Sn(1)-O(1)#1	81.4(3)
O(1)-Sn(1)-O(1)#1	144.6(4)
C(2)-C(1)-O(3)	124.0(10)
C(1)-C(2)-C(3)	120.5(9)
C(4)-O(2)-Sn(1)	115.9(8)
C(1)-O(3)-C(5)	118.0(10)
C(3)-O(1)-Sn(1)	111.3(6)
O(2)-C(4)-C(5)	122.9(10)
O(2)-C(4)-C(3)	119.7(12)
C(5)-C(4)-C(3)	117.4(10)
C(4)-C(5)-O(3)	123.3(9)
C(4)-C(5)-C(6)	125.9(11)
O(3)-C(5)-C(6)	110.8(12)
O(1)-C(3)-C(2)	124.9(9)
O(1)-C(3)-C(4)	118.3(11)
C(2)-C(3)-C(4)	116.8(10)

Appendix H: Crystal data and structure refinement for $Sn(trop)_2$ (11)

Table 9. Crystal data and structure refinement for **(11)**.

Identification code	$Sn(tropolone)_2$
Empirical formula	$C_{14}H_{10}O_4Sn$
Formula weight	360.91
Temperature	120(2)°K
Wavelength	0.71070 Å
Crystal system	Triclinic
Space group	P-1
Unit cell dimensions	a = 7.4934(7) Å α = 78.140(6)°
	b = 7.5027(10) Å β = 84.493(6)°.
	c = 12.026(2) Å γ = 74.096(5)°.
Volume	635.80(15) $Å^3$
Z	2
Density (calculated)	1.885 Mg/m^3
Absorption coefficient	2.016 mm^{-1}
F(000)	352
Crystal size	0.80 x 0.80 x 0.10 mm^3
Theta range for data collection	2.83 to 24.99°.
Index ranges	-8<=h<=8, -8<=k<=8, -14<=l<=13
Reflections collected	3801
Independent reflections	2192 [R(int) = 0.0989]
Refinement method	Full-matrix least-squares on F^2
Data / restraints / parameters	2192 / 0 / 173
Goodness-of-fit on F^2	1.109
Final R indices [I>2□(I)]	R1 = 0.0987, wR2 = 0.2524
R indices (all data)	R1 = 0.1044, wR2 = 0.2550
Largest diff. peak and hole	4.926 and -3.096 $e.Å^{-3}$
Weighting scheme	calc $w=1/[\sigma^2(Fo^2)+(0.0748P)^2+4.7143P]$ where $P=(Fo^2+2Fc^2)/3$
Extinction coefficient	0.055(11)
Extinction expression	$Fc^*=kFc[1+0.001xFc^2\lambda^3/\sin(2\theta)]^{-1/4}$

Table 10. Bond lengths [Å] and angles [°] for **(11)**.

Sn(1)-O(1)	2.140(9)
Sn(1)-O(4)	2.140(10)
Sn(1)-O(3)	2.242(10)
Sn(1)-O(2)	2.258(10)
O(4)-C(9)	1.311(16)
O(3)-C(8)	1.259(17)
O(2)-C(2)	1.287(16)
C(3)-C(4)	1.37(2)
C(3)-C(2)	1.43(2)
C(11)-C(12)	1.36(2)
C(11)-C(10)	1.41(2)
C(5)-C(6)	1.36(2)
C(5)-C(4)	1.38(2)
C(10)-C(9)	1.38(2)
C(8)-C(14)	1.443(19)
C(8)-C(9)	1.479(18)
C(14)-C(13)	1.39(2)
C(7)-C(6)	1.39(2)
C(7)-C(1)	1.42(2)
C(2)-C(1)	1.495(18)
C(1)-O(1)	1.274(18)
C(12)-C(13)	1.41(2)
O(1)-Sn(1)-O(4)	94.2(4)
O(1)-Sn(1)-O(3)	77.1(4)
O(4)-Sn(1)-O(3)	72.0(3)
O(1)-Sn(1)-O(2)	72.5(3)
O(4)-Sn(1)-O(2)	81.1(4)
O(3)-Sn(1)-O(2)	137.4(4)
C(9)-O(4)-Sn(1)	120.0(8)
C(8)-O(3)-Sn(1)	116.5(8)
C(2)-O(2)-Sn(1)	116.0(8)
C(4)-C(3)-C(2)	130.9(12)
C(12)-C(11)-C(10)	129.5(13)
C(6)-C(5)-C(4)	127.8(13)
C(9)-C(10)-C(11)	131.9(13)
O(3)-C(8)-C(14)	119.1(12)
O(3)-C(8)-C(9)	117.0(11)
C(14)-C(8)-C(9)	123.9(12)
C(13)-C(14)-C(8)	131.6(13)
C(6)-C(7)-C(1)	131.5(13)
C(3)-C(4)-C(5)	130.0(13)
O(2)-C(2)-C(3)	119.5(12)
O(2)-C(2)-C(1)	115.1(12)
C(3)-C(2)-C(1)	125.3(12)
C(5)-C(6)-C(7)	129.9(13)
O(1)-C(1)-C(7)	119.5(12)
O(1)-C(1)-C(2)	116.0(13)
C(7)-C(1)-C(2)	124.5(13)

O(4)-C(9)-C(10)	119.7(12)
O(4)-C(9)-C(8)	113.7(11)
C(10)-C(9)-C(8)	126.6(12)
C(11)-C(12)-C(13)	127.4(13)
C(14)-C(13)-C(12)	129.0(14)
C(1)-O(1)-Sn(1)	120.2(8)

Appendix I: Crystal data and structure refinement for $Zn(hino)_2$ (17)

Table 11. Crystal data and structure refinement for **(17)**.

Identification code	$Zn(hinokitiol)_2$
Empirical formula	$C_{22}\ H_{28}\ O_5\ Zn$
Formula weight	437.81
Temperature	170(2) K
Wavelength	0.71070 Å
Crystal system	Monoclinic
Space group	$P2_1/n$
Unit cell dimensions	a = 8.0820(2)Å α = 90°
	b = 17.1500(3)Å β = 100.219(1)°
	c = 14.9090(3)Å γ = 90°
Volume	2033.70(7) $Å^3$
Z	4
Density (calculated)	1.430 Mg/m^3
Absorption coefficient	1.238 mm^{-1}
F(000)	920
Crystal size	0.20 x 0.17 x 0.12 mm
Theta range for data collection	3.63 to 27.50 °.
Index ranges	0<=h<=10; -22<=k<=22; -19<=l<=19
Reflections collected	27227
Independent reflections	4666 [R(int) = 0.0431]
Reflections observed (>2σ)	4010
Refinement method	Full-matrix least-squares on F^2
Data / restraints / parameters	4666 / 1 / 262
Goodness-of-fit on F^2	1.007
Final R indices [I>2σ(I)]	R_1 = 0.0288 wR_2 = 0.0734
R indices (all data)	R_1 = 0.0375 wR_2 = 0.0774
Largest diff. peak and hole	0.379 and -0.426 $e.Å^{-3}$

Table 12. Bond lengths [Å] and angles [°] for **(17)**.

Zn(1)-O(2)	2.029(1)
Zn(1)-O(4)	2.075(1)
Zn(1)-O(1)	2.074(1)
Zn(1)-O(3)	2.107(1)
Zn(1)-O(5)	2.258(1)
Zn(1)-O(4)#1	2.171(1)
O(1)-C(1)	1.277(2)
O(2)-C(2)	1.287(2)
O(3)-C(12)	1.279(2)
O(4)-C(11)	1.306(2)
O(4)-Zn(1)#1	2.171(1)
O(5)-C(21)	1.445(2)
C(1)-C(7)	1.409(2)
C(1)-C(2)	1.481(2)
C(2)-C(3)	1.402(2)
C(3)-C(4)	1.401(2)
C(4)-C(5)	1.387(3)
C(4)-C(8)	1.524(2)
C(5)-C(6)	1.391(3)
C(6)-C(7)	1.383(3)
C(8)-C(10)	1.528(3)
C(8)-C(9)	1.532(3)
C(11)-C(17)	1.398(2)
C(11)-C(12)	1.480(2)
C(12)-C(13)	1.410(2)
C(13)-C(14)	1.379(3)
C(14)-C(15)	1.392(3)
C(15)-C(16)	1.383(2)
C(16)-C(17)	1.400(2)
C(16)-C(18)	1.528(2)
C(18)-C(19)	1.526(2)
C(18)-C(20)	1.535(2)
C(21)-C(22)	1.503(3)
O(2)-Zn(1)-O(4)	175.63(5)
O(2)-Zn(1)-O(1)	78.63(5)
O(4)-Zn(1)-O(1)	99.39(5)
O(2)-Zn(1)-O(3)	100.02(5)
O(4)-Zn(1)-O(3)	76.35(4)
O(1)-Zn(1)-O(3)	98.75(5)
O(2)-Zn(1)-O(5)	82.79(5)
O(4)-Zn(1)-O(5)	99.48(4)
O(1)-Zn(1)-O(5)	160.74(4)
O(3)-Zn(1)-O(5)	89.38(5)
O(2)-Zn(1)-O(4)#1	110.26(5)
O(4)-Zn(1)-O(4)#1	73.54(5)
O(1)-Zn(1)-O(4)#1	90.68(5)
O(3)-Zn(1)-O(4)#1	149.53(4)
O(5)-Zn(1)-O(4)#1	91.03(4)
C(1)-O(1)-Zn(1)	114.0(1)

C(2)-O(2)-Zn(1)	126.5(1)
C(12)-O(3)-Zn(1)	126.5(1)
C(11)-O(4)-Zn(1)	117.3(1)
C(11)-O(4)-Zn(1)#1	146.8(1)
Zn(1)-O(4)-Zn(1)#1	106.46(5)
C(21)-O(5)-Zn(1)	117.28(9)
O(1)-C(1)-C(7)	120.0(2)
O(1)-C(1)-C(2)	126.0(1)
C(7)-C(1)-C(2)	124.0(2)
O(2)-C(2)-C(3)	118.4(1)
O(2)-C(2)-C(1)	126.6(1)
C(3)-C(2)-C(1)	136.0(2)
C(2)-C(3)-C(4)	133.0(2)
C(5)-C(4)-C(3)	126.3(2)
C(5)-C(4)-C(8)	128.5(2)
C(3)-C(4)-C(8)	116.3(2)
C(4)-C(5)-C(6)	138.0(2)
C(7)-C(6)-C(5)	130.5(2)
C(6)-C(7)-C(1)	131.0(2)
C(4)-C(8)-C(10)	111.2(1)
C(4)-C(8)-C(9)	112.5(2)
C(10)-C(8)-C(9)	111.4(2)
O(4)-C(11)-C(17)	118.9(1)
O(4)-C(11)-C(12)	114.2(1)
C(17)-C(11)-C(12)	137.9(2)
O(3)-C(12)-C(13)	119.5(2)
O(3)-C(12)-C(11)	116.6(1)
C(13)-C(12)-C(11)	123.8(2)
C(14)-C(13)-C(12)	130.7(2)
C(13)-C(14)-C(15)	130.9(2)
C(16)-C(15)-C(14)	128.2(2)
C(15)-C(16)-C(17)	126.1(2)
C(15)-C(16)-C(18)	117.0(2)
C(17)-C(16)-C(18)	127.9(1)
C(11)-C(17)-C(16)	133.9(2)
C(19)-C(18)-C(16)	113.5(1)
C(19)-C(18)-C(20)	111.0(1)
C(16)-C(18)-C(20)	110.4(1)
O(5)-C(21)-C(22)	111.6(1)

Appendix J: Crystal data and structure refinement for $Cu(hino)_2$ (20)

Table 13. Crystal data and structure refinement for **(20)**.

Identification code	$Cu(hinokitiol)_2$
Empirical formula	$C_{20}H_{22}CuO_4$
Formula weight	389.92
Temperature	150(2) K
Wavelength	0.71069 Å
Crystal system	Monoclinic
Space group	P21/n
Unit cell dimensions	a = 16.7420(2)Å α = 90°
	b = 15.5370(2)Å β = 99.4000(6)°
	c = 18.3010(3)Å γ = 90°
Volume	4696.54(11) $Å^3$
Z	10
Density (calculated)	1.379 Mg/m^3
Absorption coefficient	1.183 mm^{-1}
F(000)	2030
Crystal size	0.25 x 0.10 x 0.10 mm
Theta range for data collection	3.80 to 27.48 °.
Index ranges	-21<=h<=21; -19<=k<=20; -23<=l<=23
Reflections collected	54148
Independent reflections	10712 [R(int) = 0.0471]
Reflections observed (>2σ)	8462
Absorption correction	Multiscan
Max. and min. transmission	1.030, 0.974
Refinement method	Full-matrix least-squares on F^2
Data / restraints / parameters	10712 / 0 / 584
Goodness-of-fit on F^2	0.915
Final R indices [I>2σ(I)]	R_1 = 0.0384 wR_2 = 0.1000
R indices (all data)	R_1 = 0.0558 wR_2 = 0.1139
Largest diff. peak and hole	0.807 and -0.644 $e.Å^{-3}$

Notes: 2½ molecules in asymmetric unit. 2 full molecules are proximate to inversion centres and hence dimerize with nearby lattice neighbours. Remaining half of one molecule has metal seated on an inversion centre. Disorder in one of the isopropyl groups successfully modelled.

Table 14. Bond lengths [Å] and angles [°] for **(20)**.

Cu(1)-O(1)	1.9186(16)	Cu(1)-O(2)	1.9196(17)
Cu(1)-O(3)	1.9321(17)	Cu(1)-O(4)	1.9330(16)
Cu(2)-O(5)	1.9154(17)	Cu(2)-O(6)	1.9210(17)
Cu(2)-O(8)	1.9221(17)	Cu(2)-O(7)	1.9388(17)
Cu(3)-O(11)#1	1.901(2)	Cu(3)-O(11)	1.901(2)
Cu(3)-O(9)	1.9098(18)	Cu(3)-O(9)#1	1.9098(18)
O(1)-C(1)	1.291(3)	O(2)-C(2)	1.298(3)
O(3)-C(11)	1.287(3)	O(4)-C(12)	1.301(3)
O(5)-C(22)	1.303(3)	O(6)-C(21)	1.292(3)
O(7)-C(31)	1.291(3)	O(8)-C(32)	1.304(3)
O(9)-C(41)	1.306(3)	O(11)-C(51)	1.300(3)
C(1)-C(7)	1.404(3)	C(1)-C(2)	1.465(3)
C(2)-C(3)	1.398(3)	C(3)-C(4)	1.395(4)
C(4)-C(5)	1.393(4)	C(4)-C(8)	1.531(4)
C(5)-C(6)	1.379(4)	C(6)-C(7)	1.386(4)
C(8)-C(9)	1.500(6)	C(8)-C(10)	1.529(6)
C(11)-C(17)	1.402(4)	C(11)-C(12)	1.465(4)
C(12)-C(13)	1.390(3)	C(13)-C(14)	1.394(4)
C(14)-C(15)	1.380(5)	C(14)-C(18)	1.530(5)
C(15)-C(16)	1.398(5)	C(16)-C(17)	1.382(4)
C(18)-C(20)	1.399(7)	C(18)-C(19)	1.471(6)
C(21)-C(27)	1.402(3)	C(21)-C(22)	1.466(3)
C(22)-C(23)	1.401(3)	C(23)-C(24)	1.399(4)
C(24)-C(25)	1.386(4)	C(24)-C(28)	1.531(4)
C(25)-C(26)	1.384(4)	C(26)-C(27)	1.385(4)
C(28)-C(30)	1.515(5)	C(28)-C(29)	1.529(5)
C(31)-C(37)	1.407(3)	C(31)-C(32)	1.464(3)
C(32)-C(33)	1.398(3)	C(33)-C(34)	1.393(3)
C(34)-C(35)	1.391(4)	C(34)-C(38)	1.527(4)
C(35)-C(36)	1.386(4)	C(36)-C(37)	1.388(4)
C(38)-C(40A)	1.380(12)	C(38)-C(39A)	1.430(11)
C(38)-C(39)	1.456(6)	C(38)-C(40)	1.649(7)
C(41)-C(42)	1.394(4)	C(41)-C(51)	1.466(3)
C(42)-C(43)	1.387(4)	C(43)-C(44)	1.388(4)
C(44)-C(45)	1.399(4)	C(45)-C(46)	1.389(4)
C(45)-C(48)	1.526(4)	C(46)-C(51)	1.403(4)
C(48)-C(49)	1.525(4)	C(48)-C(50)	1.526(4)
O(1)-Cu(1)-O(2)	83.86(7)	O(1)-Cu(1)-O(3)	99.15(7)
O(2)-Cu(1)-O(3)	165.00(8)	O(1)-Cu(1)-O(4)	177.40(7)
O(2)-Cu(1)-O(4)	93.55(7)	O(3)-Cu(1)-O(4)	83.26(7)
O(5)-Cu(2)-O(6)	84.27(7)	O(5)-Cu(2)-O(8)	174.64(7)
O(6)-Cu(2)-O(8)	93.36(7)	O(5)-Cu(2)-O(7)	97.95(7)
O(6)-Cu(2)-O(7)	166.88(7)	O(8)-Cu(2)-O(7)	83.29(7)
O(11)#1-Cu(3)-O(11)	180.0	O(11)#1-Cu(3)-O(9)	95.47(8)
O(11)-Cu(3)-O(9)	84.53(8)	O(11)#1-Cu(3)-O(9)#1	84.53(8)
O(11)-Cu(3)-O(9)#1	95.47(8)	O(9)-Cu(3)-O(9)#1	180.00(12)
C(1)-O(1)-Cu(1)	112.89(15)	C(2)-O(2)-Cu(1)	112.84(15)
C(11)-O(3)-Cu(1)	112.67(16)	C(12)-O(4)-Cu(1)	112.71(15)
C(22)-O(5)-Cu(2)	112.68(15)	C(21)-O(6)-Cu(2)	112.47(15)

C(31)-O(7)-Cu(2)	112.55(15)	C(32)-O(8)-Cu(2)	113.27(15)
C(41)-O(9)-Cu(3)	112.44(15)	C(51)-O(11)-Cu(3)	113.26(16)
O(1)-C(1)-C(7)	119.2(2)	O(1)-C(1)-C(2)	115.4(2)
C(7)-C(1)-C(2)	125.5(2)	O(2)-C(2)-C(3)	117.8(2)
O(2)-C(2)-C(1)	114.9(2)	C(3)-C(2)-C(1)	127.3(2)
C(4)-C(3)-C(2)	131.9(2)	C(5)-C(4)-C(3)	125.9(3)
C(5)-C(4)-C(8)	117.6(2)	C(3)-C(4)-C(8)	116.5(3)
C(6)-C(5)-C(4)	129.3(2)	C(5)-C(6)-C(7)	130.6(3)
C(6)-C(7)-C(1)	129.4(3)	C(9)-C(8)-C(10)	111.3(4)
C(9)-C(8)-C(4)	112.1(3)	C(10)-C(8)-C(4)	110.7(3)
O(3)-C(11)-C(17)	119.4(2)	O(3)-C(11)-C(12)	115.8(2)
C(17)-C(11)-C(12)	124.8(2)	O(4)-C(12)-C(13)	118.0(2)
O(4)-C(12)-C(11)	114.6(2)	C(13)-C(12)-C(11)	127.4(2)
C(12)-C(13)-C(14)	132.8(3)	C(15)-C(14)-C(13)	125.7(3)
C(15)-C(14)-C(18)	119.2(3)	C(13)-C(14)-C(18)	115.2(3)
C(14)-C(15)-C(16)	128.9(3)	C(17)-C(16)-C(15)	130.6(3)
C(16)-C(17)-C(11)	129.8(3)	C(20)-C(18)-C(19)	119.7(4)
C(20)-C(18)-C(14)	113.3(5)	C(19)-C(18)-C(14)	114.7(4)
O(6)-C(21)-C(27)	118.6(2)	O(6)-C(21)-C(22)	115.7(2)
C(27)-C(21)-C(22)	125.7(2)	O(5)-C(22)-C(23)	118.7(2)
O(5)-C(22)-C(21)	114.8(2)	C(23)-C(22)-C(21)	126.5(2)
C(24)-C(23)-C(22)	132.1(2)	C(25)-C(24)-C(23)	126.6(2)
C(25)-C(24)-C(28)	116.4(2)	C(23)-C(24)-C(28)	116.9(2)
C(26)-C(25)-C(24)	128.6(2)	C(25)-C(26)-C(27)	130.5(2)
C(26)-C(27)-C(21)	129.8(2)	C(30)-C(28)-C(29)	111.2(3)
C(30)-C(28)-C(24)	111.5(3)	C(29)-C(28)-C(24)	112.6(3)
O(7)-C(31)-C(37)	119.6(2)	O(7)-C(31)-C(32)	115.8(2)
C(37)-C(31)-C(32)	124.5(2)	O(8)-C(32)-C(33)	117.9(2)
O(8)-C(32)-C(31)	114.4(2)	C(33)-C(32)-C(31)	127.7(2)
C(34)-C(33)-C(32)	132.5(2)	C(35)-C(34)-C(33)	125.6(2)
C(35)-C(34)-C(38)	119.0(2)	C(33)-C(34)-C(38)	115.4(2)
C(36)-C(35)-C(34)	128.8(2)	C(35)-C(36)-C(37)	131.1(2)
C(36)-C(37)-C(31)	129.6(3)	C(40A)-C(38)-C(39A)	122.7(9)
C(40A)-C(38)-C(39)	53.0(11)	C(39A)-C(38)-C(39)	114.4(5)
C(40A)-C(38)-C(34)	113.8(6)	C(39A)-C(38)-C(34)	117.4(4)
C(39)-C(38)-C(34)	120.2(4)	C(40A)-C(38)-C(40)	61.7(12)
C(39A)-C(38)-C(40)	80.7(5)	C(39)-C(38)-C(40)	110.0(4)
C(34)-C(38)-C(40)	105.9(3)	O(9)-C(41)-C(42)	119.2(2)
O(9)-C(41)-C(51)	115.1(2)	C(42)-C(41)-C(51)	125.7(2)
C(43)-C(42)-C(41)	129.8(2)	C(42)-C(43)-C(44)	130.5(2)
C(43)-C(44)-C(45)	128.6(3)	C(46)-C(45)-C(44)	126.3(2)
C(46)-C(45)-C(48)	116.2(2)	C(44)-C(45)-C(48)	117.5(2)
C(45)-C(46)-C(51)	132.2(2)	C(49)-C(48)-C(50)	110.8(3)
C(49)-C(48)-C(45)	112.3(2)	C(50)-C(48)-C(45)	110.5(2)
O(11)-C(51)-C(46)	118.5(2)	O(11)-C(51)-C(41)	114.7(2)
C(46)-C(51)-C(41)	126.9(2)		

Appendix K: Crystal data and structure refinement for $Zn(trop)_2$ (21)

Table 15. Crystal data and structure refinement for **(21)**.

Identification code	$Zn(tropolone)_2$
Empirical formula	$C_{14}H_{10}O_4Zn$
Formula weight	307.59
Temperature	293(2) K
Wavelength	0.71069 Å
Crystal system	Monoclinic
Space group	$P2_1/c$
Unit cell dimensions	a = 6.3438(6)Å α = 90°
	b = 20.504(2)Å β = 98.840(10)°
	c = 9.3910(10)Å γ = 90°
Volume	1207.0(2) $Å^3$
Z	4
Density (calculated)	1.693 Mg/m^3
Absorption coefficient	2.040 mm^{-1}
F(000)	624
Crystal size	0.20 x 0.20 x 0.20 mm
Theta range for data collection	2.41 to 24.97 °.
Index ranges	0<=h<=7; 0<=k<=24; -11<=l<=11
Reflections collected	2449
Independent reflections	2126 [R(int) = 0.0110]
Refinement method	Full-matrix least-squares on F^2
Data / restraints / parameters	2123 / 0 / 173
Goodness-of-fit on F^2	0.837
Final R indices [$I>2\sigma(I)$]	R1 = 0.0308 wR2 = 0.0791
R indices (all data)	R1 = 0.0407 wR2 = 0.0843
Largest diff. peak and hole	0.606 and -0.890 $eÅ^{-3}$
Weighting scheme	calc $w=1/[\sigma^2(Fo^2)+(0.0740P)^2+0.3509P]$ where $P=(Fo^2+2Fc^2)/3$
Extinction coefficient	0.0007(12)
Extinction expression	$Fc^*=kFc[1+0.001xFc^2\lambda^3/\sin(2\theta)]^{-1/4}$

Table 16. Bond lengths [Å] and angles [°] for **(21)**.

Zn(1)-O(3)	2.051(2)
Zn(1)-O(1)	2.067(2)
Zn(1)-O(4)#1	2.103(2)
Zn(1)-O(2)#2	2.121(2)
Zn(1)-O(4)	2.149(2)
Zn(1)-O(2)	2.150(2)
O(1)-C(1)	1.261(3)
O(2)-C(2)	1.291(3)
O(2)-Zn(1)#2	2.121(2)
O(3)-C(8)	1.263(3)
O(4)-C(9)	1.299(3)
O(4)-Zn(1)#1	2.103(2)
C(1)-C(7)	1.417(4)
C(1)-C(2)	1.473(4)
C(2)-C(3)	1.395(4)
C(3)-C(4)	1.388(4)
C(4)-C(5)	1.359(5)
C(5)-C(6)	1.390(5)
C(6)-C(7)	1.368(5)
C(8)-C(14)	1.420(4)
C(8)-C(9)	1.473(3)
C(9)-C(10)	1.389(4)
C(10)-C(11)	1.390(4)
C(11)-C(12)	1.365(4)
C(12)-C(13)	1.390(4)
C(13)-C(14)	1.363(4)
O(3)-Zn(1)-O(1)	92.61(8)
O(3)-Zn(1)-O(4)#1	147.81(7)
O(1)-Zn(1)-O(4)#1	95.61(8)
O(3)-Zn(1)-O(2)#2	93.21(8)
O(1)-Zn(1)-O(2)#2	146.82(7)
O(4)#1-Zn(1)-O(2)#2	96.63(7)
O(3)-Zn(1)-O(4)	75.29(7)
O(1)-Zn(1)-O(4)	103.19(7)
O(4)#1-Zn(1)-O(4)	72.54(7)
O(2)#2-Zn(1)-O(4)	109.89(7)
O(3)-Zn(1)-O(2)	101.47(7)
O(1)-Zn(1)-O(2)	74.84(7)
O(4)#1-Zn(1)-O(2)	110.72(7)
O(2)#2-Zn(1)-O(2)	71.99(8)
O(4)-Zn(1)-O(2)	176.22(7)
C(1)-O(1)-Zn(1)	118.2(2)
C(2)-O(2)-Zn(1)#2	135.9(2)
C(2)-O(2)-Zn(1)	116.0(2)
Zn(1)#2-O(2)-Zn(1)	108.01(8)
C(8)-O(3)-Zn(1)	118.4(2)
C(9)-O(4)-Zn(1)#1	136.8(2)
C(9)-O(4)-Zn(1)	115.6(2)

Zn(1)#1-O(4)-Zn(1)	107.46(7)
O(1)-C(1)-C(7)	119.0(3)
O(1)-C(1)-C(2)	116.7(2)
C(7)-C(1)-C(2)	124.2(2)
O(2)-C(2)-C(3)	120.4(2)
O(2)-C(2)-C(1)	113.8(2)
C(3)-C(2)-C(1)	125.8(2)
C(4)-C(3)-C(2)	130.8(3)
C(5)-C(4)-C(3)	130.6(3)
C(4)-C(5)-C(6)	126.3(3)
C(7)-C(6)-C(5)	129.8(3)
C(6)-C(7)-C(1)	131.8(3)
O(3)-C(8)-C(14)	119.0(2)
O(3)-C(8)-C(9)	117.0(2)
C(14)-C(8)-C(9)	124.0(2)
O(4)-C(9)-C(10)	120.4(2)
O(4)-C(9)-C(8)	113.4(2)
C(10)-C(9)-C(8)	126.2(2)
C(9)-C(10)-C(11)	131.3(3)
C(12)-C(11)-C(10)	129.9(3)
C(11)-C(12)-C(13)	126.2(3)
C(14)-C(13)-C(12)	130.6(3)
C(13)-C(14)-C(8)	131.5(3)

Symmetry transformations used to generate equivalent atoms: #1 -x+1,-y,-z+1; #2 -x,-y,-z+1

Appendix L: Crystal data and structure refinement for $Cu(hino)_2.py$ (25)

Table 17. Crystal data and structure refinement for **(25)**.

Identification code	$Cu(hinokitiol)_2.pyridine$
Empirical formula	$C_{25} H_{27} Cu N O_4$
Formula weight	469.02
Temperature	293(2)°K
Wavelength	0.71069 Å
Crystal system	Monoclinic
Space group	$P2_1/n$
Unit cell dimensions	a = 8.616(2)Å α = 90°
	b = 26.848(4)Å β = 102.56(2)°
	c = 9.910(2)Å γ = 90°
Volume	2237.5(8) $Å^3$
Z	4
Density (calculated)	1.392 Mg/m^3
Absorption coefficient	1.007 mm^{-1}
F(000)	980
Crystal size	0.25 x 0.20 x 0.20 mm
Theta range for data collection	2.24 to 24.98 °.
Index ranges	0<=h<=10; 0<=k<=31; -11<=l<=11
Reflections collected	4337
Independent reflections	3928 [R(int) = 0.0326]
Refinement method	Full-matrix least-squares on F^2
Data / restraints / parameters	3922 / 0 / 278
Goodness-of-fit on F^2	0.853
Final R indices [I>2σ(I)]	R1 = 0.0441 wR2 = 0.1232
R indices (all data)	R1 = 0.1271 wR2 = 0.1681
Largest diff. peak and hole	0.343 and -0.380 $eÅ^{-3}$
Weighting scheme	calc $w=1/[\sigma^2(Fo^2)+(0.1000P)^2+0.0000P]$ where $P=(Fo^2+2Fc^2)/3$

Table 18. Bond lengths [Å] and angles [°] for **(25)**.

Cu(1)-O(4)	1.933(3)
Cu(1)-O(1)	1.940(3)
Cu(1)-O(2)	1.945(3)
Cu(1)-O(3)	1.965(3)
Cu(1)-N(1)	2.311(5)
O(1)-C(1)	1.287(5)
O(2)-C(2)	1.278(6)
O(3)-C(8)	1.287(5)
O(4)-C(9)	1.277(6)
N(1)-C(15)	1.319(7)
N(1)-C(19)	1.331(7)
C(1)-C(7)	1.408(6)
C(1)-C(2)	1.472(7)
C(2)-C(3)	1.388(7)
C(3)-C(4)	1.372(7)
C(4)-C(5)	1.379(7)
C(5)-C(6)	1.382(7)
C(6)-C(7)	1.393(6)
C(6)-C(20)	1.533(7)
C(8)-C(14)	1.389(6)
C(8)-C(9)	1.469(7)
C(9)-C(10)	1.398(7)
C(10)-C(11)	1.368(7)
C(11)-C(12)	1.397(7)
C(11)-C(23)	1.518(7)
C(12)-C(13)	1.349(6)
C(13)-C(14)	1.40
C(15)-C(16)	1.370(9)
C(16)-C(17)	1.358(9)
C(17)-C(18)	1.33
C(18)-C(19)	1.370(8)
C(20)-C(21)	1.521(7)
C(20)-C(22)	1.519(7)
C(23)-C(25)	1.501(9)
C(23)-C(24)	1.509(8)
O(4)-Cu(1)-O(1)	172.2(2)
O(4)-Cu(1)-O(2)	94.3(2)
O(1)-Cu(1)-O(2)	82.73(14)
O(4)-Cu(1)-O(3)	82.34(14)
O(1)-Cu(1)-O(3)	97.28(14)
O(2)-Cu(1)-O(3)	155.2(2)
O(4)-Cu(1)-N(1)	95.3(2)
O(1)-Cu(1)-N(1)	92.3(2)
O(2)-Cu(1)-N(1)	99.0(2)
O(3)-Cu(1)-N(1)	105.8(2)
C(1)-O(1)-Cu(1)	113.0(3)
C(2)-O(2)-Cu(1)	113.7(3)
C(8)-O(3)-Cu(1)	112.5(3)
C(9)-O(4)-Cu(1)	114.4(3)

C(15)-N(1)-C(19)	116.3(5)
C(15)-N(1)-Cu(1)	124.1(4)
C(19)-N(1)-Cu(1)	119.4(4)
O(1)-C(1)-C(7)	118.0(4)
O(1)-C(1)-C(2)	115.7(4)
C(7)-C(1)-C(2)	126.3(4)
O(2)-C(2)-C(3)	120.6(5)
O(2)-C(2)-C(1)	114.9(4)
C(3)-C(2)-C(1)	124.5(5)
C(4)-C(3)-C(2)	131.0(5)
C(3)-C(4)-C(5)	131.3(5)
C(6)-C(5)-C(4)	128.0(5)
C(5)-C(6)-C(7)	126.4(5)
C(5)-C(6)-C(20)	118.8(4)
C(7)-C(6)-C(20)	114.8(4)
C(6)-C(7)-C(1)	132.6(5)
O(3)-C(8)-C(14)	119.4(4)
O(3)-C(8)-C(9)	115.7(4)
C(14)-C(8)-C(9)	125.0(4)
O(4)-C(9)-C(10)	118.8(5)
O(4)-C(9)-C(8)	115.0(4)
C(10)-C(9)-C(8)	126.2(4)
C(11)-C(10)-C(9)	133.6(5)
C(10)-C(11)-C(12)	125.6(5)
C(10)-C(11)-C(23)	118.9(5)
C(12)-C(11)-C(23)	115.5(5)
C(13)-C(12)-C(11)	128.8(5)
C(12)-C(13)-C(14)	131.2(3)
C(8)-C(14)-C(13)	129.6(3)
N(1)-C(15)-C(16)	124.2(7)
C(17)-C(16)-C(15)	117.8(7)
C(18)-C(17)-C(16)	119.3(5)
C(17)-C(18)-C(19)	119.8(5)
N(1)-C(19)-C(18)	122.5(7)
C(21)-C(20)-C(22)	110.9(5)
C(21)-C(20)-C(6)	114.0(4)
C(22)-C(20)-C(6)	110.4(4)
C(25)-C(23)-C(24)	110.5(5)
C(25)-C(23)-C(11)	110.3(5)
C(24)-C(23)-C(11)	115.2(5)

Appendix M: Crystal data and structure refinement for Zn(1-benzyl-2-methyl-3-hydroxypyridin-4-one)$_2$ (41)

Table 19. Crystal data and structure refinement for **(41)**.

Identification code	Zn(1-benzyl-2-methyl-3-hydroxypyridin-4-one)$_2$
Empirical formula	$C_{26}H_{30}N_2O_7Zn$
Formula weight	547.89
Temperature	170(2) K
Wavelength	0.71069 Å
Crystal system	Triclinic
Space group	P-1
Unit cell dimensions	a = 9.2894(5)Å α = 97.185(3)°
	b = 11.8685(6)Å β = 108.933(3)°
	c = 12.3560(6)Å γ = 100.155(3)°
Volume	1243.8(1) Å^3
Z	2
Density (calculated)	1.463 Mg/m^3
Absorption coefficient	1.036 mm^{-1}
F(000)	572
Crystal size	0.10 x 0.10 x 0.08 mm
Theta range for data collection	3.29 to 27.52 °.
Index ranges	0<=h<=12; -15<=k<=15; -16<=l<=14
Reflections collected	14775
Independent reflections	5614 [R(int) = 0.0598]
Reflections observed (>2σ)	4338
Max. and min. transmission	0.9263 and 0.9035
Refinement method	Full-matrix least-squares on F^2
Data / restraints / parameters	5614 / 0 / 326
Goodness-of-fit on F^2	1.059
Final R indices [I>2σ(I)]	R_1 = 0.0677 wR_2 = 0.1777
R indices (all data)	R_1 = 0.0930 wR_2 = 0.1940
Largest diff. peak and hole	1.334 and -0.694 e.Å^{-3}

Possible H–bonds based on O–O distances

2.8245 (0.0055) O5 - O2
2.8238 (0.0103) O5 - O7
2.7478 (0.0061) O5 - O4_#1
2.7453 (0.0077) O3 - O6
2.8456 (0.0120) O6 - O7
2.7597 (0.0110) O6 - O7_#2

Symmetry transformations used to generate equivalent atoms:
#1 -x,-y,-z
#2 -x,-y,1-z

Table 20. Bond lengths [Å] and angles [°] for **(41)**.

Zn(1)-O(3)	2.000(3)
Zn(1)-O(2)	2.008(3)
Zn(1)-O(1)#1	2.022(3)
Zn(1)-O(4)	2.048(3)
Zn(1)-O(1)	2.136(3)
Zn(1)-Zn(1)#1	3.0460(9)
O(1)-C(2)	1.337(5)
O(1)-Zn(1)#1	2.022(3)
O(2)-C(1)	1.296(5)
O(3)-C(15)	1.338(6)
O(4)-C(14)	1.288(6)
N(1)-C(4)	1.357(7)
N(1)-C(5)	1.380(6)
N(1)-C(7)	1.479(6)
N(2)-C(16)	1.353(6)
N(2)-C(17)	1.356(7)
N(2)-C(19)	1.470(6)
C(1)-C(3)	1.398(6)
C(1)-C(2)	1.449(6)
C(2)-C(5)	1.377(5)
C(3)-C(4)	1.357(7)
C(5)-C(6)	1.497(6)
C(7)-C(8)	1.520(6)
C(8)-C(13)	1.380(7)
C(8)-C(9)	1.387(7)
C(9)-C(10)	1.389(7)
C(10)-C(11)	1.372(7)
C(11)-C(12)	1.379(8)
C(12)-C(13)	1.401(7)
C(14)-C(15)	1.396(7)
C(14)-C(18)	1.413(7)
C(15)-C(16)	1.410(6)
C(16)-C(26)	1.472(7)
C(17)-C(18)	1.354(7)
C(19)-C(20)	1.533(7)
C(20)-C(21)	1.384(7)

C(20)-C(25)	1.394(7)
C(21)-C(22)	1.397(7)
C(22)-C(23)	1.370(9)
C(23)-C(24)	1.47(1)
C(24)-C(25)	1.394(8)
O(3)-Zn(1)-O(2)	100.4(1)
O(3)-Zn(1)-O(1)#1	107.2(1)
O(2)-Zn(1)-O(1)#1	110.7(1)
O(3)-Zn(1)-O(4)	82.2(1)
O(2)-Zn(1)-O(4)	139.5(1)
O(1)#1-Zn(1)-O(4)	117.8(1)
O(3)-Zn(1)-O(1)	165.6(1)
O(2)-Zn(1)-O(1)-80.0(1)	
O(1)#1-Zn(1)-O(1)	85.8(1)
O(4)-Zn(1)-O(1)	88.2(1)
O(3)-Zn(1)-Zn(1)#1	151.1(1)
O(2)-Zn(1)-Zn(1)#1	96.47(8)
O(1)#1-Zn(1)-Zn(1)#1	44.38(7)
O(4)-Zn(1)-Zn(1)#1-00.8(1)	
O(1)-Zn(1)-Zn(1)#1	41.45(7)
C(2)-O(1)-Zn(1)#1	121.0(2)
C(2)-O(1)-Zn(1)	108.9(2)
Zn(1)#1-O(1)-Zn(1)	94.2(1)
C(1)-O(2)-Zn(1)	113.8(3)
C(15)-O(3)-Zn(1)	109.2(3)
C(14)-O(4)-Zn(1)	110.5(3)
C(4)-N(1)-C(5)	120.6(4)
C(4)-N(1)-C(7)	118.3(4)
C(5)-N(1)-C(7)	121.1(4)
C(16)-N(2)-C(17)	121.5(4)
C(16)-N(2)-C(19)	123.7(4)
C(17)-N(2)-C(19)	114.7(4)
O(2)-C(1)-C(3)	124.4(4)
O(2)-C(1)-C(2)	118.3(4)
C(3)-C(1)-C(2)	117.3(4)
O(1)-C(2)-C(5)	123.0(4)
O(1)-C(2)-C(1)	116.7(3)
C(5)-C(2)-C(1)	120.3(4)
C(4)-C(3)-C(1)	120.1(4)
N(1)-C(4)-C(3)	122.4(4)
C(2)-C(5)-N(1)	119.3(4)
C(2)-C(5)-C(6)	121.2(4)
N(1)-C(5)-C(6)	119.4(4)
N(1)-C(7)-C(8)	113.3(4)
C(13)-C(8)-C(9)	119.6(4)
C(13)-C(8)-C(7)	119.7(4)
C(9)-C(8)-C(7)	120.6(4)
C(8)-C(9)-C(10)	120.1(5)
C(11)-C(10)-C(9)	120.4(5)
C(10)-C(11)-C(12)	119.8(4)
C(11)-C(12)-C(13)	120.3(5)

C(8)-C(13)-C(12)	119.7(5)
O(4)-C(14)-C(15)	117.8(4)
O(4)-C(14)-C(18)	124.0(4)
C(15)-C(14)-C(18)	118.1(4)
O(3)-C(15)-C(14)	119.7(4)
O(3)-C(15)-C(16)	120.3(4)
C(14)-C(15)-C(16)	119.9(4)
N(2)-C(16)-C(15)	119.1(4)
N(2)-C(16)-C(26)	119.2(4)
C(15)-C(16)-C(26)	121.8(5)
C(18)-C(17)-N(2)	121.2(5)
C(17)-C(18)-C(14)	120.0(5)
N(2)-C(19)-C(20)	112.1(4)
C(21)-C(20)-C(25)	119.2(5)
C(21)-C(20)-C(19)	124.6(4)
C(25)-C(20)-C(19)	116.2(5)
C(20)-C(21)-C(22)	120.0(5)
C(23)-C(22)-C(21)	120.3(6)
C(24)-C(23)-C(22)	120.1(5)
C(23)-C(24)-C(25)	120.6(5)
C(20)-C(25)-C(24)	119.7(6)

Appendix N: Crystal data and structure refinement for Cu(1-benzyl-2-ethyl-3-hydroxypyridin-4-one)$_2$ (45)

Table 21. Crystal data and structure refinement for **(45)**.

Identification code	Cu(1-benzyl -2-ethyl-3-hydroxypyridin-4-one)$_2$
Empirical formula	$C_{30}H_{36}CuN_2O_6$
Formula weight	584.15
Temperature	293(2) K
Wavelength	0.71069 Å
Crystal system	Triclinic
Space group	P-1
Unit cell dimensions	a = 7.379(2)Å α = 110.08(2)°
	b = 10.629(4)Å β = 108.76(2)°
	c = 10.676(3)Å γ = 99.76(2)°
Volume	706.8(4) Å^3
Z	1
Density (calculated)	1.372 Mg/m^3
Absorption coefficient	0.818 mm^{-1}
F(000)	307
Crystal size	0.25 x 0.25 x 0.25 mm
Theta range for data collection	2.15 to 24.97 °.
Index ranges	0<=h<=8; -12<=k<=12; -12<=l<=12
Reflections collected	2792
Independent reflections	2474 [R(int) = 0.0090]
Refinement method	Full-matrix least-squares on F^2
Data / restraints / parameters	2474 / 0 / 176
Goodness-of-fit on F^2	1.072
Final R indices [I>2σ(I)]	R1 = 0.0384 wR2 = 0.1132
R indices (all data)	R1 = 0.0508 wR2 = 0.1200
Largest diff. peak and hole	0.820 and -0.419 eÅ^{-3}
Weighting scheme	w=1/[σ^2(Fo^2)+(0.0819P)^2+0.1178P] where P=(Fo^2+2Fc^2)/3

Table 22. Bond lengths [Å] and angles [°] for **(45)**.

Cu(1)-O(2)	1.904(2)
Cu(1)-O(2)#1	1.904(2)
Cu(1)-O(1)	1.916(2)
Cu(1)-O(1)#1	1.916(2)
O(1)-C(1)	1.292(3)
O(2)-C(2)	1.319(3)
O(3)-C(15)	1.416(4)
N(1)-C(4)	1.354(4)
N(1)-C(3)	1.373(4)
N(1)-C(6)	1.470(4)
C(1)-C(5)	1.390(4)
C(1)-C(2)	1.431(4)
C(2)-C(3)	1.379(4)
C(3)-C(13)	1.489(4)
C(4)-C(5)	1.355(4)
C(6)-C(7)	1.509(4)
C(7)-C(12)	1.377(4)
C(7)-C(8)	1.383(4)
C(8)-C(9)	1.379(5)
C(9)-C(10)	1.365(5)
C(10)-C(11)	1.358(5)
C(11)-C(12)	1.380(4)
C(13)-C(14)	1.493(4)
O(2)-Cu(1)-O(2)#1	180.00(10)
O(2)-Cu(1)-O(1)	86.32(8)
O(2)#1-Cu(1)-O(1)	93.68(8)
O(2)-Cu(1)-O(1)#1	93.68(8)
O(2)#1-Cu(1)-O(1)#1	86.32(8)
O(1)-Cu(1)-O(1)#1	180.00(16)
C(1)-O(1)-Cu(1)	110.00(17)
C(2)-O(2)-Cu(1)	109.84(16)
C(4)-N(1)-C(3)	121.0(2)
C(4)-N(1)-C(6)	117.3(2)
C(3)-N(1)-C(6)	121.7(2)
O(1)-C(1)-C(5)	125.0(3)
O(1)-C(1)-C(2)	117.4(2)
C(5)-C(1)-C(2)	117.7(3)
O(2)-C(2)-C(3)	123.2(2)
O(2)-C(2)-C(1)	116.5(2)
C(3)-C(2)-C(1)	120.3(3)
N(1)-C(3)-C(2)	119.0(3)
N(1)-C(3)-C(13)	121.8(2)
C(2)-C(3)-C(13)	119.2(2)
C(5)-C(4)-N(1)	121.6(3)
C(4)-C(5)-C(1)	120.3(3)
N(1)-C(6)-C(7)	113.0(2)
C(12)-C(7)-C(8)	118.5(3)
C(12)-C(7)-C(6)	120.9(3)
C(8)-C(7)-C(6)	120.6(3)

C(9)-C(8)-C(7)	120.4(3)
C(10)-C(9)-C(8)	120.2(3)
C(11)-C(10)-C(9)	119.9(3)
C(10)-C(11)-C(12)	120.5(3)
C(7)-C(12)-C(11)	120.5(3)
C(3)-C(13)-C(14)	113.1(3)

Symmetry transformations used to generate equivalent atoms: #1 -x,-y,-z

Appendix O: Crystal data and structure refinement for Cu(1-^{n}butyl-2-ethyl-3-hydroxypyridin-4-one)$_2$ (46)

Table 23. Crystal data and structure refinement for **(46)**.

Identification code	Cu(1-^{n}butyl-2-ethyl-3-hydroxypyridin-4-one)$_2$
Empirical formula	$C_{22}H_{32}CuN_2O_4$
Formula weight	452.04
Temperature	170(2) K
Wavelength	0.71069 Å
Crystal system	Monoclinic
Space group	$P2_1/n$
Unit cell dimensions	a = 7.3736(2)Å α = 90°
	b = 9.4780(3)Å β = 95.113(2)°
	c = 15.0544(3)Å γ = 90°
Volume	1047.92(5) Å^3
Z	2
Density (calculated)	1.433 Mg/m^3
Absorption coefficient	1.073 mm^{-1}
F(000)	478
Crystal size	0.17 x 0.15 x 0.08 mm
Theta range for data collection	3.46 to 27.48 °.
Index ranges	0<=h<=9; -12<=k<=12; -19<=l<=19
Reflections collected	15651
Independent reflections	2409 [R(int) = 0.0345]
Reflections observed (>2σ)	2141
Max. and min. transmission	0.9239 and 0.8345
Refinement method	Full-matrix least-squares on F^2
Data / restraints / parameters	2409 / 0 / 134
Goodness-of-fit on F^2	0.987
Final R indices [I>2σ(I)]	R_1 = 0.0297 wR_2 = 0.0893
R indices (all data)	R_1 = 0.0347 wR_2 = 0.0949
Largest diff. peak and hole	0.332 and -0.439 e.Å^{-3}

Table 24. Bond lengths [Å] and angles [°] for **(46)**.

Cu(1)-O(2)	1.916(1)
Cu(1)-O(2)#1	1.916(1)
Cu(1)-O(1)	2.057(1)
Cu(1)-O(1)#1	2.057(1)
O(1)-C(1)	1.297(2)
O(2)-C(9)	1.328(2)
N(1)-C(3)	1.460(2)
N(1)-C(10)	1.375(2)
N(1)-C(5)	2.597(2)
C(1)-C(2)	1.399(2)
C(1)-C(9)	1.438(2)
C(2)-C(3)	1.369(2)
C(5)-C(6)	1.526(2)
C(6)-C(7)	1.518(2)
C(7)-C(13)	1.526(2)
C(9)-C(10)	1.392(2)
C(10)-C(12)	1.515(2)
C(11)-C(12)	1.528(2)
O(2)-Cu(1)-O(2)#1	180.00(3)
O(2)-Cu(1)-O(1)	85.87(4)
O(2)#1-Cu(1)-O(1)	94.13(4)
O(2)-Cu(1)-O(1)#1	94.13(4)
O(2)#1-Cu(1)-O(1)#1	85.87(4)
O(1)-Cu(1)-O(1)#1	180.00(8)
C(1)-O(1)-Cu(1)	109.74(8)
C(9)-O(2)-Cu(1)	110.09(8)
C(3)-N(1)-C(10)	120.6(1)
C(3)-N(1)-C(5)	116.3(1)
C(10)-N(1)-C(5)	123.0(1)
O(1)-C(1)-C(2)	125.1(1)
O(1)-C(1)-C(9)	117.3(1)
C(2)-C(1)-C(9)	117.6(1)
C(3)-C(2)-C(1)	120.0(1)
N(1)-C(3)-C(2)	122.1(1)
N(1)-C(5)-C(6)	112.9(1)
C(7)-C(6)-C(5)	114.7(1)
C(6)-C(7)-C(13)	112.3(1)
O(2)-C(9)-C(10)	122.7(1)
O(2)-C(9)-C(1)	127.0(1)
C(10)-C(9)-C(1)	120.3(1)
N(1)-C(10)-C(9)	119.4(1)
N(1)-C(10)-C(12)	121.6(1)
C(9)-C(10)-C(12)	129.0(1)
C(10)-C(12)-C(11)	112.3(1)

Appendix P: Crystal data and structure refinement for Zn(1-methyl-2-ethyl-3-hydroxypyridin-4-one)$_2$ (47)

Table 25. Crystal data and structure refinement for **(47)**.

Identification code	Zn(1-methyl-2-ethyl-3-hydroxypyridin-4-one)$_2$
Empirical formula	$C_{16}H_{20}N_2O_5Zn$
Formula weight	369.71
Temperature	170(2) K
Wavelength	0.71070 Å
Crystal system	Triclinic
Space group	P-1
Unit cell dimensions	a = 7.5363(3)Å α = 79.070(2)°
	b = 14.6288(5)Å β = 84.792(2)°
	c = 15.7246(6)Å γ = 83.735(2)°
Volume	1687.6(1) Å^3
Z	4
Density (calculated)	1.455 Mg/m^3
Absorption coefficient	1.476 mm^{-1}
F(000)	768
Crystal size	0.10 x 0.08 x 0.08 mm
Theta range for data collection	3.52 to 27.55 °.
Index ranges	-9<=h<=9; -18<=k<=19; -20<=l<=20
Reflections collected	26744
Independent reflections	7724 [R(int) = 0.0438]
Reflections observed (>2σ)	6339
Absorption correction	Semi-empirical from equivalents
Max. and min. transmission	0.8911 and 0.8665
Refinement method	Full-matrix least-squares on F^2
Data / restraints / parameters	7724 / 4 / 450
Goodness-of-fit on F^2	1.039
Final R indices [I>2σ(I)]	R_1 = 0.0553 wR_2 = 0.1511
R indices (all data)	R_1 = 0.0711 wR_2 = 0.1606
Largest diff. peak and hole	1.545 and -0.663 e.Å^{-3}

Hydrogen bonds with H..A < r(A) + 2.000 Angstroms and <DHA > 110 deg.

D-H	d(D-H)	d(H..A)	<DHA	d(D..A)	A
O5-**H5A**	0.964	1.683	160.16	2.610	**O8** [x-1, y, z]
O5-**H5B**	0.951	1.731	169.07	2.671	**O6**
O10-**H10A**	0.954	1.699	164.68	2.631	**O2**
O10-**H10B**	0.959	1.703	164.73	2.640	**O4** [x+1, y, z]

Symmetry transformations used to generate equivalent atoms: #1 -x,-y,-z

Table 26. Bond lengths [Å] and angles [°] for **(47)**.

Zn(1)-O(9)	1.990(2)
Zn(1)-O(7)	2.000(3)
Zn(1)-O(10)	2.015(3)
Zn(1)-O(6)	2.063(2)
Zn(1)-O(8)	2.067(3)
Zn(2)-O(3)	2.003(2)
Zn(2)-O(5)	2.009(3)
Zn(2)-O(1)	2.018(2)
Zn(2)-O(2)	2.046(2)
Zn(2)-O(4)	2.055(2)
O(1)-C(1)	1.312(4)
O(2)-C(2)	1.305(4)
O(3)-C(9)	1.314(4)
O(4)-C(10)	1.312(4)
O(6)-C(17)	1.299(4)
O(7)-C(18)	1.315(4)
O(8)-C(26)	1.305(4)
O(9)-C(25)	1.313(4)
N(1)-C(4)	1.356(5)
N(1)-C(5)	1.378(5)
N(1)-C(6)	1.475(4)
N(2)-C(12)	1.348(5)
N(2)-C(13)	1.372(5)
N(2)-C(14)	1.482(5)
N(3)-C(20)	1.344(5)
N(3)-C(19)	1.381(5)
N(3)-C(22)	1.479(5)
N(4)-C(28)	1.346(5)
N(4)-C(29)	1.386(5)
N(4)-C(32)	1.479(5)
C(1)-C(5)	1.398(5)
C(1)-C(2)	1.447(5)
C(2)-C(3)	1.396(5)
C(3)-C(4)	1.362(5)

C(5)-C(7)	1.503(5)
C(7)-C(8)	1.533(5)
C(9)-C(13)	1.399(5)
C(9)-C(10)	1.433(5)
C(10)-C(11)	1.403(5)
C(11)-C(12)	1.364(5)
C(13)-C(15)	1.512(5)
C(15)-C(16)	1.523(5)
C(17)-C(21)	1.410(5)
C(17)-C(18)	1.436(5)
C(18)-C(19)	1.399(5)
C(19)-C(23)	1.494(5)
C(20)-C(21)	1.373(6)
C(23)-C(24)	1.526(6)
C(25)-C(29)	1.399(5)
C(25)-C(26)	1.440(5)
C(26)-C(27)	1.401(5)
C(27)-C(28)	1.358(6)
C(29)-C(30)	1.489(5)
C(30)-C(31)	1.512(7)
O(9)-Zn(1)-O(7)	135.5(1)
O(9)-Zn(1)-O(10)	118.3(1)
O(7)-Zn(1)-O(10)	117.0(1)
O(9)-Zn(1)-O(6)-00.8(1)	
O(7)-Zn(1)-O(6)	82.3(1)
O(10)-Zn(1)-O(6)	91.9(1)
O(9)-Zn(1)-O(8)	82.2(1)
O(7)-Zn(1)-O(8)	94.7(1)
O(10)-Zn(1)-O(8)	89.1(1)
O(6)-Zn(1)-O(8)	177.0(1)
O(3)-Zn(2)-O(5)	121.5(1)
O(3)-Zn(2)-O(1)	121.3(1)
O(5)-Zn(2)-O(1)	118.2(1)
O(3)-Zn(2)-O(2)	105.6(1)
O(5)-Zn(2)-O(2)	91.3(1)
O(1)-Zn(2)-O(2)	82.2(1)
O(3)-Zn(2)-O(4)	82.5(1)
O(5)-Zn(2)-O(4)	92.4(1)
O(1)-Zn(2)-O(4)	97.1(1)
O(2)-Zn(2)-O(4)	176.12(9)
C(1)-O(1)-Zn(2)	110.4(2)
C(2)-O(2)-Zn(2)	110.5(2)
C(9)-O(3)-Zn(2)	110.7(2)
C(10)-O(4)-Zn(2)	109.7(2)
C(17)-O(6)-Zn(1)	110.0(2)
C(18)-O(7)-Zn(1)	111.0(2)
C(26)-O(8)-Zn(1)	109.6(2)
C(25)-O(9)-Zn(1)	111.0(2)
C(4)-N(1)-C(5)	121.0(3)
C(4)-N(1)-C(6)	118.5(3)
C(5)-N(1)-C(6)	120.5(3)

C(12)-N(2)-C(13)	121.0(3)
C(12)-N(2)-C(14)	118.4(3)
C(13)-N(2)-C(14)	120.6(4)
C(20)-N(3)-C(19)	120.7(3)
C(20)-N(3)-C(22)	118.4(3)
C(19)-N(3)-C(22)	120.9(3)
C(28)-N(4)-C(29)	121.7(3)
C(28)-N(4)-C(32)	118.6(4)
C(29)-N(4)-C(32)	119.7(4)
O(1)-C(1)-C(5)	122.2(3)
O(1)-C(1)-C(2)	118.7(3)
C(5)-C(1)-C(2)	119.1(3)
O(2)-C(2)-C(3)	124.7(3)
O(2)-C(2)-C(1)	117.0(3)
C(3)-C(2)-C(1)	118.3(3)
C(4)-C(3)-C(2)	120.0(4)
C(3)-C(4)-N(1)	122.1(3)
N(1)-C(5)-C(1)	119.6(3)
N(1)-C(5)-C(7)	120.9(3)
C(1)-C(5)-C(7)	119.5(3)
C(5)-C(7)-C(8)	112.7(3)
O(3)-C(9)-C(13)	121.9(3)
O(3)-C(9)-C(10)	118.9(3)
C(13)-C(9)-C(10)	119.2(3)
O(4)-C(10)-C(11)	123.9(3)
O(4)-C(10)-C(9)	117.6(3)
C(11)-C(10)-C(9)	118.5(3)
C(12)-C(11)-C(10)	119.3(4)
N(2)-C(12)-C(11)	122.4(4)
N(2)-C(13)-C(9)	119.5(3)
N(2)-C(13)-C(15)	121.7(3)
C(9)-C(13)-C(15)	118.8(3)
C(13)-C(15)-C(16)	111.6(3)
O(6)-C(17)-C(21)	124.0(3)
O(6)-C(17)-C(18)	117.9(3)
C(21)-C(17)-C(18)	118.1(3)
O(7)-C(18)-C(19)	121.7(3)
O(7)-C(18)-C(17)	118.7(3)
C(19)-C(18)-C(17)	119.6(3)
N(3)-C(19)-C(18)	119.5(3)
N(3)-C(19)-C(23)	121.0(3)
C(18)-C(19)-C(23)	119.5(3)
N(3)-C(20)-C(21)	122.8(3)
C(20)-C(21)-C(17)	119.2(4)
C(19)-C(23)-C(24)	112.0(3)
O(9)-C(25)-C(29)	122.1(3)
O(9)-C(25)-C(26)	118.6(3)
C(29)-C(25)-C(26)	119.3(3)
O(8)-C(26)-C(27)	124.2(3)
O(8)-C(26)-C(25)	117.3(3)
C(27)-C(26)-C(25)	118.4(3)

C(28)-C(27)-C(26)	120.0(4)
N(4)-C(28)-C(27)	121.8(4)
N(4)-C(29)-C(25)	118.7(3)
N(4)-C(29)-C(30)	121.1(3)
C(25)-C(29)-C(30)	120.1(4)
C(29)-C(30)-C(31)	113.9(4)

Appendix Q: Crystal data and structure refinement for 2-benzylaminotropone (64)

Table 27. Crystal data and structure refinement for **(64)**.

Identification code	2-benzylaminotropone
Empirical formula	$C_{14}H_{13}NO$
Formula weight	211.25
Temperature	150(2) K
Wavelength	0.71070 Å
Crystal system	Monoclinic
Space group	P21/c
Unit cell dimensions	a = 5.57800(10)Å α = 90°
	b = 9.3640(2)Å β = 95.0710(9)°
	c = 20.8230(3)Å γ = 90°
Volume	1083.38(3) $Å^3$
Z	4
Density (calculated)	1.295 Mg/m^3
Absorption coefficient	0.082 mm^{-1}
F(000)	448
Crystal size	0.40 x 0.30 x 0.25 mm
Theta range for data collection	2.93 to 30.03 °.
Index ranges	-7<=h<=7; -11<=k<=13; -28<=l<=29
Reflections collected	14213
Independent reflections	3152 [R(int) = 0.0393]
Reflections observed (>2σ)	2690
Absorption correction	Semi-empirical from equivalents
Max. and min. transmission	1.020, 0.984
Refinement method	Full-matrix least-squares on F^2
Data / restraints / parameters	3152 / 0 / 150
Goodness-of-fit on F^2	1.058
Final R indices [I>2σ(I)]	R_1 = 0.0534 wR_2 = 0.1346
R indices (all data)	R_1 = 0.0630 wR_2 = 0.1398
Largest diff. peak and hole	0.285 and -0.243 $e.Å^{-3}$

Table 28. Bond lengths [Å] and angles [°] for **(65)**.

O(1)-C(1)	1.2573(18)	N(1)-C(2)	1.3457(18)
N(1)-C(8)	1.449(2)	C(1)-C(7)	1.433(2)
C(1)-C(2)	1.485(2)	C(2)-C(3)	1.3982(19)
C(3)-C(4)	1.398(2)	C(4)-C(5)	1.375(2)
C(5)-C(6)	1.398(2)	C(6)-C(7)	1.376(2)
C(8)-C(9)	1.519(2)	C(9)-C(14)	1.388(2)
C(9)-C(10)	1.398(2)	C(10)-C(11)	1.392(2)
C(11)-C(12)	1.388(2)	C(12)-C(13)	1.386(2)
C(13)-C(14)	1.394(2)		
C(2)-N(1)-C(8)	125.08(12)	O(1)-C(1)-C(7)	119.92(14)
O(1)-C(1)-C(2)	117.02(13)	C(7)-C(1)-C(2)	123.06(13)
N(1)-C(2)-C(3)	120.68(14)	N(1)-C(2)-C(1)	112.09(12)
C(3)-C(2)-C(1)	127.22(13)	C(4)-C(3)-C(2)	130.85(15)
C(5)-C(4)-C(3)	130.21(15)	C(4)-C(5)-C(6)	126.26(15)
C(7)-C(6)-C(5)	130.21(16)	C(6)-C(7)-C(1)	132.18(15)
N(1)-C(8)-C(9)	115.06(12)	C(14)-C(9)-C(10)	118.92(13)
C(14)-C(9)-C(8)	122.42(13)	C(10)-C(9)-C(8)	118.63(13)
C(11)-C(10)-C(9)	120.46(14)	C(12)-C(11)-C(10)	120.10(14)
C(13)-C(12)-C(11)	119.74(14)	C(12)-C(13)-C(14)	120.15(14)
C(9)-C(14)-C(13)	120.61(14)		

Symmetry transformations used to generate equivalent atoms: #1 -x,-y,-z

Appendix R: Crystal data and structure refinement for Cu(2-methylaminotropone)$_2$ (71)

Table 29. Crystal data and structure refinement for **(71)**.

Identification code	Cu(2-methylaminotropone)$_2$
Empirical formula	$C_{16}H_{16}CuN_2O_2$
Formula weight	331.85
Temperature	170(2) K
Wavelength	0.71069 Å
Crystal system	Monoclinic
Space group	$P2_1/n$
Unit cell dimensions	a = 6.7680(1)Å α = 90°
	b = 9.2410(2)Å β = 92.413(1)°
	c = 22.1370(4)Å γ = 90°
Volume	1383.29(4) Å^3
Z	4
Density (calculated)	1.593 Mg/m^3
Absorption coefficient	1.584 mm^{-1}
F(000)	684
Crystal size	0.20 x 0.20 x 0.20 mm
Theta range for data collection	3.68 to 27.47 °.
Index ranges	-8<=h<=8; -11<=k<=11; -28<=l<=28
Reflections collected	20982
Independent reflections	3149 [R(int) = 0.0292]
Reflections observed (>2σ)	2844
Absorption correction	Multiscan
Max. and min. transmission	1.014, 0.992
Refinement method	Full-matrix least-squares on F^2
Data / restraints / parameters	3149 / 0 / 191
Goodness-of-fit on F^2	0.978
Final R indices [I>2σ(I)]	R_1 = 0.0273 wR_2 = 0.0844
R indices (all data)	R_1 = 0.0317 wR_2 = 0.0882
Largest diff. peak and hole	0.403 and -0.481 e.Å^{-3}

Table 30. Bond lengths [Å] and angles [°] for **(71)**.

Cu(1)-N(2)	1.928(1)
Cu(1)-N(1)	1.931(1)
Cu(1)-O(2)	1.934(1)
Cu(1)-O(1)	1.941(1)
O(1)-C(2)	1.296(2)
O(2)-C(10)	1.309(2)
N(1)-C(3)	1.318(2)
N(1)-C(1)	1.464(2)
N(2)-C(11)	1.320(2)
N(2)-C(9)	2.560(2)
C(2)-C(8)	1.392(2)
C(2)-C(3)	1.484(2)
C(3)-C(4)	1.429(2)
C(4)-C(5)	1.376(2)
C(5)-C(6)	1.400(2)
C(6)-C(7)	1.375(2)
C(7)-C(8)	1.402(2)
C(10)-C(16)	1.382(2)
C(10)-C(11)	1.481(2)
C(11)-C(12)	1.426(2)
C(12)-C(13)	1.375(2)
C(13)-C(14)	1.399(2)
C(14)-C(15)	1.368(2)
C(15)-C(16)	1.403(2)
N(2)-Cu(1)-N(1)	175.78(5)
N(2)-Cu(1)-O(2)	82.26(5)
N(1)-Cu(1)-O(2)	97.13(5)
N(2)-Cu(1)-O(1)	98.57(5)
N(1)-Cu(1)-O(1)	82.04(5)
O(2)-Cu(1)-O(1)	179.17(4)
C(2)-O(1)-Cu(1)	114.54(9)
C(10)-O(2)-Cu(1)	114.59(9)
C(3)-N(1)-C(1)	120.4(1)
C(3)-N(1)-Cu(1)	115.4(1)
C(1)-N(1)-Cu(1)	124.1(1)
C(11)-N(2)-C(9)	120.3(1)
C(11)-N(2)-Cu(1)	115.20(9)
C(9)-N(2)-Cu(1)	124.44(9)
O(1)-C(2)-C(8)	118.5(1)
O(1)-C(2)-C(3)	125.0(1)
C(8)-C(2)-C(3)	137.5(1)
N(1)-C(3)-C(4)	122.7(1)
N(1)-C(3)-C(2)	112.7(1)
C(4)-C(3)-C(2)	124.5(1)
C(5)-C(4)-C(3)	131.8(2)
C(4)-C(5)-C(6)	131.5(2)
C(7)-C(6)-C(5)	137.6(2)
C(6)-C(7)-C(8)	130.8(2)
C(2)-C(8)-C(7)	131.1(2)

O(2)-C(10)-C(16)	118.5(1)
O(2)-C(10)-C(11)	125.0(1)
C(16)-C(10)-C(11)	126.5(1)
N(2)-C(11)-C(12)	123.1(1)
N(2)-C(11)-C(10)	113.8(1)
C(12)-C(11)-C(10)	124.2(1)
C(13)-C(12)-C(11)	131.3(2)
C(12)-C(13)-C(14)	130.4(2)
C(15)-C(14)-C(13)	126.4(2)
C(14)-C(15)-C(16)	130.7(2)
C(10)-C(16)-C(15)	132.6(2)

Appendix S: Crystal data and structure refinement for Cu(2-ethylaminotropone)$_2$ (72)

Table 31. Crystal data and structure refinement for **(72)**.

Identification code	Cu(2-ethylaminotropone)$_2$
Empirical formula	C_{18} H_{20} Cu N_2 O_2
Formula weight	359.90
Temperature	170(2) K
Wavelength	0.71070 Å
Crystal system	Monoclinic
Space group	$P2_1/c$
Unit cell dimensions	a = 15.5900(2)Å α = 90°
	b = 5.12200(10)Å β = 150.4561(15)°
	c = 19.8310(4)Å γ = 90°
Volume	780.83(2) Å^3
Z	2
Density (calculated)	1.531 Mg/m^3
Absorption coefficient	1.410 mm^{-1}
F(000)	374
Crystal size	0.20 x 0.10 x 0.10 mm
Theta range for data collection	4.17 to 30.02 °.
Index ranges	0<=h<=21; -7<=k<=7; -27<=l<=13
Reflections collected	5207
Independent reflections	2262 [R(int) = 0.0306]
Reflections observed (>2σ)	2112
Refinement method	Full-matrix least-squares on F^2
Data / restraints / parameters	2262 / 0 / 108
Goodness-of-fit on F^2	1.081
Final R indices [I>2σ(I)]	R_1 = 0.0287 wR_2 = 0.0860
R indices (all data)	R_1 = 0.0306 wR_2 = 0.0879
Largest diff. peak and hole	0.494 and -0.635 e.Å^{-3}

Table 32. Bond lengths [Å] and angles [°] for **(72)**.

Cu(1)-O(1)#1	1.9314(9)
Cu(1)-O(1)	1.9314(9)
Cu(1)-N(1)	1.9370(11)
Cu(1)-N(1)#1	1.9370(11)
N(1)-C(4)	1.3250(16)
N(1)-C(1)	1.4628(15)
O(1)-C(3)	1.2935(15)
C(1)-C(2)	1.5210(18)
C(3)-C(9)	1.3963(18)
C(3)-C(4)	1.4777(17)
C(4)-C(5)	1.4303(17)
C(5)-C(6)	1.3789(19)
C(6)-C(7)	1.402(2)
C(7)-C(8)	1.378(2)
C(8)-C(9)	1.400(2)
O(1)#1-Cu(1)-O(1)	180.000(1)
O(1)#1-Cu(1)-N(1)	97.66(4)
O(1)-Cu(1)-N(1)	82.34(4)
O(1)#1-Cu(1)-N(1)#1	82.34(4)
O(1)-Cu(1)-N(1)#1	97.66(4)
N(1)-Cu(1)-N(1)#1	180.000(1)
C(4)-N(1)-C(1)	121.23(11)
C(4)-N(1)-Cu(1)	114.76(8)
C(1)-N(1)-Cu(1)	123.99(8)
C(3)-O(1)-Cu(1)	114.60(7)
N(1)-C(1)-C(2)	112.44(11)
O(1)-C(3)-C(9)	118.08(11)
O(1)-C(3)-C(4)	115.52(10)
C(9)-C(3)-C(4)	126.39(12)
N(1)-C(4)-C(5)	123.18(11)
N(1)-C(4)-C(3)	112.69(10)
C(5)-C(4)-C(3)	124.13(11)
C(6)-C(5)-C(4)	131.71(13)
C(5)-C(6)-C(7)	130.09(14)
C(8)-C(7)-C(6)	126.33(13)
C(7)-C(8)-C(9)	129.72(13)
C(3)-C(9)-C(8)	131.62(14)

Symmetry transformations used to generate equivalent atoms: #1 -x+1,-y+1,-z+2